NOAA Technical Memorandum ERL ARL-108

METHODS FOR ESTIMATING WAKE FLOW AND EFFLUENT DISPERSION NEAR SIMPLE BLOCK-LIKE BUILDINGS

R. P. Hosker, Jr.

Air Resources Laboratories
Silver Spring, Maryland
May 1981

noaa NATIONAL OCEANIC AND ATMOSPHERIC ADMINISTRATION / Environmental Research Laboratories

DISCLAIMER

NOAA-TM-ERL-ARL--108

DE82 008600

NOAA Technical Memorandum ERL ARL-108

METHODS FOR ESTIMATING WAKE FLOW AND EFFLUENT DISPERSION NEAR SIMPLE BLOCK-LIKE BUILDINGS

R. P. Hosker, Jr.

Atmospheric Turbulence and Diffusion Laboratory
Oak Ridge, Tennessee

Air Resources Laboratories
Silver Spring, Maryland
May 1981

UNITED STATES
DEPARTMENT OF COMMERCE
Malcolm Baldrige,
Secretary

NATIONAL OCEANIC AND
ATMOSPHERIC ADMINISTRATION
James P. Walsh,
Acting Administrator

Environmental Research
Laboratories
Joseph O. Fletcher,
Acting Director

NOTICE

Mention of a commercial company or product does not constitute an endorsement by NOAA Environmental Research Laboratories. Use for publicity or advertising purposes of information from this publication concerning proprietary products or the tests of such products is not authorized.

Report is also to be published as NUREG/CR-2521, a publication of the U. S. Nuclear Regulatory Commission.

ATDL Contribution File No. 81/10

ABSTRACT

This report is intended as an interim guide for those who routinely face air quality problems associated with near-building exhaust stack placement and height, and the resulting concentration patterns. The report consolidates available data and methods for estimating wake flow and effluent dispersion near isolated block-like structures. The near-building and wake flows are described, and quantitative estimates for frontal eddy size, height and extent of roof and wake cavities, and far wake behavior are provided. Concentration calculation methods for upwind, near-building, and downwind pollutant sources are given. For an upwind source, it is possible to estimate the required stack height, and to place upper limits on the likely near-building concentration. The influences of near-building source location and characteristics relative to the building geometry and orientation are considered. Methods to estimate effective stack height, upper limits for concentration due to flush roof vents, and the effect of changes in rooftop stack height are summarized. Current wake and wake cavity models are presented. Numerous graphs of important expressions have been prepared to facilitate computations and quick estimates of flow patterns and concentration levels for specific simple buildings. Detailed recommendations for additional work are given.

THIS PAGE

WAS INTENTIONALLY

LEFT BLANK

CONTENTS

THIS PAGE

WAS INTENTIONALLY

LEFT BLANK

LIST OF FIGURES

THIS PAGE

WAS INTENTIONALLY

LEFT BLANK

LIST OF SYMBOLS

Symbols are listed below and are also defined in the text as needed. An attempt has been made to force consistency of nomenclature throughout. Consequently readers who refer to the original papers can expect changes in notation. Units (length, time, mass, temperature) are indicated in square brackets after each symbol.

a	coefficient in power law approximation of σ_z $[L]^{1-q}$
b	coefficient in expression for K/K_r as function of distance from rooftop stack
b'	coefficient in expression for K/K_r as function of stack height relative to the roof.
A,B	functions of L/H in expression for wake cavity length
$A';B';C';D'$	coefficients in "MPTER" algorithms for σ_y and σ_z [varied units]
A_c	surface area of wake cavity exposed to atmosphere $[L^2]$
A_e	exit area of effluent vent $[L^2]$
A_p	projected frontal area of an obstacle $[L^2]$
c	coefficient in expressions for building wake concentrations
d_i	inside diameter of stack [L]
D	dilution, the ratio of concentration at effluent exit point to concentration at an arbitrary location
D_b	diameter of a cylindrical building [L]
f	fraction of time plume is entrained into wake cavity by aerodynamic downwash
f_i	mass fraction of i^{th} gaseous component in an effluent mixture
F_b	buoyancy flux of effluent, $= -g\dot{V}_e\Delta/\pi$ $[L^4\ t^{-3}]$
g	gravitational acceleration, 9.8 m/s^2 $[L\ t^{-2}]$
$\tilde{h}$	height of stack relative to building roof [L]
h'	effluent release height corrected for stack tip downwash [L]

h'' effluent release height corrected for both stack tip downwash and building aerodynamic influence [L]

h_1 first approximation to stack height [L]

h_e effective stack height, compensated for stack tip downwash, building aerodynamic effects, and plume buoyancy [L]

h_{eo} virtual effective stack height (see Table 1) [L]

h_s stack height relative to ground [L]

Δh plume rise [L]

H characteristic vertical dimension of an obstacle [L]

H_c max. height of roof recirculation zone [L]

K concentration coefficient, $= \chi U A_p / Q$

K_e concentration coefficient at the effluent exit, $= (U_s/w_e)(A_p/A_e)$

L characteristic dimension of an obstacle in the along-wind direction [L]

L_c length of roof recirculation zone [L]

$\bar{m}$ molecular weight [M/mole]

n exponent of power-law velocity profiles ($U \propto z^n$). Also, the outward normal to a surface.

p an exponent

q exponent in power law approximation of σ_z

R Wilson's (1979) characteristic dimension of an obstacle,

$= \zeta_b^{2/3} \xi_b^{1/3}$ [L]

s "stretched string" distance between source and receptor on the same building [L]

t time [t]

t_d characteristic retention time for effluent in a wake cavity [t]

T absolute temperature [°K]

U mean wind speed in the x direction [Lt^{-1}]

U_A critical wind speed for closest approach to ground of isopleth of maximum allowable concentration $[Lt^{-1}]$

ΔU mean velocity defect, $= U - U_\infty$ $[Lt^{-1}]$

V_c volume of wake cavity $[L^3]$

$\dot{V}_e$ volume flow rate of effluent, $= w_e A_e$ $[L^3 t^{-1}]$

w_e effluent vertical exit speed $[Lt^{-1}]$

w_t transport velocity across a turbulent shear layer $[Lt^{-1}]$

W characteristic dimension of an obstacle in the cross-wind (horizontal) direction [L]

x,y,z along-wind, cross-wind, and vertical coordinates, respectively [L]

$\tilde{x},\tilde{y},\tilde{z}$ coordinates relative to base of a roof-mounted stack [L]

x_B location of building front face relative to upwind source [L]

x_c distance from windward edge to location of maximum height of roof recirculation zone [L]

x_r length of recirculation zone behind an obstacle, measured from the lee building face [L]

x_s point of intersection of Z_{II} and roof plane, relative to upwind roof edge (see Fig. 8) [L]

x_{yo},x_{zo} virtual source location upwind of effluent vent, such that $\sigma_{yo} = \sigma_y(x_{yo})$, $\sigma_{zo} = \sigma_z(x_{zo})$ [L]

x_o virtual source location when $x_{yo} = x_{zo} = x_o$ [L]

Y_p plume half-width [L]

z_o aerodynamic roughness length [L]

Z_e effective wake height of building, $= H + 1.5\ \zeta_b$ [L]

Z_m minimum descent height of maximum permissible concentration isopleth [L]

Z_p plume depth, for ground-level source [L]

$Z_{I,II,III}$ boundaries of flow zones above a building roof (Fig. 8) [L]

α angle of wind incidence relative to building face normal [degrees or radians]

$\tilde{\alpha}$ Halitsky's (1963a,b) configuration coefficient in expression for dilution as function of source to receptor distance (Eq. 3-21)

β ratio of average transport speed in horseshoe vortex to speed at roof height

δ boundary layer or shear layer thickness [L]

δ_c thickness of wake cavity boundary [L]

Δ relative density difference of effluent, = $(\rho_e - \rho_a)/\rho_a$

ζ_b smaller of obstacle frontal dimensions W or H [L]

η smaller of obstacle frontal dimensions H or W/2 [L]

λ a turbulent mixing length [L]

ξ_b larger of obstacle frontal dimensions W or H [L]

π 3.14159...

ρ density $[ML^{-3}]$

$\sigma_y(x)$, $\sigma_z(x)$ cross-wind and vertical Gaussian plume dispersion coefficients, as functions of along-wind distance [L]

$\sigma'_y(x)$, $\sigma'_z(x)$ wake-enhanced dispersion coefficients (Eq. 3-44) [L]

σ_{yo},σ_{zo} plume dispersion coefficients corresponding to an upwind virtual source [L]

σ_ϕ standard deviation of vertical fluctuations of wind direction [degrees or radians]

Σ_y,Σ_z total diffusion coefficients (Eq. 3-41) [L]

τ dimensionless retention time for effluent in wake cavity, = $U_\infty t_d/H$

χ effluent concentration $[ML^{-3}]$

χ_{GL} concentration at plume height due to an elevated source, no buildings present $[ML^{-3}]$

χ_{GL} ground-level concentration due to an elevated source, no buildings present $[ML^{-3}]$

χ_{GLB} ground-level concentration at windward face of a building due to an upwind source $[ML^{-3}]$

χ_{GLO} ground-level concentration due to a ground-level source, no buildings present $[ML^{-3}]$

χ_H concentration at height H due to an elevated source, no buildings present $[ML^{-3}]$

$\bar{\chi}_S$ average concentration over all building surfaces due to an elevated upwind source $[ML^{-3}]$

χ_o ground-level centerline concentration due to a ground-level source, no buildings present $[ML^{-3}]$

Subscripts

a denotes an ambient quantity

e denotes an effluent quantity, or a quantity measured at vent or stack exit

H denotes value of quantity at roof height

i denotes quantity for i^{th} step, or building

j indicates a particular stability category; in terms of P-G-T, j = 1 = "A", j = 4 = "D", etc.

k index for wind speed class

ℓ index for position downward of stack

m or min denotes a manimum value

M or max denotes a maximum value

r denotes a quantity measured in a rooftop release from a flush vent

rms indicates root-mean-square value of quantity

s denotes value of quantity at stack height

v denotes values within a vortex

∞ denotes a "freestream" value aloft

An overbar ($\overline{\ }$) denotes an average value

THIS PAGE

WAS INTENTIONALLY

LEFT BLANK

ACKNOWLEDGEMENTS

This report was prepared for the Site Safety Standards Branch of the Office of Standards Development, U.S. Nuclear Regulatory Commission, under interagency agreement AT(49-25)-1004. Preliminary work was accomplished under interagency agreements among the National Oceanic and Atmospheric Administration, the Department of Energy, and the NRC. The author is grateful to Robert Abbey, Leta Brown, and Robert Kornasiewcz of the Nuclear Regulatory Commission for their support and patience. Thanks are also due to Erma J. Yates of the Atmospheric Turbulence and Diffusion Laboratory for her expert typing and patient revisions, and to several reviewers, particularly R. N. Meroney and K. M. Kothari of Colorado State University, for their helpful comments.

EXECUTIVE SUMMARY

This report attempts to consolidate available information and provide simple estimation methods for wake flow and effluent dispersion near isolated block-like buildings. It is intended as an interim guide for those who routinely face air quality problems associated with near-building exhaust stack placement or height, and estimation of the resulting effluent concentrations. However, it should be explicitly recognized that the techniques described apply only to idealized isolated structures located in a flat, homogeneous landscape free of hills, river valleys, shorelines, or other perturbing influences; in more complicated circumstances the user is on shaky ground, and should proceed accordingly. In particular, detailed evaluations of complex sites and building clusters are generally beyond the scope of these methods, although the techniques may be useful for crude assessments and identification of potential trouble spots.

The report is organized around two major components: a description of the flow patterns near simple buildings, and methods to estimate the pollutant concentrations generated by these patterns. The flow section provides means for quantitative estimates of the frontal eddy size, the height and extent of the recirculating roof and wake cavities, and the behavior of the far wake. The intent of the section is to provide information useful for selecting good exhaust stack or air intake locations, as well as to convey some understanding of the very complex flow phenomena which are found near even simple buildings exposed to the turbulent atmosphere. The concentration calculations deal with sources upwind, near, and downwind of an isolated structure. For the upwind source, it is possible to estimate the stack height needed to avoid objectionable pollutant levels near the building, or to place upper limits on the concentrations likely to be experienced. When the source is close to the obstacle, its exact location, height, and emission characteristics are important in evaluating concentrations appearing in the complex local flows. Methods to estimate effective stack height are given, along with a discussion of the influence of rooftop stack position. Upper limits on the near-building concentrations produced by flush roof vents are suggested, and a way of accounting for roof stack elevation is described. Current wake and wake cavity concentration models are presented, along with some discussion of their agreement with the limited data available. Numerous graphs of important expressions are included to facilitate calculations and quick estimates. A summary of the most relevant procedures and recommendations for future work conclude the report. Additional research is needed to fill significant gaps in the data set available for simple building concentration model development and testing. Data from a variety of building shapes and stack locations are needed to assess the fluctuating entrainment problem. Basic information on fluid flow near rudimentary arrays of structures is necessary before plausible semi-empirical models can be developed for concentrations close to a building cluster.

THIS PAGE

WAS INTENTIONALLY

LEFT BLANK

1.0 INTRODUCTION

The behavior of effluent plumes near buildings is a concern common to architects, regulatory agencies, and air pollution meteorologists. Reliable answers to the questions of whether a pollution problem exists and, if so, how frequently it may occur, are difficult to obtain. This is particularly true in the nuclear industry, where the possible paths, concentrations, and effects of radioactive plumes must be assessed for both routine and emergency release situations. Despite the need, there is relatively little guidance available in an easy to apply format; instead, one must usually delve into the technical literature. For example, the U.S. Environmental Protection Agency's (1978) Guideline on Air Quality Models simply refers the reader to several articles on "aerodynamic downwash"; no explicit modeling recommendations are made. Turner (1969) and the American Society of Mechanical Engineers (1973) treat only the case where material emitted from a source on a building is fully entrained into the building wake. An exception is the excellent article by Meroney (1979), which suggests calculation methods for a variety of cases often encountered in practice.

This report is an attempt to consolidate the information and calculation methods presently available for wake flow and effluent dispersion near and downwind of simple block-like buildings. The flow field observed around such structures is presented in some detail, since it will generally be impossible to explain or predict effluent concentration patterns near buildings without some understanding of the aerodynamic processes responsible. The flow description is broken into five sections: an overall flow field summary, followed by more detailed descriptions of the upwind influence of a building, the flows and recirculation zones along its roof and side, the near wake, especially the recirculating cavity region, and the turbulent far wake. The viewpoint in these sections is rather fundamental, emphasizing the physical phenomena, their (often complex) theoretical explanations, and some "rules of thumb" for estimation purposes; this mode of presentation reflects the method of study commonly encountered in the fluid dynamics literature. The question of effluent dispersion in these complicated flow fields is then addressed, but in a more applied fashion, again reflecting the traditional approach of the relevant literature. The discussion covers plumes approaching a building from upwind, those emitted on or near a structure, and those released downwind. "Rules of thumb" and formulas are presented for estimating such things as appropriate stack heights and concentrations near buildings. It must be remembered, however, that such "rules" generally are valid only for quite specific building shapes and orientations; even rather small changes in these parameters may drastically alter the flow field and the resulting dispersion patterns. The user therefore must try to visualize all the flow patterns possible for the structure under study; in particular, the changes accompanying different angles of wind incidence must be explored. Guidance for cases involving even mildly complex geometry or winds along the building diagonal will often not be available; recourse to field or laboratory tests may then be necessary. In particular, fluid modeling of the situation may prove quite useful and inexpensive, if executed properly. A recent report by Snyder (1981) may be helpful in this regard.

2.0 FLOW NEAR SIMPLE BUILDINGS

2.1 General Features of the Flow.

Consider a typical deep turbulent atmospheric boundary layer normally incident on a simple building. Until fairly recently, the generally accepted conceptual model of the main flow patterns was rather simple, as shown in Figure 1. While the sketch does demonstrate some of the principal phenomena, it also neglects a few important features. A more accurate model, indicated in Figure 2, has emerged during the last decade or so from work by Morkovin (1972) and his colleagues, by Britter, Hunt, and Puttock (1976), by Woo, Peterka, and Cermak (1977), and by Hunt et al. (1978). The main features of the flow are as follows: upwind of the obstacle there is a "displacement zone" where the incident fluid is first influenced by the presence of the building. Within this zone, both wind speed and direction are affected as the flow attempts to travel around and over the body. The exposed front surfaces of the obstacle will experience a pressure higher than ambient as the approaching air decelerates. Since the incident wind speed diminishes with decreasing height, a downward-directed pressure gradient will be established as the flow decelerates near the upwind face. This gradient drives a downward-directed flow along the front surface; at the ground, this flow moves out from the building, causing the approach flow to separate from the ground some distance upwind. The result is a standing eddy in front of the lower portion of the building. The exact upwind separation location depends on the building width to height ratio, the upstream surface roughness, and the approach flow characteristics relative to the building. The behavior of the frontal eddy is discussed below.

Above this eddy, the incident flow strikes the building face, moving upward and/or sidewards depending on its proximity to the roof or side edges. On block-like structures, the resulting viscosity-induced boundary layer separates from the exposed surface at sharp edges (sides, roof) where the flow cannot follow the abrupt change in direction. On rounded obstacles, separation occurs when fluid within a boundary layer encounters a region of increasing pressure and has insufficient momentum to successfully cross this zone of adverse pressure gradient. In this situation, the exact place where the fluid adjacent to the building surface is decelerated to zero velocity and is then diverted outward from the surface depends on a complicated aerodynamic force balance. Factors such as building surface roughness, wind speed shear, and the incident turbulence characteristics are important. In this report, however, attention will be focused on the simpler case of sharp-edged buildings, where flow separation is generally limited to the roof and side edges.

The separated boundary layers move out into the surrounding fluid as free shear layers. If the obstacle is sufficiently long, the flow may reattach to the building surface at some downstream location, and eventually will separate again at the end of the body. If the obstacle is not long enough, reattachment does not occur. In either case, the separated layers curve inward toward the wake axis, feeding into a "cavity" or recirculation "bubble" immediately downwind of the body. The cavity zone is

characterized by low mean speed, high turbulence intensity, recirculation with relatively large residence times of fluid particles "trapped" within the bubble, and low, rather uniform pressure. The exact flow characteristics within this zone depend on the peculiarities of the boundary layers shed by the particular obstacle, and on the details of the turbulent mixing within the free shear layers; these are difficult to predict in any general way. In cases where the flow clings to or reattaches to the building sides and roof, the wake cavity may be further complicated by the presence of vertically-oriented vortices behind the lee side edges. These vortices interact with the main flow near roof level and bend over, streaming off downwind as an elevated counter-rotating vortex pair.

Meanwhile the turbulent shear layer above the wake cavity thickens as it diffuses into the ambient flow. Its behavior has been studied most closely for the two-dimensional case (e.g., Bradshaw and Wong, 1972), where the layer forms the cavity's upper boundary. In this case, when the layer finally strikes the ground to "close" the cavity, it divides; some of its fluid enters the cavity, and the remainder moves off downwind into the turbulent wake. The portion diverted into the cavity balances the cavity fluid lost to entrainment by the cavity boundary shear layer. Immediately downwind of the two-dimensional cavity closure, the scale (eddy size) of the near-surface turbulence present is small because of the splitting of the shear layer from which it arises; in effect, the eddies within the layer are torn in two by the process. However, a new boundary layer flow dependent on the local surface characteristics and scaling to height above the surface immediately begins to develop. Above this "surface" or "wall" layer is a mixing zone whose upper edge forms the top of the turbulent wake. At least some of the fluid within this zone originates from the split shear layer. The fluid above the wake mixing zone is ambient air, somewhat perturbed and displaced by the presence of the building and the lower portion of the associated wake, but basically dependent on the characteristics of the incident flow field and upwind fetch. Figure 3 (Counihan, Hunt, and Jackson, 1974) is an idealization of the situation behind a very wide (two-dimensional) simple structure. The three-dimensional case is considerably more complex, since fluid traveling along the separation streamline actually enters the cavity region, rather than simply bounding it (see Figure 2), while the lee-edge vortices serve to remove fluid from the cavity. Detailed studies of the flow and turbulence characteristics associated with the boundary of a three-dimensional cavity are apparently unavailable. Furthermore, since the turbulent shear layers leaving any obstacle interact with each other, with the lee-edge vortices, and with the turbulent incident flow, the cavity will in reality fluctuate in size. Consequently the descriptions just given of cavity phenomena are appropriate only in some time-averaged sense.

While the shear layer shed by the building is undergoing these changes, the frontal eddy is also interacting with the incident flow near the sides of the structure, wrapping about the obstacle and trailing off downwind on either side near ground level. Viewed from above, this vortex rather resembles a horseshoe, from which it takes its name. Although Figure 2 shows the horseshoe vortex as a system of alternating-rotation vortices (as many as seven have been seen in laboratory work), only a single vortex seems to have been observed in field studies. Since the separation point on the ground upwind of the building and the reattachment location

on the exposed building face are determined by aerodynamic force balances rather than by geometry, their locations and the frontal eddy they bound will fluctuate with perturbations of the overall flow field. Such perturbations can be introduced by ambient turbulence or unsteadiness in the approach flow, and by the feedback of turbulence generated in the obstacle wake. Hence the upwind vortex can be expected to be unsteady. Fluctuations in its strength and location will affect the trailing arms of the horseshoe vortex system, perturbing the wake flow; these can subsequently feed back to the frontal eddy. Prediction of the location and characteristics of this vortex-wake interaction will probably be possible only in a time-averaged sense.

The far wake of a building immersed in the atmospheric boundary layer is quite complex, since the presence of potentially persistent longitudinally-oriented vortices generated by the body can strongly influence the flow far downwind. For example, a trailing counter-rotating vortex pair can transport higher velocity air from above the wake down into the slower-moving central portions of the wake, producing a sort of velocity "overshoot"; i.e., the measured speeds in the wake are higher than would be found at that same location if the obstacle were not present. This is likely to be important if the building is at an angle to the incident flow, since the upwind edges of the roof then generate a strong vortex pair quite similar to the wingtip vortices of an airplane (e.g., Hansen and Cermak, 1975). Such phenomena may be most significant primarily at distances greater than 10 or 12 building heights H downwind, where ordinary momentum deficit-type wake effects have begun to die away, although vortex effects can be observed at much shorter distances, 3 to 5H downwind, say, particularly when the wind is at an angle to the building or when the flow is stably stratified. In any event, quantitative evaluation of this far wake region has largely been confined to laboratory studies, although theoretical work by Kothari, Peterka, and Meroney (1980a,b) seems very promising. More field data are vital, especially if the possible significance of vortex-type wakes is to be established. Hansen and Cermak (1975) showed that wake vortex meander due to ambient turbulence and general flow unsteadiness results in an apparently weak and rapidly decaying vortex as detected by a fixed sensor, even though the actual vortex may be quite strong and persistent. This means that vortices may be difficult to observe in the field in the wakes of buildings; their presence may have to be inferred from evidence such as velocity overshoot in the wake at large distances downwind (e.g., Colmer, 1970). Furthermore, vortices can probably be expected to rise from ground level and spread from the wake centerline with increasing downwind distance; hence measurements confined to the ground surface and wake centerline may not be very useful.

Additional discussion of the various phenomena associated with flow about obstacles and an extensive listing of the pertinent literature may be found in Hosker (1982).

2.2 Estimates of Frontal Eddy Size and the Zone of Upwind Influence.

Consider a deep boundary layer flow approaching a very wide (i.e., two-dimensional) obstruction such as a fence. The important phenomena

found upwind of the fence are sketched in Figure 4a. The undisturbed incident wind is indicated by the profile U(z); the fence height is H. The displacement zone may extend as much as 5 to 10 H ahead of the obstacle, judging from measurements near dense windbreaks (van Eimern et al., 1964), although some laboratory work has found flow perturbations to only 4 H (Souster and Lee, 1975). The distance probably depends to a great extent on the characteristics of the approach flow and on the ratios of the fence height H to surface roughness z_o and boundary layer depth δ. Strong turbulent mixing would tend to suppress the obstacle's influence until quite close to the fence, while a tall fence would present a more significant obstruction to the flow, and its influence would therefore be felt further upstream. Unsteadiness in the approach flow will also affect this distance. The main flow separates from the ground about 1 or 2 H upwind to pass above the frontal eddy, according to laboratory data (Baines, 1963; Good and Joubert, 1968; Arie et al., 1975). The exact location again seems to depend on parameters such as δ/H, the degree of flow unsteadiness, and probably on the shape of the incident wind profile as well (e.g., Corke and Nagib, 1976). Upwind of the separation line the flow near the ground is directed toward the fence; downwind of the line the surface flow is away from the fence. The separation line is a region of near-zero wind speed; consequently material suspended in the flow, such as snow flakes or dust particles, will tend to deposit on the ground along this line, as pointed out by Baines (1963).

On the face of the two-dimensional wall, the main flow will reattach above the frontal vortex at a height z/H between 0.5 and 0.8, with values near 0.6 being the most commonly cited. Above this line the flow adjacent to the fence is directed upward; below the reattachment line the fence is subjected to the locally downward motion of the eddy. Effluents released with little momentum or buoyancy from flush vents will therefore be carried up over the fence if the vent is above the reattachment line, but will be transported toward the ground, trapped within the frontal vortex, and recirculated there, if the vent location is below the reattachment line.

A semi-empirical theory is available (see Hosker, 1982, for a summary of the relevant literature) to predict the flow patterns and pressure distributions upwind of simple two-dimensional walls. The method is not entirely predictive, since information is required on the location and value of the peak pressure on the exposed face, the exact separation location and pressure at the top of the wall, and the length of the wake cavity. Given these data, excellent agreement with experimentally observed flow patterns can be obtained. This may be useful for predicting the path of passive effluents released into the flow upwind of similarly simple obstacles. The report by Bitte and Frost (1976) supplies sufficient detail to apply the theory.

Figure 4b shows the comparable situation for flow approaching a three-dimensional block-like obstacle. The location and extent of the displacement zone again will depend on factors such as δ/H, the degree of curvature of the incident wind profile, and the scale and intensity of the oncoming turbulence. Unsteadiness can also result from the turbulent wake, with the horseshoe vortex serving as a means of communication. The building width

to height ratio W/H also is important. In any event, the displacement zone will cover just a few building heights upwind. For example, Wilson and Netterville (1978) observed perturbations in incident concentrations profiles to occur only 1.3 H in front of a model building. Separation of the incident flow from the ground will occur even closer, although exact predictions are not yet feasible. For a fairly wide building, Frost and Shahabi (1977) observed separation at 0.9 H upwind. As in the two-dimensional case, particle deposition can be expected along this dividing streamline.

Reattachment of the mean flow to the building face also depends on the flow and building variables mentioned earlier. The actual wind profile seems to be particularly important. For power-law profiles such that $U \propto z^n$, Corke and Nagib (1976) observed the dividing point between upward and downward directed flow on the building centerline depended on n: for $n \cong 0.11$ (coresponding to very smooth and flat upwind terrain), reattachment occurred at 0.53 H; for $n \cong 0.23$ (typical of rural areas), reattachment moved upward to 0.72 H; for $n \cong 0.30$ (forested or urban areas), reattachment took place near 0.77 H. Evidently the diameter of the frontal vortex, which contacts the building face below this point, increases with increasing upwind surface roughness. For buildings much taller than they are wide, reattachment can be expected at a height roughly equal to the building width W (Baines, 1963).

2.3 Estimates of Flow Near Building Roof and Sides.

2.3.1 General Characteristics.

The peculiarities of flow near the roof and sides of a building are due primarily to flow separation (and sometimes subsequent reattachment) at different locations on these surfaces. Discussion here will be restricted to simple block-like structures where separation is geometrically induced along the sharp leading edges. The nomenclature used is shown in Figure 5a, where H, W, and L are the building height, crosswind width, and alongwind length, respectively. The alongwind coordinate x is measured from the upwind building face; y and z, the crosswind and vertical coordinates, are measured from the ground-level centerline. The incident turbulent atmospheric boundary layer velocity U(z) is a function only of height; the incident boundary layer depth δ is assumed much greater than H.

Consider a building which is rather thin in the alongwind direction, so that $L/H < 1$. For such a structure, the flow which separates from the windward edges generally will not reattach to the roof or sides (see Hosker, 1979, for a discussion). Figure 5b indicates the resulting flow patterns. The air immediately adjacent to the roof and sides moves forward toward the leading edges, where it separates from the building and travels outward and rearward. On the lee face of the structure the flow is mostly upward near the center, and sideward near the vertical edges. In this case of small L/H, the recirculating cavity contacts the entire roof, side, and rear faces of the building. Air pollutants emitted with little buoyancy or momentum from flush vents anywhere on these surfaces will tend to be retained within and

mixed throughout the cavity, eventually contaminating all of the surfaces "wetted" by the cavity. However, if the pollutants are very buoyant, are ejected at high speed, or are emitted from sufficiently tall stacks, they may partially or completely escape entrainment into the cavity. Methods to estimate this are discussed in Section 3.

Figure 5c illustrates the situation when the building extends far enough in the alongwind direction for flow reattachment to take place on the roof and sides. The reattachment location depends on the local aerodynamic force balance and so varies with position and with fluctuations in the flow field. The resulting unsteady "zone" of reattachment is suggested by the shaded pattern in Figure 5c. The portions of the building between the windward edges and the reattachment zone are exposed to recirculating cavities; the direction of flow adjacent to the surface within these cavities tends toward the upwind face. Pollutants released into these regions will be well mixed within the local cavity but can reach rather high concentrations because of the limited possibility of air exchange. Here again, strong buoyancy, high exit velocity, or the use of stacks can reduce or eliminate entrapment of effluents. Downwind of the fluctuating reattachment zone, the near-surface flow is basically toward the lee edges. Pollutants emitted into this flow will tend to travel off downwind, although some turbulent entrainment into the wake cavity is quite likely. At the edges of the rear face the flow separates again; the resulting turbulent free shear layer curves inward and downward to enter as well as more or less enclose the wake cavity. Effluents emitted from the rear face may initially travel upward near its center or outward near its sides, but will soon become well-mixed and recirculated to any location exposed to the wake cavity.

Figures 6a,b,c,d (based on drawings by Wilson, 1976a,b, and 1979a,b, and by Gandemer, 1976) show the approximate directions of near-surface flow for several building shapes. Zones of fluctuating reattachment are indicated by shading. The reader is cautioned not to be too precise in applying these estimates to specific cases, since seemingly small changes in the basic geometry can significantly modify the flow patterns. For example, Figures 7a,b,c,d (Wilson, 1979a) illustrate the effect on the flow over a squat building of a rather small penthouse placed at different locations.

2.3.2 Roof Phenomena.

In very simple cases, such as those of Figure 6, reasonable estimates of the flow behavior can be made if information is available about the reattachment zones and the roof and side cavities they bound. Wilson (1979a,b) has developed a method for estimating the height and extent of the cavity and high turbulence zones above a roof. Figure 8 illustrates the flow patterns along the centerline of a flat-roofed building on which reattachment occurs. The roof cavity length is L_c, and the cavity has a maximum height H_c a distance x_c from the upwind roof edge. A turbulent shear layer bounds the roof cavity from above; the upper edge of this layer is denoted by Z_{II}. Above the shear layer is the roof wake, whose upper edge is indicated by

Z_{III}. It is important to note that Z_{II} and Z_{III} are not streamlines, so that material may be transported from one region to another both by the mean flow and by turbulent diffusion.

Wilson's (1979a,b) method is as follows: let ζ_b be the smaller of the building face dimensions H and W, and let ξ_b be the larger. The characteristic length scale for the building is then given by

$$R \equiv \zeta_b^{2/3} \, \xi_b^{1/3} \qquad (2\text{-}1)$$

For relatively tall buildings where W/H < 1, we have ζ_b = W and ξ_b = H, which leads to

$$R/H = (W/H)^{2/3} \quad , \text{ if } W/H < 1 \, . \qquad (2\text{-}2a)$$

For squat buildings where W/H >1, ζ_b = H and ξ_b = W, and so

$$R/H = (W/H)^{1/3} \quad , \text{ if } W/H > 1. \qquad (2\text{-}2b)$$

Figure 9 can be used for quick estimates of the scale length R, given H and W/H. Two restrictions must be met: the ratio L/H must be at least unity or larger if roof reattachment is to occur, and the ratio W/H must not be too large (< 10 at most) or reattachment to the roof may be delayed. The roof cavity dimensions can all then be expressed in terms of the scaling parameter R.

For example, the cavity length along the roof centerline is given to within about ± 10% by

$$L_c \cong 0.9 \, R \qquad (2\text{-}3a)$$

A plot of L_c/H as a function of W/H is given for convenience in Figure 10a. Note that L_c must be smaller than L for reattachment to occur, which places a restriction on the building dimensions for wide structures: $L_c/H = 0.9 \, (R/H) = 0.9 \, (W/H)^{1/3} < L/H$, for W/H > 1. Thus for W/H $\geq$ 1.38, L/H must be greater than unity for reattachment to be possible; for W/H = 10, L/H > 1.94. Equation (2-3a) can be rewritten in terms of the alongwind building length L to facilitate estimates of roof cavity length using a scaled side view of any given building. Thus

$$L_c/L \cong 0.9 \, (L/H)^{-1} \, (R/H)$$

or, using the relations for R/H,

$$L_c/L \cong 0.9\ (L/H)^{-1}\ (W/H)^p \qquad (2\text{-}3b)$$

where p = 2/3 for W/H < 1, and p = 1/3 for W/H > 1. This expression is plotted in Figure 10b, where the restriction that L_c/L must be less than unity has been explicitly observed. This sketch can be used to estimate the centerline fraction of the roof length covered by a recirculating cavity when the building geometry ratios W/H and L/H are known.

Within experimental scatter, Wilson found the maximum height of the roof cavity to be

$$H_c \cong 0.22\ R\ , \qquad (2\text{-}4a)$$

which occurs a distance

$$x_c \cong 0.5\ R \qquad (2\text{-}4b)$$

from the upwind roof edge. These expressions are nondimensionalized with respect to building height in Figure 11a. Equation (2-4b) can be rewritten in terms of the building length as well, giving

$$x_c/L \cong 0.5\ (L/H)^{-1}\ (W/H)^p \qquad (2\text{-}4c)$$

where p = 2/3 for W/H < 1, and 1/3 for W/H > 1. This result is shown in Figure 11b for several building geometries.

The roof wake boundary Z_{III}, shown in Figure 8, is fitted fairly well by

$$Z_{III}/R \cong 0.28\ (x/R)^{1/3}\ , \qquad (2\text{-}5a)$$

which can also be written as

$$Z_{III}/H \cong 0.28\ (L/H)^{1/3}\ (R/H)^{2/3}\ (x/L)^{1/3}\ , \qquad (2\text{-}5b)$$

which gives the wake height as a function of distance along the roof. Equations (2-2) have been used with (2-5b) to generate the typical wake boundary curves of Figure 12; the restriction that W/H must be less than 1.38 if L/H = 1 has been observed.

The upper edge of the shear layer bounding the roof cavity, shown by Z_{II} in Figure 8, is approximated by

$$Z_{II} \cong 0.27\ R - 0.1\ x \quad , \qquad (2\text{-}6a)$$

which is just the equation for a straight line connecting the point of maximum cavity height H_c located at $x = x_c$ to a point x_s in the plane of the roof a distance 2.7 R from the upwind edge. In terms of the building geometric variables,

$$x_s/L \cong 2.7\ (L/H)^{-1}\ (W/H)^{p} \qquad (2\text{-}6b)$$

where p takes the values mentioned earlier, and the restriction on L/H and W/H applies to insure roof reattachment. Equation (2-6b) is shown in Figure 13. One can therefore estimate the location of the upper edge of the shear layer on a side view of a simple building by reading the maximum cavity height from Figure 11a and the location of this maximum from Figure 11a or 11b. The point of intersection x_s of the shear layer top with the roof plane can be obtained from Figure 13; a straight line is then drawn connecting the cavity top and the point x_s.

The above discussion applies to conditions along the roof centerline of the building, as noted in Figure 8. As the lateral edges of the roof are approached, the reattachment location moves forward, as shown in Figures 6a, b, d. Unfortunately, an empirical expression for the cavity length close to the roof edges of even a simple building is not yet available. One can only estimate the overall roof reattachment pattern from results such as those in Figure 6, which suggest reattachment along the roof sides occurs somewhere between 0.35 H and 0.5 H from the upwind roof edge. The breadth of the fluctuating reattachment zone appears to be between 10% and 20% of H. These estimates, based only on Wilson's (1979a,b) sketches, must be regarded as highly tentative; more data are sorely needed.

2.3.3. Flow Near the Sides.

The phenomena observed near the side faces of a building normal to the wind are rather similar to those on the roof: separated flow near the upwind edge, with the possibility of reattachment if the building is long enough. However, no quantitative expressions for features such as the reattachment length or the recirculating cavity thickness presently exist. Once again, sketches such as those of Figure 6 provide the only guidance available. The maximum cavity length along the side is perhaps 1.3 to 1.4 R, and the width of the fluctuating reattachment zone near the roof edge is about 30% of the distance from the upwind edge to the roof edge reattachment point. In at least some cases (see Figure 6d), the side reattachment zone width can be quite large, indicating significant fluctuations in the extent of the side wall recirculating cavity.

Some of the curvature and breadth of the side wall reattachment zone may be due to the influence of the horseshoe vortex which wraps about the structure, and is itself a highly variable phenomenon. The path of this vortex relative to the building sides is of considerable practical interest, since strong winds and intense turbulence accompany the vortex. However, information on the behavior of the horseshoe vortex even close to the building is rather sparse. Ogawa (1973) and Frost and Shahabi (1977) performed a limited amount of flow visualization work during their field experiments; their results only verified the presence of organized vorticity near the edges of obstacles, but did not provide data on its path, velocity, or persistence. Colmer's (1970) field measurements were also suggestive of such vortex structure in the wake. There was some indication in Colmer's (1970) work that the wake effectively rose off the ground as it moved downwind. Similar behavior has been reported in wind tunnel tests (Lemberg, 1973; Hansen and Cermak, 1975). Penwarden and Wise (1975) studied the line of maximum wind speed (y_{MS}) due to the horseshoe vortex wrapping around a rather thin (small L) model building; relative to the wake centerline, their data agree fairly well with the relation

$$y_{MS}/W \cong 0.5 + c(x/W)^{1/2} \qquad (2\text{-}7)$$

where x is measured from the front face of the building, and $c \cong 0.39$. The "constant" c must actually depend on H and L, especially when L is large and the flow reattaches to the sides, but not enough data are available to determine this dependence. The behavior and persistence of the horseshoe vortex require further study, expecially with regard to its interactions with the atmosphere and the flow patterns along the building sides.

2.4 Estimation of Flow Patterns in the Near Wake.

The wake "cavity" found behind any bluff obstacle experiencing separated flow is a zone of very complex motion, as suggested in Figures 2 and 5b,c, and described in Section 2.1. Quantitative information is generally sparse. For example, little is known about the elevated vortex pair produced by the interaction of the vertically-oriented lee-edge vortices with the mean flow near roof level (Figure 2). Colmer's (1970) field measurements and the smoke releases of Frost and Shahabi (1977) indicate the presence of these vortices, as do wind tunnel experiments (e.g. Counihan, 1971). However, even qualitative descriptions of their behavior and interactions with the mean and cavity flows and with the trailing horseshoe vortex are not yet available. Laboratory flow visualizations (e.g., Castro and Robins, 1977; Hatcher et al., 1978) suggest that, close to ground level, these lee-edge vortices are perhaps 30% of the building width in "diameter" (strictly speaking, their cross-section is probably closer to an ellipse, with the elongation in the direction of the mean wind), and their centers are located about the same distance behind the structure with the outer edges roughly in line with the building sides. The ground-level flow in these vortices is roughly parallel to the incident wind along the outer edges, and toward the lee building face on the innermost edges. Material which enters these vortices will spiral upward from near ground level to travel off downwind within the elevated vortex pair.

Even the three-dimensional extent of the cavity zone is not very well-known. Hosker (1979) examined the along-wind length x_r of the cavity relative to the rear face of the building, and suggested the empirical relation

$$\frac{x_r}{H} = \frac{A \cdot (W/H)}{1 + B \cdot (W/H)} \qquad (2\text{-}8a)$$

For a building where L/H is small, so that the flow does not reattach to the building roof and sides, the factors A and B are weak functions of L/H, where L/H must be greater than about 0.16:

$$A = -2.0 + 3.7\ (L/H)^{1/3} ,$$

$$B = -0.15 + 0.305\ (L/H)^{1/3} . \qquad (2\text{-}8b)$$

If L/H is large enough (typically > 1, for structures of moderate W/H in the atmosphere) for reattachment to occur, A and B are constants:

$$A = 1.75 ,$$

$$B = 0.25 . \qquad (2\text{-}8c)$$

The behavior of these factors is sketched for convenience in Figure 14. Figure 15 shows laboratory and field data on cavity length for cases where the flow was not reattached to the building surfaces; the shaded area was calculated using Equations (2-8a) and (2-8b) with L/H = 0.75 as a reasonable obstacle thickness ratio. Agreement with the data is only fair; the scatter is probably due to the effects of the many different incident flow fields. In most cases, however, Equations (2-8a) and (2-8b) predict the cavity length behind simple block-like obstacles without flow reattachment to within ± 50% (see Hosker, 1982, for additional discussion). Figure 16 shows cavity length data for cases where the flow was observed to reattach to the building surfaces. The comparison to Equations (2-8a,c) is somewhat better here; the predictions are within ± 30% of all the data, and are generally within ± 15% (see Hosker, 1982). Evidently the exact nature of the incident flow field is less important to the physics of wake cavity formation when the building is long enough for the flow to first reattach to the roof and sides.

Notice that the maximum predicted cavity length occurs as W/H becomes large. For the case where reattachment occurs, $(x_r/H) \rightarrow 7$; however, if reattachment does not occur, $(x_r/H)_{max}$ can be much larger (see Figure 15). The important point is that for large buildings, such as those commonly found at nuclear power plants, the wake cavity region of actual flow recirculation can be quite extensive. Consider, for example, a hypothetical but perhaps typical turbine building about 35 m high, 185 m wide, and 75 m long

(nomenclature of Figure 5a). Since $L/H \cong 2.1$, we can expect reattachment to the building roof and sides to occur under most wind conditions. Since $W/H \cong 5.3$, we can use Equations (2-8a,c) or Figure 16 to estimate a cavity recirculation zone length $x_r/H \cong 4$; i.e., the cavity extends about 140 m (roughly 460 ft) downwind of the lee building face. Personnel or buildings anywhere within this rather large distance may be subjected to possibly high concentrations of effluents released with low momentum from the turbine building into the wake cavity.

Quantitative data on other cavity dimensions are sparse. If reattachment to the building roof and sides does not occur, the cavity maximum height can be somewhere between 1.5 H and 2.5 H above ground (see Hosker, 1982, for a summary); roof slope will strongly influence this parameter. Very limited laboratory data suggest that in this non-reattached case the maximum cavity width is approximately $1.1\ W + 1.7\ W \exp(-0.55\ W/H)$; however, this relation needs field validation. If flow reattachment does occur, the situation is much simpler; the maximum cavity height and width are given by the building dimensions H and W, respectively.

2.5 Estimation of Far Wake Behavior.

The turbulent far wake of a very wide obstacle behaves somewhat like a developing boundary layer, as described in Section 2.1 and sketched for a two-dimensional obstacle in Figure 3. Within the "wall" layer which develops downwind of the wake cavity, the mean velocity depends in the usual logarithmic manner on height and local surface roughness, and the turbulence is similarly dependent on the underlying surface characteristics. The flow in the "mixing" layer above this region is "self-preserving" in the sense of many wake and boundary-layer flows (e.g., Schlichting, 1960). Within this mixing layer, the mean velocity "defect" (the difference between the velocities observed at a given location with and without the obstacle in place) and the perturbations to the turbulent shear stresses both die out for this two-dimensional body approximately as $(x/H)^{-1}$. The decay of the mean velocity defect and stress perturbations is more rapid than this in the wall layer close to the ground. The overall wake height increases roughly as $(x/H)^{1/2}$. A more detailed summary of the relevant theoretical and experimental literature can be found in Hosker (1982).

The far wake of a truly three-dimensional obstacle, such as a building, can be considerably more complex because of the presence of potentially persistent longitudinally-oriented vortices, as mentioned in Section 2.1. These are important from the dispersion point of view since elevated pollutant plumes can be swept from above the wake down to near ground level by the action of such trailing vortices. However, these may not be a significant problem in many cases of interest. For example, with a block-like building at right angles to the wind in a well-mixed atmosphere, the horseshoe and lee-edge vortices apparently dissipate rather quickly under the action of strong ambient turbulence. The wake is then essentially a pure "momentum" wake of the type commonly studied in aerodynamics. For such a building wake, the mean velocity defect is found to decay roughly

as $(x/H)^{-p}$, where p is between 1.5 and 1.6, while the mean square turbulence intensity excess (i.e., the increase over what would be observed if the building were absent) dies off as $(x/H)^{-2}$. The crosswind profile of the mean velocity defect is approximately bell-shaped, with the maximum defect occurring along the wake centerline. Generally the wake will be indistinguishable from the background (ambient) turbulence within 10 to 20 H of the building, although this distance probably depends on the building aspect ratio W/H, as well as on the ambient turbulence characteristics. However, when organized vorticity becomes important in the wake, as may occur for rounded obstacles such as hemispheres, or for block buildings at an angle to the wind, or for block buildings normal to the wind in a stable atmosphere, the far wake can be dramatically changed in character and persistence. For example, the vortices may advect the relatively high-momentum air aloft down toward the ground level wake centerline, producing a mean velocity excess, instead of the usual deficit. Mean velocity defects here appear outboard of the vortices, well off the centerline. Similarly, a wake centerline pollutant excess can be generated if the vortices interact with an otherwise elevated effluent plume, and a wake centerline temperature excess can appear if the incident flow is stable. The persistence of these features seems to vary with the characteristics of the obstacle and the ambient flow, at least in laboratory studies. For example, the mean velocity excess behind a hemisphere decays fairly slowly, roughly as $(x/H)^{-0.5}$ (Hansen and Cermak, 1975), while that for a block building in a stable atmosphere drops off as $(x/H)^{-p}$, with p ranging between 0.9 and 2.1, depending on building geometry (Kothari, Peterka, and Meroney, 1980a). It is possible that flow reattachment (or its absence) to the building's roof and sides may influence this result. The mean temperature excess observed for this same case initially increased out to roughly 8 to 15 H, and then decayed very slowly, $x^{-0.2}$ to $x^{-0.7}$, again depending on building shape. The temperature wake for this stable case was thus more persistent than the velocity wake; turbulent velocity fluctuations decayed to the background level between 7.5 to 10 H, but the temperature excess extended to at least 60 H downwind. The laboratory work generally suggests that a detectable wake of some sort may extend 50 to 100 H downwind of an obstacle, depending on ambient turbulence level, atmospheric stability, and building shape. A more detailed summary may be found in Hosker (1982). It may be somewhat difficult to detect wake vortices in the field because of their probable meander in the ambient turbulence, and because the vortices may also rise upward and spread outward from the centerline with increasing downwind distance. As suggested in Section 2.1, their presence will probably have to be inferred from evidence such as mean velocity excesses in the wake far downwind (e.g. Colmer, 1970), and it may be necessary to utilize remote-sensing instruments, towers, or tethersondes to determine such conditions above ground level and off the wake centerline.

3.0 CONCENTRATION CALCULATIONS

3.1 Effluent Source Upwind of a Building

The preceding description of the flow fields generally expected around block-like obstacles provides a basis for at least a qualitative understanding

of the concentration field near a building subjected to an isolated effluent plume. The sketches of Figures 2, 4b, 5b and c, 7, and 8 are particularly relevant here. Some detailed discussion is presented below. In many cases, however, it may be sufficient to observe that the overall effect of a building, as viewed from a distance, is to induce a rapid enlargement and dilution of the incident plume. Near the building, ground-level concentrations will be higher than would be observed in its absence, but further downwind the concentrations will generally be lower.

3.1.1 A Nearby Ground-Level Source

Consider a low-momentum, non-buoyant pollutant released at ground level directly upwind of a simple building. If the source is close enough to the structure for the plume depth to be less than about (2/3) H for a wide building, or less than about W for a tall building, then the portion of the plume striking the building's upwind face will be largely entrained into the frontal vortex, and carried off on either side of the obstacle within the arms of the horseshoe vortex. Not too much of the effluent will be transferred into the wake cavity zone, where the resulting concentration will therefore be rather low; the highest concentrations will probably be found along the outer edges of the wake. Hinds (1969) describes such a situation in field experiments. A rough mass-balance can be written to estimate the average concentration within an arm of the horseshoe vortex as follows: the frontal vortex has a diameter D_v related to the building geometry. Let $\bar{\chi}_v$ and $\bar{U}_v$ be the average concentration and the average axial mass transport speed within one vortex arm, respectively. Entrainment of the total source emission within the frontal vortex means that $Q \cong 2\ \bar{\chi}_v (\pi D_v^2/4)\ \bar{U}_v$, or

$$\bar{\chi}_v \cong \frac{2Q}{\pi\, D_v^2\, \bar{U}_v} \quad .$$

Now consider the ground-level centerline concentration which would appear in the absence of the building,

$$\chi_o = \frac{Q}{\pi \sigma_y \sigma_z U} \quad . \qquad (3\text{-}1)$$

Therefore

$$\frac{\bar{\chi}_v}{\chi_o} \cong 2\, \frac{\sigma_y \sigma_z}{D_v^2}\, \frac{U}{\bar{U}_v} \quad , \qquad (3\text{-}2)$$

where the dispersion coefficients σ_y and σ_z are evaluated at x_B, the location of the building relative to the source, and U is the average wind speed transporting the plume. We can relate σ_z to the plume depth Z_p, say, by $Z_p \cong 2\sqrt{2}\ \sigma_z$.

Also, $U = Z_P^{-1} \int_0^{Z_P} U(z)dz \cong (n+1)^{-1} U_H (Z_P/H)^n$, if U behaves as a simple power law (exponent n) with height. Finally, we estimate the average material transport speed within a vortex arm as some fraction β of the incident wind speed near the building top: $\bar{U}_v \cong \beta U_H$. Then, since $Z_P \leq D_v$ for plume capture by the vortex, we have the approximate upper bound

$$\frac{\bar{\chi}_v}{\chi_o} \leq \frac{1}{4\beta(1+n)} \frac{\sigma_y}{\sigma_z} \left[\frac{Z_P}{H}\right]^n \quad . \tag{3-3a}$$

In a region with an aerodynamic surface roughness $z_o \cong 10$ cm, $n \cong 0.2$ (Davenport, 1965); under neutral atmospheric conditions, $\sigma_z/\sigma_y \cong 0.6$ (Briggs, 1973). The value of Z_P relative to H is not very critical since n is small; assume $Z_P/H = 2/3$. Thus

$$\bar{\chi}_v/\chi_o \lesssim 0.32/\beta \quad . \tag{3-3b}$$

Laboratory data of Cook and Redfearn (1976) and Penwarden and Wise (1975) suggest that $\beta = \bar{U}_v/U_H$ may be of order 0.5 near the building corners, although this needs verification. If this is indeed a reasonable estimate for β, we have

$$\bar{\chi}_v/\chi_o \lesssim 2/3 \quad ; \tag{3-3c}$$

i.e., the average (not peak) concentration in either vortex arm near the building corners should be less than roughly two-thirds of the ground-level centerline concentration that would be produced at the building location if the structure were absent. Experimental data are essential before this result can be characterized as anything more than a crude estimate.

3.1.2 A Distant Ground-Level Source.

If the same low-momentum, non-buoyant material is released farther upwind of the structure, the plume may be deeper than the frontal vortex of the building. In this case, material striking the obstacle above the eddy will be diverted upward or sideward to pass around the building. As indicated in Figures 2 and 5b,c, some of this pollutant will probably enter the wake cavity.

Pollutant that enters the cavity zone from the sides or from above will be fairly thoroughly mixed in that region, so that concentrations over the rear face of the building will be rather uniform. If the building is sufficiently large in the along-wind direction (i.e., large L/H), the flow that has separated from the upwind roof edge may reattach, bringing the effluent closer to roof level and possibly inducing high concentrations there. However, if L/H is small the roof-level flow will not reattach, and

the incident plume will be deflected above the roof level. Concentrations on the roof then will be similar to those found on the rear face. Estimates of the wake cavity concentrations resulting from this mode of pollutant transfer cannot presently be made from basic principles; empirical results must be relied upon (see Section 3.1.3, below).

The effluent incident on the building at heights less than the frontal vortex size will probably be mostly entrained within that vortex and swept around the building corners to travel off downwind, as outlined previously. A crude estimate of the quantity of material captured in the horseshoe vortex system can be obtained by integrating the mass flux due to an unobstructed plume over the projected area of the vortex:

$$\frac{\text{captured mass}}{\text{unit time}} \cong \int_{-W/2}^{W/2} \int_{o}^{D_v} \chi \, U \, dy dz$$

$$\cong Q \, \text{erf}\left[\frac{W}{Y_P}\right] \text{erf}\left[\frac{2\,D_v}{Z_P}\right] ,$$

taking the plume half-width $Y_P \cong 2\sqrt{2}\,\sigma_y(x_B)$ and the plume depth $Z_P \cong 2\sqrt{2}\,\sigma_z(x_B)$.

This reaches the previous result for total capture, Q, when the source is so close to the building that the plume dimensions are much smaller than those of the structure. Again, this entrained material is carried off in the two ground-level trailing vortices, so that

$$\bar{\chi}_v \cong \frac{2Q}{\pi\, D_v^{\,2}\, \bar{U}_v} \, \text{erf}\left[\frac{W}{Y_P}\right] \text{erf}\left[\frac{2D_v}{Z_P}\right] .$$

Using Equation (3-1), we have

$$\frac{\bar{\chi}_v}{\chi_o} \cong 2\,\frac{\sigma_y \sigma_z}{D_v^{\,2}}\,\frac{U}{\bar{U}_v} \, \text{erf}\left[\frac{W}{Y_P}\right] \text{erf}\left[\frac{2D_v}{Z_P}\right] . \qquad (3\text{-}4)$$

This expression is similar to Equation (3-2) for a source close to the body, except for the error functions involving the ratios of building to plume dimensions ($D_v \cong (2/3)\,H$ for $H/W < 1$, and $\cong W$ for $H/W > 1$). If the source to building distance is large, these factors can significantly reduce the average in-vortex concentration, relative to the ground-level centerline value, from its nearby source value whose upper bound was estimated by Equations (3-3).

3.1.3 An Elevated Upwind Source.

Much of the previous discussion regarding vortex entrainment, plume diversion, and wake cavity entry applies as well to material impinging on a building from an isolated elevated source. Quantitative confirmation of our general expectations has been provided by a number of authors. For example, Wilson and Netterville (1978) found the influence of a building of height H on the concentration profiles due to an upwind plume emitted also at height H extended only about 1.3 H upwind of the building face. Just downwind of the structure they observed quite uniform concentrations and an elevated plume maximum about 1.1 H above the ground. Ground-level concentrations were increased locally by factors of two to five over the "no-building" values. As a useful rule of thumb, Wilson and Netterville (1978) suggested that the downwash effect generated by the building might be approximated by assuming that the concentration on all building surfaces is uniform and equal to the average of the concentrations expected at roof and ground levels with no building present. They also remarked that, at least for an incident plume released at the height of the "target" building, the concentration at ground level near the building may conservatively be taken equal to the maximum concentration intercepted by any point on the building surface.

Estimation of the average concentration over the whole building surface, $\bar{\chi}_S$, can be carried out following Wilson and Netterville's suggestion; $\bar{\chi}_S$ is approximated by

$$\bar{\chi}_S \cong 0.5\ (\chi_{GL} + \chi_H) \tag{3-5}$$

where χ_{GL} and χ_H are the concentrations due to an elevated plume expected at ground level and at height H in the absence of the building at a distance x_B from the isolated stack. The Gaussian plume formula is used to evaluate these concentrations (e.g., Gifford, 1968):

$$\chi(x,y,z) = \frac{Q}{2\pi\sigma_y\sigma_z U} \exp\left[\frac{-y^2}{2\sigma_y^2}\right]\left\{\exp\left[\frac{-(z-h_e)^2}{2\sigma_z^2}\right] + \exp\left[\frac{-(z+h_e)^2}{2\sigma_z^2}\right]\right\} \tag{3-6}$$

where the effective emission height h_e, which incorporates the effects of plume momentum and buoyancy, may be calculated using the methods of Section 3.1.4 or 3.2.1. Then

$$\chi(x_B,y,0) \equiv \chi_{GL} = \frac{Q}{\pi\sigma_y\sigma_z U} \exp\left[\frac{-y^2}{2\sigma_y^2}\right] \exp\left[\frac{-h_e^2}{2\sigma_z^2}\right], \tag{3-7}$$

while

$$\chi(x_B,y,H) \equiv \chi_H = 2\,\chi_{GL}\,\exp\left[\frac{-H^2}{2\sigma_z^2}\right]\cosh\left[\frac{Hh_e}{\sigma_z^2}\right] \quad , \qquad (3\text{-}8)$$

Equation (3-5) can be written in either of two ways:

$$\bar{\chi}_S \cong 0.5\,\chi_{GL}(1 + \chi_H/\chi_{GL}) \qquad (3\text{-}9a)$$

or

$$\bar{\chi}_S \cong 0.5\,\chi_H(1 + \chi_{GL}/\chi_H) \qquad (3\text{-}9b)$$

Equation (3-8) supplies the requisite expression for χ_H/χ_{GL} or its inverse. Use of Equation (3-9a) or (3-9b) just amounts to the selection of a suitable normalizing concentration for $\bar{\chi}_S$; for a relatively short stack χ_{GL} is probably appropriate, while χ_H is more suitable for a tall stack.

Equation (3-9a) is plotted in Figure 17 as a function of $H/\sigma_z(x_B)$ for effective emission heights $h_e < H/2$. For these short stacks, if the source is close to the building (small x_B) so that $H/\sigma_z(x_B)$ is greater than about 10, the average concentration over the whole building will be about 50% of the ground-level concentration expected at x_B from the same source if the building were not present. This is at least consistent with the earlier discussion of Section 3.1.1, which treated the capture of a ground-level plume by the frontal vortex, with subsequent transport of the pollutant around the building sides into the far wake, producing relatively little transfer into the wake cavity region. If the source is far upwind of the building on the other hand (large x_B), so that $H/\sigma(x_B)$ is less than about 0.5, effluent released from short stacks will produce an average building surface concentration about 1.5 times greater than the no-building ground-level concentration. Again, this is consistent with the notion of a downward advection of plume material in front of the building, and a rather thorough mixing of effluent from aloft into the wake cavity region; both processes should raise concentrations along the building surfaces.

Equation (3-9b) is plotted in Figure 18 for $h_e/H > 0.5$. For nearby sources, such that $H/\sigma_z(x_B)$ is greater than about 10, $\bar{\chi}_S$ will be about 50% of the value expected at roof height H if the building were absent; for a distant elevated source such that $H/\sigma_z(x_B)$ is smaller than 0.1, $\bar{\chi}_S$ will be about 75% of χ_H. At intermediate distances, $\bar{\chi}_S/\chi_H$ can approach 90% or more as $h_e/H \to 0.5$. Actually the somewhat unusual behavior at large H/σ_z for $h_e/H = 0.5$ in both Figures 17 and 18 is apparently due to mathematical singularities associated with the choice of a Gaussian plume format, and may not be too significant physically. In any case, the curves of Figures

17 and 18 should be regarded as rough approximations in need of validation, particularly since Wilson and Netterville's (1978) suggestions for χ_S seems to be largely based on work at a single distance x_B and a single stack-to-building height ratio ($h_e/H = 1$).

An upper bound on the concentration expected at ground level near the building can be established by following the second suggestion of Wilson and Netterville (1978), namely, that this value should be less than the maximum concentration intercepted by any point on the building surface. This can be estimated as follows. Let χ_{GLB} be the concentration at ground level near the building, which is supposed to be less than the maximum concentration incident on the building face. There are two possible cases. Suppose the effective stack height is smaller than the building height, $h_e < H$. The maximum concentration incident on the building will be the concentration at the center of the plume, χ_{CL}, which occurs at a height $z = h_e < H$. It is assumed that the building does not seriously change this concentration, so that it can be approximated by its no-building value (see Britter, Hunt, and Puttock, 1976, for a discussion justifying this assumption). From Equation (3-6),

$$\chi_{CL} = \frac{Q}{2\pi\sigma_y\sigma_z U} \exp\left[\frac{-y^2}{2\sigma_y^2}\right] \left\{1 + \exp\left[-2\left(\frac{h_e}{\sigma_z}\right)^2\right]\right\} . \qquad (3\text{-}10)$$

We choose the ground-level concentration due to a ground-level source as a convenient normalizing value; call this χ_{GLO}. From Equation (3-7), with $h_e = 0$,

$$\chi_{GLO} = \frac{Q}{\pi\sigma_y\sigma_z U} \exp\left[\frac{-y^2}{2\sigma_z^2}\right] . \qquad (3\text{-}11)$$

Then

$$\chi_{CL} = 0.5\ \chi_{GLO}\left\{1 + \exp\left[-2\left(\frac{h_e}{\sigma_z}\right)^2\right]\right\},$$

and so

$$\frac{\chi_{GLB}}{\chi_{GLO}} < 0.5\left\{1 + \exp\left[-2\left(\frac{h_e}{\sigma_z}\right)^2\right]\right\}. \qquad (3\text{-}12)$$

The right-hand-side of Inequality (3-12) is plotted in Figure 19. When the source is close to the building (small x_B), $h_e/\sigma_z(x_B)$ can be large; when $h_e/\sigma_z(x_B)$ is greater than about 1.5, the ground-level concentration near the building will be less than 50% of the concentration generated at that location by a ground-level release. When the source and building are far

enough apart that $h_e/\sigma_z(x_B)$ is less than about 0.1, the ground-level concentration near the structure may be close to χ_{GLO}.

Suppose on the other hand $h_e > H$. Then the maximum concentration intercepted by the building will be that at the roof top, where $z = H$. In terms of χ_{GLO},

$$\chi_H = 0.5\ \chi_{GLO}\left\{\exp\left[\frac{-H^2}{2\sigma_z^2}\left(1 - \frac{h_e}{H}\right)^2\right] + \exp\left[\frac{-H^2}{2\sigma_z^2}\left(1 + \frac{h_e}{H}\right)^2\right]\right\};$$

and so

$$\frac{\chi_{GLB}}{\chi_{GLO}} < 0.5\left\{\exp\left[\frac{-H^2}{2\sigma_z^2}\left(\frac{h_e}{H} - 1\right)^2\right] + \exp\left[\frac{-H^2}{2\sigma_z^2}\left(\frac{h_e}{H} + 1\right)^2\right]\right\}. \qquad (3\text{-}13)$$

The right hand side of Inequality (3-13) is plotted in Figure 20 for a range of possible h_e/H values. For sources close to the building, such that $H/\sigma_z(x_B)$ is large, the ground-level concentration near the building will be vanishingly small compared to χ_{GLO}. Physically, the material is simply passing over the roof and not being diverted down to the ground; this is increasingly true as h_e/H becomes large. For distant sources, $\chi_{GLB} \rightarrow \chi_{GLO}$, depending on h_e/H. This seems quite reasonable; if the source is far enough upwind, the difference in ground-level concentrations due to elevated and ground-level emissions should become small, and the distance at which this occurs must depend on the height of the release.

3.1.4 Stack Design for Upwind Sources.

Techniques to estimate the required height for an isolated stack so that hazardous or legislated effluent concentration limits are not exceeded on or near downwind buildings have been developed by Lucas (1972) and by Wilson and Netterville (1976).

Lucas' (1972) method requires a preliminary estimate of required source height using an appropriate open-terrain model, such as Equation (3-6). The height, width, and distance from the source of each downwind structure are also needed; a large number of buildings can be accomodated. Little explicit use is made of the known aerodynamic flow fields, although their consequences are reflected in the rules of thumb provided. For example, it is assumed that effluent will not be affected by surrounding structures if the stack is more than 2.5 times higher than all of the neighboring buildings. Also, it is assumed that the turbulent wake of a building can rise to 1.5 times the building width or length, whichever is less, and extends

downwind with gradually decreasing effectiveness to 10 building heights or half-widths, whichever is less. The original paper should be consulted for full details.

Lucas' (1972) recommended procedure is as follows:

(1) Let h_1 be a first approximation to the stack height. Estimate h_1 by using a standard open-terrain plume model (e.g., Equation 3-6) to determine the height required in the absence of neighboring buildings to insure that the maximum predicted ground-level concentration is less than or equal to the safe and/or legal limit for the particular effluent. Standard conservative practice should be followed.

(2) List for the i^{th} downwind building ($i = 1,2,3,...$) its distance from the stack x_i, its height H_i, and its width normal to the wind W_i (if some buildings are smaller in both height and width than a closer building, they may be ignored).

(3) For each building, let ζ_i be the smaller of H_i and W_i, and η_i the smaller of H_i and $W_i/2$. Calculate an effective wake height for each building as $Z_{ei} \equiv H_i + 1.5\ \zeta_i$.

(4) In the set of all buildings for which $x_i/\eta_i \leq 5$, select the largest value of Z_{ei} as Z_{eM}.

(5) Now consider the buildings for which $5 < x_i/\eta_i \leq 10$; ignore those for which $Z_{ei} \leq Z_{eM}$. For the remainder (if any), calculate the adjusted wake height $Z_{ai} \equiv Z_{eM} + (2.0-0.2x_i/\eta_i)(Z_{ci}-Z_{cM})$, and take the maximum value in this set as Z_{aM}.

(6) Compare Z_{eM} and Z_{aM}; call the larger Z_M.

(7) Now consider the heights H_i for those buildings where $x_i \leq 5h_1$, and the reduced heights $J_i \equiv H_i - 0.2\ x_i$ for those buildings where $5h_1 < x_i \leq 20h_1$; the largest of any of these values is taken to be H_M.

(8) Calculate the corrected physical stack height using

$$h_s = H_M + h_1 \left(1 - \frac{H_M}{Z_M}\right) \quad . \qquad (3\text{-}14)$$

Lucas suggested that his technique is appropriate for stacks of 30 m or less, but urged further comparison with experimental data to validate the method.

A somewhat similar scheme has been suggested by Wilson and Netterville (1976). They remarked that the most important effect of downwind buildings on an incident effluent plume is the mixing of the plume downward to produce a fairly uniform concentration between roof level and the ground. Hence for design purposes the concentration at roof level should be maintained below the allowable limits, regardless of the location of effluent receptors such as building air intakes. To insure this, they introduced the concept of "minimum descent height" Z_m of the maximum permissible concentration χ_M. As indicated in Figure 21a, Z_m is the height above the surface of the isopleth of maximum allowable concentration at a particular location x. This parameter is a function of the wind speed, since the lower plume boundary will be high above the ground in very light winds, while stronger winds will bend the plume over more sharply. However, strong winds also improve dilution, reducing concentrations in the plume. Consequently the isopleth of allowable concentration will first approach the ground as the wind speed at stack height U_s increases, will reach a height of closest approach (Z_m) to the surface at some critical speed U_A, say, and will then recede from the ground as U_s continues to increase. The procedure is to calculate Z_m by iteration using an initial guess for the stack height h_s, a standard plume equation (e.g., Equation 3-6) and an appropriate estimate of plume rise if necessary, and plot Z_m as a function of downwind distance (Figure 21b). All stability categories should be considered. On this graph, indicate the locations and heights of downwind structures. If Z_m intersects any existing buildings, or is too low to permit anticipated construction on the site, then the stack height should be increased, and the procedure repeated. Alternately, the method may be used to estimate maximum permissible building heights for new construction downwind of existing stacks.

The actual calculation is tedious:

(1) Take, as a first approximation, h_s equal to the minimum stack height needed in open flat terrain to produce acceptable air quality levels at all downwind surface locations. All possible atmospheric stabilities and wind speeds should be considered in this computation.

(2) Select an atmospheric stability category j, j = 1,2,...,6 ("1" corresponds to the usual "A" stability, "4" to "D", and so on). Choose the appropriate curves or functional forms for the dispersion parameters $\sigma_{yj}(x)$ and $\sigma_{zj}(x)$.

(3) Choose a particular wind speed at stack height U_k, k = 1,2,...

(4) Using a suitable plume rise estimation formula (e.g., Briggs, 1975) and known or estimated effluent and ambient characteristics, calculate the plume rise Δh_k for that wind speed.

(5) Solve the following equation for Z_{jk} at a number of downwind distances x_ℓ, ℓ = 1,2...

$$\exp\left[-\frac{(Z_{jk}-h_s-\Delta h_j)^2}{2\sigma_{zj}^2}\right] + \exp\left[-\frac{(Z_{jk}+h_s+\Delta h_j)^2}{2\sigma_{zj}^2}\right]$$

$$= \frac{2\pi\chi_M U_k \sigma_{yj}\sigma_{zj}}{Q} \quad . \tag{3-15}$$

Notice that for locations beyond the "end of the plume" (x_A in Figure 21a), no real values will be possible for Z_{jk}, while for $x_\ell < x_A$, a pair of values will be obtained at each x_ℓ. The smaller value in each pair represents $Z_{mjk}(x_\ell)$, the minimum descent height for stability category j and wind speed U_k at the location x_ℓ.

(6) Choose a new stack height wind speed U_{k+1}, and repeat steps (4) through (6) until the entire wind speed range expected in selected stability category j has been covered.

(7) Examine, for each x_ℓ, the entire set of values $\{Z_{mjk}\}$; the smallest value is $Z_{mj}(x_\ell)$, the minimum descent height for any wind speed in stability category j at the location x_ℓ.

(8) Choose a new stability category, j + 1, say, and repeat steps (2) through (7) until all possible stability categories have been considered.

(9) Examine, for each x_ℓ, the entire set of values $\{Z_{mj}(x_\ell)\}$; the smallest of these is $Z_m(x_\ell)$, the minimum descent height at location x_ℓ for <u>any</u> wind speed or stability category.

(10) Plot Z_m as a function of downwind distance, together with the locations and heights of present and/or planned buildings (e.g., Figure 20b). If the curve $Z_m(x)$ contacts any of these structures, the selected stack height h_s is too low. Increase the stack height and repeat steps (2) through (10) until satisfactory results are obtained.

The above procedure is obviously best carried out on a computer. Wilson and Netterville (1976) also presented a simpler approximate procedure that tends to overestimate $Z_m(x)$ by 20% or more within five stack heights of the source, but is within 2% of the correct value for $x/h_s \cong 20$ or more. This method, although not conservative, may be useful in cases where the buildings of concern are some distance away from the isolated stack, and may serve as a first approximation to Z_m in any case. The original paper should be consulted for details.

Wilson and Netterville (1976) made several useful comments about their procedure First, and perhaps most important, they remarked on the uncertainties inherent in all air pollution calculations. They recommended that the usual "rural"

dispersion curves be used for σ_y and σ_z, since the extra dilution provided by the larger dispersion parameters characteristic of built-up areas supplies a safety factor. And finally, they noted that in practice the critical atmospheric conditions for air pollution may be either an unstable atmosphere (e.g., looping plumes), or nocturnal plume trapping followed by morning fumigation, whereas the minimum descent height curve is usually closest to the ground under neutrally stable conditions. In other words, the stack designer must consider the full range of possibilities of effluent behavior, and not rely entirely on the technique just outlined.

3.2 Effluent Source Near A Building.

Here again the flow patterns described in Section 2 provide a qualitative understanding of the concentration fields generated by an effluent source close to or on an isolated simple building. Important flow features are the frontal eddy which becomes the horseshoe vortex, the roof and side cavity zones, the regions of flow reattachment, the lee-edge vortices, the wake cavity, and the downwash-inducing curvature of the turbulent shear layer above the wake cavity. The sketches of Figures 2, 3, 5b and c, 6, 7, and 8 are pertinent here.

Consider for example the flows induced by the frontal eddy and horseshoe vortex. Low-momentum, non-buoyant effluent released from surface vents at mid-height or below on the windward face of a building will be carried downward to ground level, and eventually swirled past the building sides. Some of this material will be advected and diffused into the cavity region, but much of it will be transported past the cavity to the far wake (Hinds, 1969; Meroney and Yang, 1970). On the upper one-third or so of the structure, flow will be directed upward and sideward, separating in the case of sharp-edged obstacles from the windward edges of the roof and sides, and carrying passive effluent from face vents on the upper portion of the obstacle out and away from other building surfaces.

If the along-wind length of the obstacle is sufficiently large, the edge-separated flow will reattach to the roof and sides, carrying effluent from vents on the windward face closer to the building, but providing better ventilation at outlets located in these reattached areas (see Figures 6 and 7). Wilson (1976a; 1977a) noticed that side vents close to the ground produced a somewhat higher effluent concentration at a given distance from the source than did more elevated vents, probably because of the lower wind speed closer to the ground. Flow that has reattached to the sides and top eventually separates again from the lee edges of those surfaces. If passive effluents are released within the separated areas of the sides or roof, the subsequent ineffective ventilation and flow recirculation can lead to locally high pollutant concentrations. If the air intake system for the building also happens to be within the separated zone, a potential health/safety hazard is created, since the high concentrations may then be readily circulated throughout the structure. If devices such as heat exchangers are located in these zones of separations and recirculation, they will be prone to self-contamination (plume reingestion) that can seriously degrade their performance and life expectancy.

If the building is at an angle to the wind, the flow will remain attached to the most exposed face, but may or may not separate and reattach on the less exposed windward side. Effluent dispersion will vary accordingly. On the roof, a counter-rotating vortex pair will be generated near the upwind corner; these vortices will transport the (possibly clean) high-momentum air aloft down to roof level. A roof cavity will not occur, and effluents from roof vents will be swept away quickly, keeping rooftop concentrations relatively low. However, these vortices may serve to transport entrained effluent to sensitive locations elsewhere on the building or in the wake.

Behind the structure, the notion of a more or less "closed" recirculating "bubble" bounded by a turbulent shear layer may remain a useful approximation for calculations (Vincent, 1977), although the likelihood of direct advection to and from this highly turbulent region must be recognized --i.e., a "leaky" bubble must be allowed. The cavity seems to be rather nonstationary in both atmospheric (Frost and Shahabi, 1977) and laboratory (Huber et al., 1980) flows, and may even intermittently collapse (Meroney, 1979). Flow adjacent to the lee face of the obstacle will be more or less upward. Material released within the cavity will be rapidly mixed throughout its volume; contamination of any surfaces contacting the flow is therefore quite likely (e.g., Meroney and Yang, 1971; Drivas and Shair, 1974; Huber and Snyder, 1976). In particular, for the case of buildings that are thin in the along-wind direction (small L/H), the separated flow from the windward edges of the top and sides becomes part of the cavity; consequently effluents can be expected to appear on the building's roof and sides as well as on its downwind face. Releases somewhat above ground level within the cavity will be mixed more rapidly throughout the region than emissions close to the ground (Drivas and Shair, 1974).

The curvature of the turbulent shear layer above the cavity induces downwash of the "outer" flow, especially near the bubble closure. Material released above the cavity but subject to this flow can be advected close to the ground, producing higher concentrations than would be expected if the building were absent. This process has important implications for stack height and placement decisions.

3.2.1 Estimation of Effective Stack Height.

Concentration patterns near an obstacle are intimately related to the characteristics of the effluent discharge and its interaction with local flows. Effluents that are released too close to the structure and/or at too low an exhaust speed w_e will generally produce high concentrations near the building. Therefore, successful stack or vent design must take account of building and chimney aerodynamics and effluent buoyancy. Some recent work incorporating such effects is outlined below. The reader is also referred to comprehensive survey reports by Wilson (1976a) and Meroney (1979), and a series of papers by Wilson (1977a,b; 1979a,b) for additional information.

In any stack design methodology, some attention must be directed toward the aerodynamic effect of the stack itself on the plume. Sherlock and Stalker

(1941) described the production in strong wind of vertically-oriented vortices shed by the stack, as well as a longitudinally-oriented counter-rotating vortex pair generated at the stack outlet. These latter vortices serve to transfer emitted material downward into the stack wake, resulting in a lower effective release height for the material, and producing features such as the commonly observed blackening of chimney tops. Scorer (1968) mentioned the use of flat horizontal disks installed at the stack mouth. If the diameter of these plates is roughly equal to three stack diameters, they will prevent effluent from being drawn down into the stack wake cavity, thus preserving the entire useful height of the stack.

Downwash behind the stack is probably best avoided by keeping the efflux momentum significantly higher than that of the ambient flow. Sherlock and Stalker (1941) observed downwash distances of only one stack diameter or so for an efflux to stack-height-wind speed ratio of $w_e/U_s = 1$. For $w_e/U_s = 1.5$, practically no downwash was observed. The latter value has become rather widely used, but should be viewed as a lower bound for design work -- i.e., w_e/U_s should be maintained greater than 1.5 whenever possible to prevent downwash and increase the momentum rise of the effluent plume (e.g., Turner, 1969; ASME, 1973). The effluent density enters the problem as the square root of its ratio to the ambient density, $\sqrt{\rho_e/\rho_a}$ (e.g., Wilson, 1976a,b), and in many cases may have a rather modest effect on the value of w_e/U_s needed to avoid downwash. Of course the density may be important for very hot or cold and high or low molecular weight effluents.

It has been recognized for many years that the best way to avoid plume interference by the aerodynamic flow field around an obstruction is to release the material via a tall stack. The familiar "2 and 1/2 times" rule, stating that the stack outlet should be 2.5 times the height of neighboring flow obstacles above the ground, makes use of the rough approximation that the zone of influence of a hill or structure generally reaches less than 2.5 H from the surface. Hence material emitted above this height is ejected into a more or less unperturbed flow, permitting reasonable travel distances and significant plume dilution before the effluent diffuses to the ground. Three things limit across-the-board use of this rule of thumb: economics, aesthetics, and the fact that it is in many instances needlessly conservative. In particular, concentrations are often low enough at the stack exit that the maximum amount of dilution possible is unnecessary to avoid objectionable levels of contamination, or the actual zone of disturbance above the obstacle may be significantly lower than the rule would suggest. This latter point is commonly realized for tall thin structures (e.g., Snyder and Lawson, 1976). The U.S. Environmental Protection Agency (1980) now recommends a stack height $h_s = H + 1.5\zeta_b$, where ζ_b is the smaller of the building face width or height, as good engineering practice.

Briggs (1973) has outlined a procedure for estimating effective emission height which considers an individual building's geometry and the resulting perturbations of the flow. Corrections for stack downwash and buoyancy effects are also included. The method applies to buildings where the flow does not

reattach to the roof and sides. Model studies by Snyder and Lawson (1976) on neutrally-buoyant non-downwashing stack emissions have verified for a short wide building and a tall thin building that Briggs' alternative to the "2½ times rule" is adequate to avoid building-induced effects on effluent concentration. The procedure is as follows:

(1) Compensate for stack-induced downwash by calculating a corrected release height h': if the stack outlet is not vertical, set $h' = h_s$; if the outlet is vertical,

$$h' = h_s + 2\,[(w_e/U_s) - 1.5]d_i \quad , \tag{3-16}$$

where d_i is the inside diameter of the stack of height h_s*. The ratio h'/h_s has been plotted for convenience in Figure 22 as a function of the exhaust to wind speed ratio w_e/U_s, over a range of possible stack diameter to height ratios d_i/h_s.

(2) Calculate the release height h" corrected for building aerodynamic effects. Let ζ_b be the <u>smaller</u> of the frontal building dimensions H or W. If $h' > H + 1.5\zeta_b$, the plume is above the region of building influence; set $h'' = h'$ and go to step (4). If $h' < H$, set

$$h'' = h' - 1.5\,\zeta_b \quad ; \tag{3-17a}$$

if h' is between H and $H + 1.5\,\zeta_b$, set

$$h'' = 2h' - (H + 1.5\zeta_b) \tag{3-17b}$$

and go to step (3). Equation (3-17a) is based on the idea that when $h' < H$, the effluent will be at least partially entrained within the wake cavity; however, complete capture and recirculation down to ground level is unlikely for tall ($W/H < 1$) buildings unless h' is quite small, as discussed in Step (3). For intermediate values of h' between H and $H + 1.5\,\zeta_b$, the plume is just displaced downward ("downwashed") by the building flow field. For convenience, the results of Step (2) have been plotted in Figure 23 for several building aspect ratios W/H. The figure may be used as follows: determine h'/h_s from Equation (3-16) or Figure 22 using known or estimated stack and efflux characteristics. Multiply the result by the stack to building height ratio to find h'/H. Locate this value on Figure 23; move upward on the graph until the line of appropriate W/H is intersected. Read the corresponding value of h"/H at the left. The lower boundary line below which h"/H is undetermined corresponds to complete plume capture within the wake cavity,

*The factor of 2 preceding the momentum-induced plume rise is a conservative value; factors as large as 3 have sometimes been used (e.g., Briggs, 1975). The value 2 may be especially appropriate close to the source, where the plume may not have reached its final rise height.

and is determined in Step (3). Notice that Equations (3-17a,b) can lead to negative values for h"; this is not really a problem since h" is merely an computational parameter subject to further tests (in Step 3) of its ability to represent the physical situation. This is clear from Figure 23, where the lower boundary line insures that all "allowed" values of h" are positive.

(3) The plume may remain aloft or may be entrained into the wake cavity, essentially becoming a ground level source. If $h'' > 0.5\zeta_b$, the plume remains elevated; go to step (4). On the other hand, if $h'' < 0.5\zeta_b$, the plume is trapped in the cavity and mixed down to ground level. It therefore is treated as a ground source of initial plume cross-sectional area $\cong \zeta_b^2$. A virtual source location may be determined to facilitate plume calculations. Go to step (5).

(4) Compensate for plume buoyancy by calculating the effective height of emission h_e. If the effluent is mostly ($\geq$ 98%) air and its temperature is within 2 or 3°C of the ambient, buoyancy is negligible and $h_e = h''$; go to step (5). Otherwise, determine the relative density difference of the plume using

$$\Delta = \frac{\bar{m}_e}{\bar{m}_a}\frac{T_a}{T_e} - 1 \quad , \tag{3-18}$$

where subscripts "e" and "a" refer to effluent and ambient, respectively, T is temperature in degrees Kelvin, and $\bar{m}$ denotes the molecular weight (28.8 gm/mole for air). The mean molecular weight of the effluent is determined from the mass fraction, f_i, say, of each of the component gases through the relation $\bar{m}_e^{-1} = \sum \bar{m}_i^{-1} f_i$. For many sources, the dominant component will be air, so that $\bar{m}_e \cong \bar{m}_a$. If the effluent contains water (liquid or vapor), evaporation or condensation may affect the buoyancy; see Briggs (1975). If $\Delta > 0$, the plume is denser than air. A comprehensive treatment of the behavior and resultant concentrations of dense plumes may be found in Hoot, Meroney, and Peterka (1973), and in Meroney's (1979) excellent survey chapter. If $\Delta < 0$, the plume is buoyant. Evaluate the buoyancy flux $F_b = -g\dot{V}_e\Delta/\pi$, where $\dot{V}_e$ is the volume of effluent emitted per unit time. Then calculate the buoyant plume rise Δh using standard procedures (e.g., Briggs, 1969, 1975). Set $h_e = h'' + \Delta h$, and go to step (5).

(5) Calculate downwind concentrations using standard plume dispersion formulations (e.g., Equation 3-6); wherever a source height is required, use h_e, the effective height of emission.

As mentioned above, Briggs' (1973) method applies only to buildings which are sufficiently short in the alongwind direction (i.e., small L/H) that reattachment of the edge-separated flow to the building roof and sides does not occur. Often, however, reattachment will take place. In such cases, Wilson's (1979a,b) suggestions may prove useful for avoiding contamination of air intakes or other critical locations by effluent from a stack mounted somewhere along the roof centerline. The approximate size and position of

the roof cavity and the boundary shear layer above it have been described in Section 2.3.2 (Equations 2-1 through 2-6) and Figure 8. If the stack is high enough that the effluent plume's lower edge remains above the shear layer (zone II of Figure 8), contamination of the roof is unlikely; if the plume clears the wake boundary Z_{III} as well, there is no danger of contamination. The required height depends on the rate of plume spread. Wilson suggested that it is generally adequate to draw an indicator line of slope 0.2 in the upwind direction from a point on either the zone II or zone III boundary (depending on the safety margin needed) immediately above the air intake or other critical receptor closest to the lee edge of the roof. The effective stack exit should then lie above this line. This slope corresponds to a standard deviation of wind vertical fluctuation angle σ_ϕ of perhaps 0.1 radians (5.7°), which seems reasonable, although σ_ϕ values greater than 0.3 (17.2°) have been observed over open country under some conditions (Lumley and Panofsky, 1964). Whether this value is appropriate to flow over a roof is therefore uncertain. An indicator line of slope steeper than 0.2 may be advisable for some critical contaminants. In any case, the effluent to wind speed ratio w_e/U_s should be kept above about 1.5 to prevent stack-induced downwash.

Neither of the above techniques deal adequately with the effect of stack placement. The Briggs' (1973) method makes no allowance at all for the effect of different stack locations; it requires only that the stack be on the roof, or anywhere within $\zeta_b/4$ of the building, or within 3 ζ_b directly downwind of the structure. Provided the stack is located somewhere within these bounds, the calculated effective height is the same for all locations. The Wilson (1979a,b) approach can account for roof stack placement provided the stack is somewhere along the roof centerline; additional empirical information on the roof cavity and shear layer reattachment characteristics would be necessary to extend the technique to arbitrary locations on the roof. Nevertheless, stack placement can have an important impact on the effective stack height and resulting concentration patterns because of the very different flow fields encountered by the exiting effluent at various stack locations.

Koga and Way (1979a,b) studied in a wind tunnel the consequences of different stack locations on the roof of a squat simple building (L/H = W/H = 2) for a range of stack to building height and efflux velocity to wind speed ratios. The effect of wind incidence angle was also examined. Figure 24 demonstrates the dissimilar plumes resulting from three stack positions along the building centerline when the wind is normal to the structure, while Figure 25 shows the same situation but with the stacks along the roof side edge. Figure 26 shows the consequences of eliminating the stack or of increasing the efflux to wind speed ratio. Figure 27 displays the plumes from different stack locations when the wind is along the building diagonal, while Figure 28 illustrates the changes induced by eliminating the stack or by increasing the efflux velocity. Koga and Way examined many of the possible combinations of these parameters; their reports should be consulted for details. They found that a combination of stack height and position could strongly affect (average factor of three) the ground-level concentrations behind the building. For example, if the emission takes place at the lee edge center, a flush roof vent produces much higher ground-level concentrations than a stack would generate. On the other hand, a stack at the upwind edge center also induces high concentrations behind the structure, apparently because of the

downwash produced by the curved shear layer over the roof and wake cavity zones. Building orientation relative to the wind is also an important factor; wind along the diagonal produced concentrations a factor of three more than those observed for flow at normal incidence to the building, probably because of downwash induced by the vortices generated at the upwind roof corner.

Koga and Way (1979a,b) also presented a very useful (but limited) guide to the behavior of plumes released from roof-mounted stacks at various locations, depending on the exit velocity to wind speed ratio and the stack to building height ratio. Figure 29 defines their four classes of plume behavior: "E" denotes a plume which is essentially unaffected by the building's flow field and "escapes" from the vicinity. A plume which is somewhat influenced by the near-building flow but is mainly just washed downward a bit is indicated by "W". A plume which is substantially influenced by the building, and may be partially or intermittently captured in the wake cavity, is denoted by "D-W". Some plumes are completely downwashed and entrained into the wake cavity, and these are designated "D". Using these categories of plume behavior, Koga and Way developed transition lines separating the different plume behavioral regimes as functions of efflux to wind speed ratio and stack to building height ratio, for several stack positions and two building orientations. Figure 30 shows the various modes of plume behavior for stacks or vents on the roof of a squat building (W/H = L/H = 2) placed normal to the wind. Consider the roof center position, Figure 30a. All four modes of plume behavior were observed for this case; a flush vent (h_s/H =1) and low efflux velocity can lead to a fully downwashed plume (category "D"), while taller stacks, with h_s/H between 2.0 and 3.5, can lead to either mild wake-induced downwash ("W") or no building influence at all ("E"), depending on w_e/U_∞. If the stack was at the center of the upwind roof edge, a fully downwashed mode "D" was not observed; stacks at the center of the lee edge produced only categories "W" or "E", as did stacks at the center of the side edge. Figure 31 shows the results of similar experiments for wind along the building diagonal; the main features of interest here are that complete downwash and wake cavity entrapment (mode "D") were possible for all the stack positions tested, and that a complete escape from building influence (mode "E") was not possible for a stack on the upwind corner (position 8), regardless of stack height or efflux speed. The efflux to freestream wind speed ratio which appears in these figures can be converted to the more usual ratio based on stack-height windspeed, $w_e/U_s \equiv w_e/U(z = h_s)$ using a rough power law approximation to Koga and Way's wind tunnel flow: $U_s/U_\infty \cong 0.76\ (h_s/H)^{0.17}$.

Koga and Way offer a few conclusions: they recommend the center of the roof as the best general site for a stack if the ambient wind direction is unknown or highly variable; this agrees with the findings of Wilson (1979b). If the stack must be placed near a building edge because of engineering or architectural constraints, it should be at least 1.5 times the building height at the leeward edge. If the leeward edge is not readily apparent, a stack of 2 to 2.5 H should be adequate for any rooftop location. Finally, they suggest that the Briggs' (1973) method of compensation for stack-induced downwash (Equation 3-16) works fairly well at low flow rates ($w_e/U_\infty \leq 1$), but increasingly underestimates the effective stack height as the flow rate increases ($1.5 \leq w_e/U_\infty \leq 2$). From

the viewpoint of air contamination estimates, this is favorable; i.e., Equation (3-16) becomes increasingly conservative as the ratio w_e/U_∞ becomes larger.

The reader is cautioned to remember, however, that the work of Koga and Way (1979a,b) was confined to a wind tunnel study of a single building shape; changes in obstacle geometry will probably result in substantial modifications of Figures 30 and 31. In particular, one should not generalize the results from this simple case where L/H = W/H = 2 to an arbitrary block-like structure; only the general trends are likely to be similar. Li, Meroney, and Peterka (1981) have recently reported tests on a simple cube. It would be very helpful for design purposes if such work were extended to a much wider range of building geometries and types of incident flow field.

3.2.2 Concentrations on Building Roof and Sides

At this time it is not possible to calculate in any general way the concentration patterns generated on the roof and sides of an arbitrary stack or vent located on or very close to the structure. Instead, one must largely rely on empirical data, mostly from wind tunnel experiments. Only certain combinations of building shapes and stack characteristics have been explored, and our ability to generalize these is severely restricted. However, it does seem possible to at least place upper bounds on the anticipated concentrations at a point some given distance from the source, and to examine in a limited way the changes in concentrations expected as a consequence of changes in important parameters such as effective stack height.

For this discussion it is convenient to introduce the nondimensional concentration coefficient (e.g., Halitsky, 1961):

$$K \equiv \chi U A/Q \quad , \tag{3-19}$$

where χ is concentration, Q is source strength, A is a characteristic area (often A_p, the projected frontal area) of the obstacle under study, and U is wind speed at the effective release height. Note that K can take any non-negative value.

Another useful quantity is the dilution D, given by the ratio of the concentration at the effluent exit point to the concentration at any arbitrary location:

$$D \equiv \chi_e/\chi = K_e/K \quad , \tag{3-20}$$

where the subscript e denotes exit conditions. In any practical situation, $D \geq 1$; in fact, D will often assume very large values.

Halitsky (1963a,b) published an extensive study of concentrations on building side and roof surfaces for a variety of flush vent locations and exhaust conditions. Figures 32a,b,c show the effects of changes in the effluent velocity ratio w_e/U_H, where U_H is the wind speed at roof (vent) height. The highest roof concentrations naturally were obtained with the lowest tested value of w_e/U_H, 0.5; a doubling of this value reduced the maximum values by a factor of two or three, depending on receptor location. A further doubling of w_e/U_H, however, only reduced the concentration by a factor of 1.5 or less, with the main effect being felt close to the exhaust. Comparison of Figures 32a and 32d shows the rather dramatic changes, especially above roof level, induced by installation of a relatively small stack. The modification reduced peak concentration by a factor of almost five, while the values over the whole roof became much more uniform. The reasons for this reduction are discussed in more detail below. Figures 32e,f,g show the effects of different building geometry. Notice that in all but Figure 32g, the rooftop concentration maxima are found upwind of the vent location. This result is due to the strong reverse flow within the roof cavity of these models; the incident flow separated at the windward roof edge and apparently never reattached to the surface. The flow close to the roof was consequently directed toward the upwind building edge, and carried effluent from flush vents toward the front of the roof. The long, tall building of Figure 32g, on the other hand, experienced flow reattachment to the roof somewhere near the vent, greatly reducing the quantity of material transported in the upwind direction.

Halitsky's (1963a,b) experiments were conducted in a uniform, low-turbulence flow not very typical of the atmosphere. His results should therefore be compared with those of Wilson (1976a,b), whose work was accomplished in a simulated atmospheric surface layer. Figures 33 reproduce some of Wilson's (1976a,b) data. Zones of observed flow reattachment are indicated on the building surfaces. Upwind of the reattachment lines the near-surface flow is directed more or less toward the front of the structure, while the flow after reattachment is predominantly parallel to the incident wind direction (see Figures 6). The K values shown in these figures are significantly higher than those cited by Halitsky (1963a,b). Tests by Wilson (1976a; 1977b) suggest that this result is due largely to the much lower efflux velocity ratio used by Wilson ($w_e/U_H \cong 0.3$ to 0.4, compared to 1.0 for most of Halitsky's tests). Figure 33a shows reattachment on the roof of the building, a feature commonly observed in turbulent boundary layer winds, as discussed in earlier sections. However, since reattachment took place considerably behind the vent, effluent was carried forward, generating patterns quite similar to those in Figures 32a,b,c. The rather squat building in Figure 33b, on the other hand, experienced reattachment close to the upwind roof edge; hence the vent was subjected only to a rearward flow. The concentration pattern may be compared to that of Figure 32e where reattached flow did not occur. Rather similar behavior is apparent in Figure 33c; the reattachment line was not given for this structure, but the isopleth pattern suggests it lies ahead of the exhaust location. Figure 32f is the no-reattachment counterpart of this example. Finally, Figure 33d shows reattachment just behind the vent; some material was evidently advected toward the front of the roof, although most was carried toward the lee edge. This case may be compared to Figure 32g which also had flow reattachment somewhere near the vent -- but probably a bit further back, judging by the concentration patterns.

Wilson (1976a,b) also reported tests of a variety of flush roof vent locations. These data are potentially quite useful since exhausts often cannot be installed in the exact center of a building roof. A few examples are shown in Figures 34; the original reports should be consulted for others. Additional building surface concentration data may be found in Li, Meroney, and Peterka (1981).

Halitsky (1963a,b) may have been the first to suggest that, for a flush-vent-type source and a receptor somewhere on the surface of the same building, the dilution $D \equiv K_e/K$ is proportional to the square of the shortest distance between the vent and the measurement site. He gave the relation, plotted in Figure 35,

$$D \cong [\ \tilde{\alpha} + 0.11\ (1 + \tilde{\alpha}/5)(s/\sqrt{A_e})]^2 \qquad (3\text{-}21)$$

where s is the "stretched string" distance between the two points, A_e is the vent exit area, and $\tilde{\alpha}$, a number between 1 and about 20, depends on the specific building/vent/atmospheric configuration. A lower bound on D is obtained by setting $\tilde{\alpha} = 1$. This expression is based, however, on tests conducted in a uniform, low-turbulence flow, with an efflux to wind speed ratio $w_e/U_H = 1$. Later, similar tests on a more complex building resulted in an expression recommended by ASHRAE (1974) which explicitly utilized this speed ratio:

$$D \cong [\ 4.66 + 0.147\ (s/\sqrt{A_e})]^2\ (U_H/w_e). \qquad (3\text{-}22)$$

Wilson's (1976a,b; 1977a) tests in boundary layers, on the other hand, used low values for w_e/U_H, 0.1 to 0.3 (depending on gas density), which might be more typical of vents with rain deflectors or louvers. He suggested a lower bound to the dilution, for buildings normal to the wind, was

$$D_{min} \cong 0.11\ K_e s^2/A_p. \qquad (3\text{-}23)$$

This expression cannot be quite correct since it does not reduce to the limit $D_{min} = 1$ as $s \to 0$; it should be adequate, however, for receptors not very close to the flush roof vent. Equation (3-23) is plotted in Figure 36; given the shortest distance s between the roof vent and some critical receptor, and the building's projected area A_p, one can estimate the lower bound on the dilution at the receptor if the concentration coefficient at the vent exit K_e, can be determined.

For a flush roof vent, where $U_s = U_H$,

$$K_e \equiv \frac{\chi_e U_H A_p}{Q} = \frac{U_H A_p}{\dot{V}_e} \quad , \tag{3-24a}$$

where $\dot{V}_e$ is the volume flow rate of effluent, so that

$$K_e = \frac{U_H A_p}{w_e A_e} \quad . \tag{3-24b}$$

Equation (3-24a) is plotted in Figure 37 over a range of possible values of $A_p/\dot{V}_e$, for likely wind speeds at building roof height U_H. Given the building dimensions and the volume flow rate of the effluent exhaust system, K_e can be estimated at various wind speeds. If the effluent exhaust to wind speed ratio is known, it may be more convenient to use Equation (3-24b) to determine K_e. In either case, Figure 36 may then be used to estimate the lower bound on dilution at the receptor location, D_{min}.

Two alternate forms of Wilson's D_{min} can be written:

$$D_{min} \cong 0.11(w_e/U_H)^{-1}(s^2/A_e), \tag{3-25a}$$

which has the same variables as Halitsky's expression (Equation 3-21), and

$$D_{min} \cong 0.11\ U_H(s^2/\dot{V}_e) \quad . \tag{3-25b}$$

Equation (3-25a) is shown for convenience in Figure 38, while Equation (3-25b) is given in Figure 39. Equations (3-23) and (3-25a,b) are entirely equivalent; selection of a particular form simply hinges on the information available in a particular design or evaluation problem.

The concentration coefficient K at a receptor point somewhere on the building surface must then be less than or equal to K_e/D_{min}, which can now be calculated. Actually, if K_e and D_{min} are of no real interest in themselves, an upper limit on the receptor concentration coefficient can be obtained directly:

$$D \equiv K_e/K \geq D_{min} \ ;$$

use Equation (3-23) to get

$$K \leqq K_{max} \cong 9.1\ A_p/s^2 \ . \qquad (3\text{-}26)$$

K_{max} is shown for convenience in Figure 40; it depends only on the area of the windward building face and the shortest distance between the receptor and the flush roof vent.

The definition of K (Equation 3-19) can be combined with Equation (3-26) to find the upper bound on the concentration to source strength ratio χ/Q for a flush roof vent:

$$\chi/Q \leqq (\chi/Q)_{max} \cong 9.1/(U_H s^2)\ m^{-3} \ , \qquad (3\text{-}27)$$

where U_H and s are given in m/s and m, respectively. Figure 41 shows $(\chi/Q)_{max}$ as a function of source to receptor distance along the building surface, for some likely values of roof-top wind speed U_H.

Comparisons of Equations (3-21) and (3-23 -- or its variants) with data from several experiments indicate (Li, Meroney, and Peterka, 1981; Wilson, 1976a,b, 1977a; Wilson and Britter, 1981; Halitsky, private communication) that Equation (3-21), with $\tilde{\alpha} = 1$, is a very conservative lower bound on dilution. On block-like structures it may be an order of magnitude smaller than actual measurements. In this instance Equation (3-23) provides somewhat less conservatism, providing a lower bound to the data in most situations. However it overpredicts (Halitsky, private communication) dilutions for block-like buildings at an angle to the wind, and for a non-idealized structure (Clinical Center of the National Institute of Health in Bethesda). Equation (3-22) was specifically developed for this latter site. Overall, it appears that Equation (3-23) is probably an adequate lower bound to dilution for most cases, particularly those involving mere nuisance contaminants (e.g., odors). If the effluent is especially troublesome, however, an extra margin of safety may be available using Equation (3-21), with $\tilde{\alpha} = 1$. More data, particularly from field tests, would be helpful in validating this guideline. If the building is at an angle to the wind, Li, Meroney, and Peterka (1981) recommend that the minimum dilution estimated from Equation (3-23) be decreased to account for building orientation; they suggest multiplying the right-hand side of the equation by $(1+4\alpha/\pi)^{-1}$, where α is the wind approach angle (in radians) relative to the normal of the building face. Consult their report for further details.

If the vent is somewhere on the sides of the building, rather than the roof, Wilson (1977a) found that Equation (3-23) was still a good lower bound to the dilution, except when the effluent emerged on the front of the structure and subsequently contaminated an air intake close to the ground on the building side. To compensate for this, Wilson suggested that the calculated minimum dilution be further reduced by a factor of five if any potential receptors were located at or below H/5 above the ground; i.e., if the receptor height $z \leqq H/5$, set $D_{min} = D_{min}(\text{Eq.31})/5$.

For more exact work, on-building concentration coefficients K can be found in the literature (e.g., Halitsky, 1963a,b, 1968; Smith, 1975, 1978; Wilson, 1976a,b; and many others). The results are often but not always for very specific building configurations, such as a particular nuclear reactor. Nevertheless, a great deal of general guidance can be obtained from a careful study of these results and their variation with important parameters such as w_e/U_s and h_s/H. The experimental conditions must be cautiously examined however, particularly for laboratory work, to assess the degree of validity of the data. For example, many early wind tunnel studies were conducted in uniform speed, low turbulence flows not very typical of the atmosphere; consequently important phenomena such as flow reattachment to the building roof or sides did not occur, and the resulting concentration patterns were probably considerably in error. A compendium of these data, together with a discussion of their general applicability and accuracy, would be most helpful.

In the meantime, one can only say that quite large K values can be expected on building surfaces very close to an effluent source of negligible momentum, buoyancy, and height. For example, Wilson (1976a,b; see Figures 33 and 34) observed isopleths of K as large as 500 close to roof-mounted vents with low efflux to wind speed ratio, although maximum K values closer to 100 were common, and maxima as low as 50 were found, depending on the building geometry and the vent position. On the other surfaces of the building, well away from the roof vent, the maximum K value is generally about 5, although values greater than 10 can occur if the effluent plume is deflected toward the surface -- as may happen on the lee building face, for example. If the material is ejected with significant momentum or buoyancy, or is emitted from a stack, the concentrations on the surface nearest the source (e.g., the roof) can be considerably decreased (perhaps a factor of ten) from the flush vent values, while the concentration reductions on the other surfaces will be noticeable but less dramatic (factor of two, say).

Suppose that the concentration patterns on a particular building are known for some given stack height, efflux to wind speed ratio, and buoyancy. The sensitivity of these patterns to variations in the parameters which determine the effective stack height is then of considerable interest, particularly with regard to the cost-effectiveness of engineering modifications such as increases in stack height or effluent exhaust speed. Smith (1975, 1978) conducted detailed field experiments on a small building fitted with a variable-height stack at the roof center; he determined concentrations on the roof, sides, and within 5 H downwind for a variety of source and atmospheric conditions. The most prominent feature of his results is the strong dependence of roof concentrations on the ratio h_s/H. For example, a 10% increase in h_s/H caused a 67% decrease in roof concentration, as well as a 25% reduction in concentration on the lee face. Smith also remarked on the varying sensitivity of the results to changes in other parameters. The most significant variables, after h_s/H, are, in order of importance, the efflux velocity ratio w_e/U_s, the angle of wind incidence α, the turbulence intensity σ_u/U_s, and the atmospheric stability as categorized by, say, the Richardson number. Smith observed roof concentrations nearly

an order of magnitude lower than the lee face concentration for all stack heights except flush vents. This suggests that roof-mounted air intakes will generally be better than side-mounted inlets if the stack height and/or efflux velocity are large enough to keep the emissions from direct contact with the roof.

Wilson (1976a, 1977b) has prepared a simple argument to demonstrate the sensitivity of roof concentrations to vent height. Effluent is emitted with negligible momentum and buoyancy from a short stack of height $\tilde{h}$ relative to the roof (i.e., $h_s = \tilde{h} + H$). Reattachment of the flow is assumed to occur upwind of the vent, so that the wind seen by the effluent is directed toward the lee edge of the roof. A coordinate system is selected such that $\tilde{x} = 0 = \tilde{y} = \tilde{z}$ at the stack base. The effluent centerline concentration on the roof is then estimated from a standard plume equation; e.g. $\chi \cong Q\,(\pi\sigma_y\sigma_z U_s)^{-1}\exp(-\tilde{h}^2/2\sigma_z^2)$, so that the nondimensional concentration coefficient is given by $K \equiv \chi U_s A_p/Q \cong A_p(\pi\,\sigma_y\,\sigma_z)^{-1}\exp(-\tilde{h}^2/2\sigma_z^2)$. For a flush vent, $\tilde{h} = 0$ and $U_s = U_H$, so $K_r \cong A_p(\pi\,\sigma_{yr}\sigma_{zr})^{-1}$, where the subscript "r" here indicates spreading appropriate to a roof-level release, and A_p is the projected frontal area of the building. After some algebra, we see that the concentration coefficient relative to that for a flush roof vent is given by

$$K/K_r \cong \exp(-b'\,\tilde{h}^2/2\sigma_z^2)\ , \qquad (3\text{-}28)$$

where b' depends on the receptor location and the character of the turbulent dispersion over the building. Equation (3-28) can be used to evaluate the relative effectiveness of two stack heights, $\tilde{h}_1$, and $\tilde{h}_2$, by forming the ratio of the concentration coefficients for each of the stack heights:

$$K_2/K_1 \cong (K_1/K_r)^{(\tilde{h}_2/\tilde{h}_1)^2-1} \qquad (3\text{-}29a)$$

or, in terms of the dilution $D \equiv K_e/K$,

$$D_2/D_1 \cong (D_1/D_r)^{(\tilde{h}_2/\tilde{h}_1)^2-1}\ . \qquad (3\text{-}29b)$$

K_e, the effluent exit concentration coefficient, is defined by Equation (3-24a or b). Given the concentration coefficient K_1 or the dilution D_1 produced by a stack of relative height $\tilde{h}_1$, compared to K_r or D_r for a flush roof vent, the concentration coefficient K_2 or dilution D_2 produced by a stack of

relative height $\tilde{h}_2$ can be calculated. The behavior of Equations (3-29a,b) is demonstrated in Figures 42a,b. Consider for example a short stack of relative height $\tilde{h}_1$, which produces a dilution D_1 of, say, 800 compared to a dilution D_r of, say, 100 produced by a flush roof vent. If the stack height is increased by, say, 50% to $\tilde{h}_2 = 1.5\tilde{h}_1$, the $D_2/D_1 \cong 13.4$, or $D_2 \cong 10{,}800$. However, if $\tilde{h}_1$ only produces a dilution D_1 of, say, 200 compared to the flush vent value $D_r = 100$, then the same percentage increase in stack height only gives $D_2/D_1 \cong 2.4$, or $D_2 \cong 476$. In other words, a modest increase in stack height produces really significant decreases in roof-level concentration only if the stack being improved upon was already high enough to cause much more dilution than a flush vent. Major increases in stack height are necessary to achieve significant improvements in K_2 or D_2 if K_1/K_r is not $<< 1$, or if D_1/D_r is not $>> 1$. If values of K_1/K_r or D_1/D_r can be obtained from field or laboratory data for a particular building and relative stack height $\tilde{h}_1$, then the consequences of changes in relative stack height can be explored using Equations (3-29a,b) or Figures 42a,b. A compilation of K_1/K_r and D_1/D_r ratios would be very helpful.

Wilson (1979a) has recently improved the argument leading to Equation (3-28) to incorporate any plume rise Δh due to effluent momentum and/or buoyancy. If the resulting effective relative stack height $\tilde{h} + \Delta h$ is not too large, so that the plume spreading rates and plume rise at the stack are not very different than those for a flush roof vent, then

$$K/K_r \cong \exp[-(\tilde{h}^2 + 2\tilde{h}\,\Delta h)/2\sigma_z^2] \; . \qquad (3\text{-}30)$$

The vertical dispersion parameter σ_z can be approximated as a power law in terms of downwind distance of the roof-level receptor from the stack base, $\sigma_z = a\tilde{x}^q$, where a depends on the properties of the turbulence and q is typically between 0.5 and 1.0. The characteristic building scale R, defined by Equation (2-1), can be used to nondimensionalize all lengths. Equation (3-30) then becomes

$$K/K_r \cong \exp[-b(\tilde{h}^2 + 2\,\tilde{h}\,\Delta h)/R^{2-2q}\tilde{x}^{2q}] \qquad (3\text{-}31a)$$

Wilson (1979a) found $q \cong 0.75$ and $b \cong 11$ for his wind tunnel concentration data; i.e.,

$$K/K_r \cong \exp[-11(\tilde{h}^2 + 2\tilde{h}\,\Delta h)/R^{0.5}\tilde{x}^{1.5}]. \qquad (3\text{-}31b)$$

This result was found to agree well with data when the stack and receptor point were both well downwind (about $2L_c$ or more from the upwind roof edge, L_c given by Equations 2-3a,b and Figure 10) of the roof cavity and reattachment zone (see Figure 8). Agreement was also improved when the stack and receptor were not close to any of the building edges. Neither of these limitations are surprising in view of the assumption of essentially unperturbed plume spread underlying Equations (3-28) and (3-31). Equation (3-31b) for K/K_r has been plotted in Figure 43 as a function of $\tilde{h}^2/R^{0.5}\tilde{x}^{1.5}$ for a range of possible momentum or buoyancy-induced plume rises, $\Delta h/\tilde{h}$. Given the stack height relative to the roof, $\tilde{h}$, and the building dimensions, the rooftop concentration coefficient K (relative to that produced by a flush roof vent, K_r) can be estimated from Figure 43 for various stack-to-receptor distances $\tilde{x}$, and different values of plume rise Δh. Once K/K_r has been evaluated for one stack height, the consequences of increasing $\tilde{h}$ can be explored using Figure 42a. Equation (3-26) or Figure 40 can then be used to place an upper bound on K_r (and hence on K_1 or K_2) if K_r isopleths are not available for the particular building shape under study. If a very conservative upper limit on K_r is needed, as may be the case for certain dangerous or noxious materials, Halitsky's (1963a,b) value given in Equation (3-21) may be used, taking $\tilde{\alpha} = 1$, to determine a new $K_{r\ max}$ in place of Equation (3-26). It should be noted that if the stack is located close to the building edges, or within the roof cavity (ahead of the roof reattachment zone), or near regions of vortex generation, the above analysis will not be valid. In such cases, empirically obtained values for K are the only recourse; special field or laboratory tests of that particular building-stack-atmosphere configuration may be necessary.

3.2.3 Concentrations in the Wake Cavity

As pointed out by Barry (1964) and more recently by Meroney (1979), most of the expressions proposed for concentration estimates within the cavity proper take the form

$$\chi \cong \frac{Q}{c\ U\ A_p} \quad , \tag{3-32a}$$

or equivalently,

$$K \cong \frac{1}{c} \quad , \tag{3-32b}$$

where the coefficient c is given values between 0.5 and 5.0. The effluent is presumed to be entirely captured in the wake. Evidently $K \cong$ constant, with values between 0.2 and 2.0. A glance at Figures 32, 33, and 34, where the concentrations on the lee face should be fairly representative of the cavity as a whole, indicates that these are indeed reasonable values. Little understanding of the physical mechanisms that generate this result is conveyed, however, and, in particular, there is nothing to suggest why the result might vary from one building to another. Actually, wake cavity concentrations are probably not really constant (e.g., Koga

and Way, 1979b; Li, Meroney, and Peterka, 1981; Wilson, 1977a); the mixing process is not rapid enough to overcome the nonuniformities resulting from advection of pollutant into and from the cavity region. This is particularly likely to be true when intermittent downwash of an elevated plume occurs (Koga and Way's (1979b) case "D-W"; see Figure 29 and Section 3.2.1). Lawson (1967), Johnson et al. (1975), and Thuillier and Mancuso (1980) have all observed this phenomenon in field experiments. Its influence on peak concentrations within the wake cavity region cannot be quantified at this time; however, the average values observed in these cases must implicitly include the downwash contribution. Intermittent downwash is further discussed in Section 3.2.4, below.

Briggs' (1973) recommendation takes at least some account of the effective stack height and building size. He defined the concentration coefficient for the cavity in terms of the smaller of the upwind face building dimensions, ζ_b:

$$K_{BRIGGS} \equiv \chi \, U \, \zeta_b^2 \, / Q. \qquad (3\text{-}33)$$

Consider the momentum and stack downwash-compensated effluent release height h', given by Equation (3-16); the pollutant is emitted above the building roof a distance h' - H. If h' - H is greater than about 0.35 ζ_b, then $K_{BRIGGS} \leq 1$ throughout the wake cavity. Conversely, if h' - H < 0.35 ζ_b, K_{BRIGGS} is typically 1.5, and perhaps as large as 3.0, except close to the effluent source, where K_{BRIGGS} can be quite large (100 or more). Smith (1978) supports Briggs' estimates to within about a factor of two.

A slightly more physical hypothesis is based on Vincent's (1977, 1978) ideas. As detailed in earlier sections, the cavity "bubble" is not, strictly speaking, a closed zone of recirculation with material transfer possible only across the turbulent shear layer bounding the region. Advection into and from the cavity can occur as well (see Figures 2 and 5b,c). Vincent's (1978) experiments suggest, however, that much of the material transfer may be conducted by turbulent exchange across the cavity boundary, with only relatively minor contributions from direct advection. The cavity can therefore be modeled, at least to a first approximation, as a volume V_c bounded by an active surface of area A_c (Figure 44). Material is emitted or entrained into this volume at a rate Q, is mixed more or less thoroughly to an average concentration $\bar{\chi}$ by the circulation within the bubble, and is finally lost from the region because of turbulent transfer through the active surface. The net flux of matter through the boundary is approximated by $\lambda \, w_t \, \partial\bar{\chi}/\partial n$, where λ is a turbulent mixing length, w_t is a turbulent transport velocity, and n is the local normal to the surface A_c. The mass balance equation is

$$\frac{d}{dt} (\bar{\chi} \, V_c) \cong Q - \lambda \, w_t \int_{A_c} \frac{\partial \bar{\chi}}{\partial n} \, dA$$

where $\bar{\chi}$ is the average concentration within the cavity. The integral is approximated by $\bar{\chi}\ A_c/\delta_c$, where δ_c is the thickness of the cavity boundary across which the concentration changes from its internal value ($\bar{\chi}$) to its external value (0). The equation becomes

$$\frac{d\bar{\chi}}{dt} + \frac{\bar{\chi}}{t_d} \cong \frac{Q}{V_c} \qquad (3\text{-}34a)$$

where t_d is a characteristic time for turbulent mass transfer:

$$t_d \equiv \frac{1}{w_t} \frac{\delta_c}{\lambda} \frac{V_c}{A_c} . \qquad (3\text{-}34b)$$

Two cases can be immediately treated. Case (i): constant source. At $t = 0$, $\bar{\chi} = 0$ and Q = constant. Then

$$\bar{\chi} \cong \frac{Qt_d}{V_c} [1 - e^{-t/t_d}] . \qquad (3\text{-}35a)$$

Case (ii): initial puff. At $t = 0$, $\bar{\chi} = \bar{\chi}_o$ and $Q = 0$; then

$$\chi \cong \bar{\chi}_o\ e^{-t/t_d} . \qquad (3\text{-}35b)$$

Note that the latter result provides a convenient means of evaluating t_d by injecting a known amount of material into the cavity, and plotting the logarithm of the resulting concentrations versus time. This procedure was carried out in field measurements by Drivas and Shair (1974). The steady-state limit of Equation (3-35a) is just $\bar{\chi} \cong Q\ t_d/V_c$, so that the average cavity concentration coefficient $\bar{K} \equiv \bar{\chi}\ U\ A_p/Q$ is

$$\bar{K} \cong A_p U\ t_d/V_c . \qquad (3\text{-}36)$$

This expression can be interpreted as the ratio of the volume of clean air intercepted by the building in time t_d to the volume of polluted air in the cavity. A more interesting interpretation is available if the cavity volume is approximated* by $V_c \sim A_p x_r$, where x_r is the cavity length; then

*This may be most appropriate for flow that has reattached to the building roof and sides.

$$\bar{K} \sim \frac{t_d}{x_r/U} \quad . \tag{3-37a}$$

That is, the cavity concentration coefficient is a measure of the characteristic diffusion time t_d relative to the characteristic "flushing" time of the cavity, x_r/U. In terms of the nondimensional time constant $\tau \equiv U\, t_d/H$, the average coefficient is

$$\bar{K} \sim \frac{\tau}{x_r/H} \quad . \tag{3-37b}$$

This result may be more convenient to evaluate in some cases, since τ and x_r/H may be available from experiments (e.g., Vincent, 1977, 1978) or from empirical formulations such as Equation (2-8). For a tall thin building or a short wide structure, the height H may not be the dimension most characteristic of the structure; in such cases $\sqrt{A_p}$ or Wilson's (1979a,b) R should probably be substituted for H in the above expressions. For example, in the field work of Drivas and Shair (1974), W/H = 5.3 and L/H = 1.4, not counting the penthouse on the roof. The velocity U was about 2.5 m/sec, the cavity reached about 3 H (36m) from the lee face of the building, and the characteristic diffusion time $t_d \cong 60$ sec. Direct use of Equation (3-37a) gives $\bar{K} \cong 4.2$, which seems somewhat large, though not unacceptable. If, however, we use $\tau = U t_d / \sqrt{A_p}$ for this rather wide building, $\tau \cong 5.2$ and so $\bar{K} \cong 1.7$, which appears quite reasonable. Before Equations (3-36) and (3-37) can be used routinely, they must be checked experimentally. For example, direct evaluation of $\bar{K}$ using the limited data of Vincent (1978) and Equation (3-37b) gives a concentration coefficient roughly a factor of three larger than those cited by Barry (1964). A suitable adjustment factor may be required to compensate for the approximations implicit in the model and for the liberties taken with the turbulent flux parameterization. Direct measurements of $\bar{K}$, τ, and x_r/H are needed to verify this.

It must be emphasized that this simple model of mass transfer from a building's near wake is somewhat at odds with present understanding of the very complex advective and turbulent exchange processes which feed and drain recirculation zones (e.g., Section 2.1, and Figures 2 and 5b,c). Additional work is needed to elucidate the significance of the advective components in particular. In the meantime, the simple scheme just outlined must be regarded as highly tentative.

Some useful estimates have recently been made of the peak-to-mean concentration ratios that may be expected at building roof or lee face receptors due to effluent emitted with negligible momentum and buoyancy from flush roof vents. Wilson (1967a) assumed the probability density function for concentration to be log-normal (e.g., Csanady, 1973), and suggested that the concentration fluctuations would exceed the local mean value by more than a factor of two only about 10% of the time or less, by a factor of five about 5% of the time or less, and by a factor of ten only 1% of the time or less. Meroney (1979) deduced an empirical expression relating the intensity of the concentration fluctuations to the distance of the particular receptor from the source. Li,

Meroney, and Peterka (1981) conducted additional measurements behind a simple cube, and verified that the log-normal probability distribution was indeed followed fairly closely. They reported somewhat smaller peak values than those of Wilson; their fluctuations exceeded the local mean by a factor of two less than 10% of the time, by a factor of two and a half less than 5% of the time, and by only a factor of three less than 1% of the time. The individual reports should be consulted for details. Further configuration tests would be most useful.

One last comment should be made about locating sources within the cavity: use of a stack roughly equal to the local cavity height can lead to surprisingly high concentration levels. The work of Huber et al. (1976) on stacks behind a long model ridge illustrates this effect fairly well. In particular, they noted that a stack height ratio $h_s/H = 1.5$ produced the highest observed ground level concentrations near the point of cavity closure. Evidently the effluent was caught in the upper portion of the recirculation pattern and carried fairly directly to the ground. This is one situation where a shorter stack may provide lower concentrations than a tall one. Some understanding of the local flow patterns and their likely consequences can be particularly helpful in such cases.

3.2.4 Concentrations Downwind of the Wake Cavity.

Downwind of the cavity zone, the wake concentration is no longer even approximately uniform. A number of techniques to compute the decay of wake concentration with distance have evolved over the years. For example, for plumes emitted near buildings, but not entrained completely in their wakes, the method of Briggs (1973), outlined in Section 3.2.1, above, can be used to estimate an effective stack height for the release. This height is then used in the standard Gaussian plume expression for an elevated source (Equation 3-6). Briggs suggests that if the downwash-corrected stack height h' is less than $H + 1.5\ \zeta_b$, where ζ_b is the smaller of H or W, and the release point is on the roof, or anywhere within roughly $\zeta_b/4$ of the building, then the plume is within the zone of building influence, and should be treated as discussed earlier (see Equations 3-17 and following). In particular, the plume may under some circumstances behave much like a ground level source with finite initial dimensions.

In cases of complete plume entrainment into the wake cavity, the methods generally used are based on simple modifications to the Gaussian plume equation for a ground source:

$$\chi = \frac{Q}{\pi\ \sigma_y\ \sigma_z\ U}$$

along the plume centerline (Equation 3-1). In terms of the concentration coefficient,

$$K = A_p/\pi\ \sigma_y\ \sigma_z \quad . \tag{3-38}$$

For example, one can account for the initial rapid mixing of the effluent into the wake by introducing a virtual source at some location upwind of the actual vent. A binormal distribution of material is assumed, with $\sigma_{yo} \cong W/4.3$ and $\sigma_{zo} \cong H/2.15$ (e.g. Turner, 1969) representing the dispersion parameters at the building. Notice that the Turner method does not distinguish between cases of flow reattachment and no reattachment to the building roof and sides, even though the initial broadening of the wake is determined by this. Strictly speaking, the Turner appraisal of σ_{yo} and σ_{zo} is probably appropriate for the case where flow has reattached. For buildings of small L/H, where reattachment does not occur, the wake cavity dimensions are roughly twice those of the building; therefore $\sigma_{yo} \cong 2W/4.3$ and $\sigma_{zo} \cong 2H/2.15$ should be somewhat better approximations. Next, evaluate the virtual locations x_{yo} and x_{zo} (Figure 45) corresponding to those parameters such that $\sigma_y(x_{yo}) = \sigma_{yo}$ and $\sigma_z(x_{zo}) = \sigma_{zo}$. Equations (3-1) or (3-38) are then used, taking $\sigma_y = \sigma_y(x + x_{yo})$ and $\sigma_z = \sigma_z(x + x_{zo})$, where x is the physical distance between the building lee face and the receptor site. If $x_{yo} \cong x_{zo} \cong x_o$, say, then σ_y and σ_z can be evaluated at the same distance $x + x_o$. In this case, the stability-dependent curves of the product $\sigma_y\sigma_z$ from Turner's (1969) workbook can be used to compute K. Figure 46 shows this simplified solution of Equation (3-38) for the case $A_p = 1000\ m^2$. The solution for any arbitrary building frontal area can be obtained simply by multiplying these results by $A_p/1000$, once the virtual source to receptor distance has been calculated for the building under study.

Meroney (1979), using Robins' (1975) data, found it best to also allow for a virtual effective emission height, h_{eo}, when the near-building source was not at ground level. Equation (3-6) for an elevated source is then used to calculate the concentration downwind of the cavity, taking $h_e = h_{eo}$. Meroney suggested virtual source locations for a few stack or vent to building height ratios which provide upper and lower bounds on the estimated wake concentration; these are reproduced in Table 1. It is assumed in the table that $x_{yo} \cong x_{zo} \cong x_o$. The most negative value of x_o and the largest value of h_{eo} in each case will determine the lower bound on the concentration, while the least negative x_o and smallest h_{eo} will establish the upper bound.

A second method, introduced by Gifford (1960) utilizes the idea (attributed to Fuquay) of the building wake providing an initial plume dilution proportional to the product of wind speed and projected building area. Ground-level concentrations along the plume centerline are then given by

Table 1 Virtual source locations for estimates of maximum and minimum building wake concentrations using Equations (3- Complete entrainment in the wake is assumed.

Source type	Actual emission height h_s/H	Virtual source location x_o/H	Virtual source height h_{eo}/H
Point	0.13	$-5 \leqq x_o/H \leqq +0.5$	0
Point	0.88	$-1 \leqq x_o/H \leqq -0.5$	$0.8 \geqq h_{eo}/H \geqq 0.55$
Line	0.88	$-1 \leqq x_o/H \leqq -0.5$	$0.8 \geqq h_{eo}/H \geqq 0.55$
Flush roof vent	1.0	0	$0.8 \geqq h_{eo}/H \geqq 0.55$

Based on Meroney (1979).

$$\chi = \frac{Q}{(\pi \sigma_y \sigma_z + c A_p)U} \quad . \tag{3-39a}$$

In terms of the concentration coefficient, this is

$$K^{-1} = (\pi \sigma_y \sigma_z / A_p) + c \quad . \tag{3-39b}$$

The constant c was estimated on intuitive grounds (e.g., Gifford, 1975) to be between 1/2 and 2, with the smaller value being the more conservative, as well as providing fairly good agreement with assorted test results (see Gifford, 1975, 1976). Here again no distinction is made between instances of reattached and nonreattached flow, although the initial plume dilution must depend on this. One would expect the smaller values of c, say $c = 1/2$ to 1, to correspond to obstacles long enough for roof and side reattachment to occur; larger c values (2, or possibly as large as 4) should be more appropriate for structures of small L/H where reattachment does not take place. Regardless of the value selected for c, the dispersion parameters can be obtained from the usual "Pasquill-Gifford" curves (e.g., Gifford, 1968, or Turner, 1969) as functions of the distance x between the building lee face and some receptor site on the wake centerline. Figure 47 shows the quantity $\pi\sigma_y\sigma_z/A_p$ calculated from Turner's (1969) curves, with $A_p = 1000\ m^2$. Values for any other building frontal area can be computed by multiplying by $1000/A_p$. To the value thus obtained, add an appropriate value for c; K is the reciprocal of this sum. It is clear from the figure that the initial wake broadening introduced through the quantity c is significant in the calculation of K only for x less than a few hundred meters, depending on A_p and the atmospheric stability condition prevailing.

Huber and Snyder (1976) and Huber et al. (1980) reported that Equation (3-39) performed fairly well for wind tunnel tests of simple buildings if the source was at ground level, using c = 1. Hatcher et al. (1978) found similar results downwind of a model of the EOCR site. However, Start et al. (1977, 1980) observed that this simple model did not correlate well with concentrations behind the Rancho Seco and EOCR reactor complexes, at least with c = 1/2. Allwine, Meroney, and Peterka (1980) found similarly poor performance in their wind tunnel tests of the Rancho Seco site, again with c = 1/2. Equation (3-39) does not reflect any of the complexity of the flow patterns expected at these reactor sites, so its inadequacy under these conditions is understandable. Hatcher, Smith, and Schulman (1979) remark that field studies by Martin (1965) and Smith (1975, 1978) suggest that c = 1/2 is appropriate for the near wake behind relatively simple buildings.

Murphy and Campe (1974) modified this method to allow c to depend on the distance s between the building and the receptor location:

$$c = [2 + 3\ (D_b/s)^{1.4}]^{-1} \quad . \qquad (3\text{-}40)$$

This expression was deduced from early wind tunnel data (Halitsky et al., 1963) on a model of the EBR-II rounded containment building of diameter D_b. Equation (3-40) gives $c \to 0$ as s/D_b becomes small, while $c \to 1/2$ for large s/D_b. The U.S. Nuclear Regulatory Commission has used this equation as part of an interim methodology for estimating concentrations near leaking containment buildings, regardless of the actual building geometry. However, as Halitsky (1968) points out, one can raise serious questions as to whether the modeled flow patterns were adequate representations of the real situation; in particular, the separation points on the model yielded a wake which was probably wider and taller than that of the prototype. Furthermore, extrapolation of wake data from a rounded structure to a block-like one is generally improper because of the very different flow characteristics. Finally, the data on which the Murphy-Campe relation is based were obtained over the fairly narrow range $0.5 < s/D_b < 3$; use of Equation (3-40) outside these distances represents yet another extrapolation. In short, the combination of Equations (3-39) and (3-40) should probably be restricted to use in the immediate lee of rounded structures, and may not be totally correct even there. Sagendorf et al. (1980) found that Equation (3-39) and (3-40) predicted maximum χ/Q values only within a factor of 10 in field work at the EOCR site, and within a factor of 100 at the Rancho Seco reactor complex. In only one case (out of forty-three) was $(\chi/Q)_{max}$ underpredicted; i.e., the Murphy-Campe approach seems to be nearly always conservative, often by a considerable margin, in field tests involving complex geometries.

A third method for wake concentration calculation introduces "total diffusion" parameters Σ_y and Σ_z (Gifford, 1968, attributed to Davidson):

$$\chi = \frac{Q}{\pi \Sigma_y \Sigma_z U} \quad , \tag{3-41a}$$

where

$$\Sigma_y \equiv \left[\sigma_y^2 + c\, A_p/\pi\right]^{1/2} \quad , \tag{3-41b}$$

$$\Sigma_z \equiv \left[\sigma_z^2 + c\, A_p/\pi\right]^{1/2} \quad .$$

The same values and comments regarding c apply here as in the discussion following Equations (3-39). In terms of K,

$$K = A_p/\pi \Sigma_y \Sigma_z \quad , \tag{3-42}$$

which is quite similar to Equation (3-38).

As mentioned earlier, in many practical cases the effluent plume will be neither completely elevated nor entrapped by the building wake; instead, a fluctuating partial entrainment may occur, in which portions of the plume are intermittently captured by the wake (e.g., Section 3.2.1). Johnson et al. (1975) introduced the so-called "split-h" model to account for the two different effective release heights generated by this intermittency. The model assumes that, in any given hour, a fraction f of the plume will be entrained. The average concentration over an hour is then given by

$$(\chi/Q)_{ave} = f\,(\chi/Q)_{entr} + (1 - f)\,(\chi/Q)_{elev}. \tag{3-43}$$

Johnson et al. calculated the concentration for the entrained portion from Equation (3-42), assuming a Gaussian crosswind distribution, while the elevated concentration was computed from a standard Gaussian formulation (Equation 3-6) with an effective source height estimated from Briggs' (1973) procedure, given above. The entrainment fraction f actually depends on parameters such as w_e/U_s, h_s/H, stack location, building geometry, atmospheric stability and turbulence intensity, and wind speed and direction. For the particular case of the Millstone nuclear reactor with a particular set of (fixed) geometric parameters, Johnson et al. (1975) found the dominant influence was w_e/U_s, and suggested an empirical form for f based on this; their result is very probably not appropriate, however, for other sites. In fact, Thuillier and Mancuso (1980) observed poor agreement with field data at the Duane Arnold Energy Center, using Johnson et al.'s form for f. Koga and Way (1979a,b) have recently shown the strong dependence of partial entrainment on h_s/H and vent location, as well as w_e/U_s, for a simple block structure (see Figures 30 and 31, for example). Experiments such as theirs may eventually produce schemes to estimate f for a particular set of conditions, but this capability is not presently available.

All of these methods have two potential drawbacks, as pointed out by Gifford (1975, 1976). The first, which is not really the fault of the model, is that the dispersion parameters generally used do not provide an adequate representation of the plume meander typically observed under light-wind stable conditions. In these circumstances, use of standard expressions or curves for σ_y and σ_z will probably provide significant overestimates of the concentration. Use of site-specific values for the dispersion parameters would alleviate this unwarranted conservatism. The second shortcoming of the methods is inherent in their assumption that the dispersive characteristics of the atmosphere are unaltered by the presence of the building, which serves only to introduce some initial dilution. Far downwind the building effect is assumed negligible. This may or may not be true since, as described earlier, wakes under some conditions display a pronounced vortex character far downwind. This is particularly apt to occur for buildings at an angle to the wind. These highly persistent vortices typically exhibit rather low swirl velocities, considerable meander, and tend to rise away from the ground with increasing downwind distance. Material entrained within them will not spread in the normal fashion, and may wind up as an elevated plume. Concentrations, especially aloft, may then drop off much more slowly with distance than the simple Gaussian formulation would predict. It is conceivable, then, that the Gaussian predictions will not be conservative under certain circumstances (e.g., buildings at an angle to the wind, or rounded buildings), predicting concentrations lower than those actually available. Kothari, Cermak, and Greenway (1982) have in fact observed such behavior downwind of a power plant model. There is a real need for field programs to attempt the detection of such organized vorticity in the wake of isolated structures and to assess its effect on concentration patterns. If significant vorticity effects are detected downwind of buildings then it will be necessary to utilize more complex models for wake diffusion which account for the effects of vortex flows on the concentration pattern (e.g., Kothari, Peterka, and Meroney, 1980a).

Some attention has been devoted recently to development of "improved" expressions for σ_y and σ_z that better account for the effects of an obstacle on the concentration field. Huber and Snyder (1976) examined concentrations in the wake of a model building for various effluent release heights. They observed that emissions occuring between ground level and roof height were dispersed rapidly in both the vertical and crosswind directions, while releases above roof level experienced only enhanced vertical dispersion, at least for wakes without significant organized vorticity. On the basis of this work, Huber (1977, 1979) recommended forms based on the concept of spread enhancement generated first by the building cavity and secondly by the decaying turbulence excess produced by the building (Huber and Snyder, 1976). For $3 \leqq x/H \leqq 10$, these forms are, for a squat building,

$$\sigma_y' = 0.7(W/2) + 0.067\ (x - 3\ H)$$

$$\sigma_z' = 0.7\ H + 0.067\ (x - 3\ H) \qquad (3\text{-}44a)$$

while for $x/H \geqq 10$, a virtual source model is used:

$$\sigma'_y = \sigma_y(x + x_{yo})$$

$$\sigma'_z = \sigma_z(x + x_{zo}) \quad . \tag{3-44b}$$

Huber uses these in the Gaussian plume model, which along the ground-level centerline is a simpler version of Equation (3-7):

$$\chi = \frac{Q}{\pi\, \sigma'_y\, \sigma'_z\, U} \exp(-h_s^2 / 2\sigma_z'^2) \quad . \tag{3-45}$$

The virtual source locations x_{yo} and x_{zo} are calculated by matching the dispension parameters at 10 building heights downwind: $\sigma'_y(10H) \cong 0.7\ (W/2) + 0.5\ H = \sigma_y(x + x_{yo})$, and $\sigma'_z(10H) \cong 1.2\ H = \sigma_z(x + x_{zo})$, where x is measured from the lee building face. If the unmodified "P-G" parameters are larger than those suggested in Equations (3-44), as usually happens in unstable conditions, for example, then the standard curves are used directly. When the effective stack height is < 1.2 H, wake-induced enhancement of <u>both</u> the lateral and vertical dispersion is presumed (i.e., σ'_y and σ'_z are used). For release heights above 1.2 H, only enhancement of the <u>vertical</u> dispersion is assumed, so σ_y and σ'_z are used. Notice that atmospheric stability effects appear only for $x/H \geq 10$. Kothari (private communication) has pointed out that wakes with trailing vortices may inhibit the dispersion enough for the observed σ_z to be smaller than the above discussion would suggest; see, e.g., Kothari, Cermak, and Greenway (1982).

Figure 48 illustrates Equations (3-44a) over the range $3 \leq x/H \leq 10$; since the relations were determined only for squat obstacles, only aspect ratios $W/H \geq 1$ were used in calculating σ'_y. The maximum appropriate value of W/H is not known, but is probably 10 or less; for wider buildings probably only the height H is significant in the dispersion modification. Similarly, if the relations (3-44a) are extended to tall buildings, one would expect the smaller dimension W to then be the dominant influence, replacing H in the dispersion parmameter estimates. For distances greater than 10 H, the virtual source relations (3-44b) can be used with, say, Turner's (1969) curves of σ_y and σ_z to generate the dispersion parameters for the distant wake. Figure 49 displays σ'_y and σ'_z for three sample cases, to show the effects of a change in H (Figures 49a and b), and a change in W (Figures 49b and c). The overall result of Huber's (1977, 1979) recommendation is an initial enhancement of diffusion with a rather slow transition to the normal curves, especially for neutral to stable atmospheric conditions where the wake influence is more persistent.

The use of "handbook" plots of σ_y and σ_z to determine the virtual source locations x_{yo} and x_{zo} and to then estimate σ'_y and σ'_z is straightforward,

but quite tedious. However, the procedure can be accomplished on a desktop computer or programmable calculator by using best-fit approximations for the σ_y and σ_z curves. For example, the "MPTER" diffusion code (Pierce and Turner, 1980)* approximates Turner's (1969) curves by the following algorithms:

$$\sigma_y(x) = (465.116\ x)\ \tan\ \theta(x), \qquad (3\text{-}46a)$$

$$\theta(x) = (A' - B'\ \ell n\ x)\ /\ 57.2958, \qquad (3\text{-}46b)$$

$$\sigma_z(x) = C'\ x^{D'}\ . \qquad (3\text{-}46c)$$

In Equation (3-46b), the quantities A' and B' depend only on the atmospheric stability category, while the terms C' and D' in (3-46c) depend on distance as well as on stability; $\sigma_z(x)$ is thus approximated in a piecewise fashion. Table 2, deduced from "MPTER"[2] (K. S. Rao, private communication) gives the values and ranges of applicability of A', B', C', and D' to accurately approximate Turner's (1969) curves. In this table and in Equations (3-46), distance x is given in kilometres, while the resulting values of σ_y and σ_z are in metres.

Using Equations (3-46) and Table 2, a computational scheme can be devised to match Huber's (1977, 1979) expressions for σ'_y and σ'_z (Equations 3-44a) to Turner's (1969) curves at x = 10 H, to obtain the virtual source locations x_{yo} and x_{zo}. For example, consider the matching

$$\sigma'_y(10\ H) = (465.116\ \tilde{x})\ \tan\ \theta(\tilde{x}),$$

where $\tilde{x} \equiv 10\ H + x_{yo}$. This can be solved by successive approximations; evaluate

$$\tilde{x}_{i+1} = [\sigma'_y(10\ H)\ /\ 465.116]\ \cot\ \theta(\tilde{x}_i)\ ,$$

where $\theta(\tilde{x}_i) = (A' - B'\ \ell n\ \tilde{x}_i)\ /\ 57.2958$. The computation is repeated until $(\tilde{x}_{i+1} - \tilde{x}_i)/\tilde{x}_i$ is arbitrarily small, say 0.001. The virtual source location crosswind dispersion is then given by $x_{yo} = \tilde{x}_{i+1} - 10\ H$. The virtual source for vertical dispersion is more straightforward:

$$x_{zo} = [\sigma'_z(10\ H)\ /\ C'\ ]^{1/D'} - 10\ H,$$

*The author is indebted to Dr. K. S. Rao, NOAA/ATDL, for this material.

Table 2 Factors required for approximation of the Turner (1969) workbook curves of dispersion parameters σ_y and σ_z, as in Equations (3-46), from "MPTER" (Pierce and Turner, 1980).

Stability class "A".

σ_y (m): A' = 24.167, B' = 2.5334

σ_z (m): x (km)	C'	D'
x < 0.10	122.80	0.9447
0.10 ≦ x < 0.15	158.08	1.0542
0.15 ≦ x < 0.20	170.22	1.0932
0.20 ≦ x < 0.25	179.52	1.1262
0.25 ≦ x < 0.30	217.41	1.2644
0.30 ≦ x < 0.40	258.89	1.4094
0.40 ≦ x < 0.50	346.75	1.7283
0.50 ≦ x < 3.11	453.85	2.1166

For x ≧ 3.11 km, use σ_z = 5000 m.

Stability class "B".

σ_y (m): A' = 18.333, B' = 1.8096

σ_z (m): x (km)	C'	D'
x < 0.2	90.673	0.93198
0.2 ≦ x < 0.4	98.483	0.98332
0.4 ≦ x < 35	109.30	1.09710

For x ≧ 35 km, use σ_z = 5000 m.

Stability class "C".

σ_y (m): A' = 12.50, B' = 1.0857

σ_z (m): x (km)	C'	D'
all x	61.141	0.91465

Table 2 (continued)

Stability class "D".

σ_y (m): $A' = 8.3333$, $B' = 0.72382$

σ_z (m): x (km)	C'	D'
$x < 0.3$	34.459	0.86974
$0.3 \leqq x < 1.0$	32.093	0.81066
$1.0 \leqq x < 3.0$	32.093	0.64403
$3.0 \leqq x < 10$	33.504	0.60486
$10 \leqq x < 30$	36.650	0.56589
$30 \leqq x$	44.053	0.51179

Stability class "E".

σ_y (m): $A' = 6.250$, $B' = 0.54287$

σ_z (m): x (km)	C'	D'
$x < 0.1$	24.260	0.83660
$0.1 \leqq x < 0.3$	23.331	0.81956
$0.3 \leqq x < 1.0$	21.628	0.75660
$1.0 \leqq x < 2.0$	21.628	0.63077
$2.0 \leqq x < 4.0$	22.534	0.57154
$4.0 \leqq x < 10$	24.703	0.50527
$10 \leqq x < 20$	26.970	0.46713
$20 \leqq x < 40$	35.420	0.37615
$40 \leqq x$	47.618	0.29592

Table 2 (continued)

Stability class "F".

σ_y (m): A' = 4.1667, B' = 0.36191

σ_z (m): x (km)	C'	D'
x < 0.2	15.209	0.81558
0.2 ≦ x < 0.7	14.457	0.78407
0.7 ≦ x < 1.0	13.953	0.68465
1.0 ≦ x < 2.0	13.953	0.63227
2.0 ≦ x < 3.0	14.823	0.54503
3.0 ≦ x < 7.0	16.187	0.46490
7.0 ≦ x < 15	17.836	0.41507
15 ≦ x < 30	22.651	0.32681
30 ≦ x < 60	27.074	0.27436
60 ≦ x	34.219	0.21716

Table provided by K. S. Rao, NOAA/ATDL (private communication), based on U.S. EPA's "MPTER" diffusion code.

although one must be careful to choose the proper range of $\tilde{x} \equiv x_{zo} + 10\ H$, so that the correct values of C' and D' are used in the calculation. Both x_{yo} and x_{zo} must be non-negative to be valid virtual source locations.

Figure 50 compares Huber's (1979) estimates of $\chi\ U\ /\ Q$ for the single case of W/H = 2, H = 25 m, using wake-enhanced dispersion parameters, to those calculated using a standard point source Gaussian model. For effective stack heights ≦ H, both horizontal and vertical enhancement were assumed, while for release heights > H, only vertical enhancement was permitted. Notice that wake-induced enhancement produces lower concentrations everywhere only for a ground-level source. For all elevated sources considered, the enhanced dispersion model produced higher maximum ground-level concentrations at locations closer to the stack. The effects diminished with decreasing stability and decreasing stack height.

The agreement with Huber et al.'s (1980) wind tunnel data is fairly good (Figure 51), especially for source heights $h_s \leqq 1.5$ H. Notice that the simple initial dilution model (Equation 3-39) also does quite well for a ground level source, using c = 1. However, Hatcher et al. (1978) found that concentrations close behind a model reactor complex were underpredicted by the Huber method for elevated effluent releases, although ground-level releases were again estimated fairly well. The discrepancy may be at least partially due to the influence of surrounding structures on the wake of the main reactor building, with subsequent modification of the rates of wake

spread and decay. Agreement with field data seems to range from poor to good on a case by case basis (see Huber, 1979, for individual comparisons). Part of the difficulty is that virtually all of the field work has involved clusters of buildings; it is therefore difficult to determine appropriate single building heights and widths for use in the model, and the wake behavior may differ from that of an isolated obstacle. Also, the presence of other buildings between the source and receptor locations in some of these experiments may have diverted material to other regions. Finally, none of the field studies determined the vertical plume height; only ground-level measurements of the horizontal spread were made. It is impossible to say at this time, therefore, whether or not the model assumptions (i.e., enhancement in both parameters for low sources, but for the vertical parameter only for higher sources) are verified in the field. As remarked before, field studies which determine both horizontal and vertical dispersion characteristics are urgently needed.

Concentration measurements behind simple isolated buildings in the field are rather rare, and seem to have been restricted largely to the near-wake region (e.g., Smith, 1975, 1978). The work of Hinds (1969) appears to have been conducted to greater distances downwind than any other, and even it reached only to about 5 $\sqrt{A_p}$. Since the tracer material in his tests was released on the windward side of the building, the near-wake region was not very well mixed (as shown by his isopleth patterns), and the resulting rapid change of concentration with distance is probably not at all typical of that behind a building with a cavity-entrained plume.

Meroney and Yang (1970, 1971) examined the concentrations behind a cubical model to 30 or more building heights downwind. For ground level releases, their concentration coefficient K decreased roughly as x to the -0.6 to -0.7 power. This decrease represents a much slower decay rate than would be estimated from the open terrain Gaussian model, which would predict powers of -1.3 to -1.6, depending on stability. Examination of Huber et al.'s (1980) data in Figure 51 indicates that between, say, 10 H and 30 H downstream of a ground-level source near a building, a line through the data points will behave roughly as $x^{-0.8}$. Beyond 30 H, however, the wake-enhanced Gaussian model appraoches a -1.3 power. Meroney and Yang (1971) on the other hand carried out measurements to more than 50 building heights downwind with no sign of a similar increase in decay rate. Meroney and Yang (1971) hypothesized that the latter result was due to a very persistent horseshoe vortex that restricted lateral spread of the wake, but the detailed flow measurements needed to confirm this explanation were not available. Symes and Meroney (1970) reported concentration measurements behind a short cylinder and a sequence of cone frustrums of various tapers. The isopleth patterns varied somewhat with the body shape, but the centerline ground-level concentrations beyond $x/H \cong 10$ were all quite similar, decaying as x to the -0.8 to -1.0 power. The measurements extend to about 35 H downwind; a trend to more rapid change with distance is not evident in the data.

3.2.5 The Building Cluster Problem

Nearly all field studies of diffusion in building wakes actually have involved clusters of structures, typically at major industrial sites such as power stations. It is consequently often difficult to separate general trends from special effects generated by site-dependent flow interactions among and behind the obstacles. Such complicated flows may be at least partially responsible for the observed variations in far wake behavior in particular; such speculation can only be confirmed or repudiated by further measurements. Only a brief discussion of the available data is possible at this time.

Fortunately, much of the field work accomplished in the near wake region of building clusters is probably equally applicable to single building wakes, since flow visualizations (smoke) and effluent releases are usually carried out on or immediately adjacent to some dominant structure such as a reactor containment vessel. For example, Abbey (1976) and Start et al. (1977) described the rather similar strong vertical mixing of smoke throughout the cavity of two quite dissimilar reactor buildings. During low wind speed stable conditions in particular, the building wake acts to convert a ground-level source into an effectively elevated one; the plume concentration maxima appear aloft downwind of the primary obstacle.

Preliminary experiments with a pair of single cubes placed in tandem along the mean wind direction in a simulated atmospheric boundary layer have been described by Meroney, Peterka, and Kothari (1980). Effluent was emitted from the upwind cube at the roof center, using either a flush vent or a short stack, or at the center of the rear face. Higher concentrations were observed on the lee face of the downwind building than were found on its windward face. The effluent was apparently lifted up and out of the recirculation zone behind the upwind cube, reducing the concentrations on the upwind face of the downwind structure. This escaping effluent was then carried into the wake cavity of the downwind cube through the shear layer generated by this structure, giving high concentrations on the lee face. Further experiments of this type, combined with flow visualization procedures to help elucidate the very complex flow patterns, are needed to provide a better understanding of the general building cluster problem. Variations in building size, shape, and relative orientation should be treated. The more or less spatially homogeneous repetitive building array typical of an urban area has been studied by numerous investigators; see Hosker (1982) and Meroney (1979) for surveys of the relevant literature.

A number of investigators have noted "critical" windspeeds in building clusters above which stack or roof-emitted effluents were downwashed into the wake cavity (e.g., Davies and Moore, 1964; Martin, 1965; Munn and Cole, 1967a,b; Rodliffe and Fraser, 1971). A bimodal state is often postulated for such cases, such that the plume remains aloft for low wind speeds, but is fully entrained for others. Lawson (1967) treated the data of Munn and Cole (1967a) in this manner, plotting their values of $\chi\, x^2/Q$ versus U to get two distinct curves. The upper branch apparently corresponded to direct cavity entrainment and followed the (probably site-specific) empirical form $\chi\, x^2/Q \cong 0.0136\ U$.

In all cases corresponding to this high concentration line, the wind speed U was greater than w_e, the effluent velocity. The lower branch seemed to correspond to a plume that remained elevated, even though U was larger than w_e in a few cases. For this branch, after a few simple assumptions, Lawson (1967) estimated that the maximum ground-level concentration occurred at $x_M = 0.32\ h_e\ U$, and was given by $\chi\ x_m^2/Q = 0.00576\ U$, about one-half his cavity entrainment value for a given wind speed. The wind tunnel work of Meroney, Cermak, and Chaudhry (1968), among others, demonstrated that the downwash was actually first intermittent, as U neared a critical speed, and then became permanent as U increased further. Attempts to utilize a simple model such as Lawson's (1967) for long-term dose estimates would require use of the wind speed frequency distribution for the specific site to assess the percentage of time spent in either the high or low concentration state. The intermittency model of Johnson et al. (1975) requires rather similar information (see Equation 3-43), but estimates concentrations in a slightly different way.

Downwind of the cavity behind the structure where effluent is released, but still within or close to the building cluster as a whole, observed concentration isopleths display widely varied behavior, especially when other large obstacles are present in the cluster. For example, Figures 52 illustrate patterns produced during individual tests when effluent impinged on large cooling towers a short distance downwind of the release site (Start et al., 1977). Figures 52a and b were obtained for quite similar release and atmospheric conditions, but with different wind directions, while Figures 52c and d resulted from test runs with similar wind and stability conditions but using two different release points. Generalizations are obviously risky. However, signs of significant wake behavior behind the cooling towers appear in all of these examples. In particular, small zones of concentration maxima are visible in the immediate lee of the towers, perhaps reflecting strong mixing of initially elevated effluent down to the ground in the tower wake cavities. Some evidence of strong dilution between the cooling towers may be seen in Figures 52b and d; a possible explanation is flow "jetting" between the towers. It is clear that individual test results will vary widely from case to case, changing significantly with modest changes in wind characteristics and source location. Strong site-dependence is inevitable. Allwine, Meroney, and Peterka (1980), Hatcher and Meroney (1977), and Thuiller and Mancuso (1980) reported a similar sensitivity to test conditions in their wind tunnel and field studies of various reactor complexes. Mathematical modeling of near-field behavior for such sites on an episode by episode basis will be extremely difficult, if not impossible.

On the other hand, Dickson, Start, and Markee (1966) presented average concentration isopleths for lapse and inversion conditions, for an ensemble of 15 tests (Figure 53). These patterns are much more like those of a classical isolated plume, although there has obviously been significant initial broadening. Simple modeling efforts may be effective for predicting such ensemble average behavior (e.g., Huber's (1979) work discussed above), which is significant for the chronic exposure problem.

Halitsky (1977) has developed a moderately complicated mathematical model for a building complex and applied it to the EBR-II site studied by Dickson, Start, and Markee (1969). The model, based on measurements of unbounded uniform flow past a flat plate normal to the wind, predicts that the wake boundary grows in the horizontal and vertical as $x^{1/3}$, and that the mean velocity defect and turbulence intensity excess both decay as $x^{-2/3}$. These predictions do not agree with those made by Counihan, Hunt, and Jackson (1974) for the wake behind an isolated building, which seems somewhat more appropriate to the problem. However, Halitsky's (1977) mean velocity defect prediction appears to agree well with at least Dickson, Start, and Markee's (1969) data. By adjustment of a free parameter related to the size of the complex the excellent agreement in concentration patterns shown in Figure 54 was obtained. It may be that the present field data do not have sufficient accuracy, resolution, and density to permit distinguishing between theoretical formulations for wake behavior.

Abbey (1976) has summarized the observed decrease of concentration with downwind distance in the far wakes of building clusters. Figures 55a and b show the results of field tests and wind tunnel studies, respectively, for neutral and unstable atmospheric conditions, while Figure 55c combines the field and laboratory data for stable conditions. Beyond a few hundred meters downwind, a power-law dependence on distance is evident. For field tests under neutral and unstable conditions, the power-law exponent ranges between -1.1 and -1.8. The wind tunnel tests, on the other hand, have exponents between -0.3 and -1.9. A laboratory study by Hatcher and Meroney (1977), not shown in Abbey's figures, found a decay rate of x to the -1.8 power with little dependence on stability. Halitsky's (1977) mathematical model for wake concentration seems to decrease as x to the -1.2 power, agreeing rather well with Dickson, Start, and Markee's (1969) field value of $K \equiv \chi U A_p/Q \cong 5(x/H)^{-1.3}$ at large values of x, where H is the containment vessel height. Under stable conditions, the field data in Figure 55c behave as $x^{-1.3}$ or so, while both laboratory results decay much more slowly, as $x^{-0.7}$. The "Islitzer" result in this figure decays very rapidly, as x^{-3}, but Abbey (1976) remarks that it is due to only a single test, and may therefore not be too reliable.

The reasons for such serious discrepancies between wind tunnel and field building cluster far wake data are unknown, although some speculation is possible. For example, under stable light wind conditions, wind "meander" is well known as an important contributor to plume dilution. Start et al. (1977) noted wind direction fluctuations so large that lateral plume spreading induced by the building complex being studied was nearly obscured. Other examples are common in the literature. Such meander is virtually impossible

to duplicate* in the laboratory, a fact that may help to account for the relatively slow decrease of concentration with distance that is observed in the wind tunnel studies. It may also be true that persistent vortex-containing wakes are more significant in the laboratory than in the field; if so, the resulting slow spread of the wake would inhibit plume dispersion, producing a lower concentration decay rate than would be observed in field experiments. The possible enhanced importance of such vortex phenomena in laboratory work could be due to many factors, such as lower Reynolds number, incomplete simulation of the turbulence properties of the incident wind, and improper scaling of the model buildings relative to the incident boundary depth, turbulence scales, and other properties (see Snyder, 1981, for a good discussion of the possible pitfalls of laboratory modeling). Additional study to resolve this dilemma is needed; in the meantime, wind tunnel data on far wake concentration patterns behind building clusters must be interpreted with some care.

3.3 Effluent Source Downwind of a Building

Relatively little guidance is presently available for estimating the concentrations produced by a source located some distance downwind of an isolated building, so this section is necessarily somewhat speculative. Suppose the source is located some distance behind the structure, but still within the wake cavity. If it is a low or ground-level vent, then the effluent will travel toward the building's lee face, and be well stirred throughout the cavity in the process. However, a higher stack at this same location may have its effluent transported fairly directly to the surface by the downwind curving shear layer above the cavity (see Figures 2 and 5b,c). If the cavity is fluctuating or collapsing, these building wake effects will be intermittently important. If the source is off the wake centerline, and if the horseshoe vortex system does not break down rapidly in the ambient turbulence, then effluent may be entrained in one of the vortices (e.g., Figure 2) and be carried off downwind, possibly rising from the surface. If an elevated vortex pair is important, as may be true for buildings at an angle to the wind, then vortex entrainment and transport may be observed for an elevated source as well. In this case one might find effluent reaching the surface far downwind of the structure. Similar arguments may be appropriate for sources downwind of the cavity closure. For a simple building normal to the wind, one generally expects the enhancement to turbulent diffusion by the building wake to be the dominant effect, so that effluent from an elevated source will be mixed to the ground fairly rapidly; consequently, concentrations far downwind are lower than if the building were not present. If organized vorticity is present in the wake, however, it may be able to transfer rather concentrated material aloft to the surface at large distances downwind, producing maxima at locations of either side of the wake centerline. The model of

*Bouwmeester, Kothari, and Meroney (1980), among others, have used time-weighting of wind tunnel data to reproduce the effect of meander on average concentrations, with promising results. Laboratory data corresponding to the stability conditions and wind directions encountered onsite are necessary; these are weighted according to their relative contributions to concentrations in the field. Adjustments for wind speed and profile, source strength, and building reference area are also feasible. Their report should be consulted for details.

Kothari, Peterka, and Meroney (1980a) may be able to deal properly with such es.

Briggs (1973) suggested that his method of incorporating building wake effects into the effective stack height should be confined to cases where the stack is within $3\zeta_b$ downwind of the building, where ζ_b is the smaller of H or W. That is, the stack is still within the cavity zone. His recommended model for computing downwind concentrations if the effective stack height h_e is zero is essentially Equation (3-39a), with c = 1. If the plume remains aloft, he suggests $\chi = 0$ for short distances x such that $\sigma_z(x) < \sqrt{2/\pi}\, h_e$, while $\sigma_z > \sqrt{2/\pi}\, h_e$,

$$\chi \cong \frac{Q}{\pi\, \sigma_y\, (\sigma_z + \sqrt{2/\pi}\, h_e) U} \quad . \tag{3-47}$$

That is, dispersion behind the building is enhanced only in the vertical for an elevated release; this assumption is similar to that of Huber (1977, 1979). No building contribution to dispersion is allowed by Briggs if the source is more than $3\zeta_b$ downwind. Huber (1977, 1979) commented that the Huber and Snyder dispersion enhancement model (Equation 3-44 and 3-45) is best applied to sources with $h_e < H + 1.5\zeta_b$, located within 2 H of a building. No recommendation was made for more distant sources.

In fact, there seems to have been rather little study of the concentration field produced by a source located downwind of the cavity zone of a building or building cluster, despite its practical importance. Barrett, Hall, and Simmonds (1978) studied the case of a single model building at an angle to the wind for a range of stack heights and downwind locations. They remarked that examination of just the velocity and turbulence profiles behind the structure would suggest that the wake is virtually dissipated by $x/H \cong 8$, yet the effects of the building on the concentration field can be observed out to at least 24 H downwind. They attributed this result to downwash along the wake centerline induced by a persistent trailing horseshoe vortex. Figure 56 shows their maximum ground-level concentration coefficient $K_{max} \equiv \chi_{max} U_H H^2/Q$ as a function of nondimensional stack height h_s/H, for a range of stack locations downwind. Further study and field validation of these results are needed for a variety of building shapes and orientations.

4.0 SUMMARY AND RECOMMENDATIONS

4.1 Caveats.

This document is intended as only an interim guide for users in the architectural, industrial, nuclear, and regulatory fields who must routinely deal with air quality problems associated with near-building exhaust stack placement and height, and the resulting concentration patterns. Two decades of research have supplied methods to at least approximately answer such needs -- but only for very simple cases. Even for an isolated block-like

structure our predictive abilities are somewhat less than satisfactory, largely because of our incomplete understanding of the very complex fluid dynamic processes which occur when the turbulent atmosphere is obstructed by a building. In more complicated cases, such as building clusters, or in the presence of major perturbations like hills, river valleys, or shorelines, the air quality specialist still stands on very shaky ground. However, rough assessments and identification of potentially troublesome situations may be possible in mildly complex cases, especially if additional information on the local flow is available. In questionable cases, it will generally be wise to resort to experiment. Properly executed laboratory modeling may often be of considerable assistance at reasonable cost.

4.2 Flow Summary.

The most significant phenomena encountered in flow near a simple building at right angles to the incident wind are illustrated in Figures 2 through 5, and described in detail in Section 2. The features which determine the paths and concentrations of effluent plumes include deflection of the mean flow, vortex production, flow separation or reattachment, zones of recirculation, and the turbulent wake. These phenomena vary with the characteristics of the atmospheric boundary layer, and with the geometry of the individual building. Even small changes in the structure may significantly alter the flow field (e.g., Figure 7). Quantitative generalizations are therefore difficult for all but the simplest shapes, for which empirical results are available. Even these cases require additional experimental validation for certain geometric ranges.

For the simplest cases, one can presently estimate the region of downwash on the windward building face, the length and maximum height of the recirculating roof cavity which occurs if the building geometry permits flow reattachment, and the length of the wake cavity. However, the behavior of the flow near ground level and along the building sides is not very well known. Flow patterns within the wake cavity are also not well understood. Although it has become clear over the last few years that material may enter or leave the wake cavity by advection as well as turbulent diffusion, it is not yet possible to assess the cavity mass balance in a general and quantitative way. Downwind of the cavity, building-induced wake effects generally seem to disappear after a distance of 10 or 20 building heights, at least at ground level. However, the presence under some circumstances of organized vorticity in the wake, possibly as an elevated counter-rotating vortex pair, may significantly alter the far wake -- at least in laboratory work. Such vortices seem to persist to great distances, and serve to transfer material between the surface and regions aloft. Whether such vortices are significant in the real atmosphere is still unclear; if they occur, they may be difficult to detect with normal ground-level instruments since the vortices probably rise up and outward from the wake centerline with increasing downwind distance, and meander about under the influence of ambient turbulence.

4.3 Summary of Concentration Estimation Procedures.

When an isolated point source is located some distance upwind of a building, the structure acts mainly to induce a rapid enlargement and dilution of the

impinging effluent plume. Close to the building, the ground level concentration will be larger than if no building were present, but farther downwind tl concentration will be smaller than the no-building case. Equations (3-5) through (3-13) provide quantitative limits on the concentrations likely near the building; Figures 17 through 20 provide computational aids. If one must estimate the minimum height needed for a new stack to be constructed upwind of an existing building, or, alternately, must calculate the maximum permissible height for a new structure to be located downwind of an existing source, two reasonable methods (Lucas, 1972; Wilson and Netterville, 1976) are described in Section 3.1.4. In critical cases, a prudent designer would apply both techniques, and then use the higher of the two calculated stack heights or the smaller of the possible building heights. It should be recognized, however, that certain meteorologically-induced phenomena such as looping plumes or morning fumigation may serve to transfer initially elevated pollutants quite directly to the ground, largely negating the benefits of using a stack. In other words, the designer must remember that the near-building aerodynamic flow field may not be the main influence on a plume under some circumstances, even close to the structure.

If effluent is released from stacks or vents on or close to a structure, the complex near-building flow patterns can yield objectionably high local concentrations, or can entrain sufficient pollutant into the wake to affect sites some distance downwind. The first aerodynamic influences encountered by a plume are generally the tip vortices and wake of the stack itself; the effluent momentum should be maintained at least 1.5 times larger than the momentum of the surrounding air to avoid downwash into the stack wake. The flow about any nearby structures also acts to decrease the effective stack height. If the building is short enough in the along-wind direction so that reattachment of the edge-separated roof and side flows does not occur (Figure 5b), then Briggs' (1973) suggestions can be used to estimate the effective release height (see Equations 3-16 through 3-18, and the associated text). On the other hand, if the building is long enough for roof reattachment to occur (Figure 5c), then Wilson's (1979a,b) approximations of the near-roof flow field can significantly assist stack height selection and placement, as long as the stack can be located somewhere along the roof centerline. When roof-mounted stacks are not close to the centerline, the plume paths and concentrations will depend in a very complicated and largely unpredictable way on the interactions among the building geometry, the atmosphere, and the stack characteristics and location. Experiments like those of Koga and Way (1979a,b; see Figures 24 through 31) are badly needed for guidance on the likelihood of plume downwash or wake entrainment. In most cases, quantitative estimates are not yet possible for the resulting effective stack height, or even for the time fraction that the plume is downwashed or trapped in the building wake.

Near-building concentration estimates are straightforward in the unfortunately rare instances when nondimensional isopleths of $K = \chi U A / Q$ have been determined for a specific architectural configuration. Such data should be quite reliable when properly adjusted to account for differences in sampling time (e.g., see Allwine, Meroney, and Peterka, 1980, or Bouwmeester, Kothari, and Meroney. 1980). Generally, however, the K-patterns are not known a priori. If the effluent is released with negligible momentum and buoyancy from a flush roof vent into a zone of reattached flow not too far off the roof centerline,

then it is at least possible to place an approximate upper bound on the concentrations which may occur at arbitrary locations on the building surfaces using Equations (3-23) through (3-27), and Figures 36 through 41. If the pollutant is particularly worrisome, a more conservative limit can be obtained using Equation (3-21) and Figure 35, with $\tilde{\alpha} = 1$. If a similarly placed stack replaces the flush vent, Equations (3-28) or (3-30) through (3-31b) and Figure 43 can provide estimates of rooftop nondimensional concentrations relative to those produced by the flush vent. Once this ratio K/K_r is evaluated for some stack height, the consequences of a change in height can be explored with Equations (3-29) and Figures 42a and b. However, if the flush vent or stack is located near the roof edges, or within the recirculating roof cavity, or near regions of vortex generation (such as upwind corners), the methods described are not applicable. No alternate analyses are presently available. In such cases the designer will usually have to conduct special tests of the individual building-stack-atmosphere configuration.

It is often necessary to estimate concentrations at points away from the building surfaces, but still within the wake cavity region. Most published formulations for a fully entrained plume give $K \cong 1/c$ (Equation 3-32), where the constant c depends (at least) on the building and atmospheric characteristics; i.e., the concentration within the cavity is assumed uniform. One can also treat this case using a rough mass transfer analysis of the cavity. The cavity concentration turns out (Equations 3-35 to 3-37) to be a measure of the characteristic time for effluent removal by turbulent transfer (and possibly by advection) relative to the time required for the mean flow to "flush" a similar volume; this ratio will usually be larger than 1. The parameters needed to apply this result can be measured fairly easily; available semi-empirical estimates (e.g., Equations 2-8) may also be useful. However, the technique requires further validation and "calibration" before it can be considered reliable. Furthermore, if the effluent is emitted from a stack, not all of the material may be captured within the wake cavity. Briggs' (1973) recommendations, described in Equation (3-33) and the corresponding text, can be used to approximate the consequences of stack-tip and building-induced downwash, depending on the stack height relative to the building. The user should bear in mind that the uniform cavity concentrations assumed by all of these schemes are unlikely to be found in practice, particularly near the source where the concentrations can be expected to increase sharply (see, e.g., Wilson, 1977a, and Wilson and Britter, 1981). No general method to account for such in-cavity nonuniformities presently exists, although very close to the source a plume-like distance-dependent model may apply. It should also be recognized that moderately tall stacks located within the wake cavity zone may lead to rather high ground level concentrations near the end of the cavity. This occurs when the pollutant is emitted close to the top of the cavity, so that it can be transported rather directly to the surface by the curved shear layer above the cavity. Under these conditions a shorter stack would probably result in better mixing and lower ground level concentrations.

Downwind of the cavity, wake concentrations become decidedly nonuniform. The model of Kothari, Peterka, and Meroney (1980b) may be of use. If cavity entrainment never occurs, one can also simply apply the point source model of Equation (3-6) after an effective stack height is estimated following Section

3.2.1. However, cavity entrainment is likely to be intermittent in many case The Johnson et al. (1975) model, Equation (3-43), seems suitable, although their empirical estimate of the time fraction during which entrainment occurs is almost certainly site-specific and inappropriate for locations other than the Millstone reactor. Generally, specialized tests will be necessary if intermittent wake capture is expected to be a problem.

Under continuing severe downwash conditions, the source will effectively be at ground level. Simple modifications to the usual Gaussian model are then generally proposed for the far wake concentration. A virtual source location determined from the building dimensions is feasible, as are modifications based on an initial plume dilution keyed to building size, followed by turbulent diffusion characteristic of an unmodified atmosphere. A more recent method postulates that turbulent diffusion out to about 10 H is determined entirely by the building geometry; at greater distances, a virtual source approximation is matched to the initial spread. This model, Equations (3-44) and (3-45), seems to agree fairly well with wind tunnel data behind simple buildings (see Figure 51), although the initial dilution model of Equation (3-39) does about as well for ground-level releases. Both of these models apply to cases where organized wake vorticity is unimportant. The far wake results behind building complexes are not as satisfactory, probably because of the substantial site-dependent changes in the flow field. It is also difficult to select an appropriate "equivalent building" height and width for a group of structures, although this information is needed to evaluate initial plume spread. In the far wake, wind tunnel data behind single obstacles suggest a rather slow concentration decrease with distance, roughly $x^{-0.8}$, out to 30 H or more. Building cluster results sometimes fall off more quickly (e.g., $x^{-1.8}$ for Hatcher and Meroney's 1977 study). Field data were generally collected behind building clusters, which may help explain the fairly rapid concentration decrease, $x^{-1.1}$ to $x^{-1.8}$, not much different than a Gaussian far wake model would predict.

Generally speaking, the building cluster problem remains intractable. Many of the phenomena associated with isolated buildings can be found close to individual structures within the complex. However, mutual aerodynamic interferences can severely distort the expected flow pattern, producing unusual concentration distributions. Zones of strong convergence ("jetting") and modifications of wake structure are commonly encountered. Nevertheless, the ensemble-average experimental results of Dickson, Start, and Markee (1969) appear amenable to mathematical modeling efforts, suggesting that it may be possible to attack at least the chronic exposure problem downwind of building clusters. Episodic releases will probably have to be addressed experimentally on a case by case basis.

Very little precedent exists for making concentration estimates when the source is downwind of a building. If the stack is still within the wake cavity zone, and the effective stack height is small, one can follow Briggs' (1973) suggestion of a ground level source model with some initial dilution (Equation 3-39a). If the plume does remain aloft, then the ground level concentration is negligible until the effluent has traveled far enough to

diffuse down to the surface; after this point, the concentration is calculated by assuming some enhancement of the vertical dispersion (Equation 3-47). Barrett, Hall, and Simmonds (1978) reported perturbations to concentrations for stacks as much as 24 H downwind of a cubical model; the structure was at an angle to the wind, however, and the persistent wake influence may be due to organized wake vorticity. No quantitative guidance is available; the designer must appeal to what may be known of the fluid dynamics of a particular wake to estimate effluent dispersion from downwind sources.

4.4 Recommendations.

For calculations of flow and dispersion near simple block-like buildings, the techniques described in the text and summarized above are generally helpful, although subject to uncertainties. Considerable additional research is required to improve this situation. A major obstacle to the development of better predictive techniques is our still inadequate understanding of the detailed flow patterns near buildings of different geometry and orientation. The following questions must be answered:

Under what conditions can reattachment of the initially separated roof and side flows be expected? What are the flow patterns along and near the roof and sides with and without reattachment?

How persistent is the horseshoe vortex in the real atmosphere, and how does it move and behave with increasing downwind distance?

How large and intense are the lee-edge vortices; how do they interact with the wake cavity and with the mean flow?

What are the wake cavity dimensions under different circumstances, and how does material enter and leave this region? How significant are turbulent diffusion and direct advective transport in the cavity mass balance?

How strong and persistent are the vortices generated at the windward roof corner of a building at an angle to the wind? How are their size and spread related to building geometry and atmospheric characteristics?

How well do present mathematical models predict the vertical and horizontal spread and decay of a turbulent wake in the real atmosphere? Are the behavior with increasing downwind distance of the mean and turbulent velocity components and the eddy scale adequately understood?

It is also clear that systematic study of building clusters is needed; this should probably begin with small groups (i.e., 2, 3, or 4 structures) of buildings to examine the mutual aerodynamic interferences and flow patterns as functions of building geometry, relative size, spacing, and orientation. Reliable, quantitative, and general models of building cluster wake behavior probably cannot be developed until the fluid dynamics of these simple cases are better understood. If laboratory data are used to answer these questions, field validation of the work is imperative. The laboratory results may be doubly valuable in this regard, since they can provide information on the types and placement of instruments needed in the field measurement program.

Additional work is also needed on the spatial distribution of concentrations near isolated simple buildings of different geometries. Data on near-building concentrations produced by upwind sources with stack heights between 0 and, say, 3 H are needed for various stack-to-building distances to check and improve the estimation procedures suggested by Lucas (1972) and Wilson and Netterville (1976,1978).

The complex and practically important problem of effluents released on or close to a structure also requires considerable research:

Verify equations such as (3-16) which compensate effluent release height for stack-induced downwash and efflux momentum.

Test Briggs' (1973) suggestions for the effect of building-induced downwash on effective release height, over a wide range of building geometries and effluent release position and heights.

Check Wilson's (1979a,b) results for roof cavity and wake behavior over a range of building shapes and atmospheric stabilities, to facilitate placement and height selection for roof-mounted stacks. Extend this work to locations off the roof center-line, so the whole roof flow field is adequately understood.

Generate quantitative data on plume path, degree of entrainment, and frequency of wake capture, for a wide range of building geometries and release positions, heights, and momenta. Combine these data with models such as that of Johnson et al. (1975) to estimate concentrations due to intermittently entrained effluent.

Further verify predictions such as Equations (3-23) or (3-25) for building surface concentrations produced by flush roof vents. Map out non-dimensional concentration (K) isopleths for a large variety of building and vent configurations and orientations, using an adequately simulated atmospheric boundary layer.

Check estimates such as Equations (3-28) or (3-31) for the rooftop concentrations produced by a roof-mounted stack at various locations. Examine the adequacy of Equation (3-29) for estimating the relative effect of changes in roof stack height.

Study wake cavity concentrations as functions of building geometry and effluent release location to elucidate cavity mass balance mechanisms, and to clarify the uniformity of concentration that can be anticipated within the cavity under different circumstances. Test the adequacy of Equations (3-33) and (3-36) or (3-37) over a range of building geometries. Provide theoretical and/or empirical estimates of wake cavity characteristic diffusion time to permit use of expressions such as (3-37) on a routine basis.

Examine the influence of vortex generation near upwind roof corners on effluent concentrations close to buildings for a variety of stack or vent locations.

Data behind isolated simple buildings is especially important for evaluating far wake models, since clusters of buildings may have quite different wake flow characteristics. Given these data, the relative accuracy of concentration models such as Equations (3-39), (3-41), and (3-44) can be assessed. The influence of organized vorticity in the far wake region is still unclear; field work would be particularly useful here because of the possible Reynolds number dependence of laboratory simulations of the phenomenon.

Finally, the problem of a source downwind of a building does not seem to have been adequately addressed. The influences of building geometry and orientation must be examined, and concentration models such as Equation (3-47) must be checked, extended, and improved. Separation distance, stack and building size, and atmospheric stability must all be considered, so that reliable models can be developed.

THIS PAGE

WAS INTENTIONALLY

LEFT BLANK

5.0 REFERENCES

Abbey, R. F., Jr., 1976: Concentration measurements downwind of buildings: previous and current experiments. In Preprints of Third Symposium on Atmospheric Turbulence, Diffusion and Air Quality, Raleigh, NC, Oct. 19-22 (Amer. Meteorol. Soc., Boston, MA), pp 247-254.

Allwine, K. J., R. N. Meroney, and J. A. Peterka, 1980: Rancho Seco Building Wake Effects on Atmospheric Diffusion: Simulation in a Meteorological Wind Tunnel. U.S. NRC report NUREG/CR-1286 (avail. NTIS, Springfield, VA), xi and 176 pp.

Arie, M., M. Kiya, H. Tamura, M. Kosugi, and K. Takaoka, 1975: Flow over rectangular cylinders immersed in a turbulent boundary layer, part 2, flow patterns and pressure distributions. Bulletin of J.S.M.E. 18, no. 125, pp 1269-1276.

ASHRAE, 1974: Laboratories. Chapter 15 in Handbook and Product Directory, 1974, Applications (Amer. Soc. Heating, Refrig., and Air-Cond. Engineers, New York), pp 15.9 ff.

ASME, 1973: Recommended Guide For The Prediction of Airborne Effluents, second edition (Amer. Soc. Mech. Engineers, New York), xii and 85 pp.

Baines, W. D., 1963: Effects of velocity distribution on wind loads and flow patterns on buildings. In Proc. of Symposium on Wind Effects on Buildings and Structures, National Physical Laboratory, Teddington, Middlesex, England, June 26-28, (Her Majesty's Stationery Office, London, 1965), vol. I, pp 197-225.

Barrett, C. F., D. J. Hall, and A. C. Simmonds, 1978: Dispersion from chimneys downwind of cubical buildings -- a wind-tunnel study. In Proc. of 9th Internat. Tech. Meeting on Air Poll. Modeling and its Application, at Toronto, Canada, Aug. 28-31 (North Atlantic Treaty Organization/CCMS, Umweltbundesamt, W. Berlin, Fed. Rep. of Germany), pp 37-44.

Barry, P. J., 1964: Estimation of downwind concentration of airborne effluents discharged in the neighbourhood of buildings. Atomic Energy of Canada, Ltd. report no. 2043 (AECL, Chalk River, Ontario), 16 pp.

Bitte, J., and W. Frost, 1976: Atmospheric Flow Over Two-Dimensional Bluff Surface Obstructions. NASA contractor report NASA CR-2750 (October), (avail. NTIS, Springfield, VA), xviii and 207 pp.

Bouwmeester, R. J. B., K. M. Kothari, and R. N. Meroney, 1980: An Algorithm to Estimate Field Concentrations Under Nonsteady Meteorological Conditions From Wind Tunnel Experiments. U.S. NRC report NUREG/CR-1474 (avail. NTIS, Springfield, VA), ix and 85 pp.

Bradshaw, P., and F. Y. F. Wong, 1972: The reattachment and relaxation of a turbulent shear layer. J. Fluid Mech. 52, part 1, pp 113-135.

Briggs, G. A., 1969: Plume Rise. U.S. AEC no. TID-25075 (avail. NTIS, Springfield, VA), vi and 81 pp.

Briggs, G. A., 1973: Diffusion estimation for small emissions. In Atmospheric Turbulence and Diffusion Laboratory 1973 Annual Report (NOAA/ATDL, Oak Ridge, TN, publication no. ATDL-106), pp 83-145.

Briggs, G. A., 1975: Plume rise predictions. Chapter 3 in Lectures on Air Pollution and Environmental Impact Analyses, Boston, Sept. 29-Oct. 3 (Amer. Meteorol. Soc., Boston, MA), pp 59-111.

Britter, R. E., J. C. R. Hunt, and J. S. Puttock, 1976: Predicting pollution concentrations near buildings and hills. Presented at Institution of Measurements and Control's Conference on Systems and Models in Air and Water Pollution, London, Sept. 22-24, pp 7-1 to 7-15.

Caput, C., Y. Belot, G. Guyot, C. Samie, and B. Seguin, 1973: Transport of a diffusing material over a thin wind-break. Atmos. Environment 7, no. 1, pp 75-86.

Castro, I. P., 1979: Relaxing wakes behind surface-mounted obstacles in rough wall boundary layers. J. Fluid Mech. 93, part 4, pp 631-659.

Castro, I. P., and J. E. Fackrell, 1978: A note on two-dimensional fence flows with emphasis on wall constraint. J. Indust. Aerodynamics 3, no. 1, pp 1-20.

Castro, I. P., and A. G. Robins, 1977: The flow around a surface-mounted cube in uniform and turbulent streams. J. Fluid Mech. 79, part 2, pp 307-335.

Chang, S.-C., 1966: Velocity Field In Separated Flow Behind A Model Hill. M. S. thesis, Colorado State University (Dept. of Civil Engineering), xiv and 101 pp.

Colmer, M. J., 1970: Some Full-Scale Measurements of the Flow in the Wake of a Hanger. Royal Aircraft Establishment/Aeronautical Research Council C. P. no. 1166, replacing RAE Tech. Report 70202-ARC32863 (Her Majesty's Stationery Office, London, 1971), 28 pp.

Cook, N. J., and D. Redfearn, 1976: Calibration and use of a hot-wire probe for highly turbulent and reversing flows. J. Indust. Aerodynamics 1, no. 3, 221-231.

Corke, T. C., and H. M. Nagib, 1976: Sensitivity of Flow Around and Pressures On a Building Model to Changes in Simulated Atmospheric Surface Layer Characteristics. Illinois Institute of Technology Fluids and Heat Transfer Report R76-1, (I.I.T., Mechanics & Mech. & Aerospace Engineering Dept., Chicago, IL), xxiii and 268 pp.

Counihan, J., 1971: An Experimental Investigation of the Wake Behind a Two Dimensional Block and Behind a Cube in a Simulated Boundary Layer Flow. Central Electricity Research Laboratories note no. RD/L/N 115/71 (CERL, Leatherhead, Surrey, England), 45 pp.

Counihan, J., J. C. R. Hunt, and P. S. Jackson, 1974: Wakes behind two-dimensional surface obstacles in turbulent boundary layers. J. Fluid Mech. 64, part 3, pp 529-563.

Csanady, G. T., 1973: Turbulent Diffusion in the Environment. Vol.3 in Geophysics and Astrophysics Monographs, B. M. McCormac, ed. (D. Reidel Pub. Co., Boston), xii and 248 pp.

Davenport, A. G., 1963: The relationship of wind structure to wind loading. In Wind Effects on Buildings and Structures, Proc. of conference at NPL, Teddington, Middlesex, U.K., June 26-28 (Her Majesty's Stationary Office, London, 1965), vol. I, pp 54-101.

Davies, P. O. A. L., and D. J. Moore, 1964: Experiments on the behavior of effluent emitted from stacks at or near the roof level of tall reactor buildings. Internat. J. Air Water Pollution 8, no. 10, pp 515-533.

de Bray, B. G., 1971: Protection by fences. Presented at a Seminar on Wind Effects on Buildings and Structures, Univ. of Auckland, New Zealand (May), paper no. 9, 24 pp.

Dickson, C. R., G. E. Start, and E. H. Markee, Jr., 1969: Aerodynamic effects of the EBR-II reactor complex on effluent concentration. Nuclear Safety 10, no. 3, pp 228-242.

Drivas, P. J., and F. H. Shair, 1974: Probing the air flow within the wake downwind of a building by means of a tracer technique. Atmos. Environment 8, no. 11, pp 1165-1175.

Frost, W., and A. M. Shahabi, 1977: A Field Study of Wind Over a Simulated Block Building. NASA report no. CR-2804 (avail. NTIS, Springfield, VA), xii and 119 pp.

Gandemer, J., 1976: Inconfort dû au Vent Aux Abords Des Bâtiments: Concepts Aérodynamiques. Cahiers du Centre Scientifique et Technique du Batiment, no. 170, Cahier 1384 (CSTB, Nantes, France). Available in translation as NBS technical note 710-9, March, 1978, 48 pp.

Gifford, F. A., 1960: Atmospheric dispersion calculations using the generalized Gaussian plume model. Nuclear Safety 2, no. 2, pp 56-59.

Gifford, F. A., 1968: An outline of theories of diffusion in the lower layers of the atmosphere. Chapter 3 in Meteorology and Atomic Energy-1968, D. Slade, editor. U.S. AEC no. TID-24190, (avail. NTIS, Springfield, VA), pp 65-116.

Gifford, F. A., 1975: Atmospheric dispersion models for environmental pollution applications. Chapter 2 in Lectures on Air Pollution and Environmental Impact Analyses, Boston, Sept. 29-Oct. 3. (Amer. Meteorol. Soc., Boston, MA), pp 35-58.

Gifford, F. A., 1976: Turbulent diffusion-typing schemes: a review. Nuclear Safety 17, no. 1, pp 68-86.

Good, M. C., and P. N. Joubert, 1968: The form drag of two-dimensional bluff-plates immersed in turbulent boundary layers. J. Fluid. Mech. 31, part 3, pp 547-582.

Halitsky, J., 1961: Diffusion of Vented Gas Around Building. Paper no. 61-35, presented at 54th Annual Meeting of Air Poll. Control Assoc., New York, June 11-15, 26 pp.

Halitsky, J., 1963a: Gas Diffusion Near Buildings. N.Y.U. Meteorol. and Oceanog. Geophys. Sciences Lab. report 63-3 (New York Univ., College of Engineering, New York), vii and 163 pp.

Halitsky, J., 1963b: Gas diffusion near buildings, ASHRAE Trans. 69, paper no. 1855, pp 464-485.

Halitsky, J., 1968: Gas diffusion near buildings. Chapter 5-5 in Meteorology and Atomic Energy-1968, ed. by D. H. Slade, U.S. AEC TID-24190 (avail. NTIS, Springfield, VA), pp 221-255.

Halitsky, J., 1977: Wake and dispersion models for the EBR-II building complex. Atmos. Environment 11, no. 7, pp 577-596.

Halitsky, J., J. Golden, P. Halpern, and P. Wu, 1963: Wind Tunnel Tests of Gas Diffusion From a Leak in the Shell of a Nuclear Power Reactor and From a Nearby Stack. N.Y.U. Meteorol. and Oceanog. Geophys. Sciences Lab. report 63-2 (New York Univ., College of Engineering, New York).

Hansen, A. C., and J. E. Cermak, 1975: Vortex-Containing Wakes of Surface Obstacles. Colorado State Univ. Fluid Dynamics and Diffusion Lab. report CER75-76ACH-JEC16 (Col. State Univ., Ft. Collins), xiv and 163 pp.

Hatcher, R. V., and R. N. Meroney, 1977: Dispersion in the wake of a model industrial complex. In Preprints of Joint Conference on Applications of Air Pollution Meteorology, Salt Lake City, Nov. 29-Dec. 2 (Amer. Meteorol. Soc., Boston, MA), pp 343-346.

Hatcher, R. V., R. N. Meroney, J. A. Peterka, and K. Kothari, 1978: Dispersion in the Wake of a Model Industrial Complex. U.S. NRC report NUREG-0373 (avail. NTIS, Springfield, VA), xiv and 231 pp.

Hatcher, R. V., D. G. Smith, and L. L. Schulman, 1979: Building downwash modeling -- recent developments. Presented at 72nd annual meeting of Air Poll. Control Assoc., Cincinnati, June 24-29, paper no. 79-2.6, 13 pp.

Hinds, W. T., 1969: Peak-to-mean concentration ratios from ground-level sources in building wakes. Atmos. Environment 3, no. 2, pp 145-156.

Hoot, T. G., R. N. Meroney, and J. A. Peterka, 1973: Wind Tunnel Tests of Negatively Buoyant Plumes. Colorado State Univ. Fluid Dynamics and Diffusion Lab. report CER73-74TGH-RNM-JAP13 (Col. State Univ., Ft. Collins, CO).

Hosker, R. P., 1979: Empirical estimation of wake cavity size behind block-type structures. In Preprints of Fourth Symposium on Turbulence, Diffusion, and Air Pollution, Reno, NV, Jan. 15-18 (Amer. Meteorol. Soc., Boston, MA, 1979), pp 603-609.

Hosker, R. P., 1982: Flow and dispersion near obstacles. Chapter 7 in Atmospheric Science and Power Production, D. Randerson, editor (U.S. Dept. of Energy Tech. Info. Center, Oak Ridge, TN -- in press).

Huber, A. H., 1977: Incorporating building/terrain wake effects on stack effluents. In Preprints of Joint Conference on Application of Air Pollution Meteorology, Salt Lake City, Nov. 29-Dec. 2 (Amer. Meteorol. Soc., Boston, MA), pp 353-356.

Huber, A. H., 1979: An evaluation of obstacle wake effects on plume dispersion. Presented at Fourth Symposium on Turbulence, Diffusion, and Air Pollution, Reno, NV, Jan. 15-18, (Amer. Meteorol. Soc., Boston, MA), 8 pp.

Huber, A. H., and W. H. Snyder, 1976: Building wake effects on short stack effluents. In Preprints of Third Sympos. on Atmospheric Turbulence, Diffusion, and Air Quality, Raleigh, NC, Oct. 19-22 (Amer. Meteorol. Soc., Boston, MA), pp 235-242.

Huber, A. H., W. H. Snyder, R. S. Thompson, and R. E. Lawson, Jr., 1976: Stack Placement in the Lee of a Mountain Ridge. U.S. E.P.A. Environmental Sciences Research Laboratory report no. EPA-600/4-76-047 (avail. NTIS, Springfield, VA), x and 44 pp.

Huber, A. H., W. H. Snyder, R. S. Thompson, and R. E. Lawson, Jr., 1980: The Effects of a Squat Building on Short Stack Effluents. U.S. EPA Environmental Sciences Research Lab. report no. EPA-600/4-80-055 (avail. NTIS, Springfield, VA), x and 108 pp.

Hunt, J. C. R., C. J. Abell, J. A. Peterka, and H. Woo, 1978: Kinematical studies of the flows around free or surface mounted obstacles: applying topology to flow visualization. J. Fluid Mech. 86, part 1, pp 179-200.

Islitzer, N. F., 1965: Aerodynamic Effects of Large Reactor Complexes Upon Atmospheric Turbulence and Diffusion. U.S. AEC Nat. Reactor Test. Station report IDO-12041 (U.S. Weather Bureau, Idaho Falls, ID), 15 pp.

Jensen, M., and N. Franck, 1963: Model-Scale Tests in Turbulent Wind, part I (Danish Tech. Press, Copenhagen), viii and 97 pp.

Johnson, W. B., E. Shelar, R. E. Ruff, H. B. Singh, and L. Salas, 1975: Gas Tracer Study of Roof-Vent Effluent Diffusion at Millstone Nuclear Power Station. Atomic Industrial Forum report AIF/NESP-007b (A.I.F., Inc., Washington, DC), xiii and 295 pp.

Koga, D. J., and J. L. Way, 1979a: Effects of stack height and position on pollutant dispersion in building wakes. In vol. 2 of Proc. of Fifth Internat. Wind Engineering Conf., Fort Collins, CO, July, J. E. Cermak, editor (Pergamon Press, New York, NY), 1003-1017.

Koga, D. J., and J. L. Way, 1979b: Effects of Stack Height and Position on the Dispersion of Pollutants in Building Wakes. Illinois Institute of Technology Fluids and Heat Transfer report no. R79-2 (I.I.T., Mechanics & Mech. & Aerospace Eng. Dept., Chicago, IL). xxiii and 238 pp.

Kothari, K. M., J. E. Cermak, and A. R. Greenway, 1982: Wind-tunnel modeling of dispersion of power plant emissions. In Extended Abstracts of AMS/APCA 3rd Joint Conf. on Appl. of Air Poll. Meteorol. San Antonio, TX, Jan. 12-15 (Amer. Meteorol. Soc., Boston, MA), pp 245-247.

Kothari, K. M., J. A. Peterka, and R. N. Meroney, 1980a: Stably Stratified Building Wakes. U.S. NRC report NUREG/CR-1247 (avail. NTIS, Springfield, VA), xiv and 143 pp.

Kothari, K. M., J. A. Peterka, and R. N. Meroney, 1980b: The Wake Structure Behind a Model Industrial Complex. U.S. NRC report NUREG/CR-1473 (avail. NTIS, Springfield, VA).

Lawson, T. V., 1967: Discussion of "Turbulence and diffusion in the wake of a building". Atmos. Environment 1, no. 2, pp 177-181.

Lemberg, R., 1973: On the Wakes Behind Bluff Bodies in a Turbulent Boundary Layer. Ph.D. thesis and Boundary Layer Wind Tunnel report no. BLWT-3-73 (University of Western Ontario, London, Ontario, Canada), xiv and 159 pp.

Li, W. W., R. N. Meroney, and J. A. Peterka, 1981: Wind-Tunnel Study of Gas Dispersion Near a Cubical Model Building. U. S. NRC report NUREG/CR-2395 (avail. NTIS, Springfield, VA).

Lucas, D. H., 1972: Choosing chimney heights in the presence of buildings. In Proc. Internat. Clean Air Conf., Melbourne Univ., Australia, May (Clean Air Society of Australia and New Zealand, 1972), pp 47-52.

Lumley, J. L., and H. A. Panofsky, 1964: The Structure of Atmospheric Turbulence (John Wiley - Interscience, New York, NY), xii and 239pp.

Martin, J. E., 1965: The Correlation of Wind Tunnel and Field Measurements of Gas Diffusion Using Krypton-85 as a Tracer. Ph.D. Thesis and report no. MMPP-272 of Michigan Memorial Phoenix Project (Univ. of Michigan, Ann Arbor), x and 130 pp.

Meroney, R. N., 1979: Turbulent diffusion near buildings. Chapter 11 in Engineering Meteorology, E. J. Plate, editor (Elsevier Press, to be published).

Meroney, R. N., J. E. Cermak, and F. H. Chaudhry, 1968: Wind-tunnel Model Study of Shoreham Nuclear Power Station Unit I for Long Island Lighting Company. Colorado State Univ. Fluid Dynamics and Diffusion Lab. report CER68-69RNM-JEC-FHC1 (Col. State Univ., Ft. Collins, CO), vi and 65 pp.

Meroney, R. N., J. A. Peterka, and K. M. Kothari, 1980: Wind-Tunnel Measurements of Dispersion and Turbulence in the Wakes of Nuclear Reactor Plants. U. S. NRC report NUREG/CR-1475 (avail. NTIS, Springfield, VA), xiii and 45 pp.

Meroney, R. N., and B. T. Yang, 1970: Gaseous plume dispersion about isolated structures of simple geometry. Presented at Second Internat. Clean Air Congress of the Internat. Union of the Air Poll. Prevention Assoc., Washington, DC, Dec. 6-11, 32 pp.

Meroney, R. N., and B. T. Yang, 1971: Wind-Tunnel Study on Gaseous Mixing Due to Various Stack Heights and Injection Rates Above an Isolated Structure. Colorado State Univ. Fluid Dynamics and Diffusion Lab. report CER71-72RNM-BTY16 (Col. State Univ., Ft. Collins, CO), v and 42 pp.

Morkovin, M. V., 1972: An approach to flow engineering via functional flow modules. In Beiträge z. Strömungsmechanik, A. Walz 65th Anniversary Volume, Deutsche Luft-und Raumfahrt Forschungsvericht no. 72-27.

Munn, R. E., and A. F. W. Cole, 1967a: Turbulence and diffusion in the wake of a building. Atmos. Environment 1, no. 1, pp 33-43.

Munn, R. E., and A. F. W. Cole, 1967b: Some strong-wind downwash diffusion measurements at Douglas Point, Ontario, Canada. Atmos. Environment 1, no. 5, pp 601-604.

Murphy, K. G., and K. M. Campe, 1974: Nuclear power plant control room ventilation system design for meeting General Criterion 19. In Proc. of 13th AEC Air Cleaning Conf., San Francisco, Aug. 12-15, M. W. First, editor, U.S. AEC CONF-740807, vol. 1 (avail. NTIS, Springfield, VA), pp. 401-430.

Nagabhushanaiah, H. S., 1961: Separation Flow Downstream Of A Plate Set Normal to A Plane Boundary. Ph.D. thesis, Colorado State University (Dept. of Civil Engineering), xx and 153 pp.

Ogawa, Y., 1973: Effects of Building and Thermal Boundary Layer On Diffusion. Ph.D. thesis, Hokkaido Univ., Sapporo, Japan (Dept. of City Environmental Engineering), xv and 327 pp.

Penwarden, A. D., and A. F. E. Wise, 1975: Wind Environment Around Buildings. Building Research Establishment Report (Her Majesty's Stationery Office, London), vii and 52 pp.

Pierce, T. E., and D. B. Turner, 1980: User's Guide for MPTER. U.S. EPA report EPA-600/8-80-016 (avail. NTIS, Springfield, VA), viii and 239 pp.

Plate, E. J., and C. W. Lin, 1965: The Velocity Field Downwind From A Two-Dimensional Model Hill, Part 1. Colorado State Univ. Fluid Dynamics and Diffusion Lab. report CER65-EJP-14 (Col. State Univ., Ft. Collins), iv and 75 pp.

Raine, J. K., and D. C. Stevenson, 1977: Wind protection by model fences in a simulated atmospheric boundary layer. J. Indust. Aerodynamics 2, no. 2, pp 159-180.

Robins, A. G., 1975: Plume Dispersion in the Vicinity of a Surface Mounted Cube. Central Electricity Generating Board report R/M/R220 (CEGB, Marchwood Engng. Labs., Marchwood, Southhampton, Hampshire, England), 49 pp.

Rodliffe, R. S., and A. J. Fraser, 1971: Measurements on the release of gaseous activity from a short stack. Atmos. Environment 5, no. 4, pp 193-208.

Sagendorf, J. F., N. R. Ricks, G. E. Start, and C. R. Dickson, 1980: Diffusion
Near Buildings as Determined From Atmospheric Tracer Experiments. NOAA Tech. Memo. ERL-ARL-84 (NOAA/ARL, Silver Spring, MD), iv and 26 pp.

Schlichting, H., 1960: Boundary Layer Theory, 4th edition (McGraw-Hill, New York, Toronto, and London), xxii and 647 pp.

Scorer, R. S., 1968: Air Pollution (Pergamon Press, Oxford, London, New York, Toronto, and Paris), xiv and 151 pp.

Sheih, C.M., P. J. Mulhearn, E. F. Bradley, and J. J. Finnigan, 1978: Pollutant transfer across the cavity region behind a two-dimensional fence. Atmos. Environment 12, no. 12, pp 2301-2307.

Sherlock, R. H., and E. A. Stalker, 1941: A Study of Flow Phenomena in the Wake of Smokestacks. Univ. of Michigan Dept. of Engineering Research Bulletin no. 29 (Univ. of Michigan Press, Ann Arbor), vi and 49 pp.

Smith, D. G., 1975: Influence of meteorological factors upon effluent concentrations on and near buildings with short stacks. Presented at 68th Annual Meeting of Air Poll. Control Assoc., Boston, June 15-20, paper no. 75-26.2, 25 pp.

Smith, D. G., 1978: Turbulent Dispersion Around a Building in the Natural Wind and Effluent Reentry. Ph.D. thesis, Harvard Univ. (School of Public Health, Boston, MA), xvi and 150 pp.

Snyder, W. H., 1981: Guidelines for Fluid Modeling of Atmospheric Diffusion. U.S. E.P.A. report no. EPA-600/8-81-009 (avail. NTIS, Springfield, VA), xvi and 185 pp.

Snyder, W. H., and R. E. Lawson, Jr., 1976: Determination of a necessary height for a stack close to a building. Atmos. Environment 10, no. 9, pp 683-691.

Souster, C. G., and B. E. Lee, 1975: The Measurement of Airflow Patterns Upstream of Some Simple Building Shapes. Univ. of Sheffield Dept. of Building Science report BS 26 (Univ. of Sheffield, England), 33 pp.

Start, G. E., J. H. Cate, C. R. Dickson, N. R. Ricks, G. R. Ackermann, and J. F. Sagendorf, 1977: Rancho Seco Building Wake Effects on Atmospheric Diffusion. NOAA Tech. Memo. ERL-ARL-69 (NOAA/ARL, Idaho Falls, ID), iv and 185 pp.

Start, G. E., N. F. Hukari, J. F. Sagendorf, J. H. Cate, and C. R. Dickson, 1980: EOCR Building Wake Effects on Atmospheric Diffusion. U.S. NRC report NUREG/CR-1395; NOAA Tech. Memo. ERL-ARL-91 (avail. NTIS, Springfield, VA), iv and 220 pp.

Symes, C. R., and R. N. Meroney, 1970: Cone Frustrums in a Shear Layer. U.S. AEC report COO-2053-4, Colorado State Univ. Fluid Dynamics and Diffusion Lab. report CER70-71CRS-RNM11 (Colo. State Univ., Ft. Collins, CO), xi and 131 pp.

Tani, I., 1957: Experimental investigation of flow separation over a step. In Proc. of Boundary Layer Research Symposium at Freiburg, Aug. 26-29, 1957, H. Görtler, editor (Springer-Verlag, Berlin and Göttingen, 1958), pp 377-386.

Thuillier, R. H., and R. L. Mancuso, 1980: Building Effects on Effluent Dispersion From Roof Vents at Nuclear Power Plants. EPRI report no. NP-1380, project no. 1073-1 (avail. Electric Power Research Institute, Palo Alto, CA), xx and 218 pp.

Tillman, W., 1945: British Min. of Aircraft Prod. Völkenrode Translation MAP-VG 34-45T (cited by Bradshaw and Wong, 1972).

Turner, D. B., 1969: Workbook of Atmospheric Dispersion Estimates. U.S. Dept. of HEW, Public Health Service, Publication no. 999-AP-26, viii and 84 pp.

U.S. E.P.A., 1978: Guidelines on Air Quality Models. Environmental Protection Agency Office of Air Qual. Planning and Stds. report no. EPA-450/2-78-027 (OAQRS no. 1.2-080) (U.S. EPA, Research Triangle Park, NC), viii and 84 pp.

U.S. E.P.A., 1980: Guidelines for Determination of Good Engineering Practice Stack Height (technical support document for stack height regulations). Environmental Protection Agency Office of Air Qual. Planning and Stds. report no. EPA-450/4-80-023 (draft), (U.S. EPA, Research Triangle Park, NC), iv and 80 pp.

van Eimern, J., R. Karschon, L. A. Razumova, and G. W. Robertson, 1964: Windbreaks and Shelterbelts. Tech. Note no. 59, WMO-No.147.TP.70 (Secretariat of the World Meteorological Organization, Geneva, Switzerland), xvi and 188 pp.

Vincent, J. H., 1977: Model experiments on the nature of air pollution transport near buildings. Atmos. Environment 11, no. 8, pp 765-774.

Vincent, J. H., 1978: Scalar transport in the near aerodynamic wakes of surface mounted cubes. Atmos. Environment 12, no. 6/7, pp 1319-1322.

Wilson, D. J., 1976a: Contamination of Building Air Intakes from Nearby Vents. Univ. of Alberta Dept. of Mech. Engng. report no. 1 (Univ. of Alberta, Edmonton, Alberta, Canada), iv and 126 pp.

Wilson, D. J., 1976b: Contamination of air intakes from roof exhaust vents. ASHRAE Trans. 82, part 1, pp 1028-1038.

Wilson, D. J., 1977a: Dilution of exhaust gases from building surface vents. ASHRAE Trans. 83, part 1, pp 168-176.

Wilson, D. J., 1977b: Effect of vent stack height and exit velocity on exhaust gas dilution. ASHRAE Trans. 83, part 1, pp 157-167.

Wilson, D. J., 1979a: Height and Location of Exhaust Stacks to Reduce Recirculation to Air Intakes. ASHRAE final report no. RP204; Univ. of Alberta Dept. of Mech. Engng. report no. 15 (Univ. of Alberta, Edmonton, Alberta, Canada), iv and 93 pp.

Wilson, D. J., 1979b: Flow patterns over flat-roofed buildings and application to exhaust stack design. ASHRAE Trans. 85, part 2, pp 284-295.

Wilson, D. J., and R. E. Britter, 1981: Predicting maximum building surface concentrations from nearby point source emissions. Presented at Air Pollution Aerodynamics Symp., Amer. Soc. Civil Engnrs'. Fall Convention, St. Louis, MO, Oct. 26-30, 43 pp.

Wilson, D. J., and D. D. J. Netterville, 1976: Influence of downwind high-rise buildings on stack design. J. Air Poll. Control Assoc. 26, no. 10, pp 976-980.

Wilson, D. J., and D. D. J. Netterville, 1978: Interaction of a roof-level plume with a downwind building. Atmos. Environment 12, no. 5, pp 1051-1059.

Woo, H. G. C., J. A. Peterka, and J. E. Cermak, 1977: Wind-Tunnel Measurements in the Wakes of Structures. NASA contractor report NASA CR-2806 (avail. NTIS, Springfield, VA), xvi and 226 pp.

Woodruff, N. P., and A. W. Zingg, 1952: Wind-Tunnel Studies of Fundamental Problems Related to Windbreaks. U.S. Dept. of Agriculture Soil Conservation Service report SCS-TP-112, 25 pp.

Yang, B. T., and R. N. Meroney, 1970: Gaseous Dispersion Into Stratified Building Wakes. Colorado State Univ. Fluid Dynamics and Diffusion Lab. report CER70-71BTY-RNM-8 (Col. State Univ., Ft. Collins, CO), xi and 103 pp.

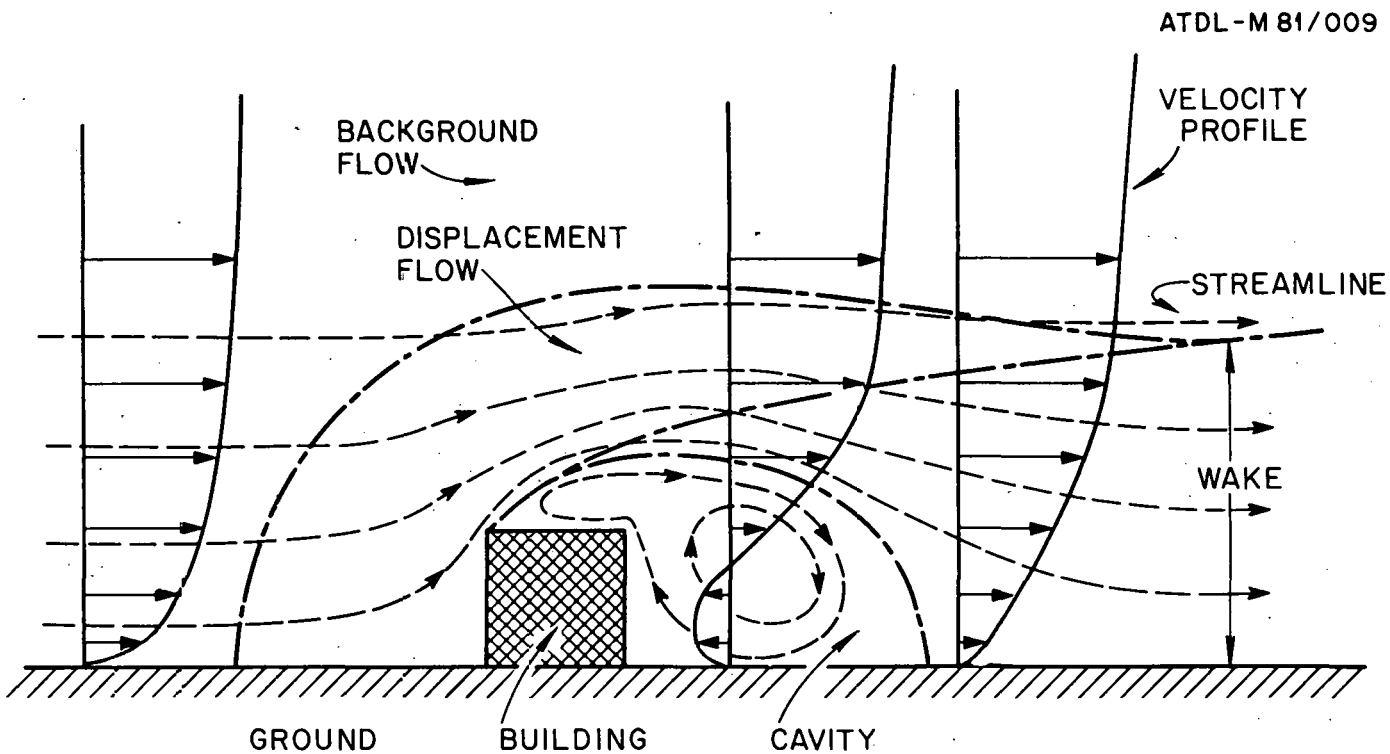

Figure 1. Simplified early model of centerline flow near a sharp-edged building normal to a deep boundary layer wind (from ASME, 1973).

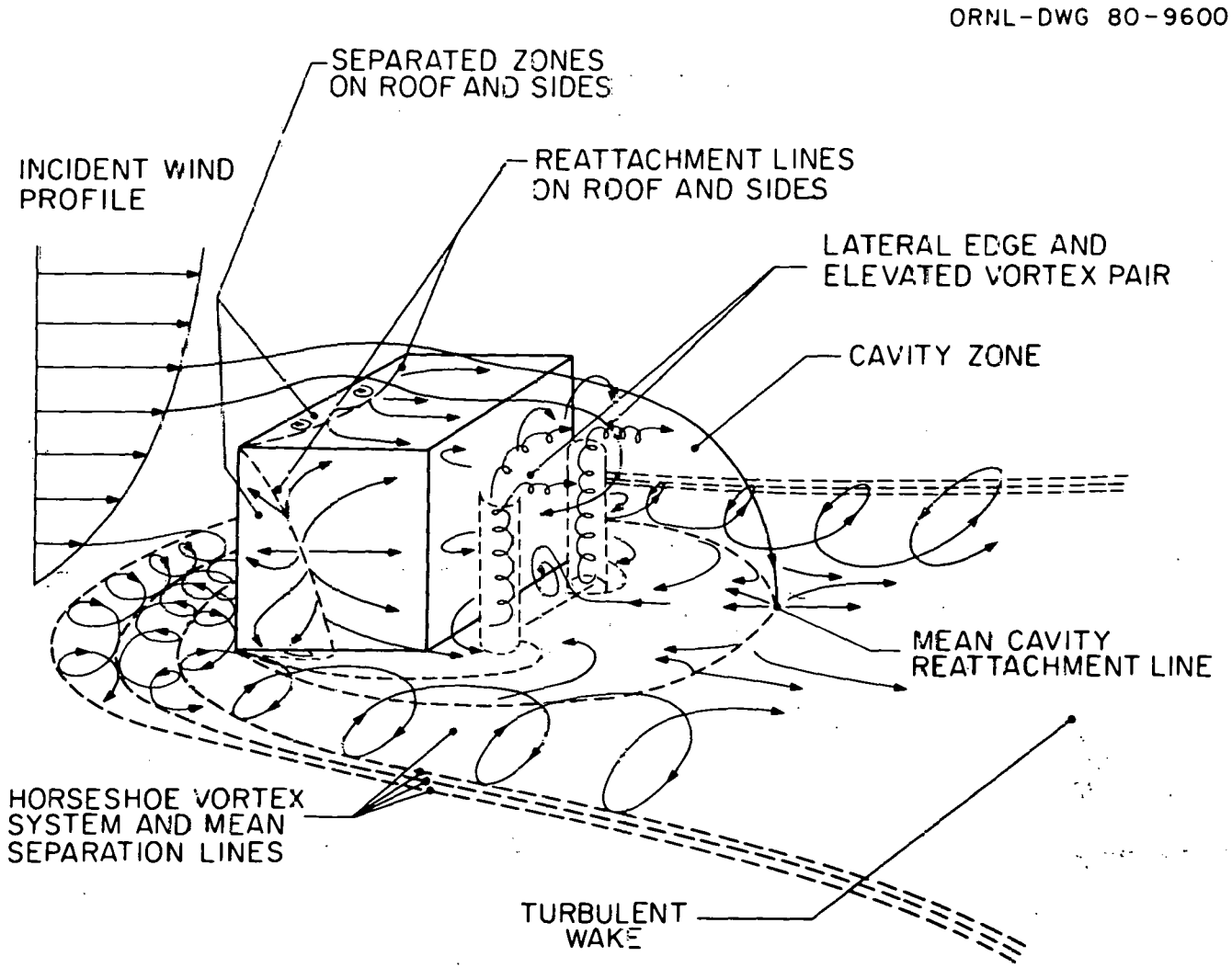

Figure 2. Recent model of flow near a sharp-edged building normal to a deep boundary layer wind (based on Woo, Peterka, and Cermak, 1977, and Hunt et al., 1978).

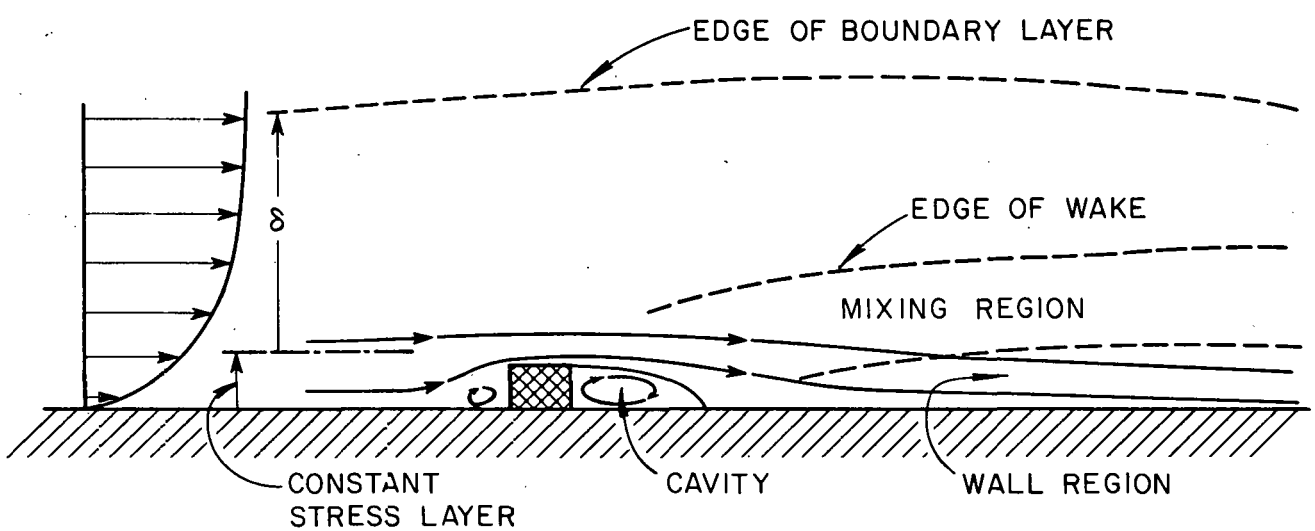

Figure 3. Two-dimensional obstacles in a deep turbulent boundary layer wind (based on Counihan, Hunt, and Jackson, 1974).

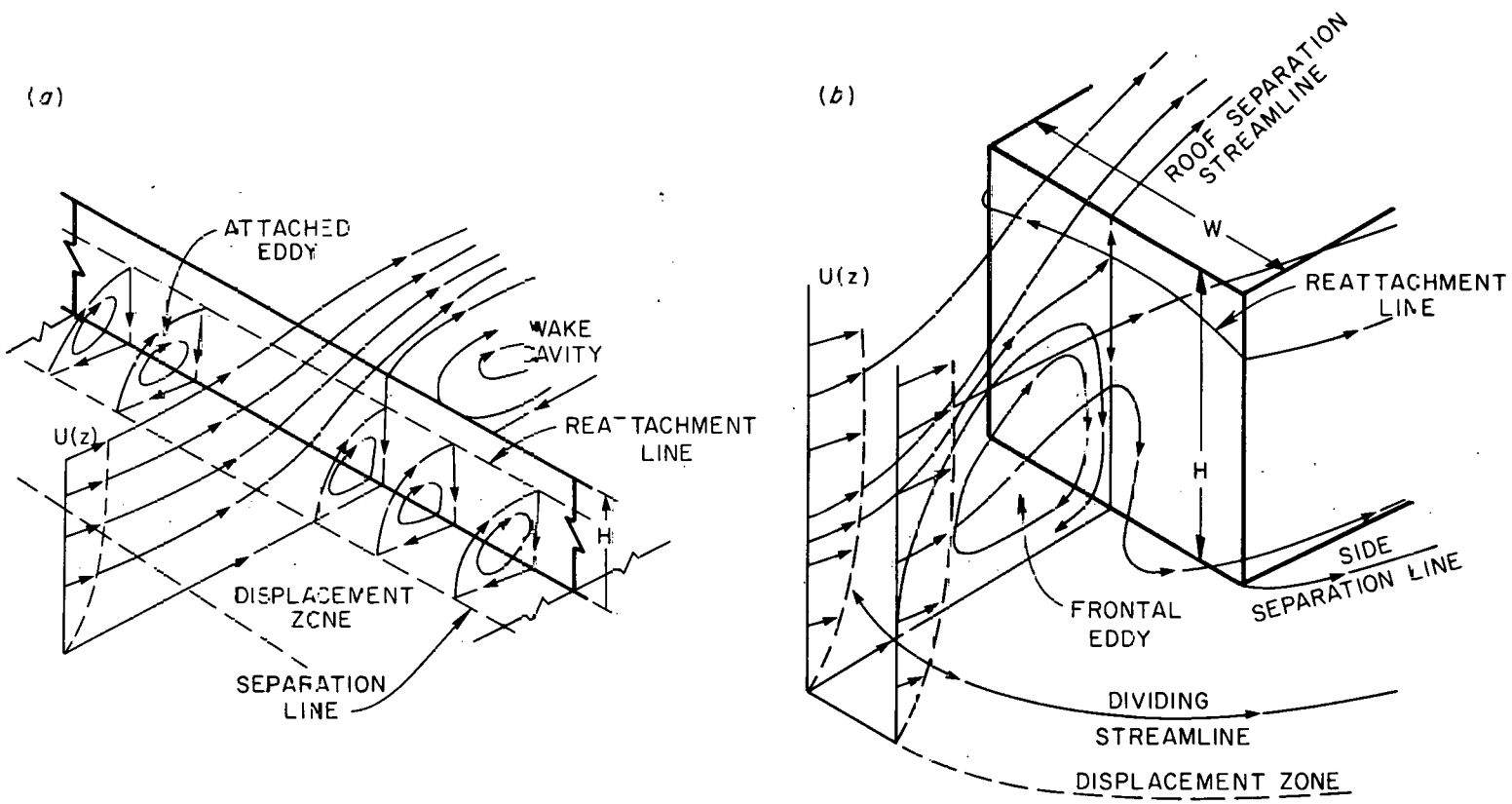

Figure 4. Deep boundary layer winds approaching obstacles. (a) two-dimensional fence; (b) three-dimensional block (based on Baines, 1963).

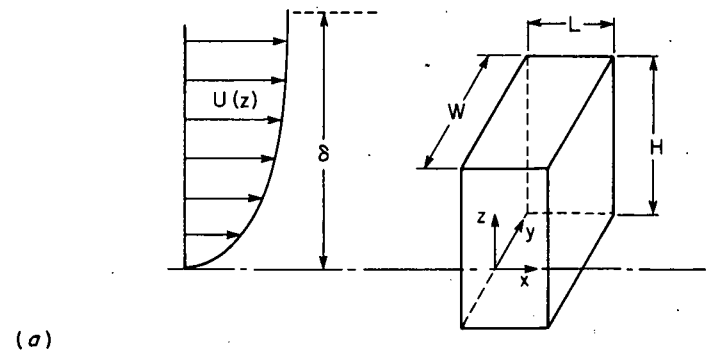

(a)

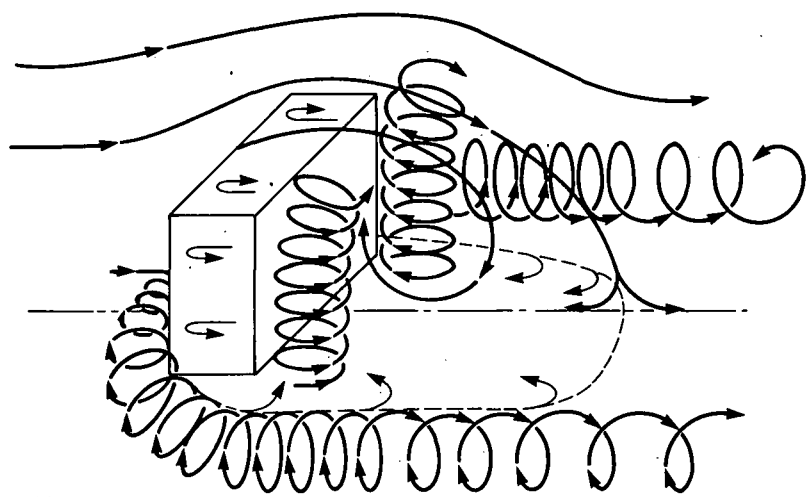

(b)

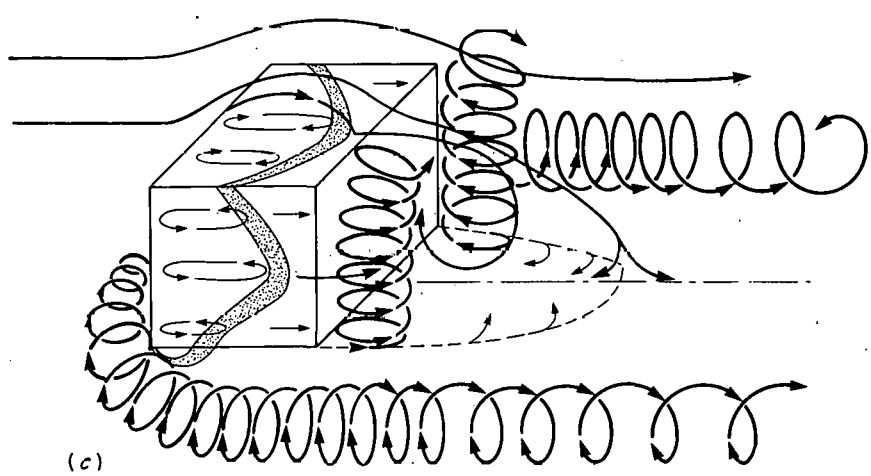

(c)

Figure 5. Flow patterns near buildings of different L/H normal to boundary layer wind. (a) nomenclature; (b) L/H small enough that roof and side reattachment do not occur; (c) L/H large, so reattachment does occur.

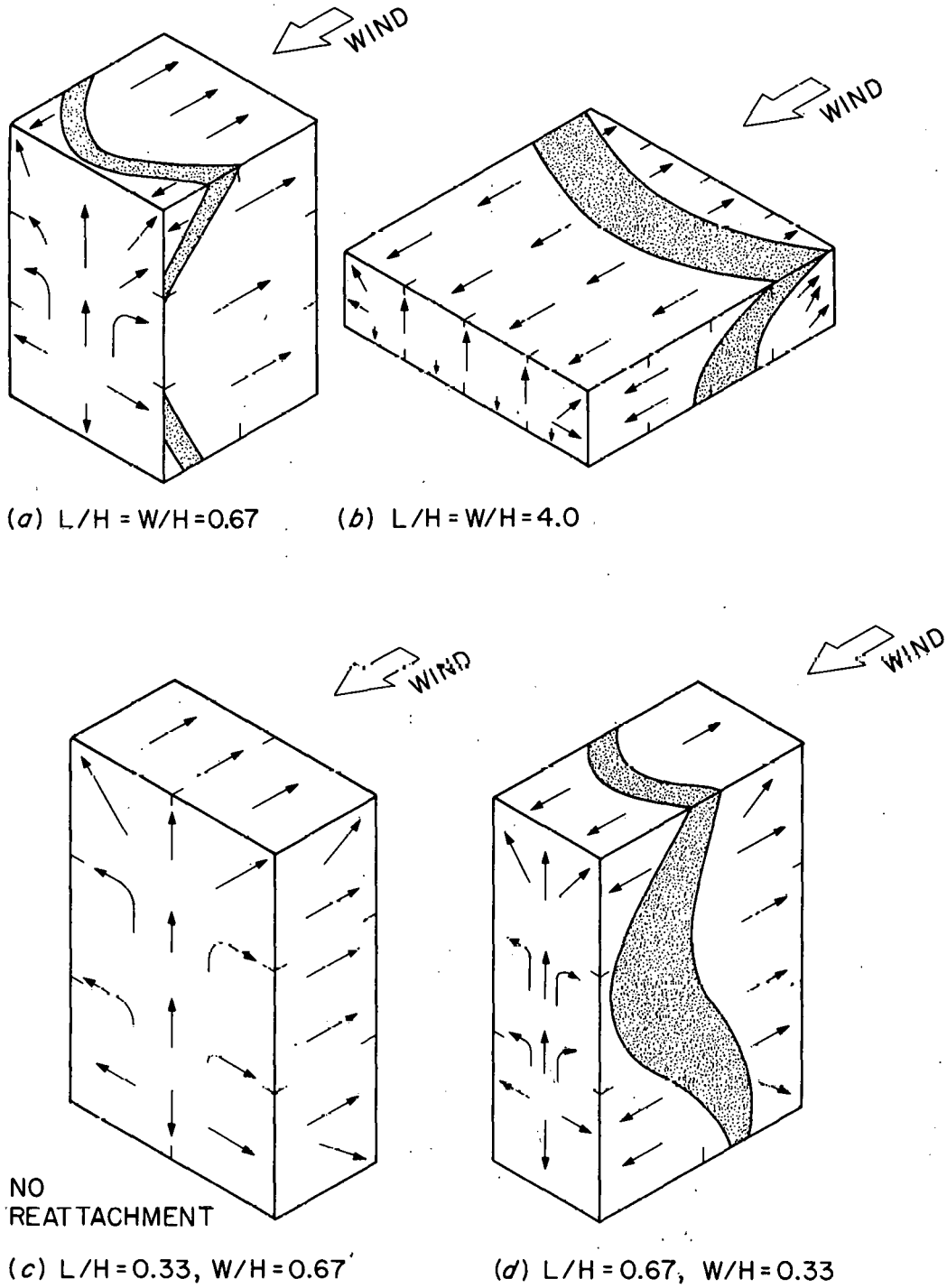

Figure 6. Near-surface flow patterns and reattachment zones on various block-like buildings in turbulent boundary layer wind (based on Wilson, 1976a,b, and Gandemer, 1976).

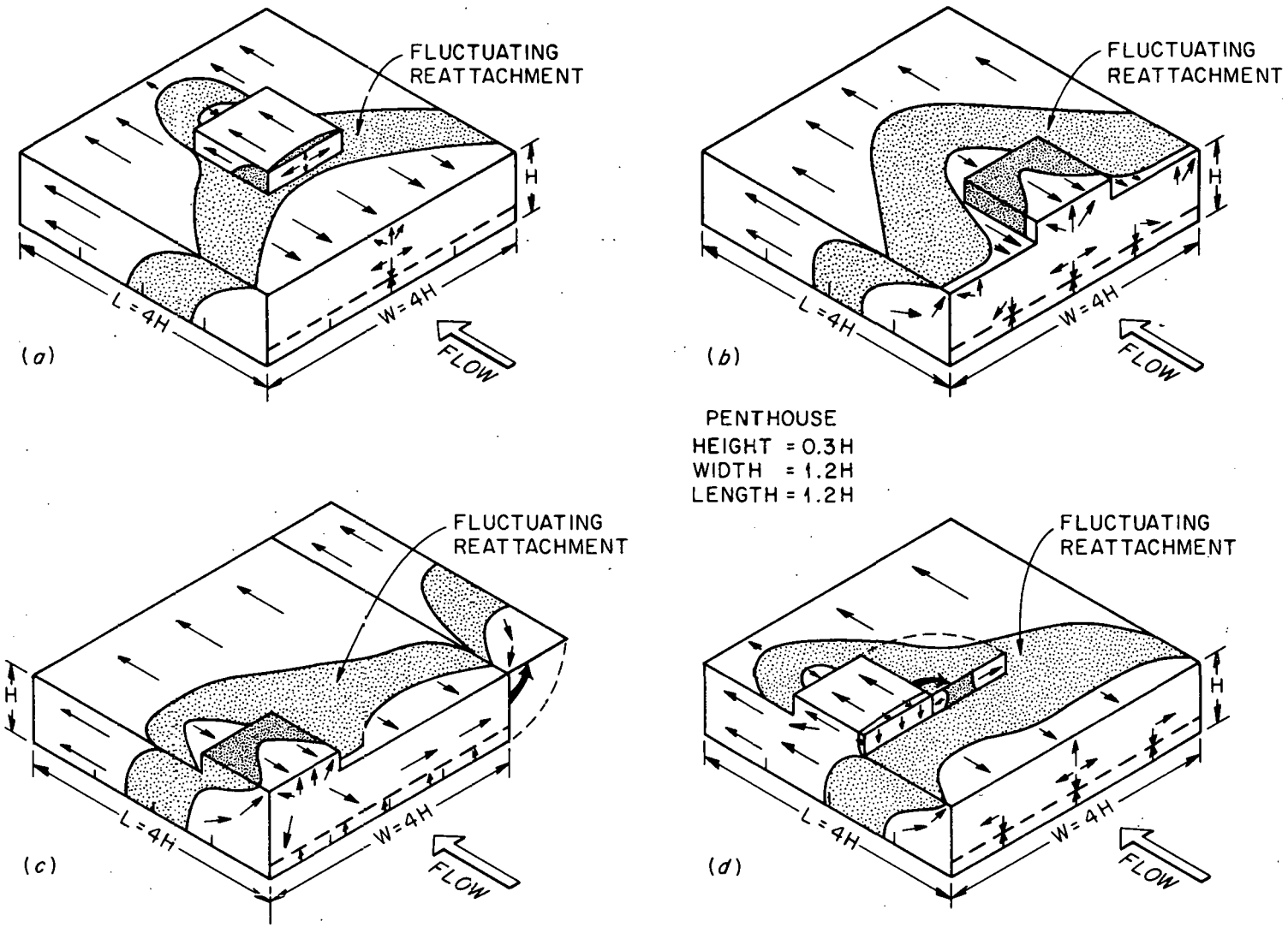

Figure 7. Surface flow patterns and reattachment zones for squat building with penthouse at different locations (after Wilson, 1979a).

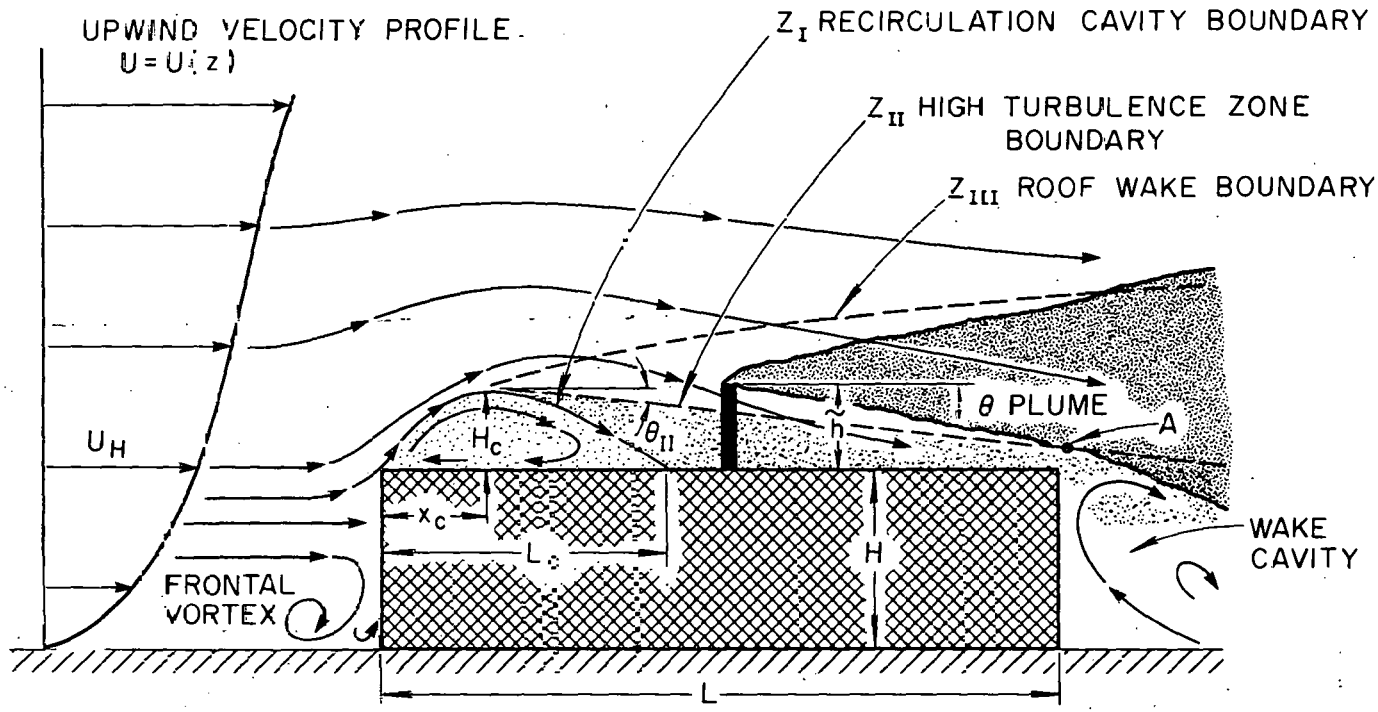

Figure 8. Flow near centerline of long, flat building roof for wind normal to exposed building face (after Wilson, 1979a,b).

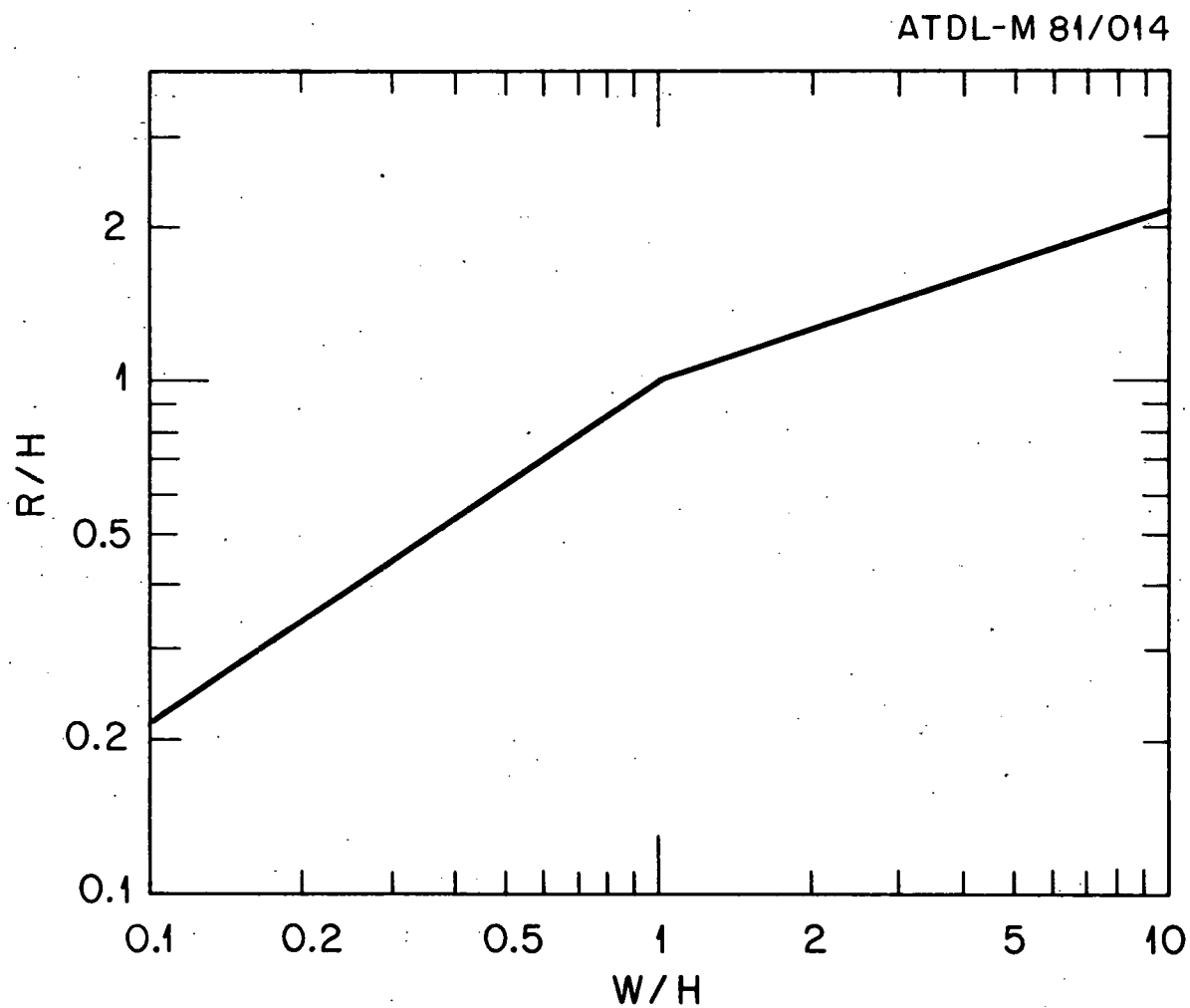

Figure 9. Wilson's (1979a,b) scale length R, relative to building height H, as function of building aspect ratio W/H. Valid only for L/H large enough to allow flow reattachment on roof.

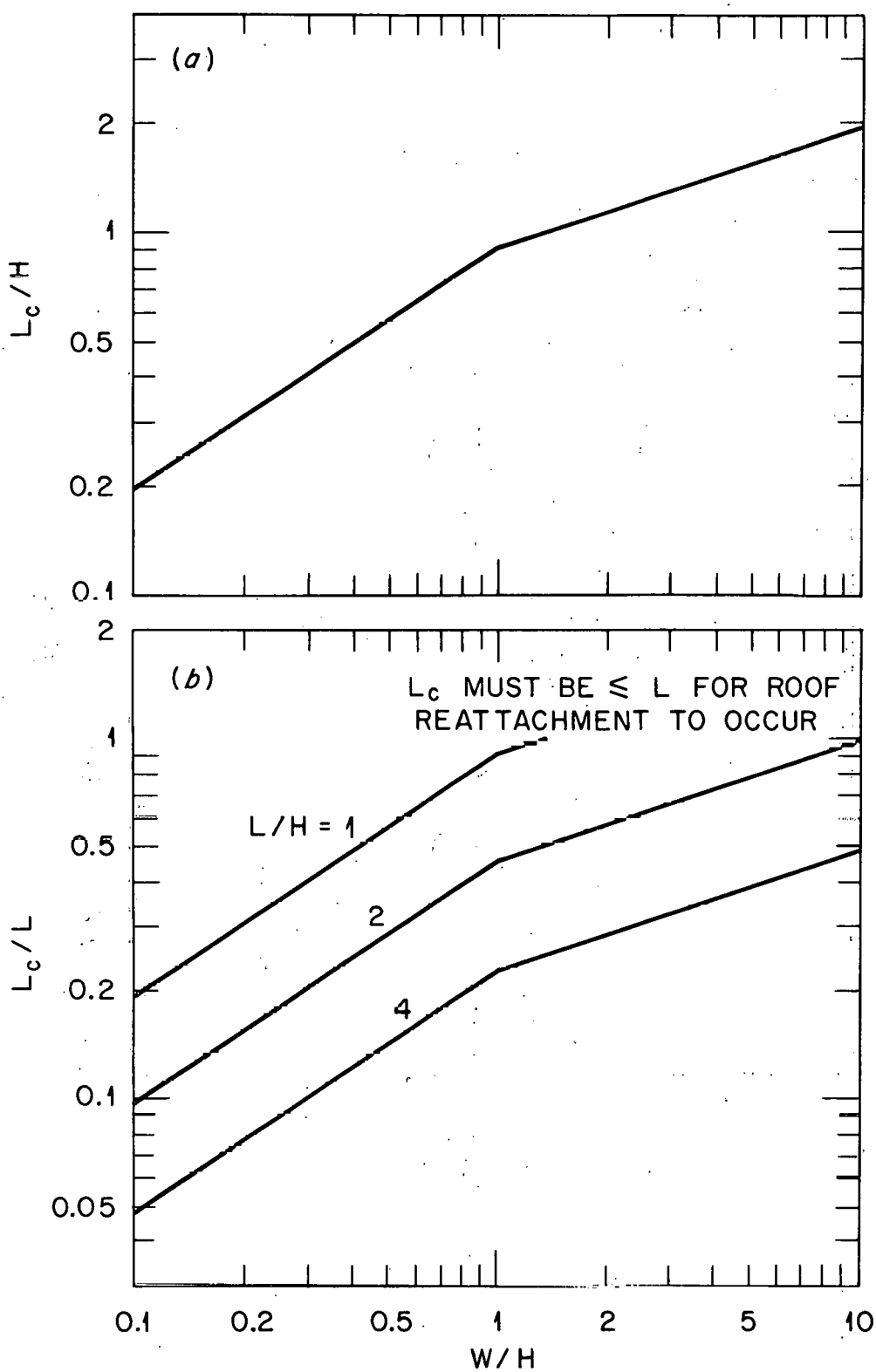

Figure 10. Centerline roof cavity length L_c relative to (a) building height H, and (b) along-wind length L, as function of aspect ratio W/H.

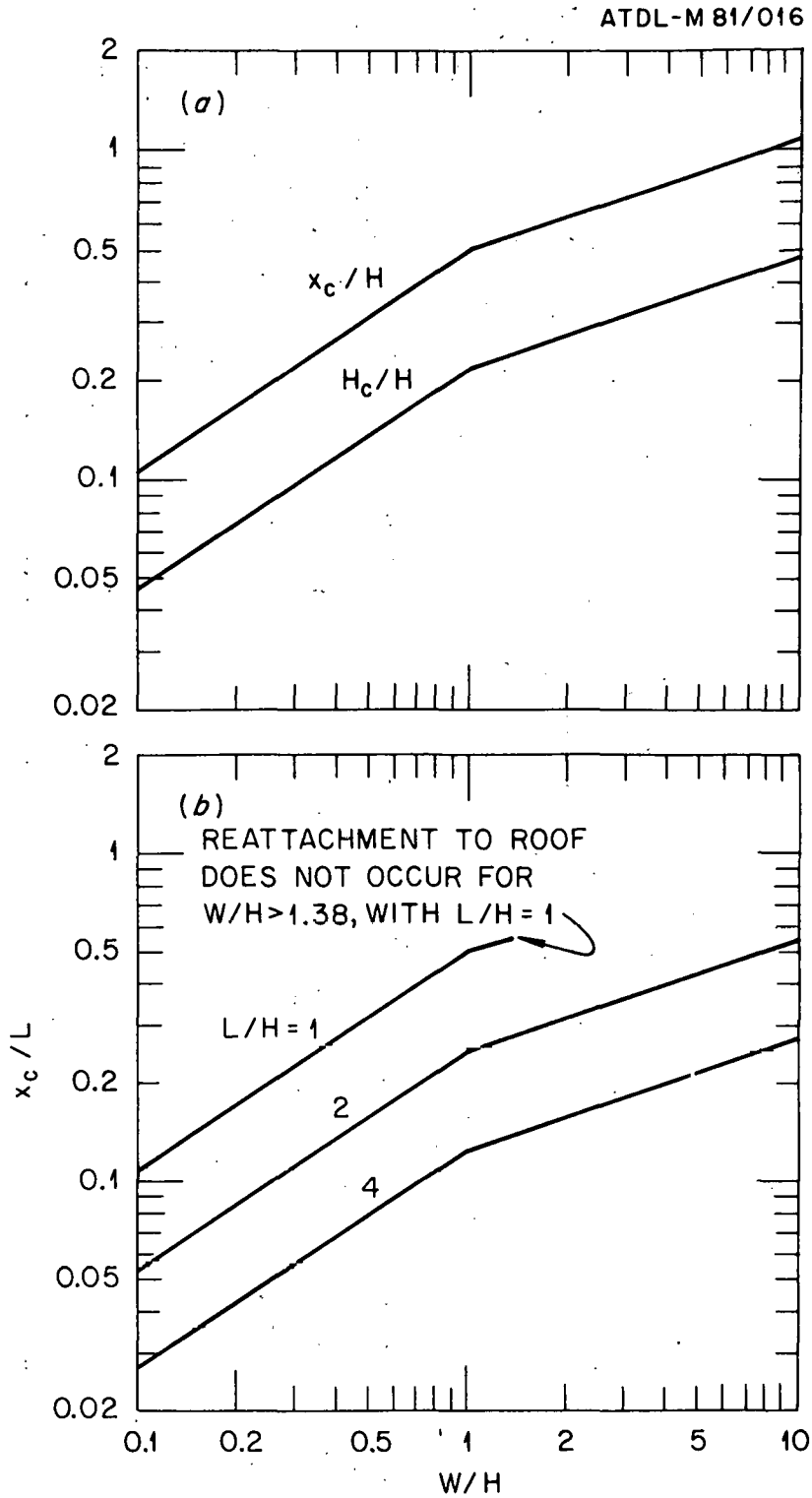

Figure 11. Maximum roof cavity height H_c, and its location x_c, as functions of aspect ratio W/H.

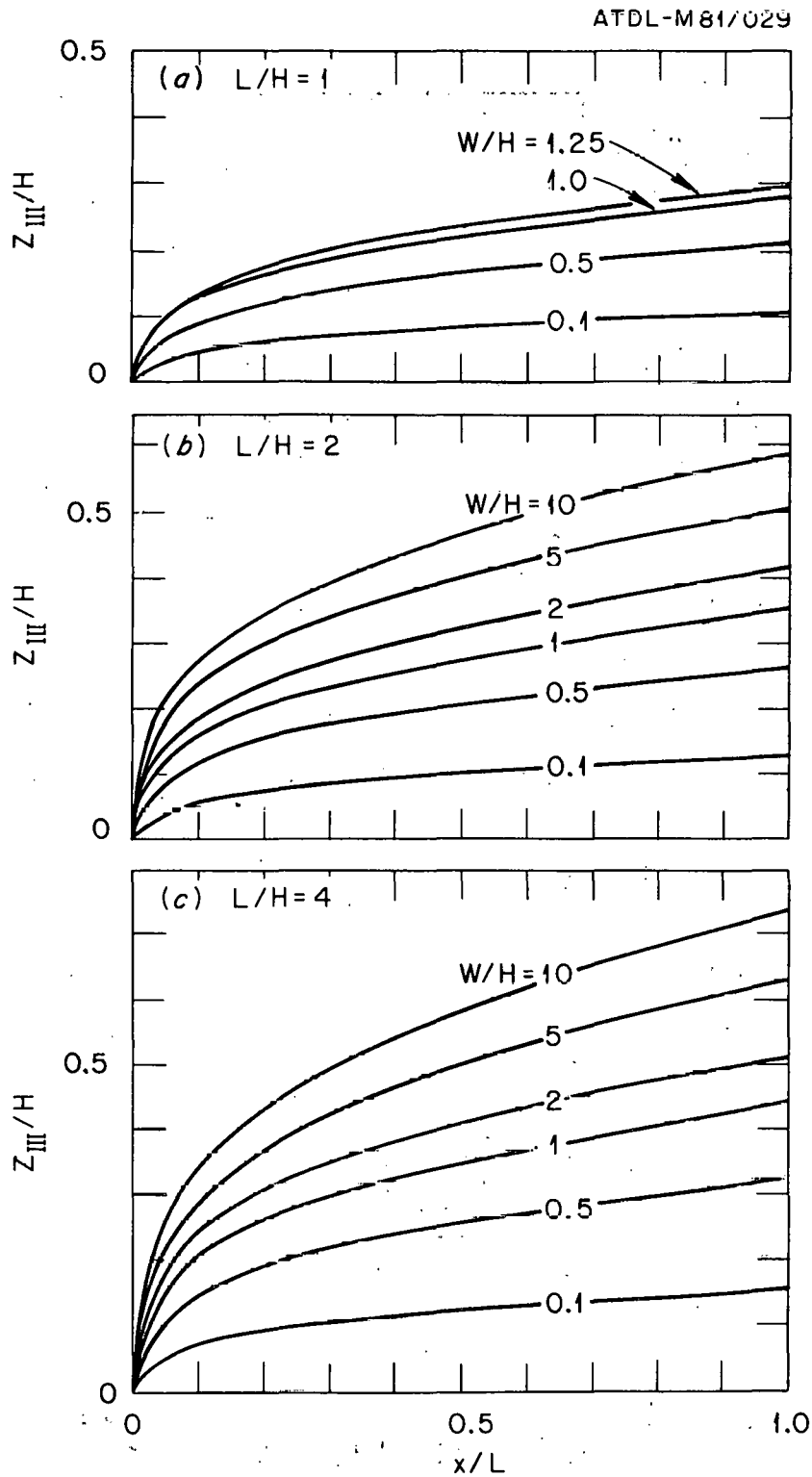

Figure 12. Centerline roof wake boundary Z_{III}/H as function of along-roof distance x/L, for several W/H and L/H ratios.

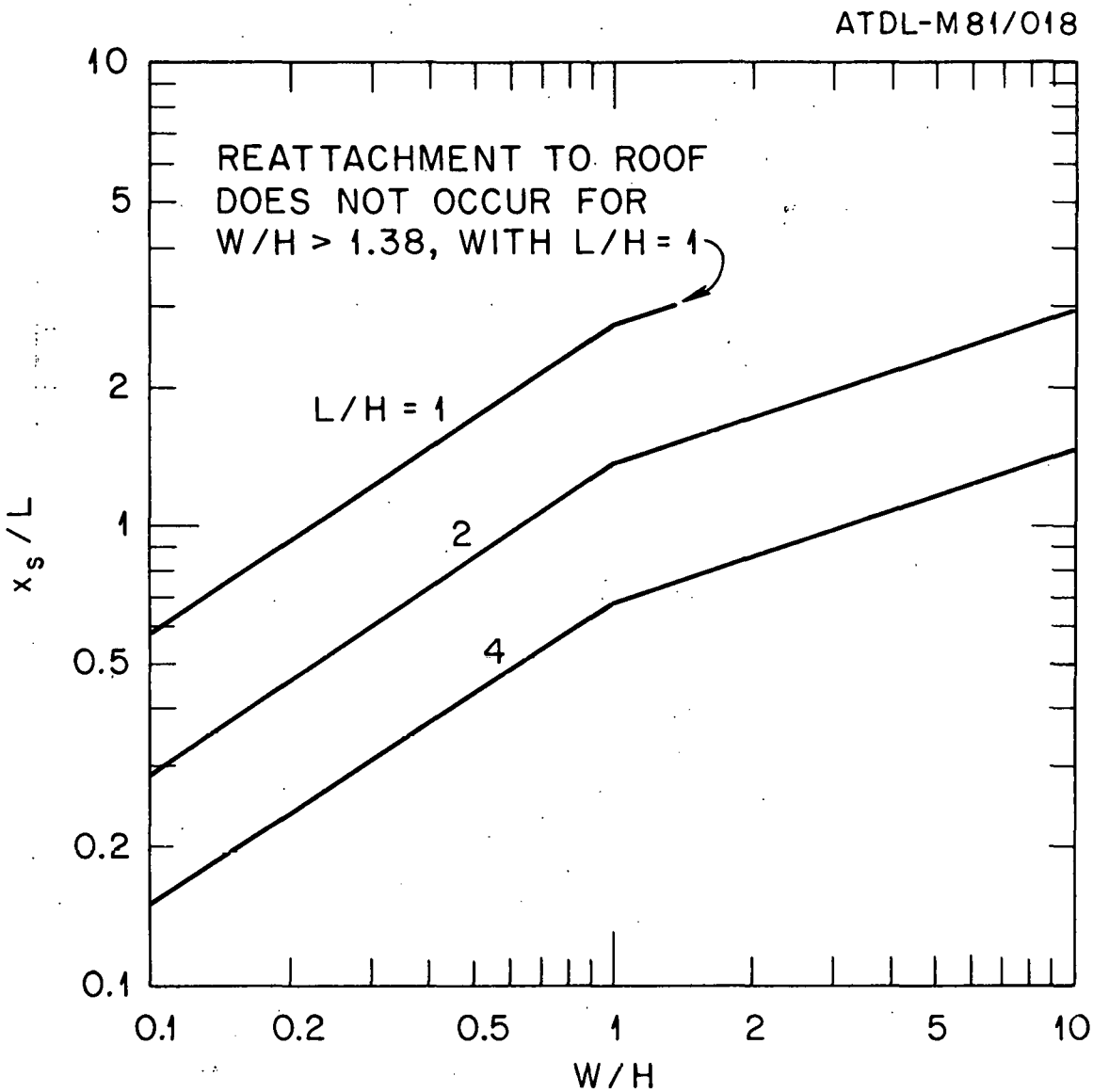

Figure 13. Point of intersection of roof cavity shear layer with roof plane, along centerline, as function of aspect ratio W/H, for several L/H.

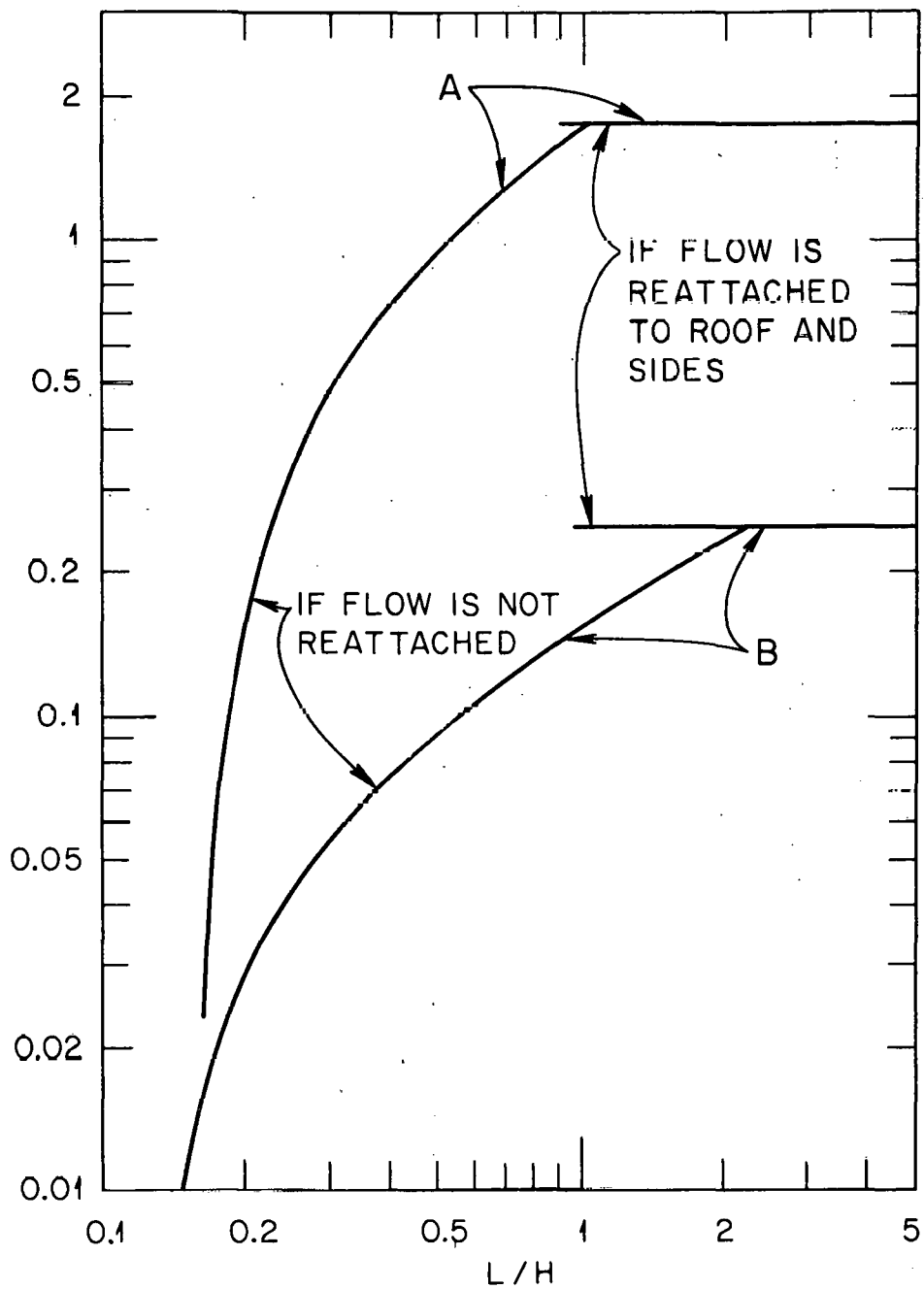

Figure 14. Factors A and B as functions of L/H, for calculating wake cavity length x_r using Equation 2-8.

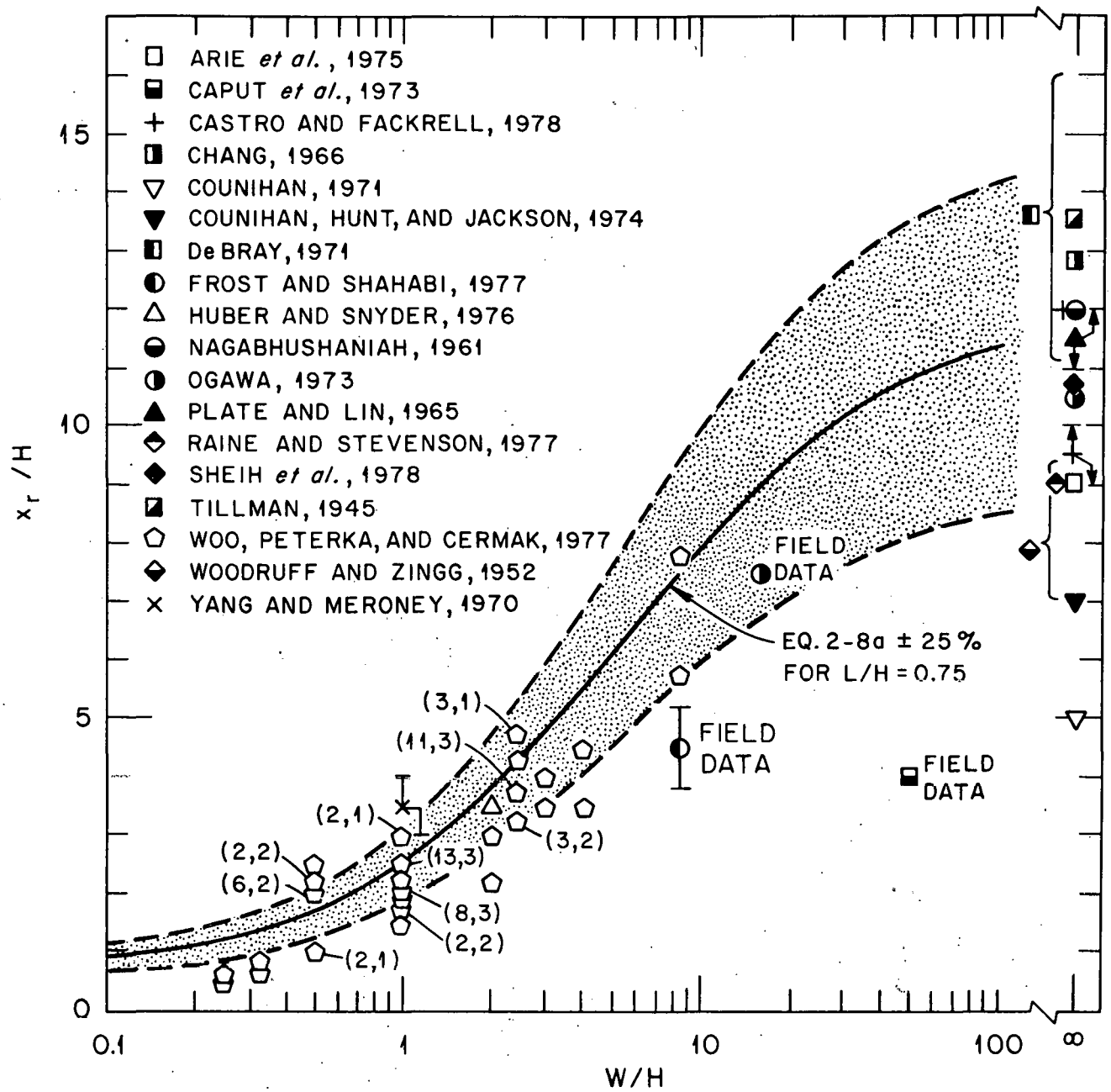

Figure 15. Wake cavity length data for structures where roof reattachment was not observed, compared to Equations 2-8a,b ± 25%. Distances measured relative to lee building face.

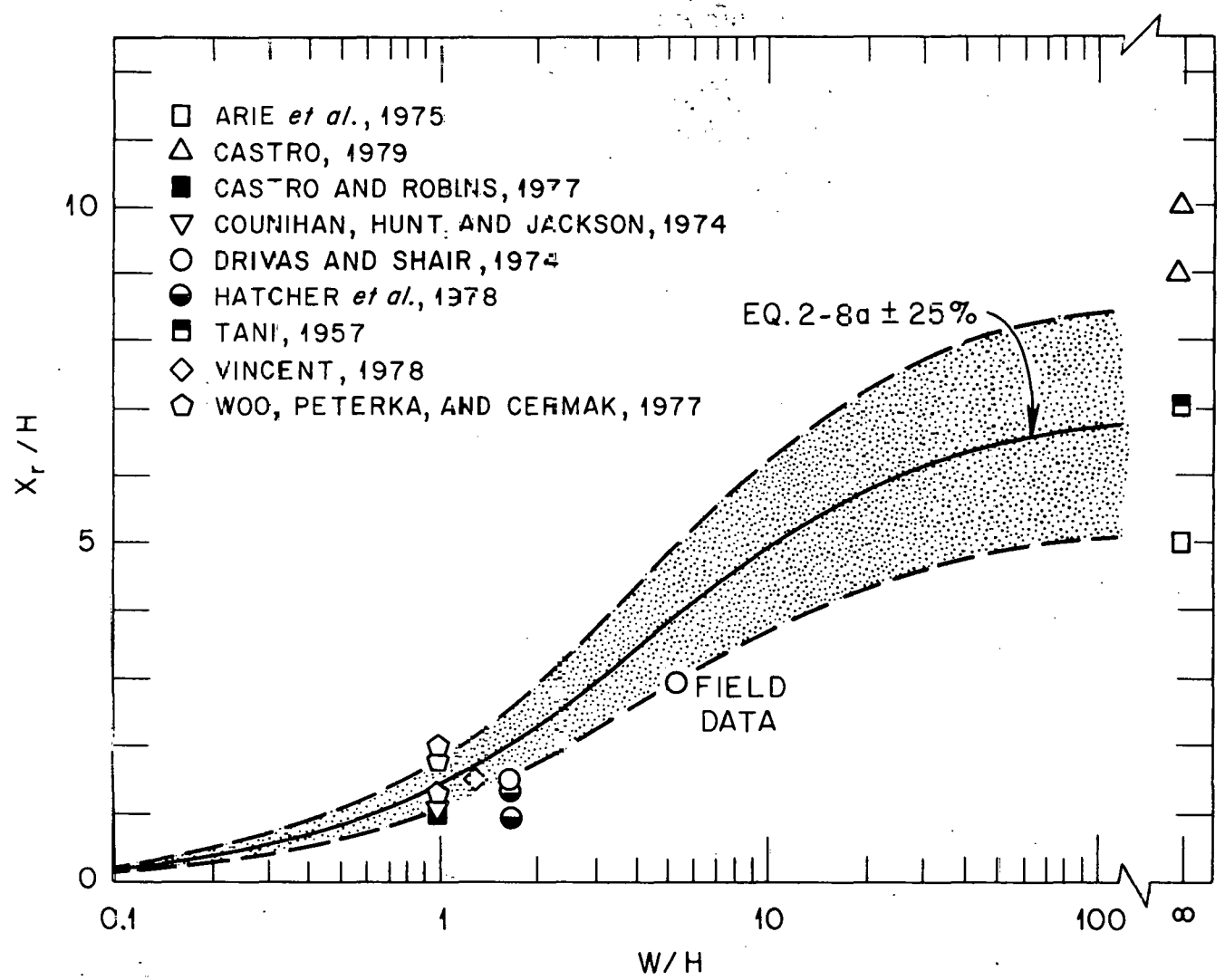

Figure 16. Wake cavity length data for structures where roof reattachment was observed, compared to Equations 2-8a,c ± 25%. Distances measured relative to lee building face.

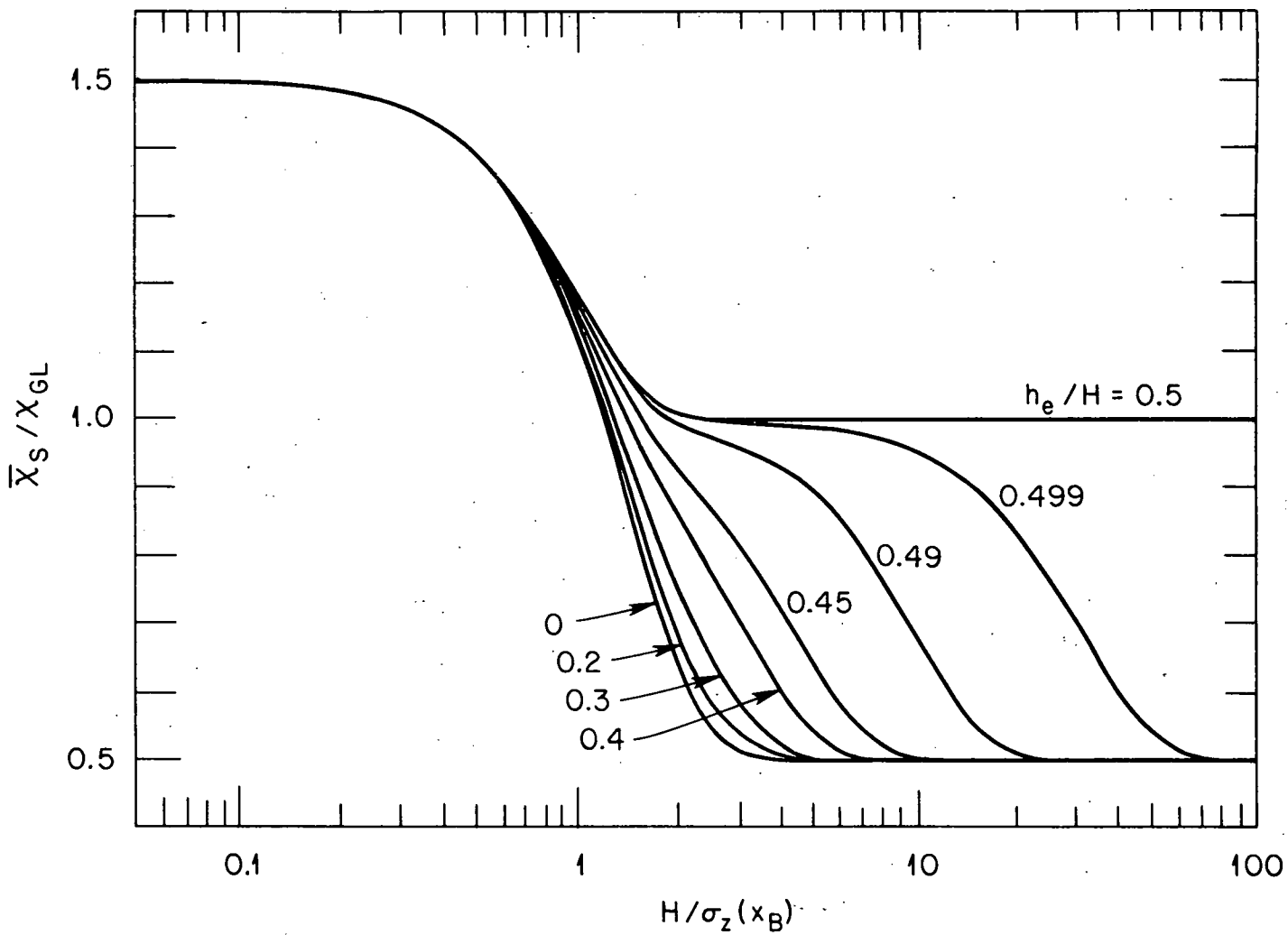

Figure 17. Estimated average concentration over building surface due to upwind source, relative to ground-level concentration without building, as function of $H/\sigma_z(x_B)$, for effective stack heights < 0.5 H.

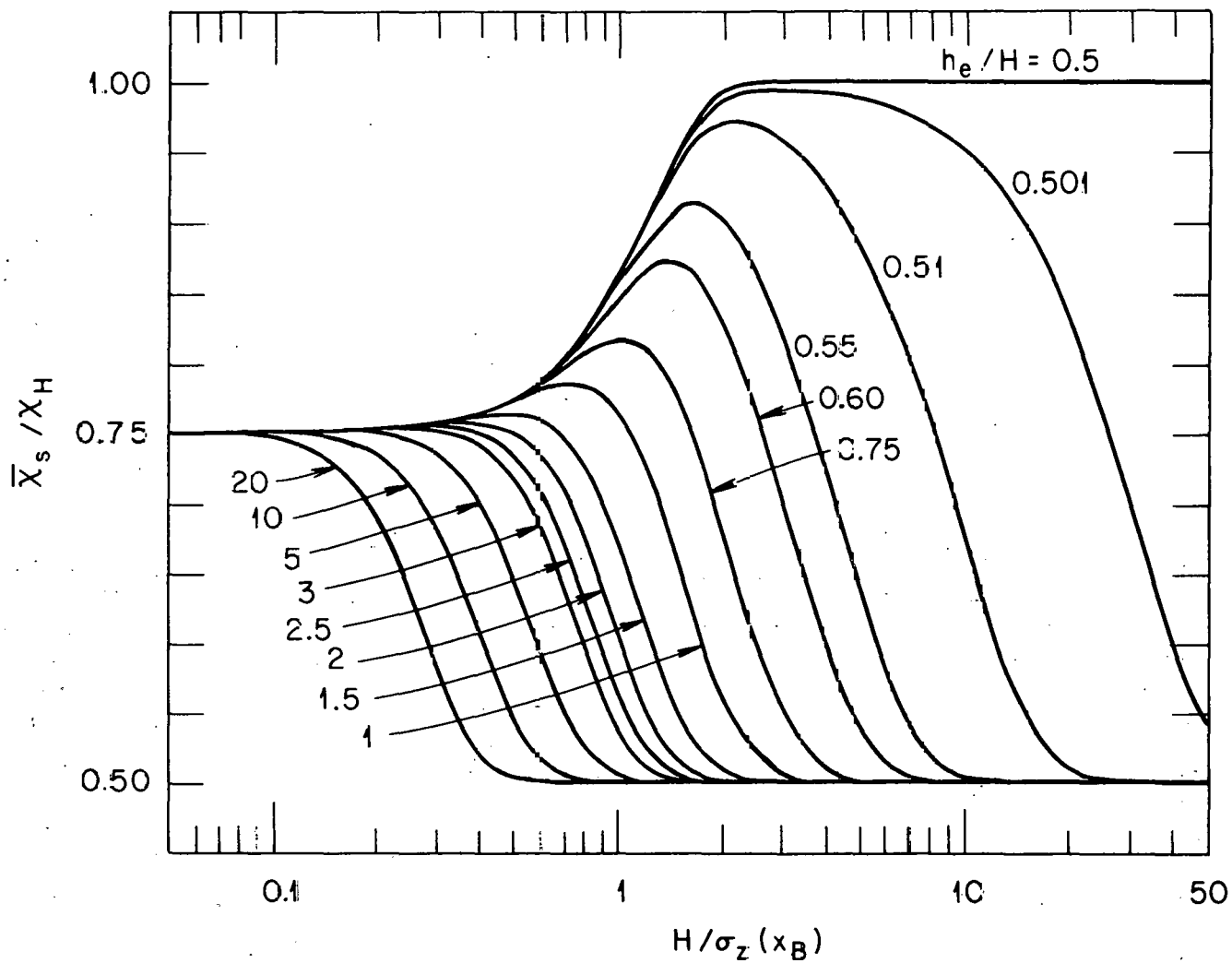

Figure 18. Estimated average concentration over building surface due to upwind source, relative to concentration at height H without building, as function of $H/\sigma_z(x_B)$, for effective stack heights > 0.5 H.

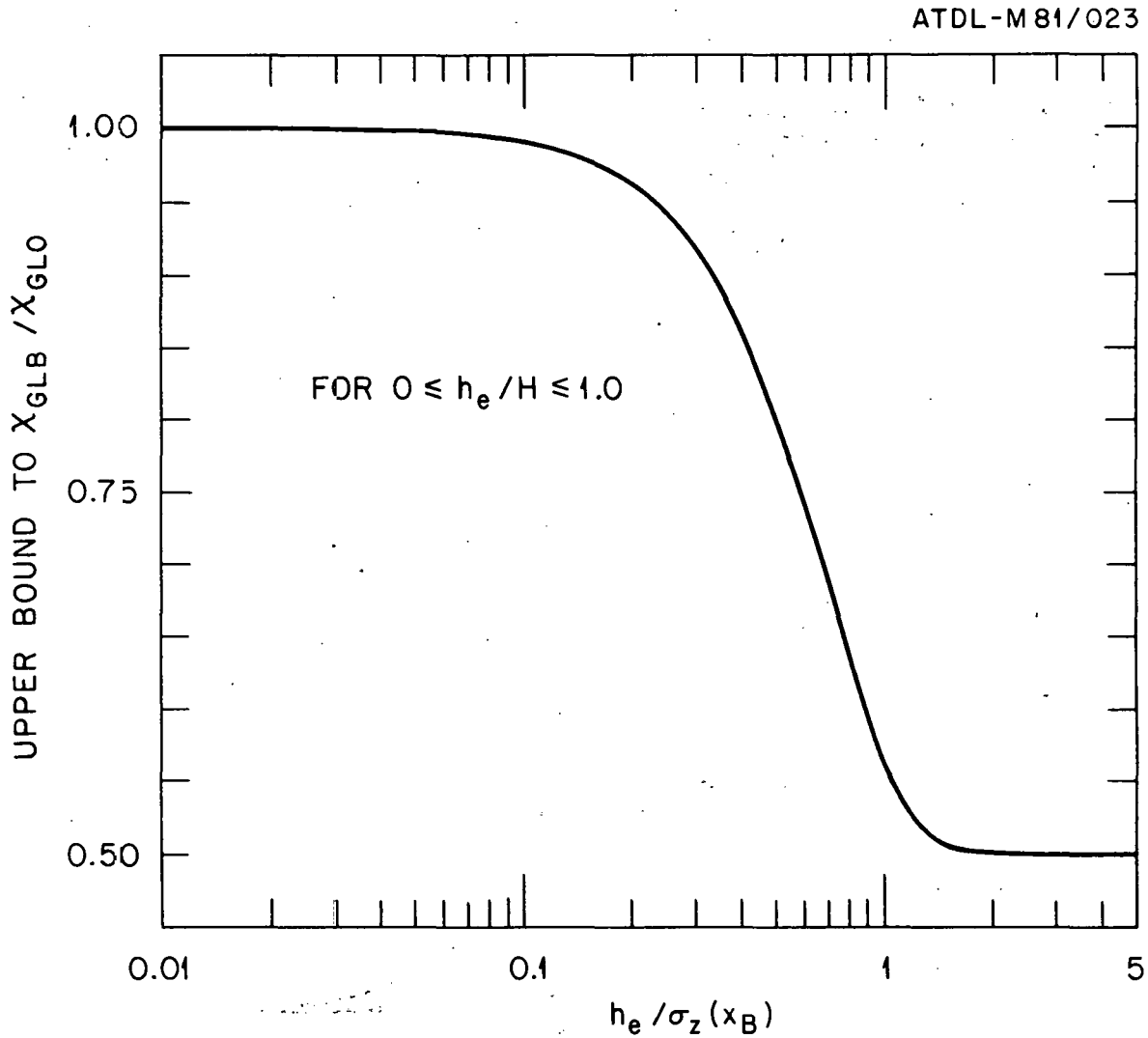

Figure 19. Upper bound on ground-level concentration near building due to upwind source, relative to ground-level concentration produced by ground-level source with no building, as function of $h_e/\sigma_z(x_B)$, for effective stack heights $\leq H$.

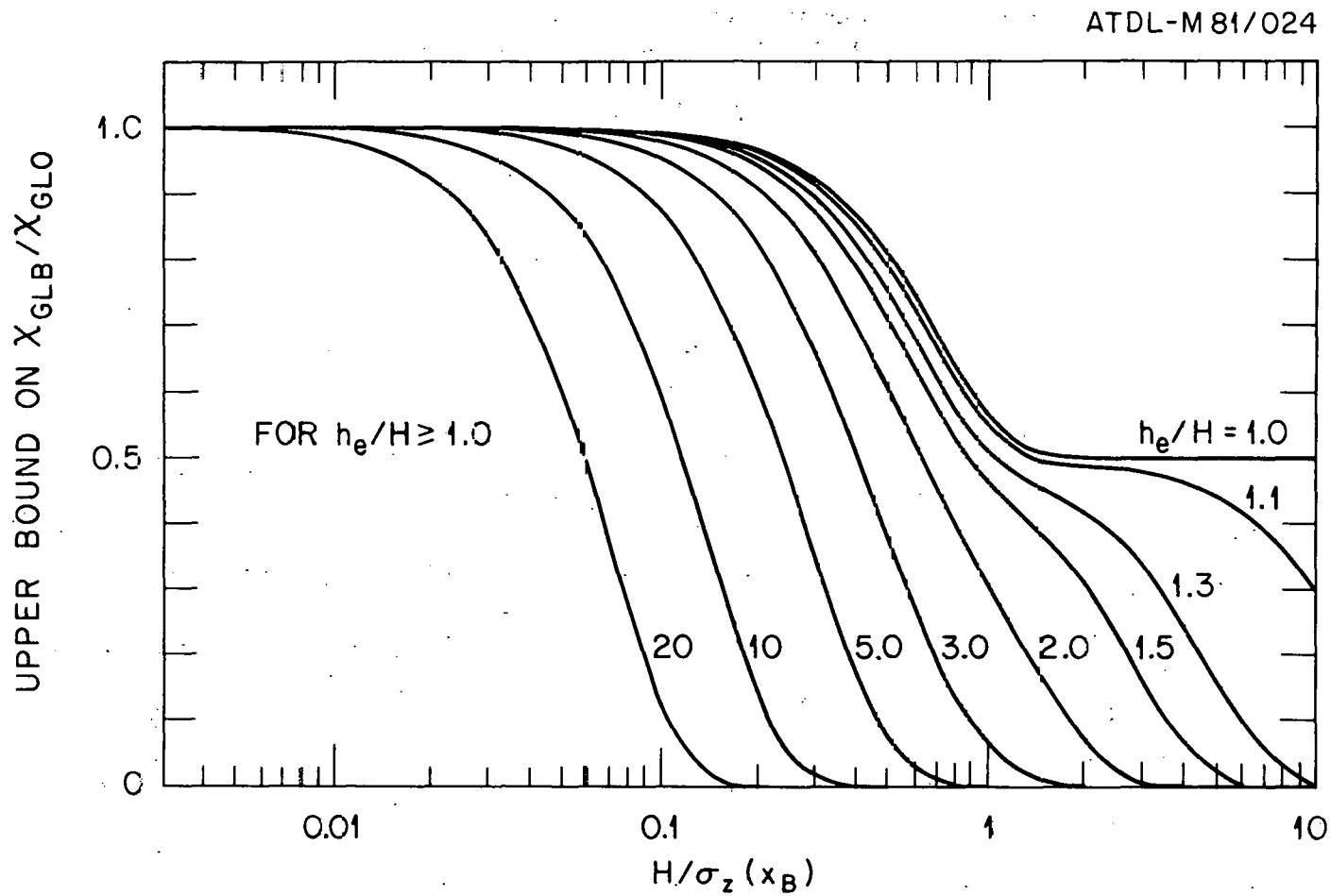

Figure 20. Upper bound on ground-level concentration near building due to upwind source, relative to ground-level concentration produced by ground-level source with no building, as function of $H/\sigma_z(x_B)$, for various $h_e/H \geq 1$.

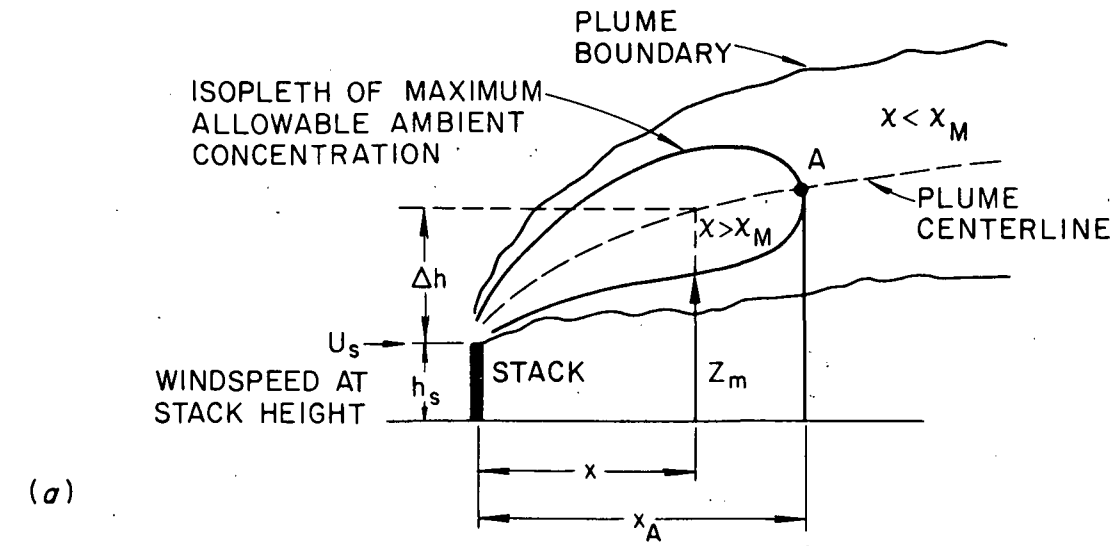

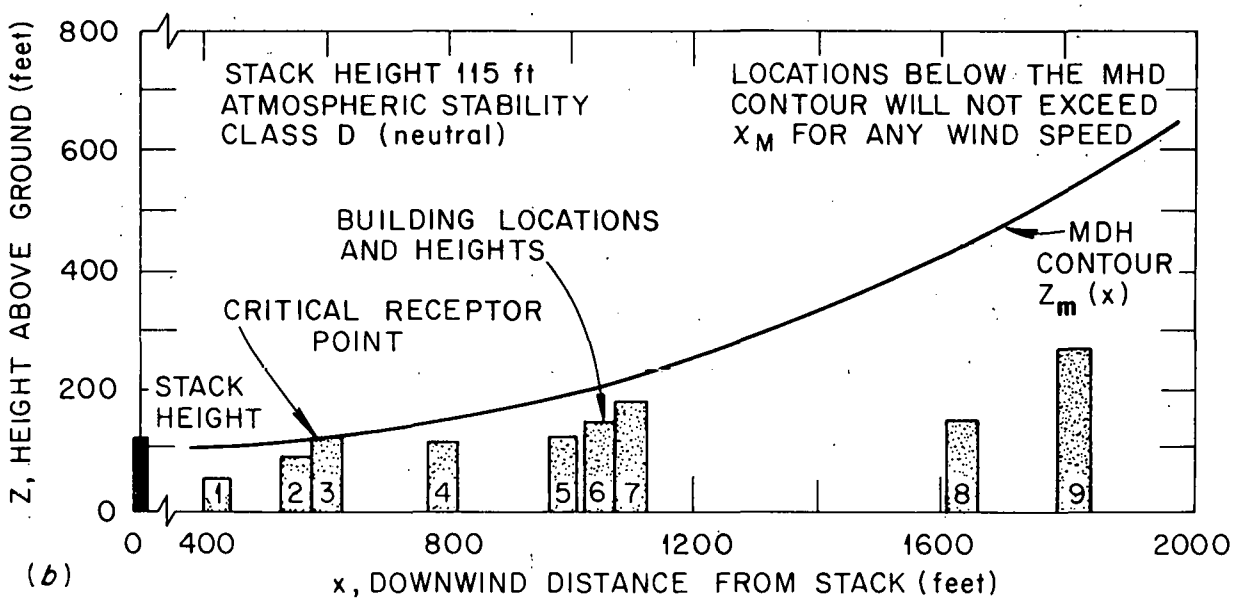

Figure 21. Definition (a), and sample computation result (b), for the "minimum descent height" Z_m of the maximum allowable concentration isopleth (after Wilson and Netterville, 1976).

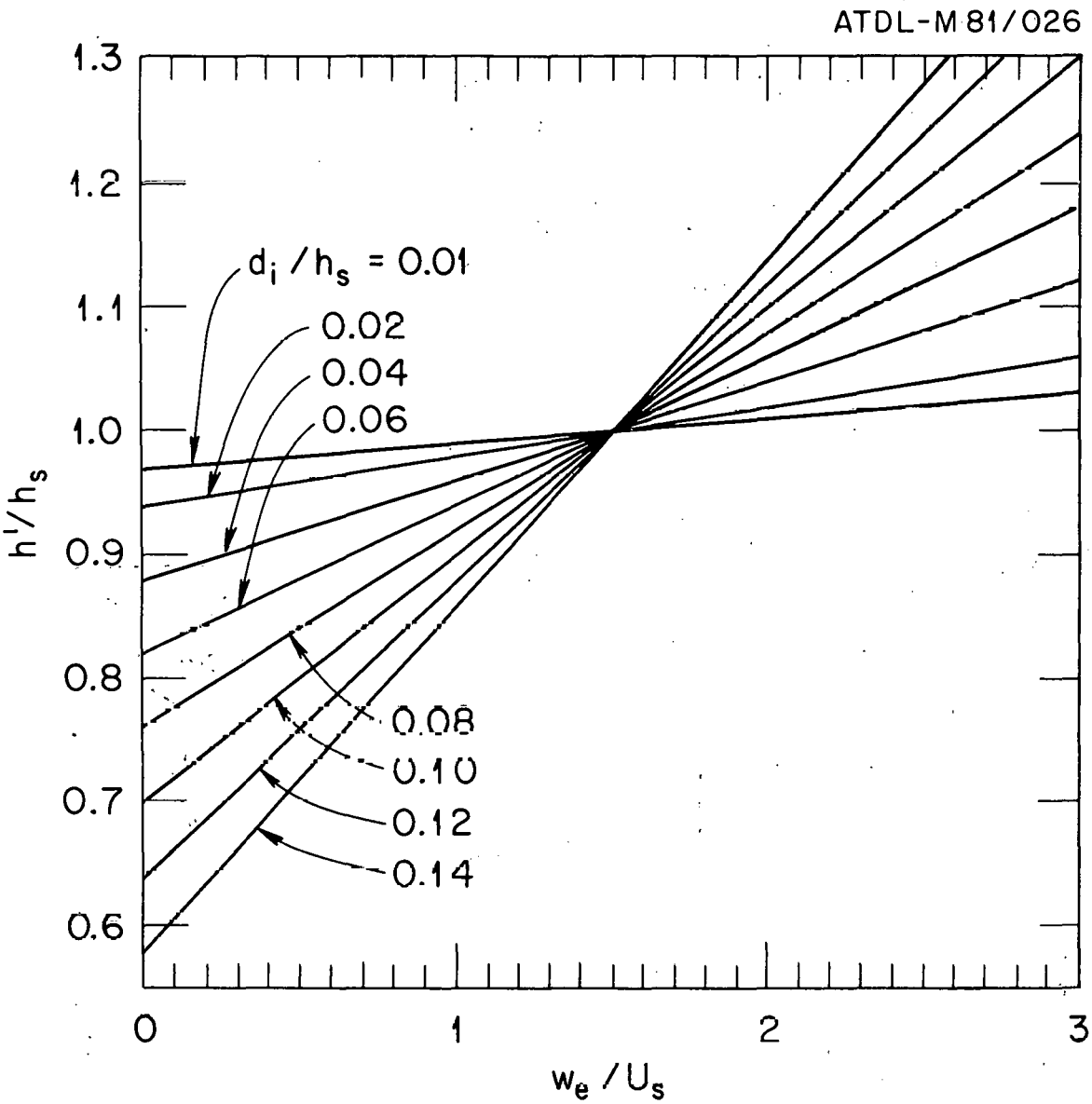

Figure 22. Effluent emission height corrected only for stack-induced tip downwash, relative to physical stack height, as function of exhaust to wind speed ratio, for several stack internal diameter to height ratios.

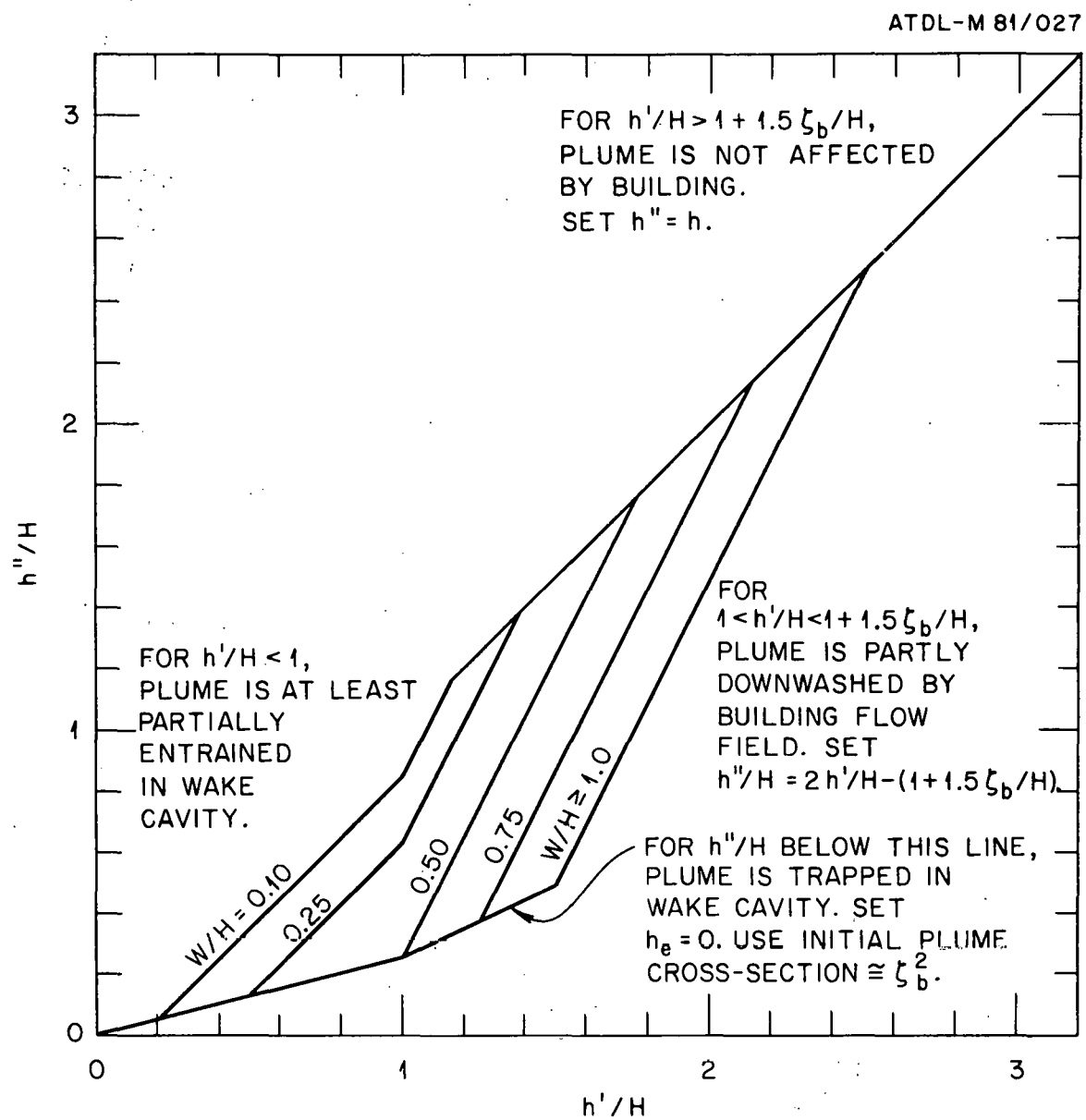

Figure 23. Emission height corrected for building aerodynamic effects, relative to building height, as function of stack downwash-corrected emission height, for several building aspect ratios W/H.

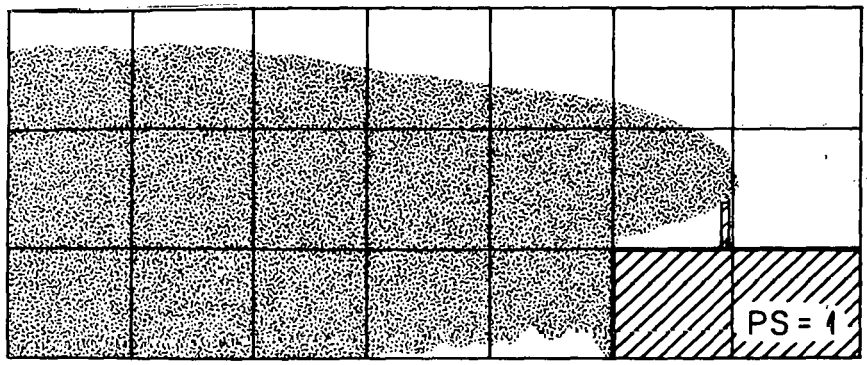

(*a*) POSITION 1, CENTER.

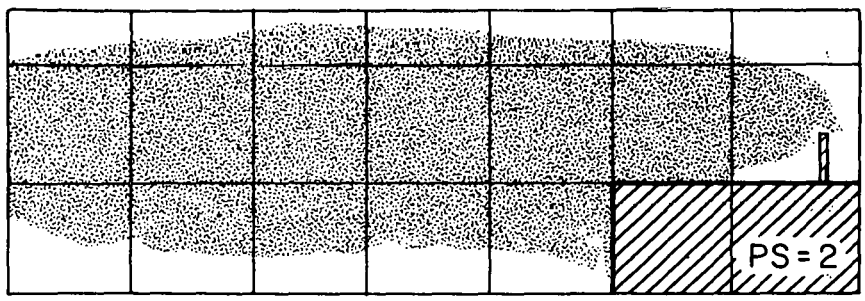

(*b*) POSITION 2, CENTER OF WINDWARD EDGE.

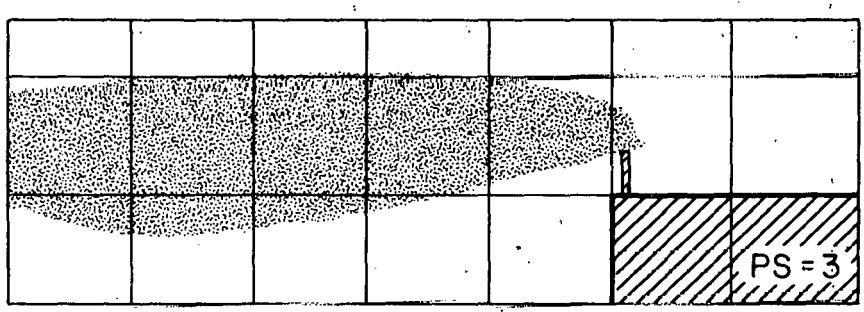

(*c*) POSITION 3, CENTER OF LEE EDGE.

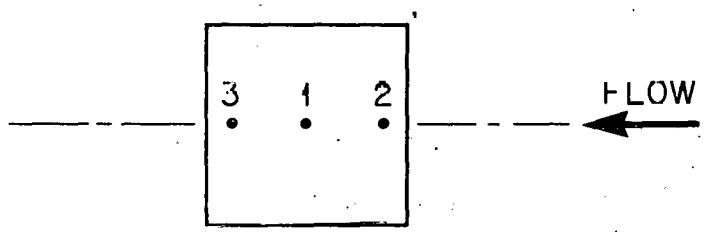

(*d*) PLAN VIEW SHOWING STACK POSITIONS.

Figure 24. Plumes from roof-centerline-mounted stacks, with h_s = 1.5 H, $w_e \cong 1.2\ U_s$ (after Koga and Way, 1979a,b).

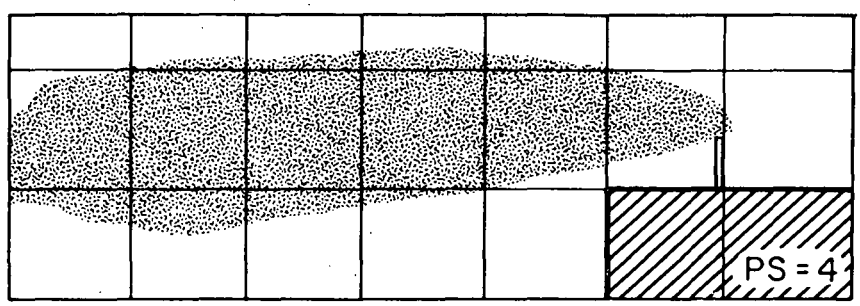

(*a*) POSITION 4, CENTER OF SIDE.

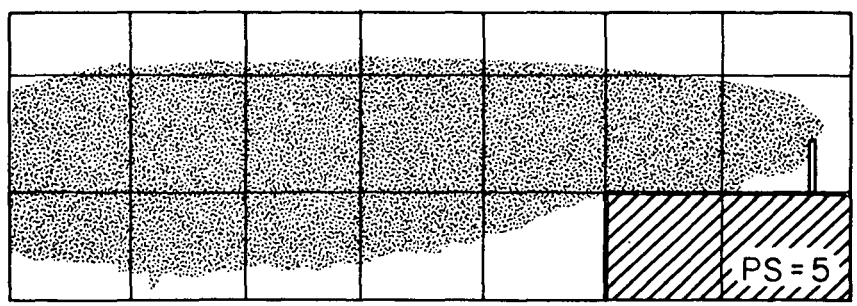

(*b*) POSITION 5, WINDWARD EDGE OF SIDE.

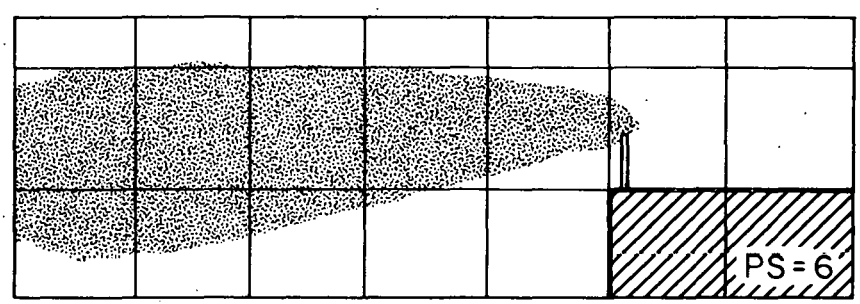

(*c*) POSITION 6, LEE EDGE OF SIDE.

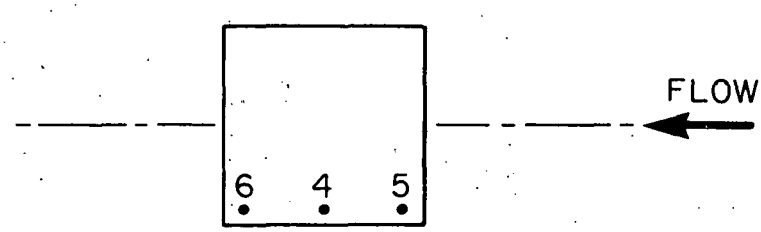

(*d*) PLAN VIEW SHOWING STACK POSITIONS.

Figure 25. Plumes from roof-edge-mounted stacks, with h_s = 1.5 H, $w_e \cong 1.2\ U_s$ (after Koga and Way, 1979a,b).

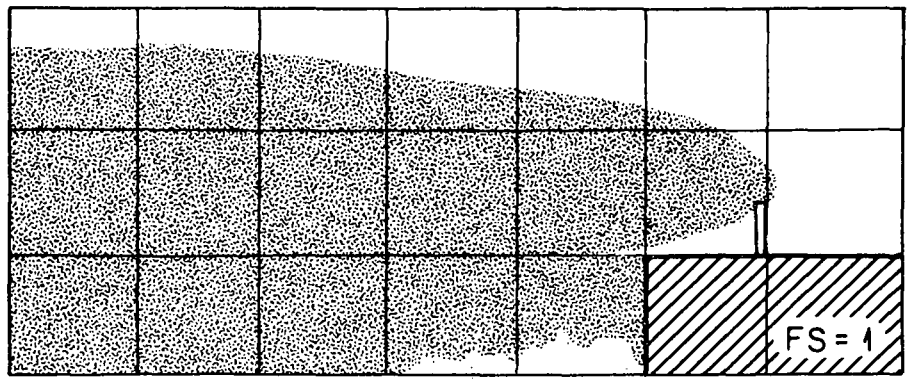

(*a*) CENTRAL STACK, $h_s/H = 1.5$, $w_e/U_s \cong 1.2$.

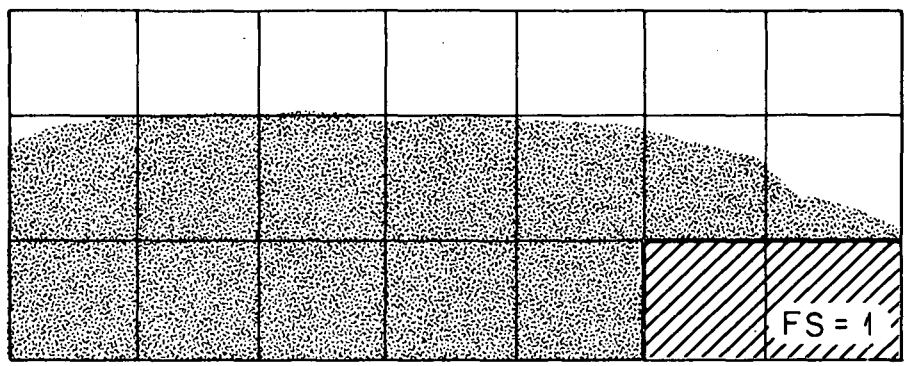

(*b*) CENTRAL VENT, $h_s/H = 1.0$, $w_e/U_s \cong 1.3$.

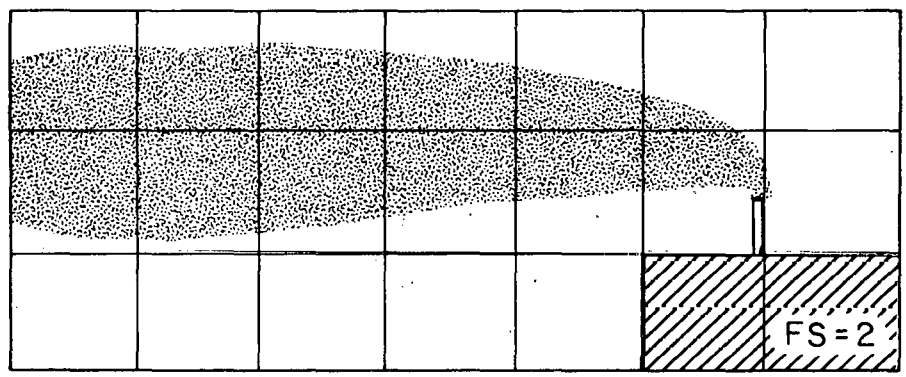

(*c*) CENTRAL STACK, $h_s/H = 1.5$, $w_e/U_s \cong 2.4$.

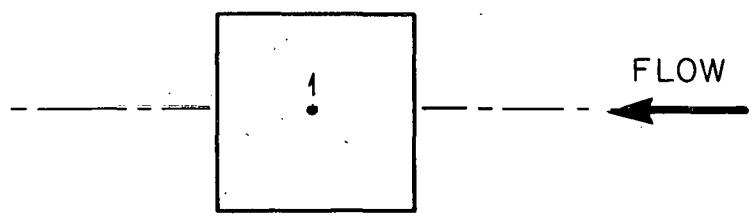

(*d*) PLAN VIEW SHOWING STACK OR VENT POSITION.

Figure 26. Plumes from roof-center stack or vent, showing effects of different stack heights (a and b), and different efflux velocities (a and c) (after Koga and Way, 1979a,b).

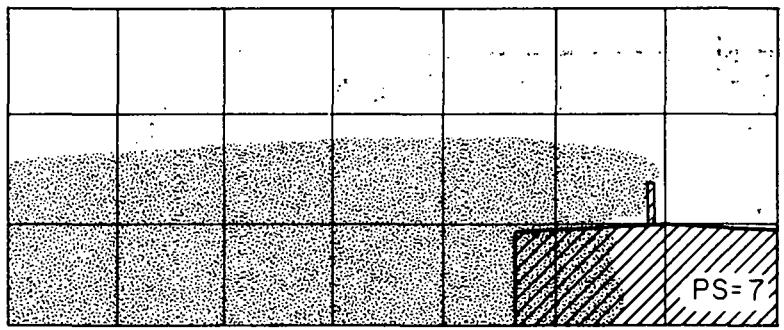

(*a*) POSITION 7, CENTER.

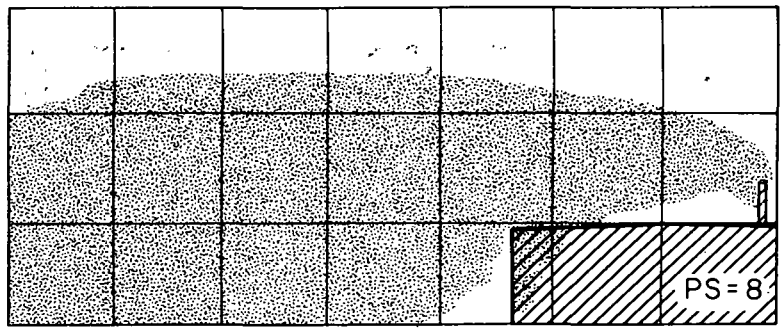

(*b*) POSITION 8, WINDWARD EDGE.

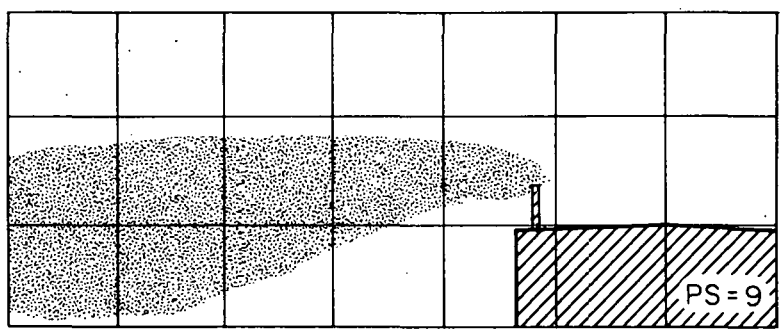

(*c*) POSITION 9, LEE EDGE.

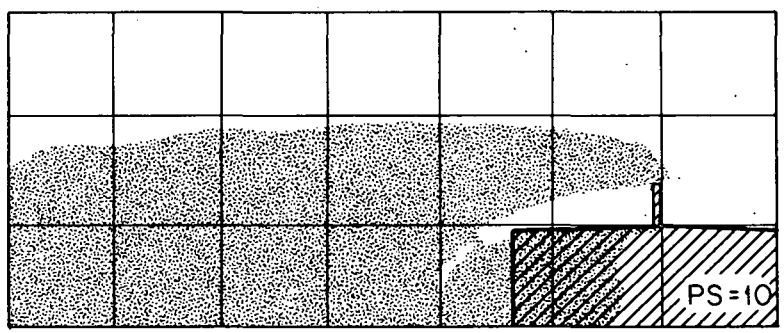

(*d*) POSITION 10, SIDE.

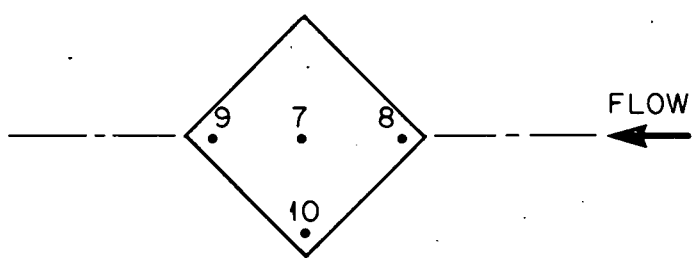

(*e*) PLAN VIEW SHOWING STACK POSITIONS.

Figure 27. Plumes from roof-mounted stacks at various positions for wind at 45° to building, with h_s = 1.5 H, $w_e \cong 1.2\ U_s$ (after Koga and Way, 1979a,b).

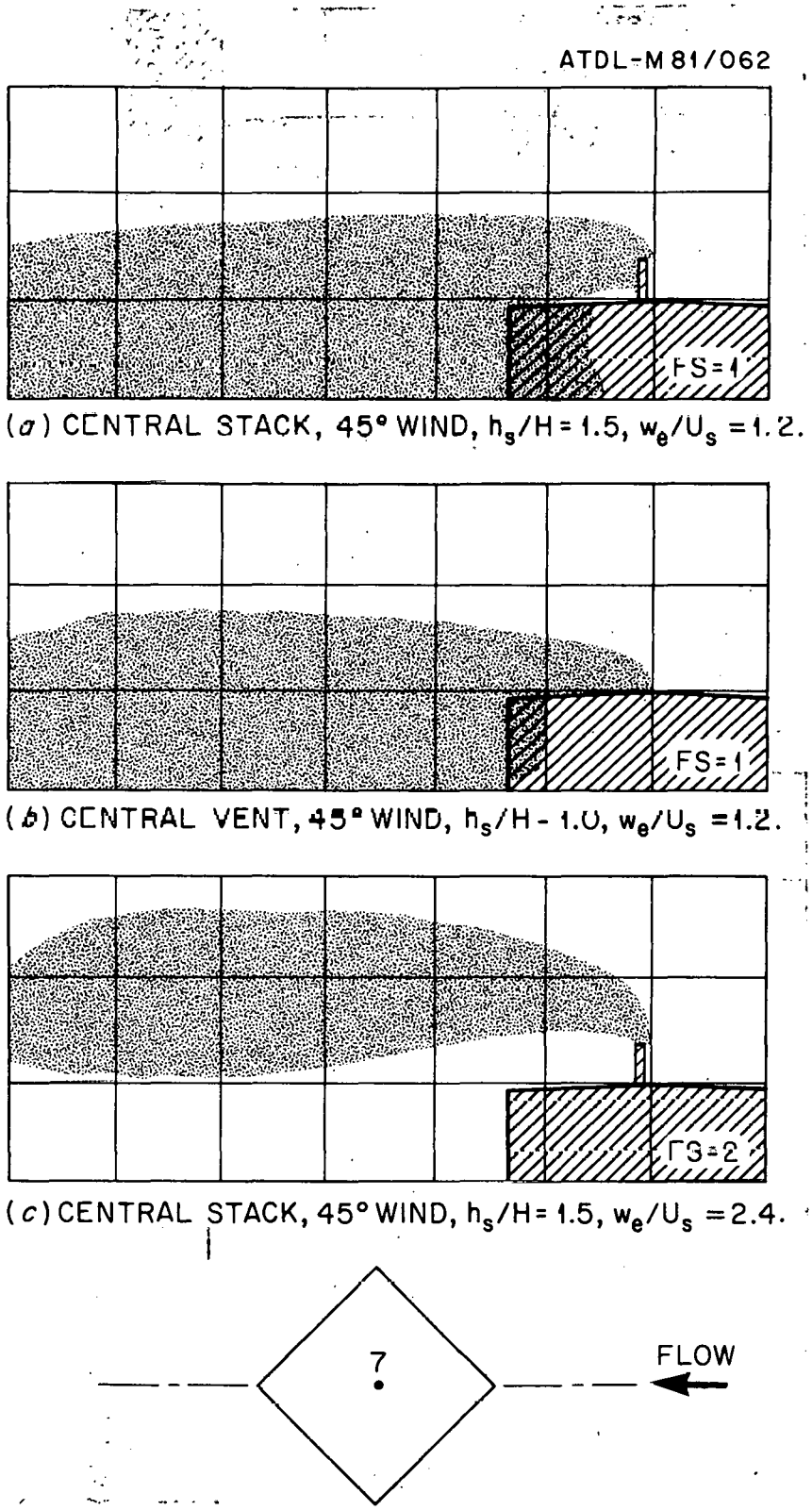

Figure 28. Plumes from roof-center stack or vent, showing effects of different stack heights (a and b) and different efflux velocities (a and c), for wind at 45° incidence (after Koga and Way, 1979a,b).

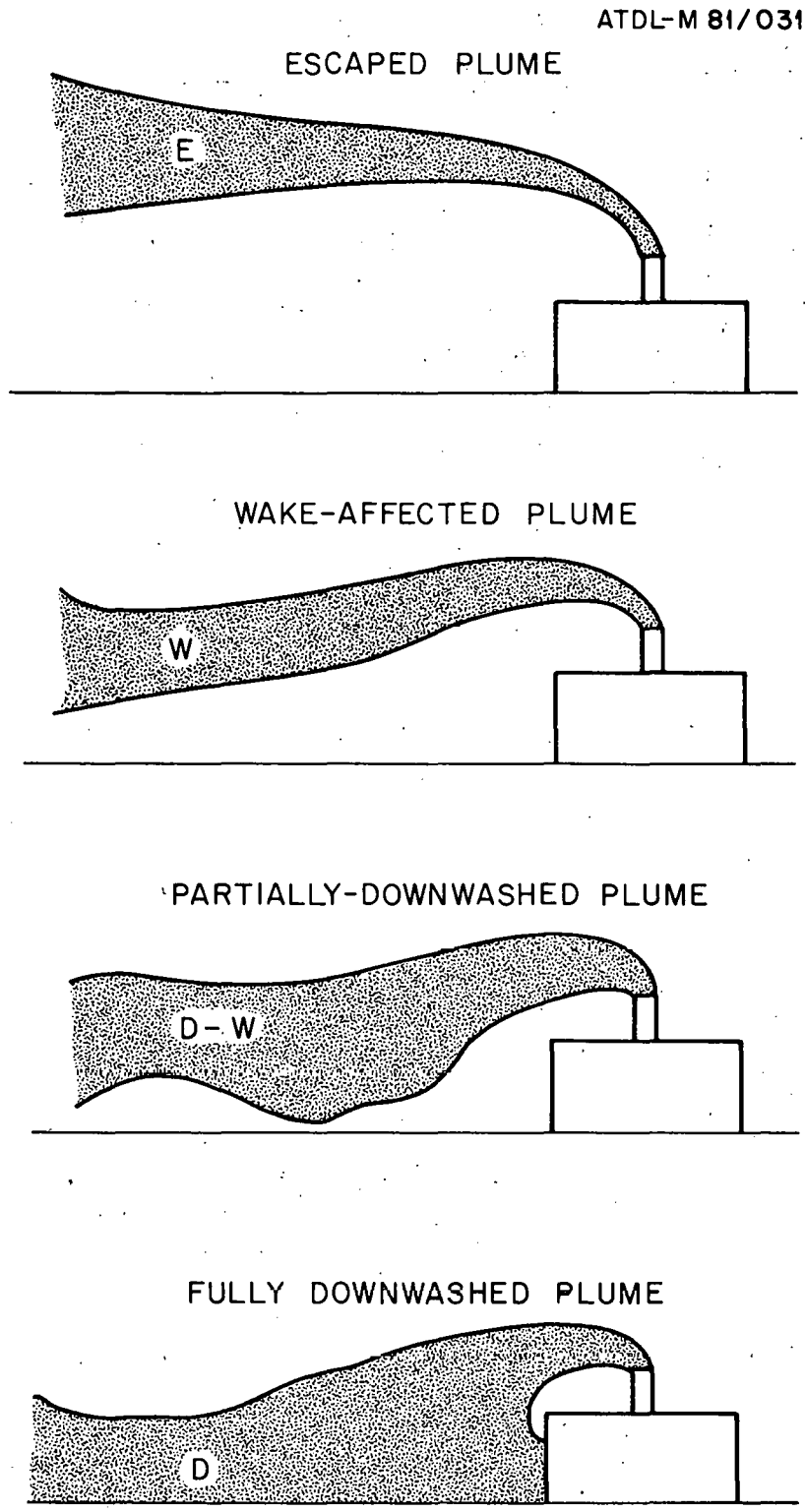

Figure 29. Koga and Way's (1979b) categories of plume behavior for effluent emitted from roof-top stacks or vents.

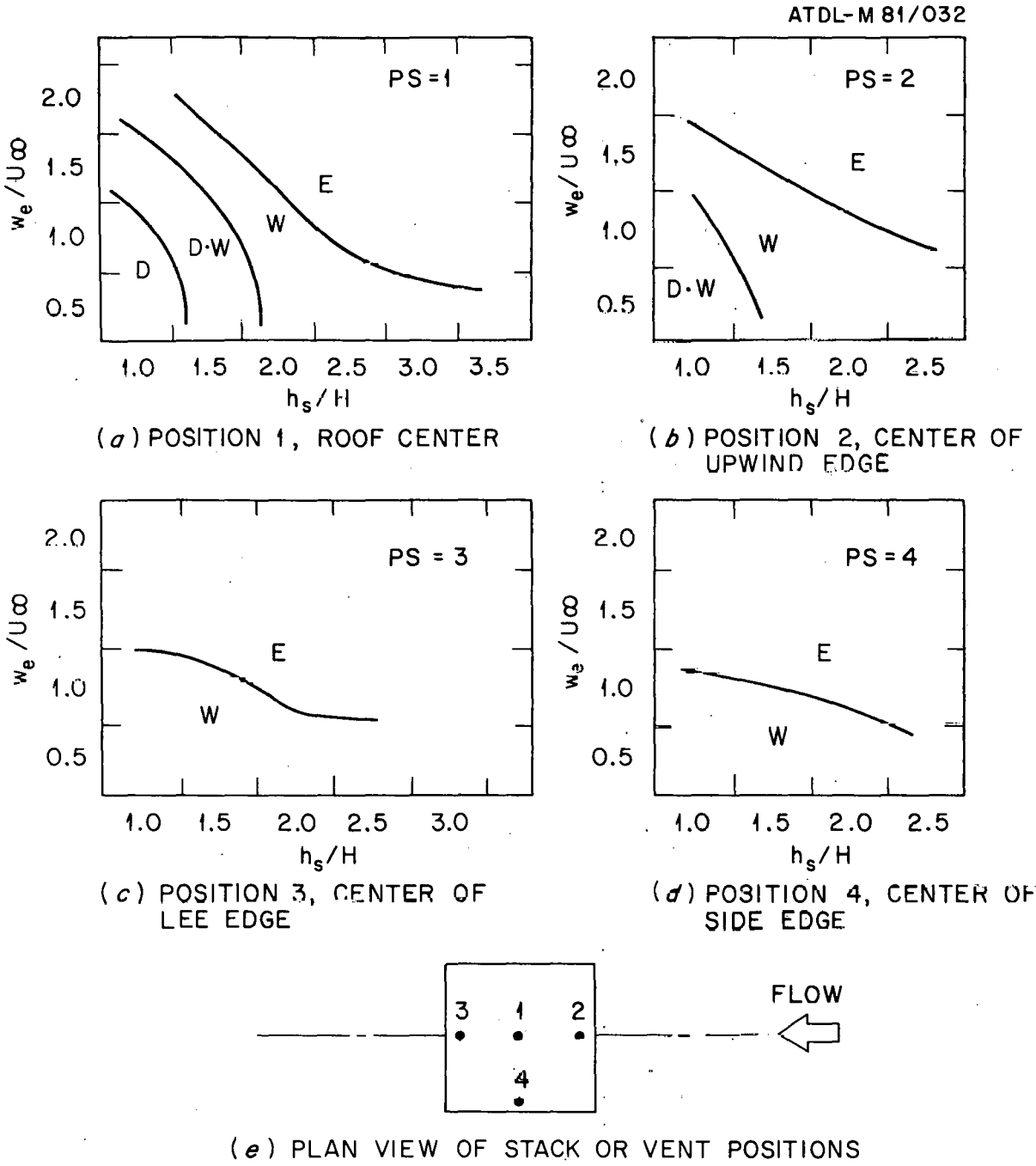

(*a*) POSITION 1, ROOF CENTER

(*b*) POSITION 2, CENTER OF UPWIND EDGE

(*c*) POSITION 3, CENTER OF LEE EDGE

(*d*) POSITION 4, CENTER OF SIDE EDGE

(*e*) PLAN VIEW OF STACK OR VENT POSITIONS

Figure 30. Modes of plume behavior for various stack positions, wind normally incident on squat building, as functions of stack to building height ratio and efflux to freestream wind speed ratio (after Koga and Way, 1979a,b).

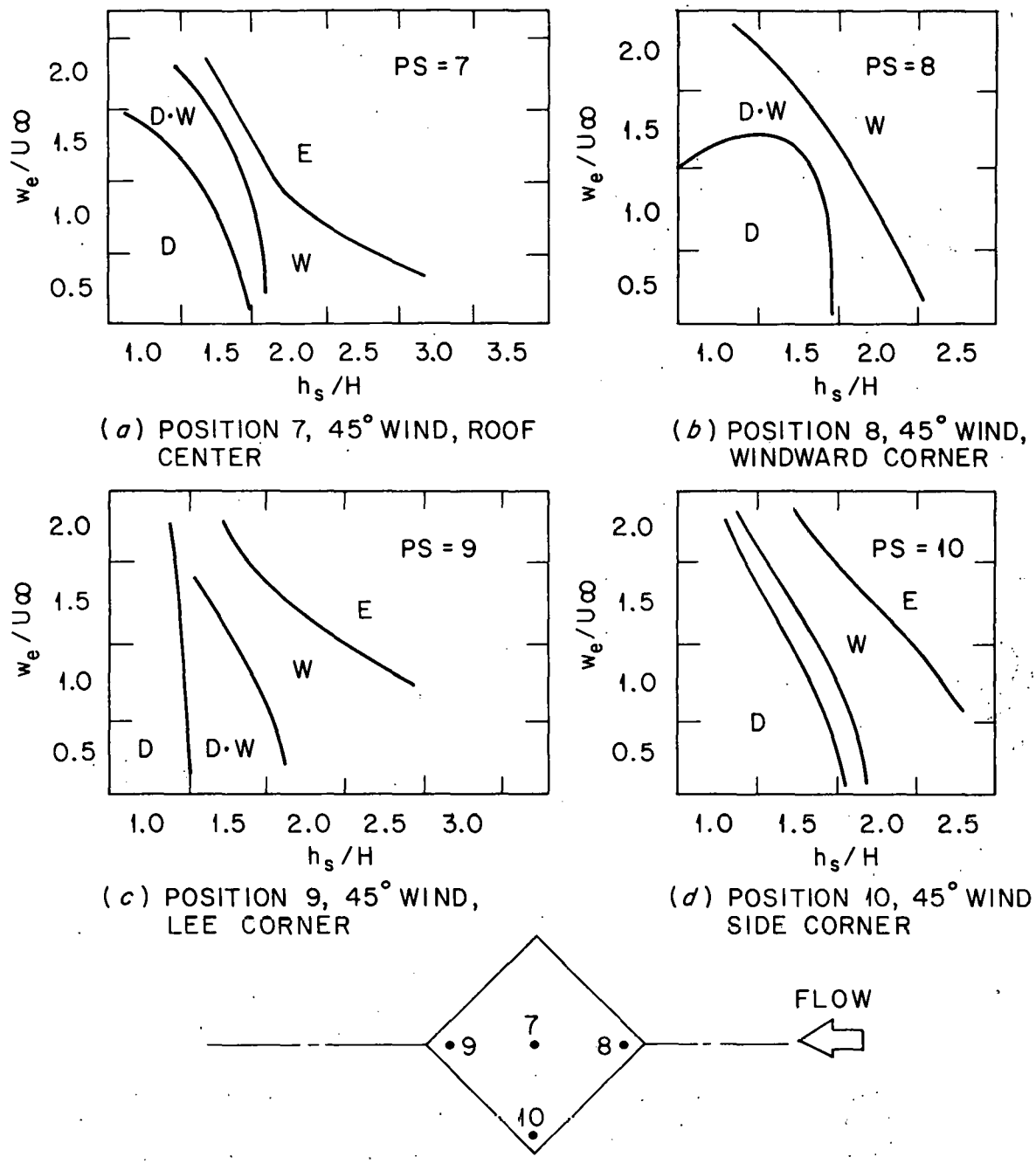

Figure 31. Modes of plume behavior for various stack positions, wind along diagonal of squat building, as functions of stack to building height ratio and efflux to freestream wind speed ratio (after Koga and Way, 1979a,b).

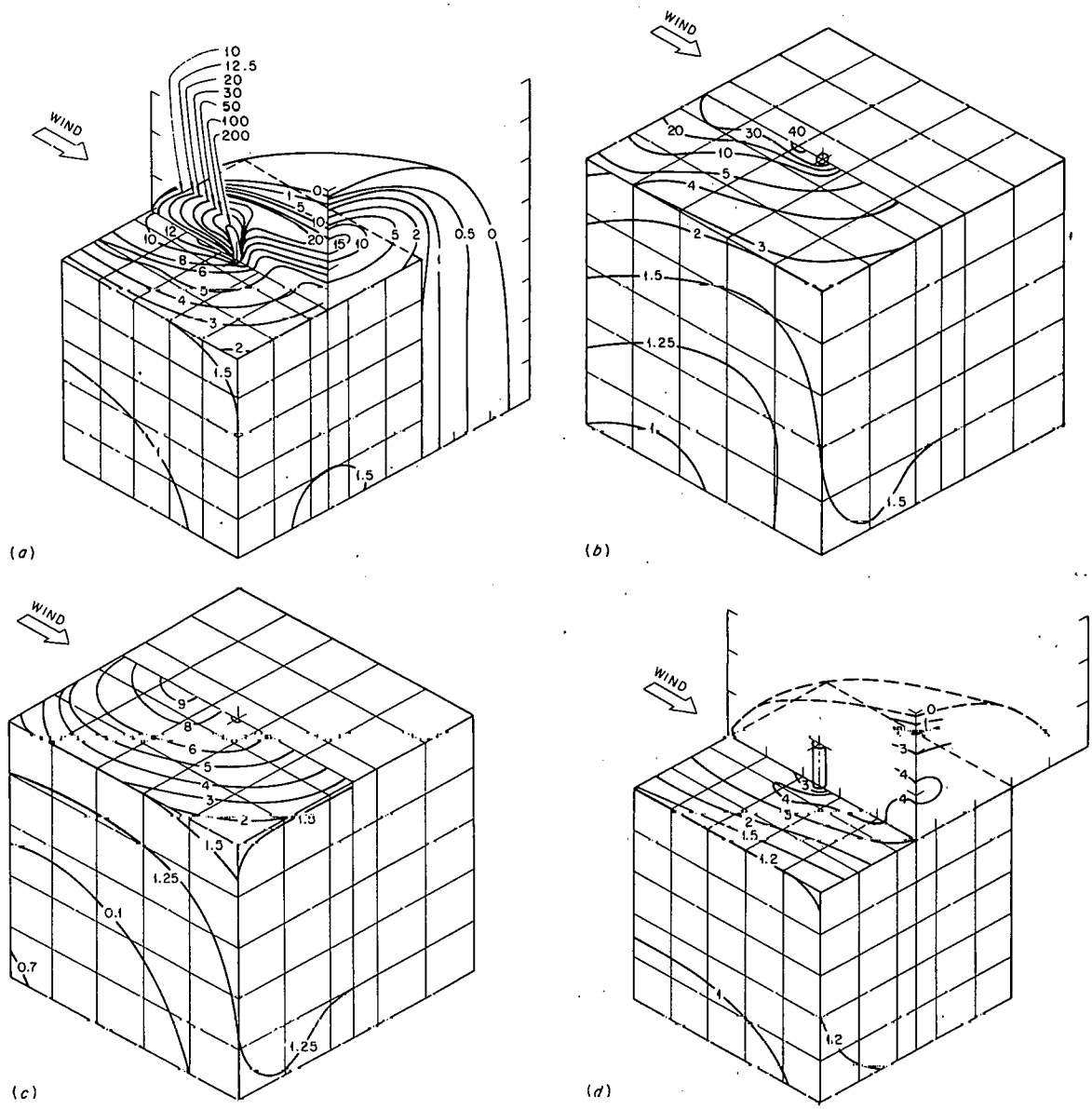

Figure 32. Nondimensional concentration coefficient contours on simple buildings, as measured in a non-boundary layer flow by Halitsky (1963a). (a) L/H = 1.0 = W/H, flush vent, $w_e/U_H \cong 1.0$; (b) L/H = 1.0 = W/H, flush vent, $w_e/U_H \cong 0.5$; (c) L/H = 1.0 = W/H, flush vent, $w_e/U_H \cong 2.0$; (d) L/H = 1.0 = W/H, short stack 0.2H above roof, $w_e/U_H \cong 1.0$.

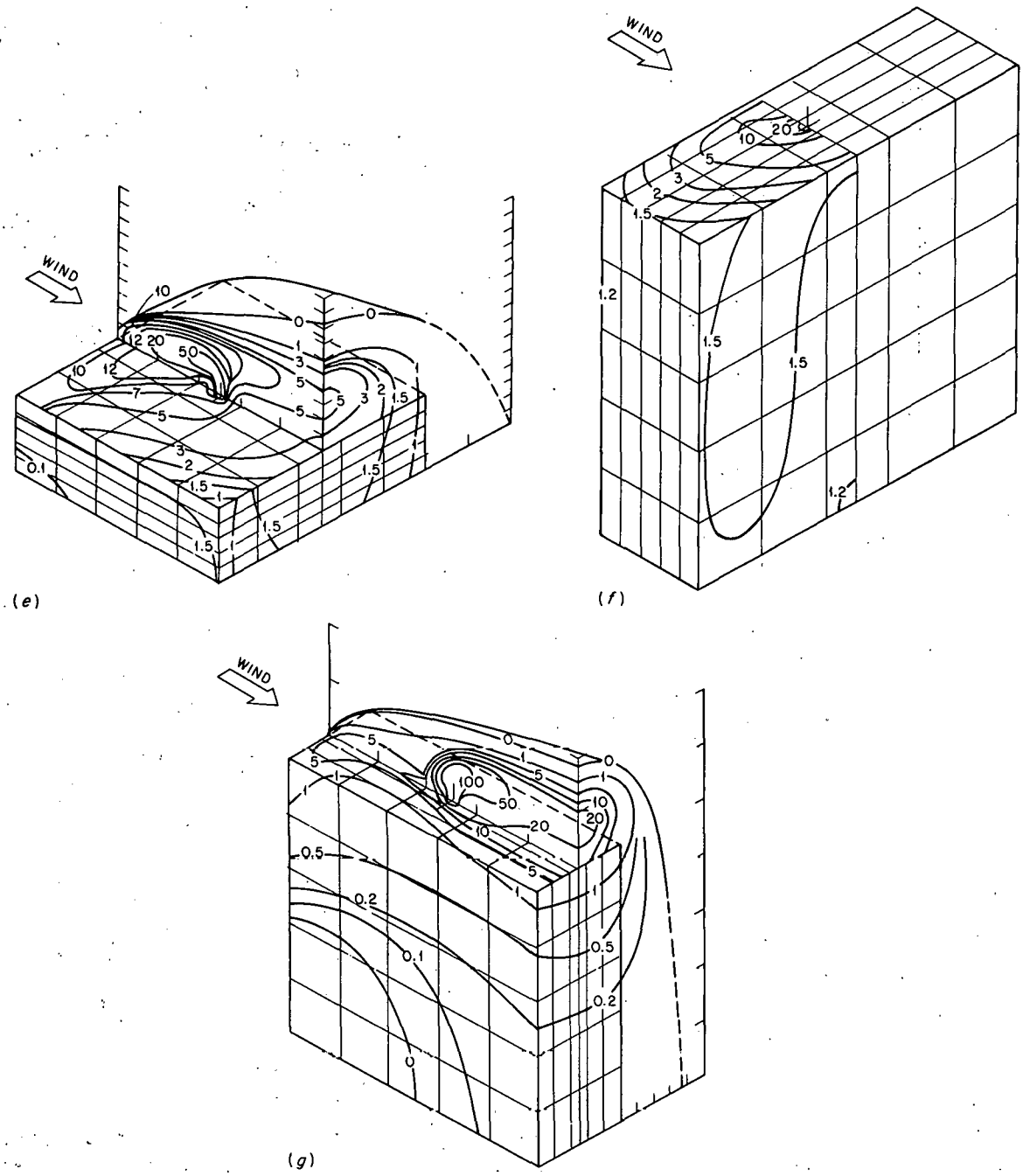

Figure 32 (continued). (e) L/H = 3.0 = W/H, flush vent, $w_e/U_H \cong 1.0$; (f) L/H = 0.33, W/H = 1.0, flush vent, $w_e/U_H \cong 1.0$; (g) L/H = 1.0, W/H = 0.33, flush vent, $w_e/U_H \cong 1.0$.

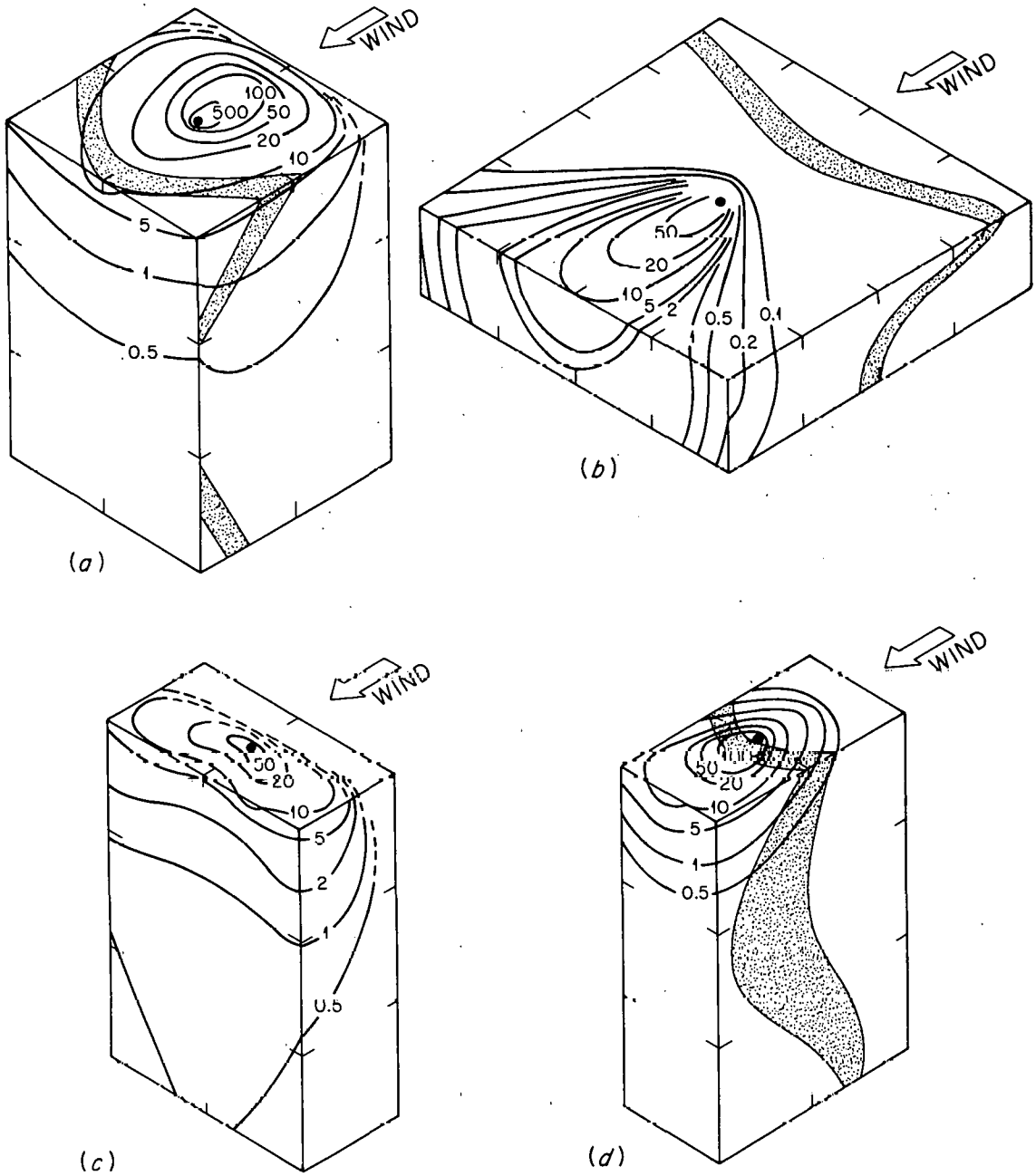

Figure 33. Nondimensional concentration coefficient contours and zones of roof and side reattachment on simple buildings, for roof-center vents, as measured in a simulated atmospheric boundary layer by Wilson (1976a,b). (a) L/H = 0.67 = W/H, w_e/U_H = 0.3; (b) L/H = 4.0 = W/H, w_e/U_H = 0.39; (c) L/H = 0.33, W/H = 0.67, w_e/U_H = 0.29; (d) L/H = 0.67, W/H = 0.33, w_e/U_H = 0.29.

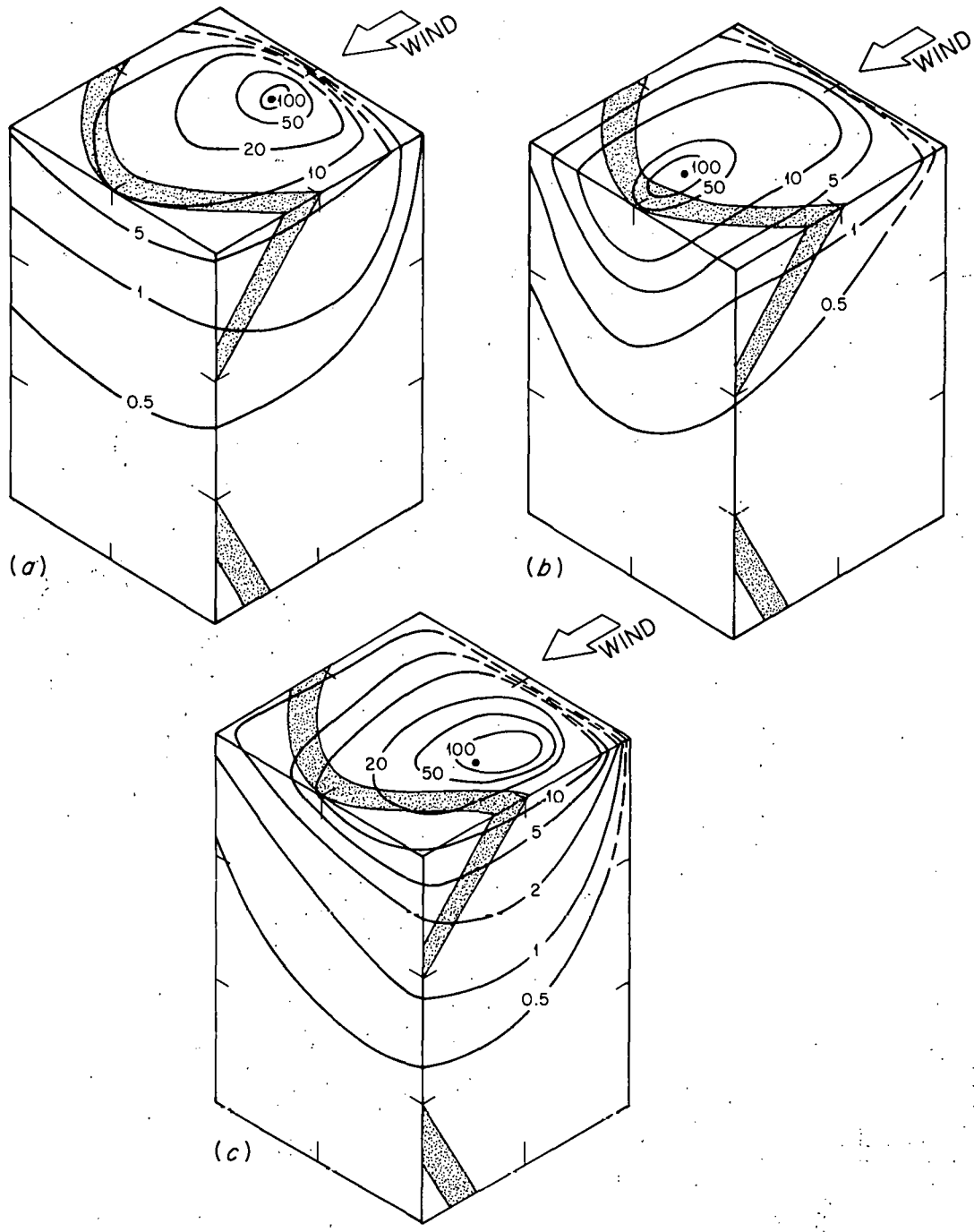

Figure 34. Nondimensional concentration coefficient contours and zones of roof and side reattachment on simple buildings, for off-center roof vents, as measured in a simulated atmospheric boundary layer by Wilson (1976a,b). $L/H = 0.67 \simeq W/H$, $w_e/U_H \simeq 0.3$, for all cases.

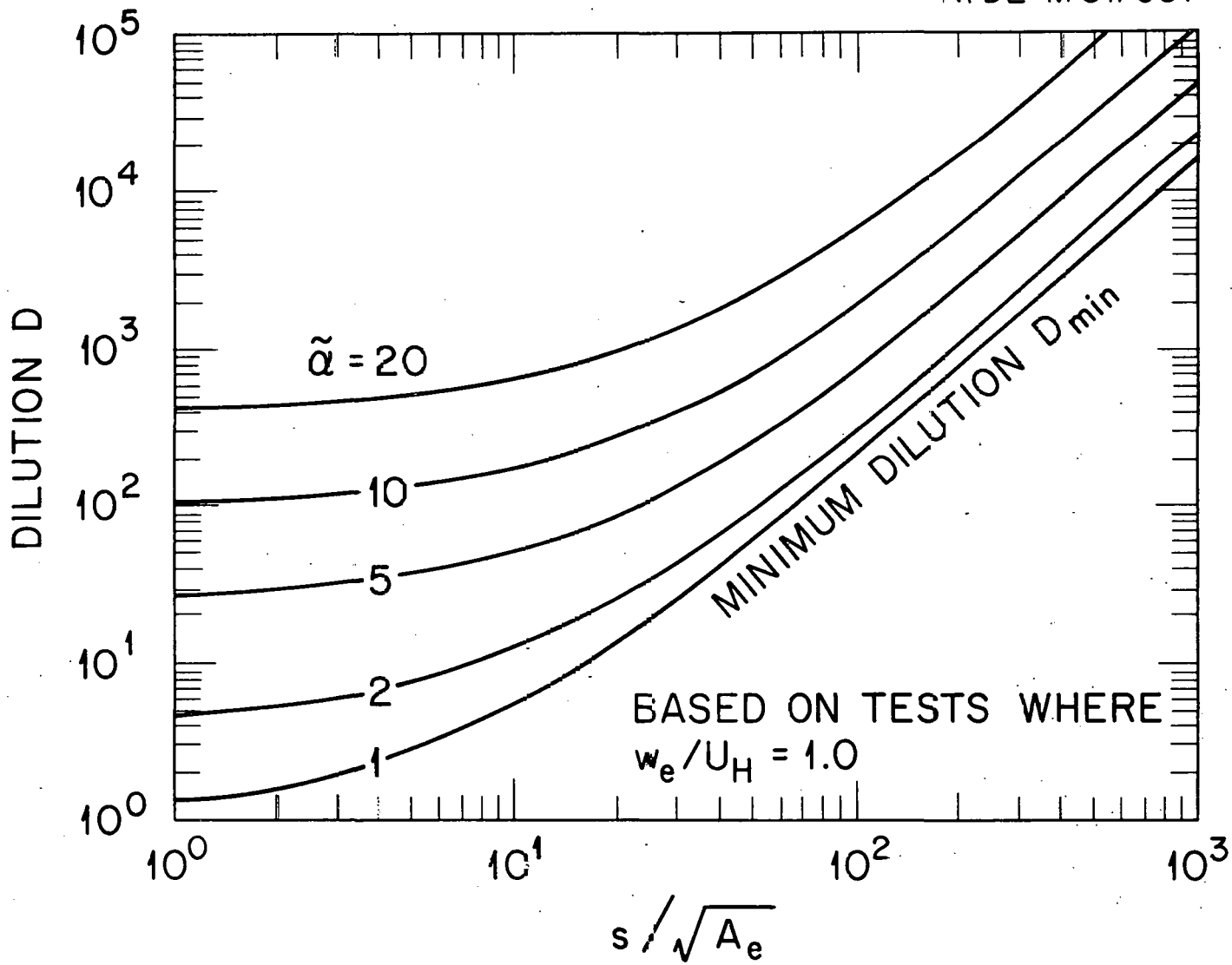

Figure 35. Halitsky's (1963a,b) relation between dilution and "stretched string" distance s, for receptor locations on surfaces of simple building fitted with flush roof exhaust vents. Minimum dilution occurs for $\tilde{\alpha}$ = 1.

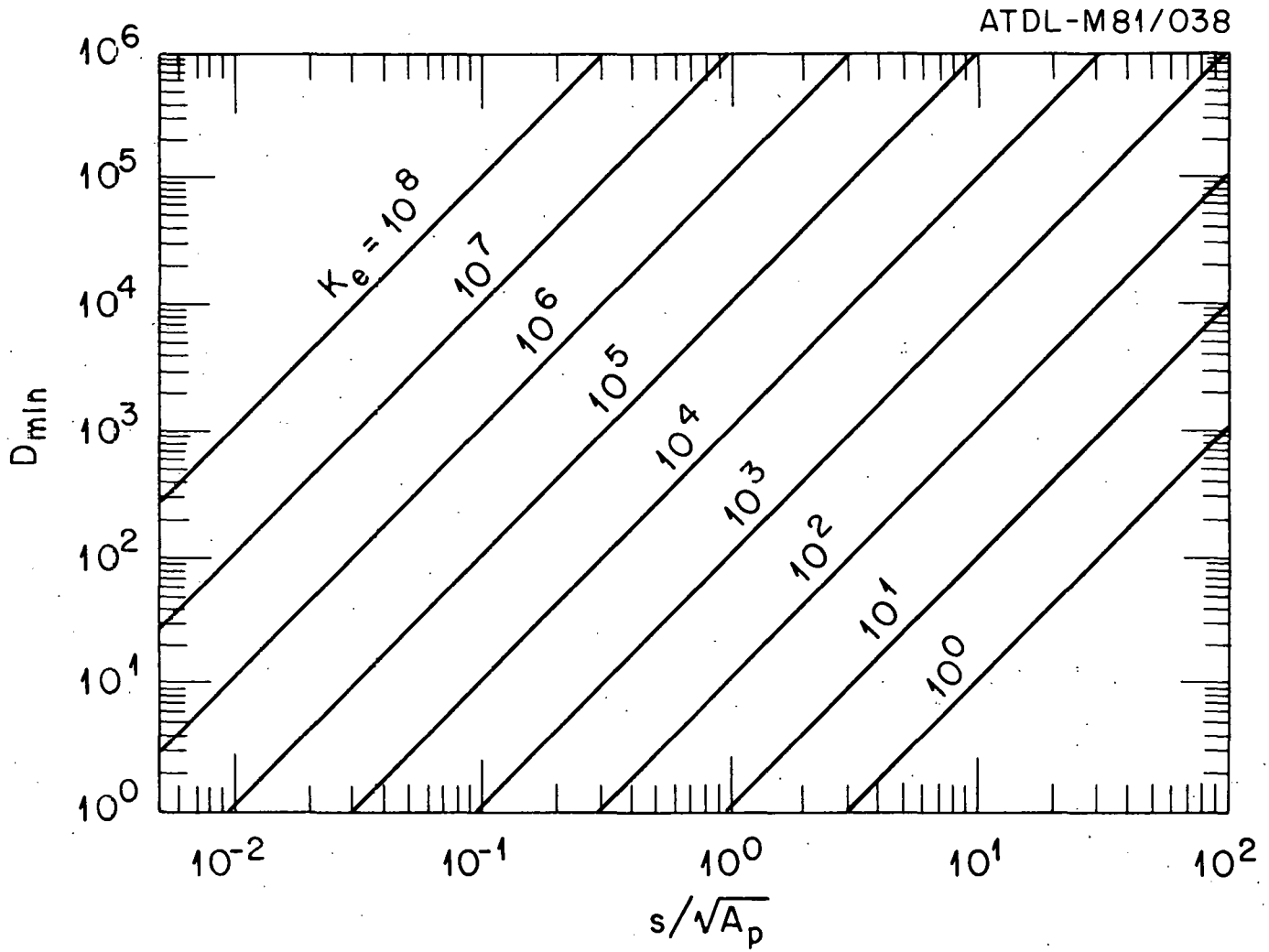

Figure 36. Wilson's (1976a,b; 1977a) recommended lower bound on dilution along surfaces of buildings with flush roof vents as a function of shortest source-to-receptor distance, for several effluent exit concentration coefficients K_e.

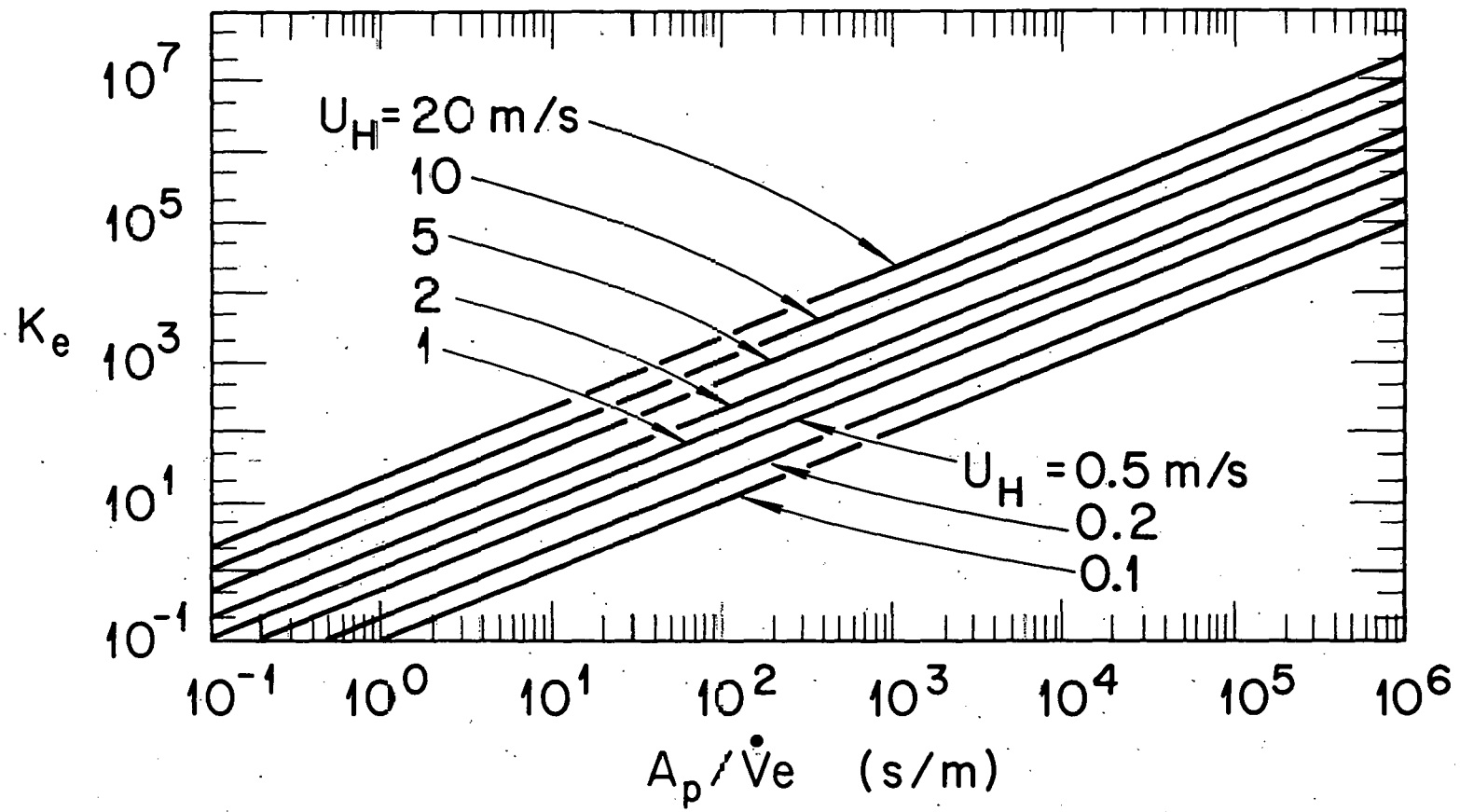

Figure 37. Effluent exit concentration K_e at a flush roof vent as function of building projected area A_p and effluent volume flow rate $\dot{V}_e$, for several roof-level wind speeds.

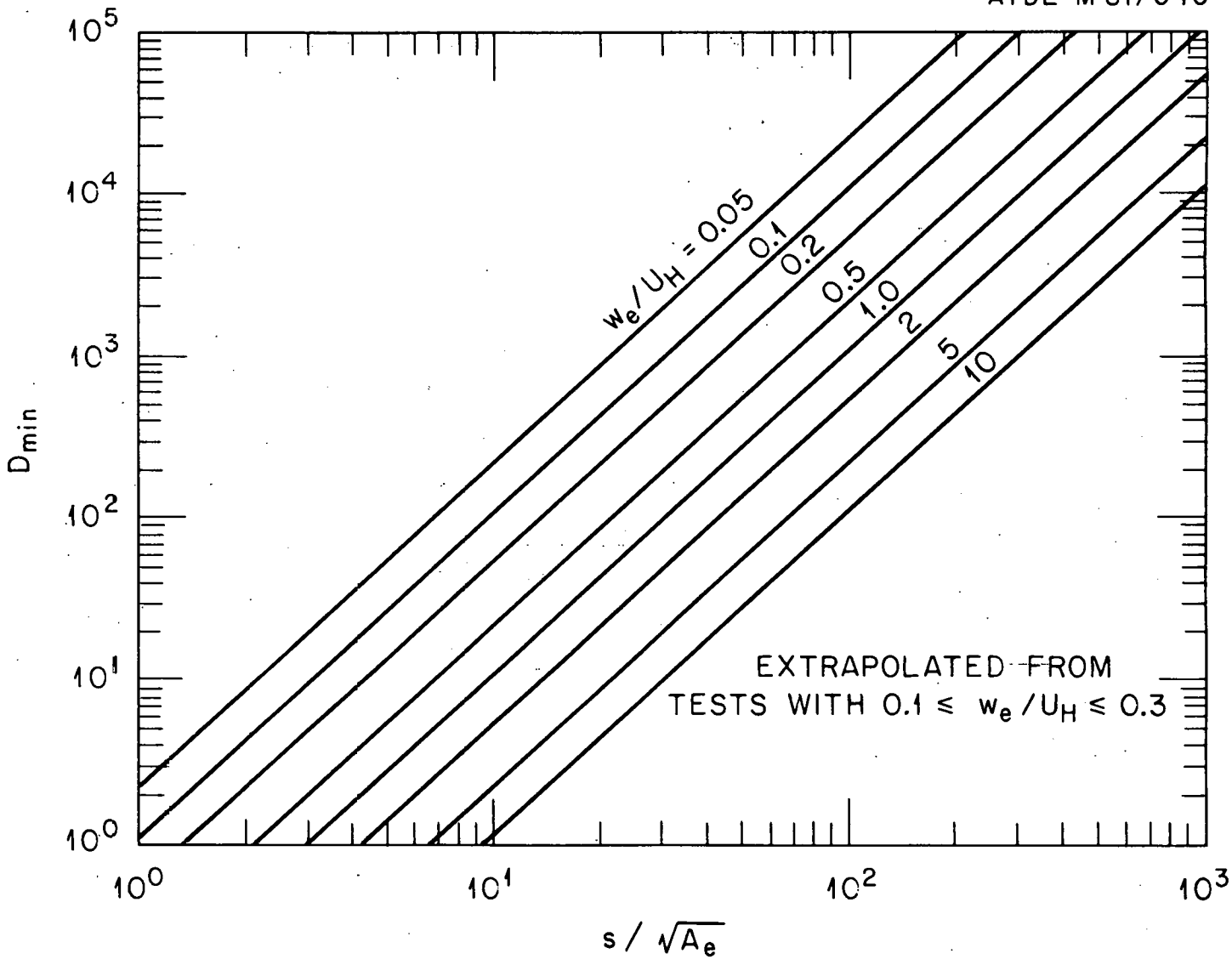

Figure 38. Wilson's (1976a,b; 1977a) lower limit on dilution for locations on surfaces of simple buildings with flush roof vents, as function of source-to-receptor distance, for several effluent to wind speed ratios.

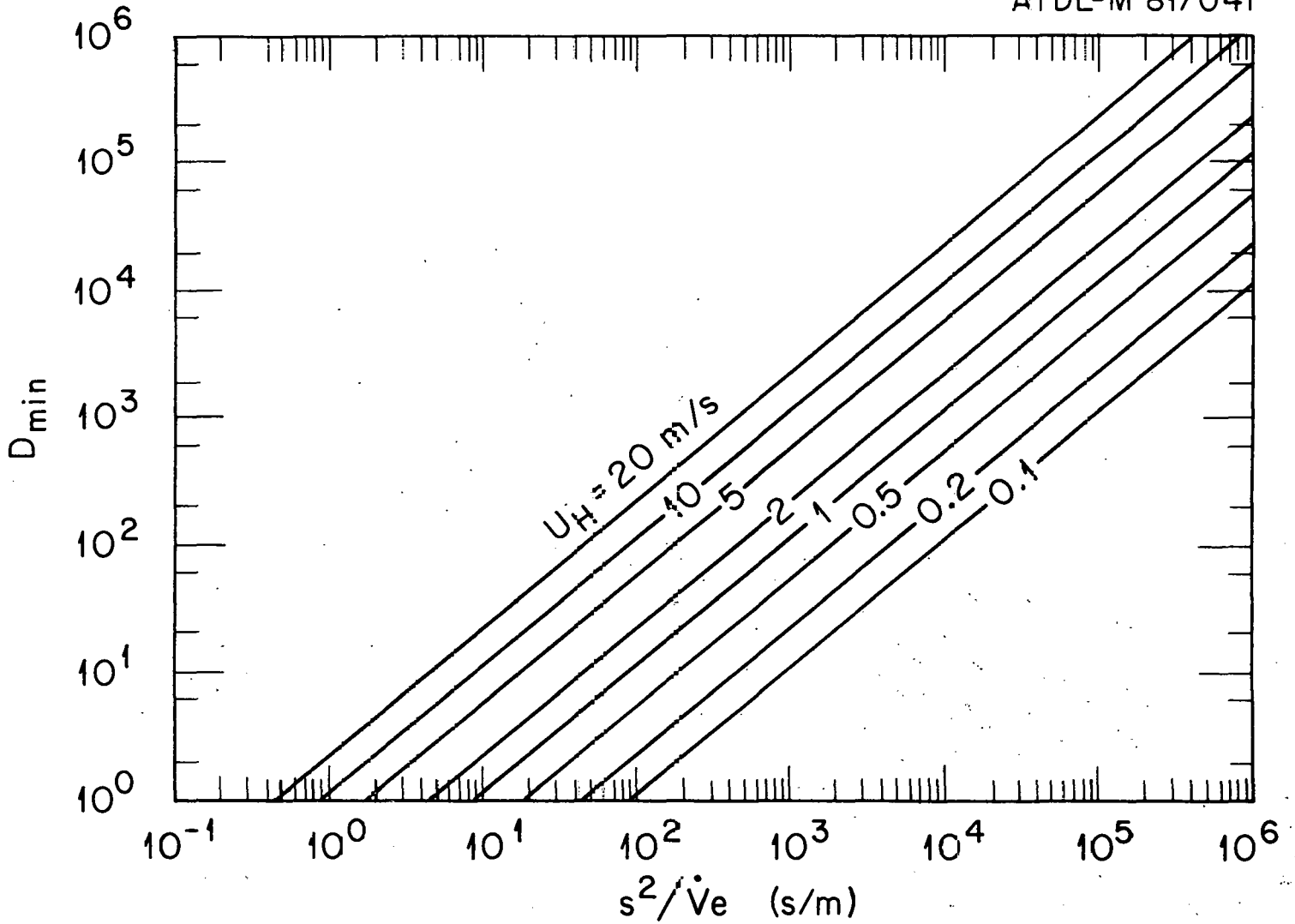

Figure 39. Wilson's (1976a,b; 1977a) lower limit on dilution, as function of source-to-receptor distance and effluent volume flow rate, for several roof-level wind speeds.

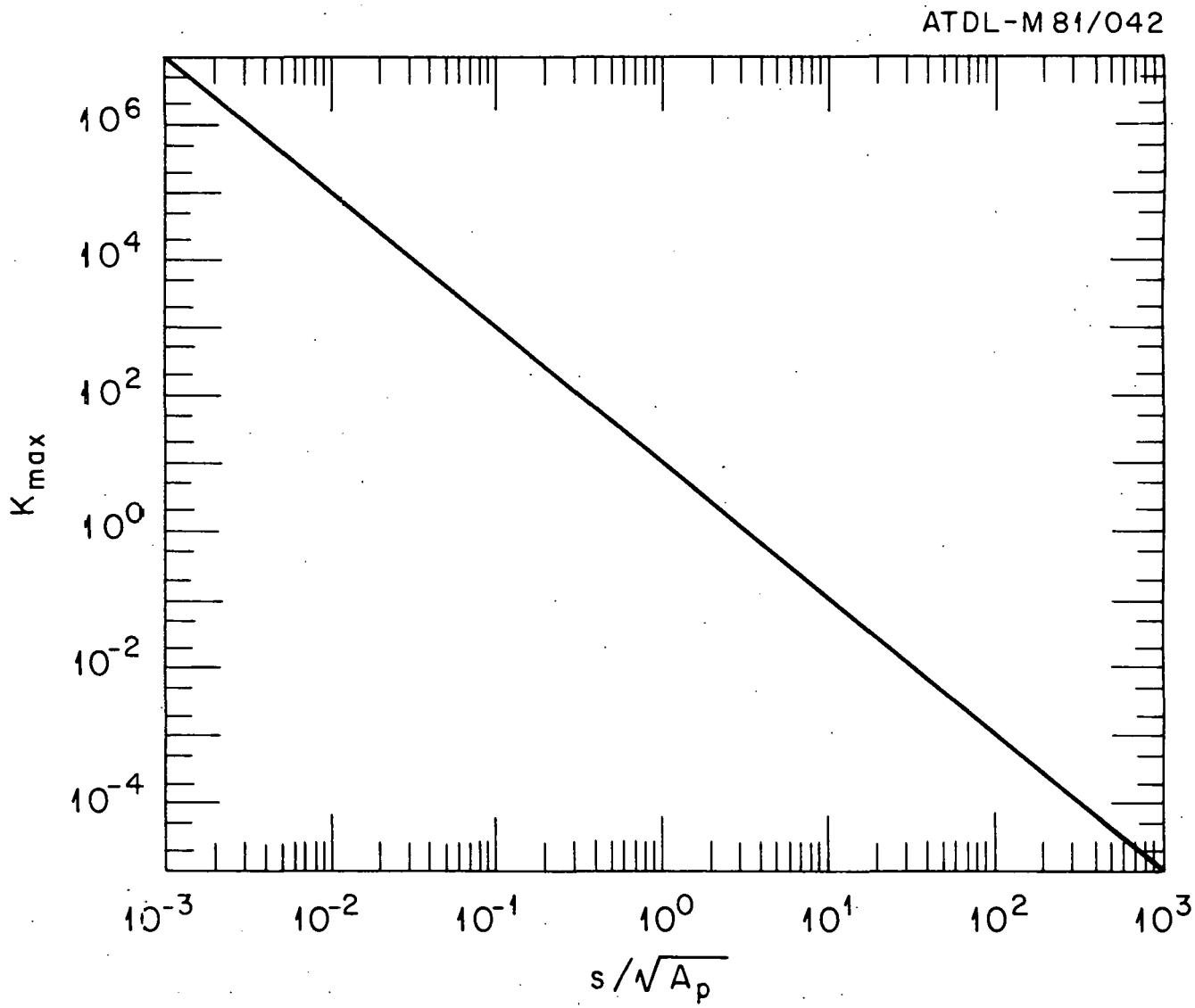

Figure 40. Upper limit on concentration coefficient at points on simple building with flush roof vents, as function of vent-to-receptor distance and building size.

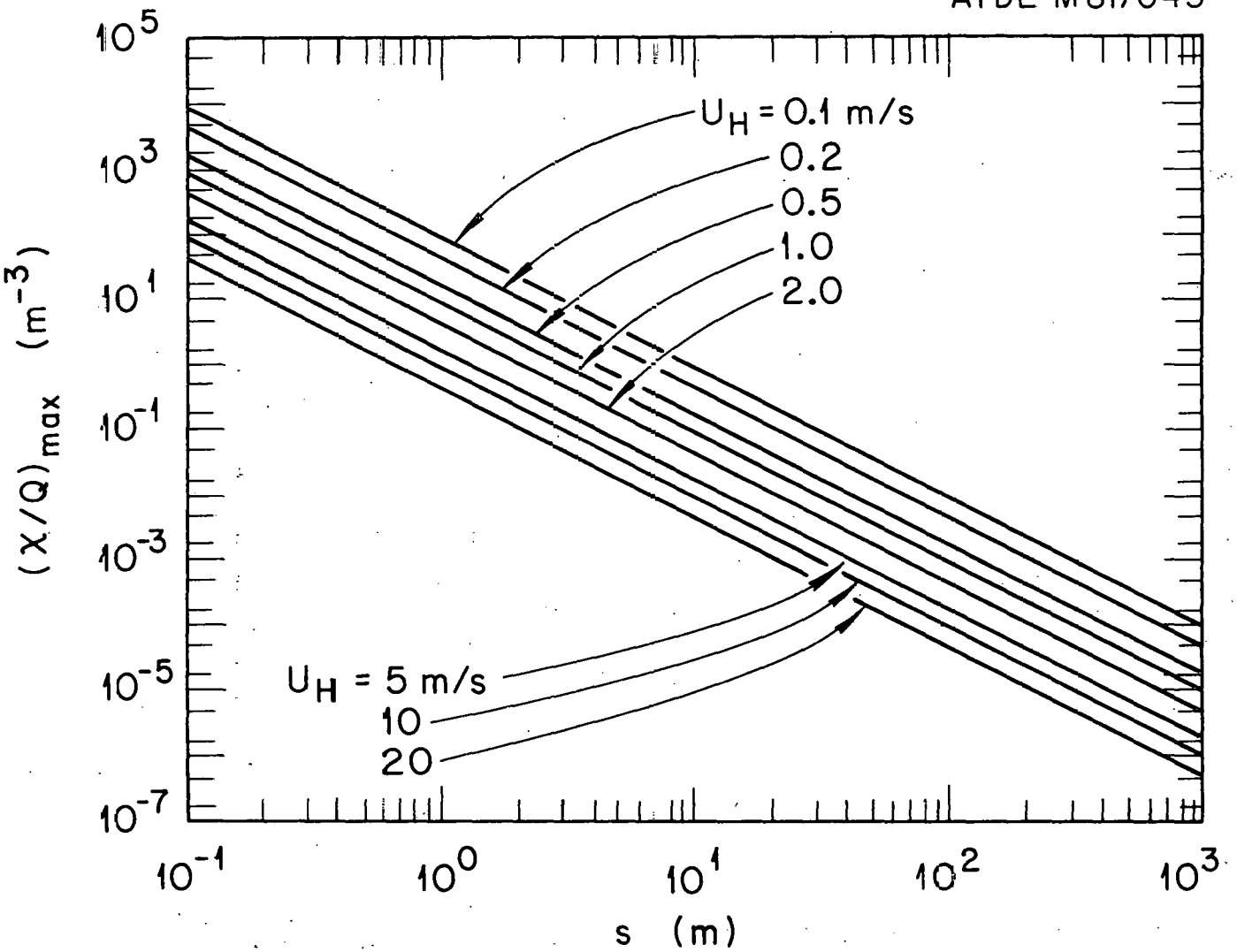

Figure 41. Upper limit on χ/Q at points on simple building with flush roof vents, as function of vent-to-receptor distance, for several roof-level wind speeds.

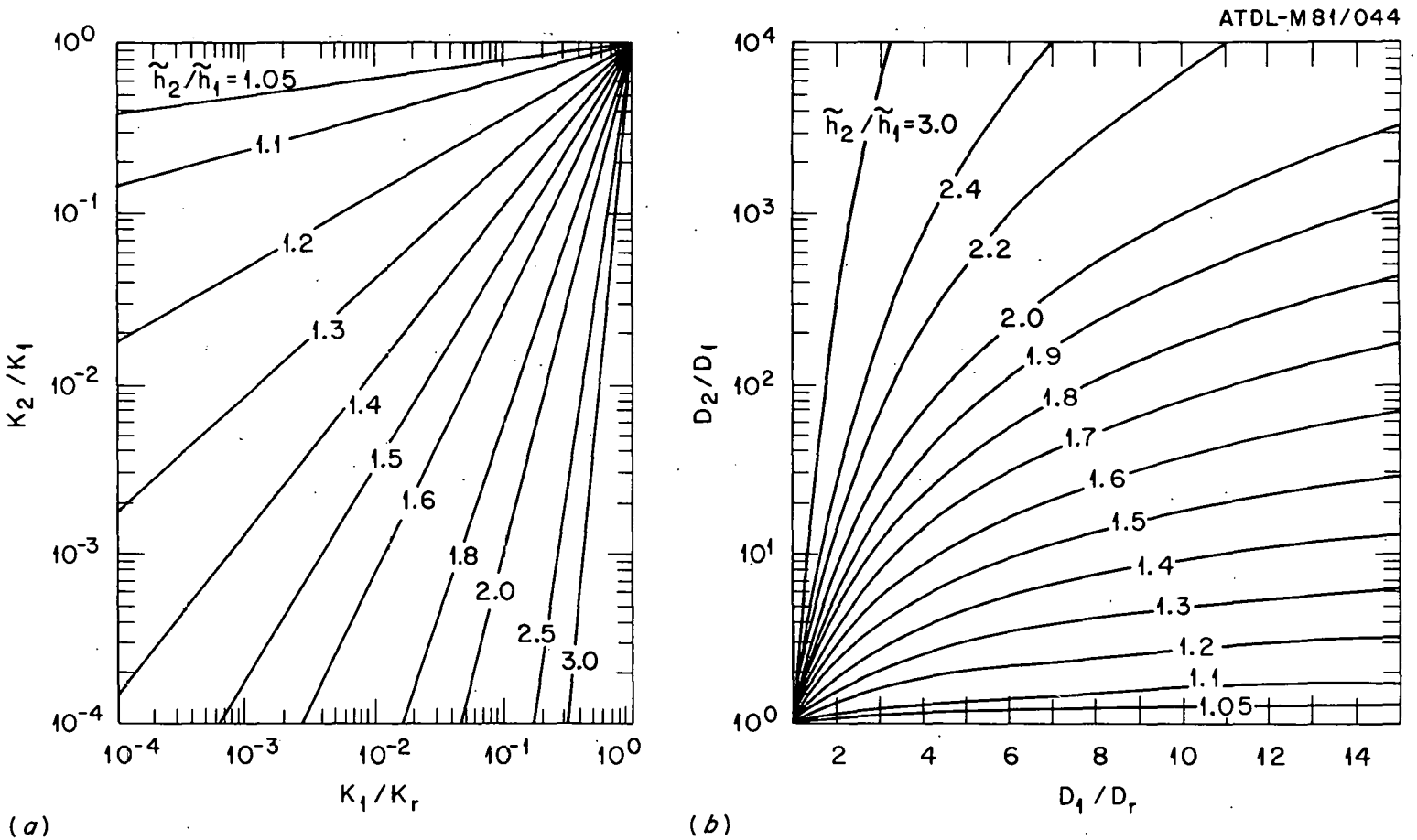

Figure 42. Roof-top concentration coefficient K_2 and dilution D_2 produced by roof-mounted stack of relative height $\tilde{h}_1$, as function of K_1 (D_1) relative to concentration K_r (D_r) due to a flush roof vent, for several ratios $\tilde{h}_2/\tilde{h}_1$.

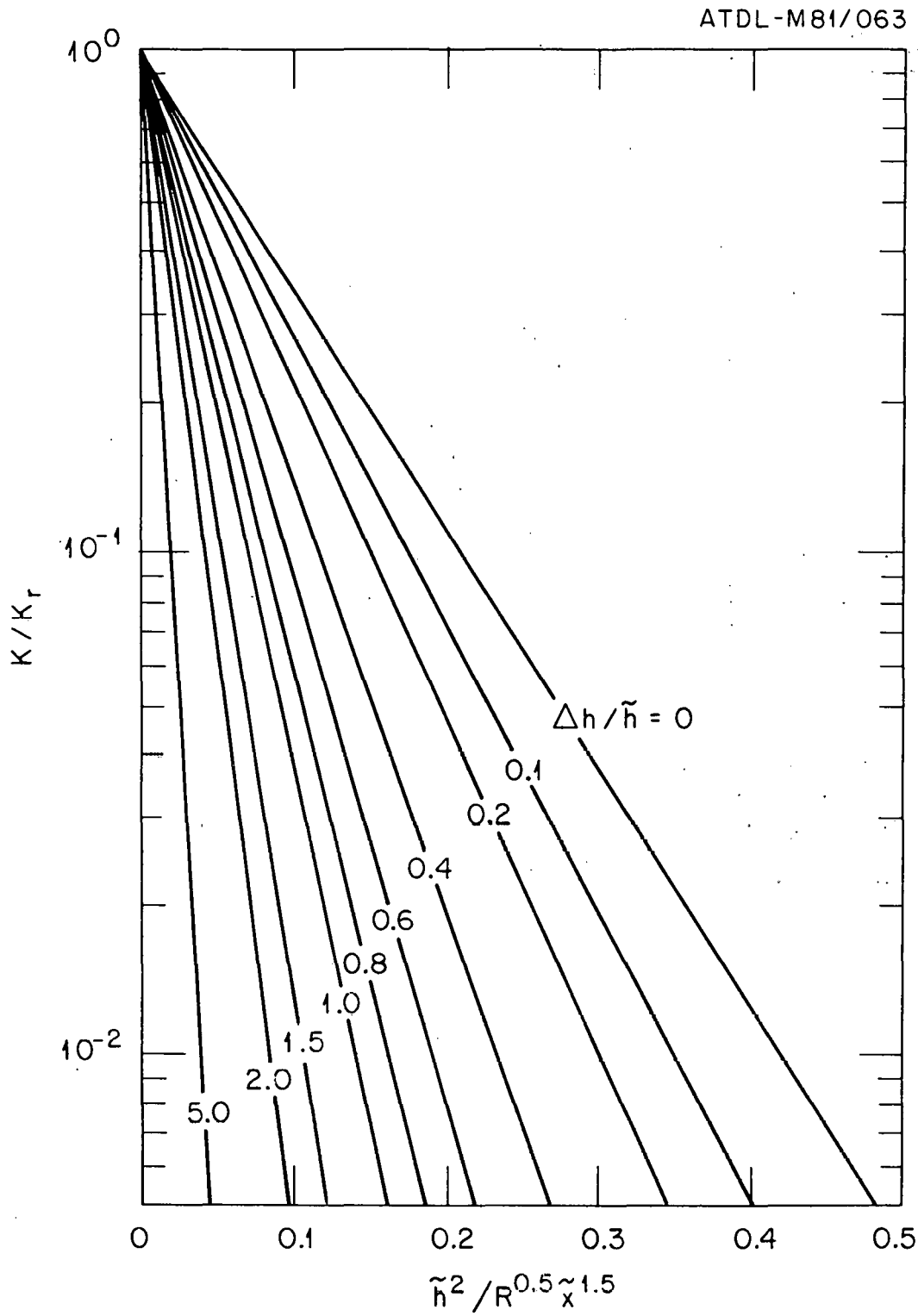

Figure 43. Wilson's (1979a) estimate of rooftop concentration K produced by a roof-mounted stack of relative height $\tilde{h}_1$, relative to concentration K_r produced by a flush vent, as function of building scale length R and stack-to-receptor distance x, for various plume rises Δh.

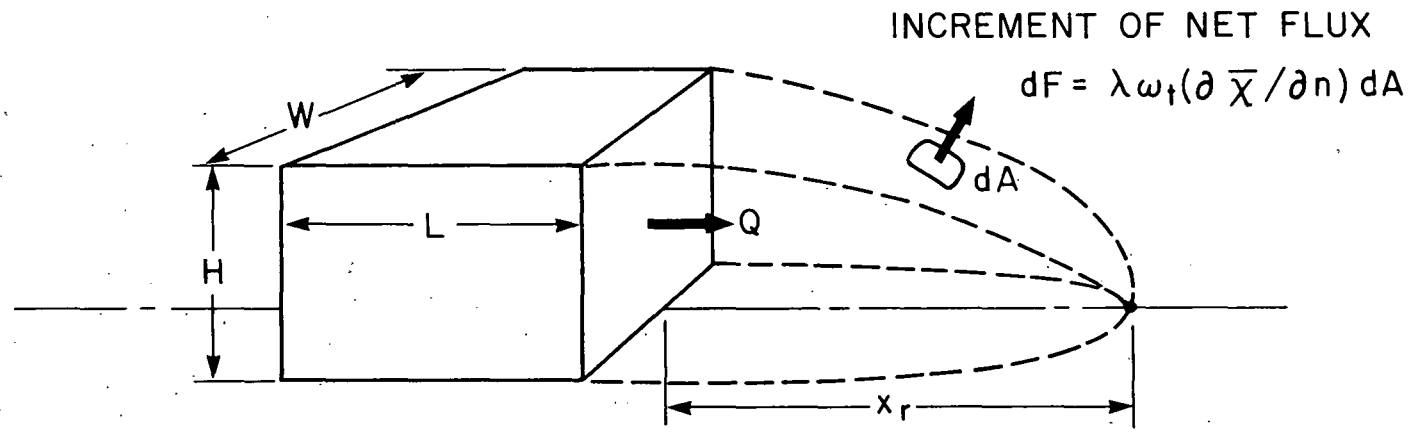

Figure 44. Simple conceptual model of recirculating wake cavity with mass transfer via turbulent diffusion across bounding shear layer.

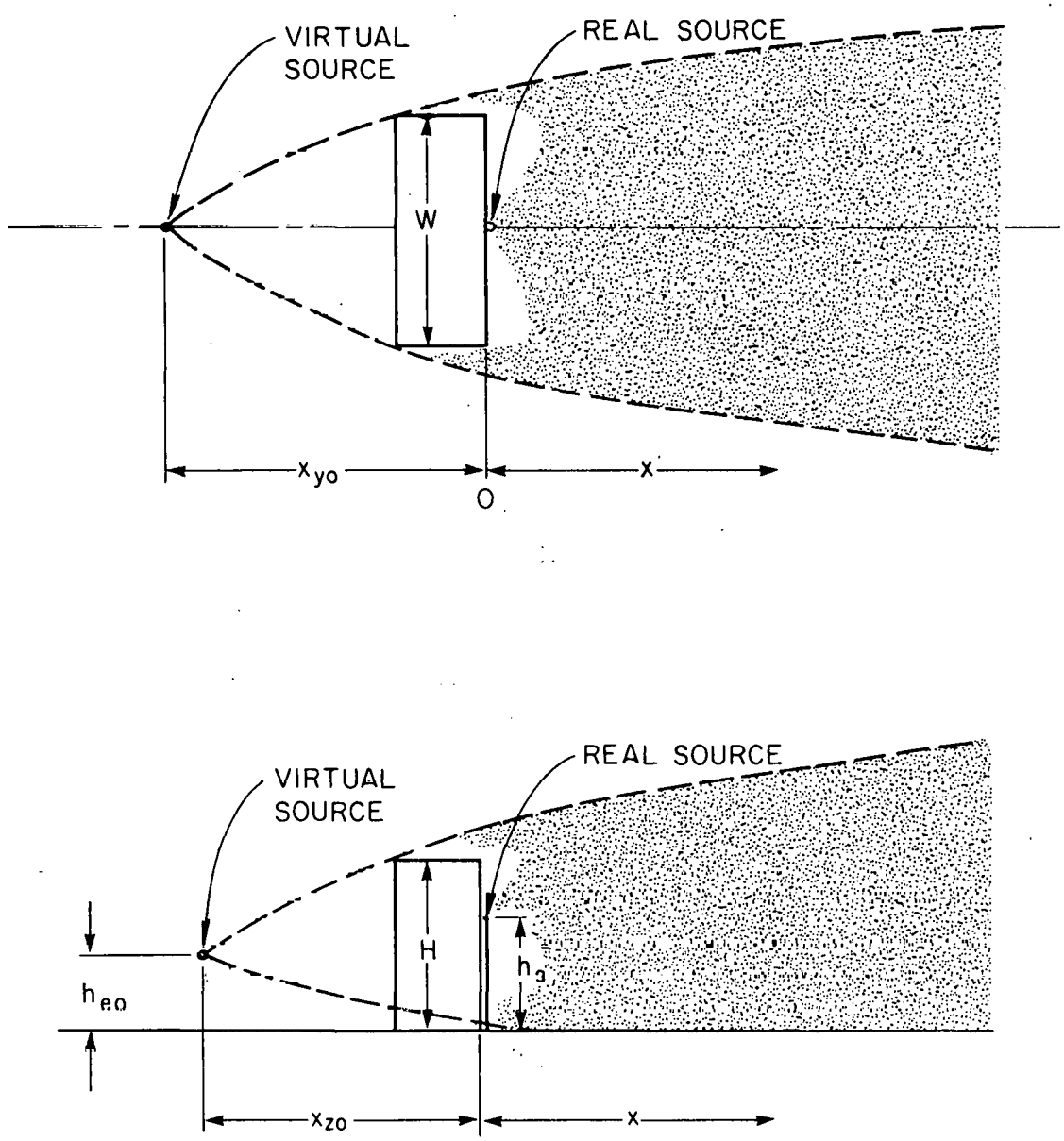

Figure 45. Schematic of horizontal and vertical virtual source locations and height for simple model of wake-entrained effluent dispersion.

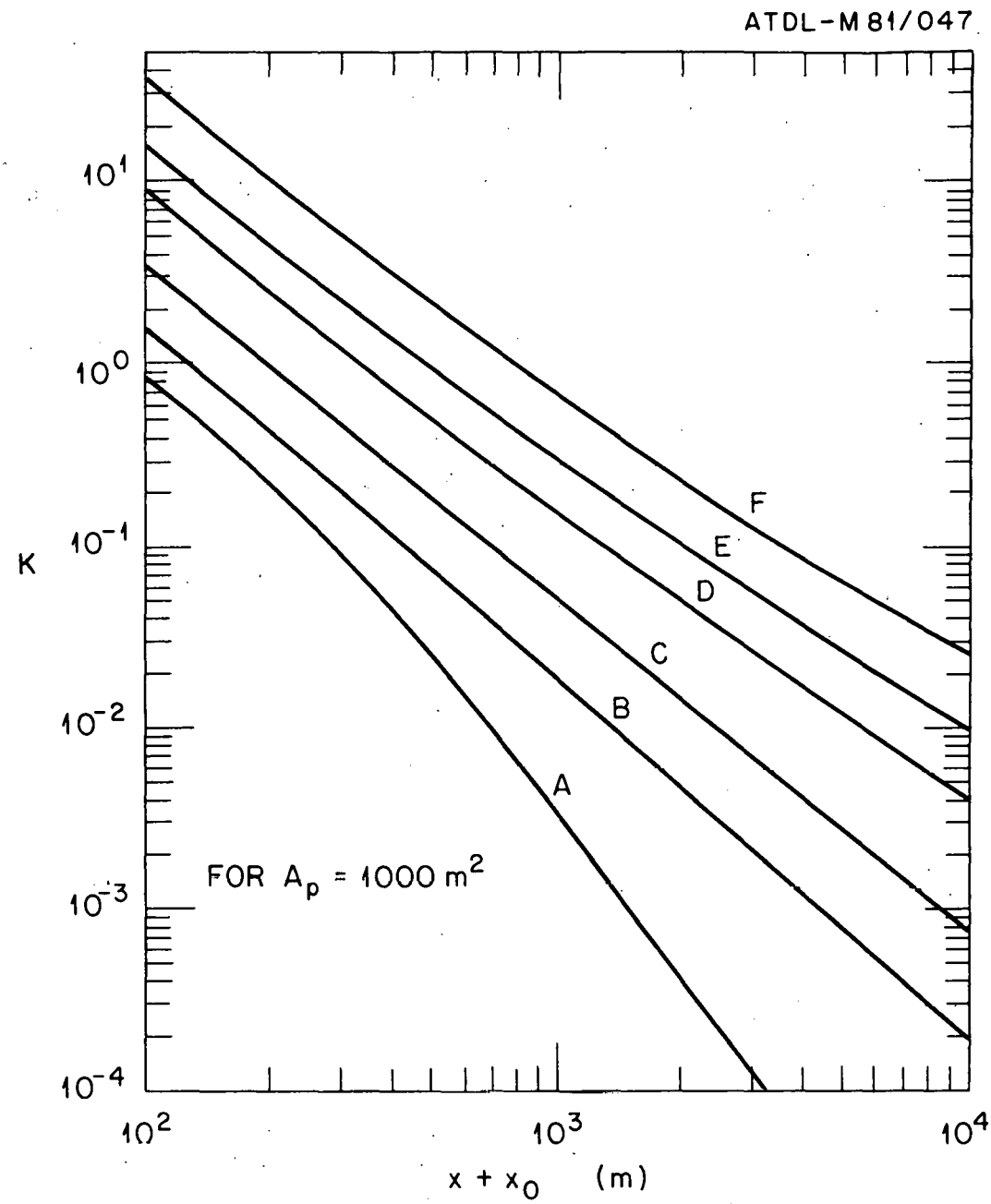

Figure 46. Nondimensional ground-level concentration K along wake centerline, calculated from virtual source model (common horizontal and vertical virtual source location x_o) as function of downwind distance x, for various atmospheric stabilities, assuming building projected area A_p = 1000 m^2.

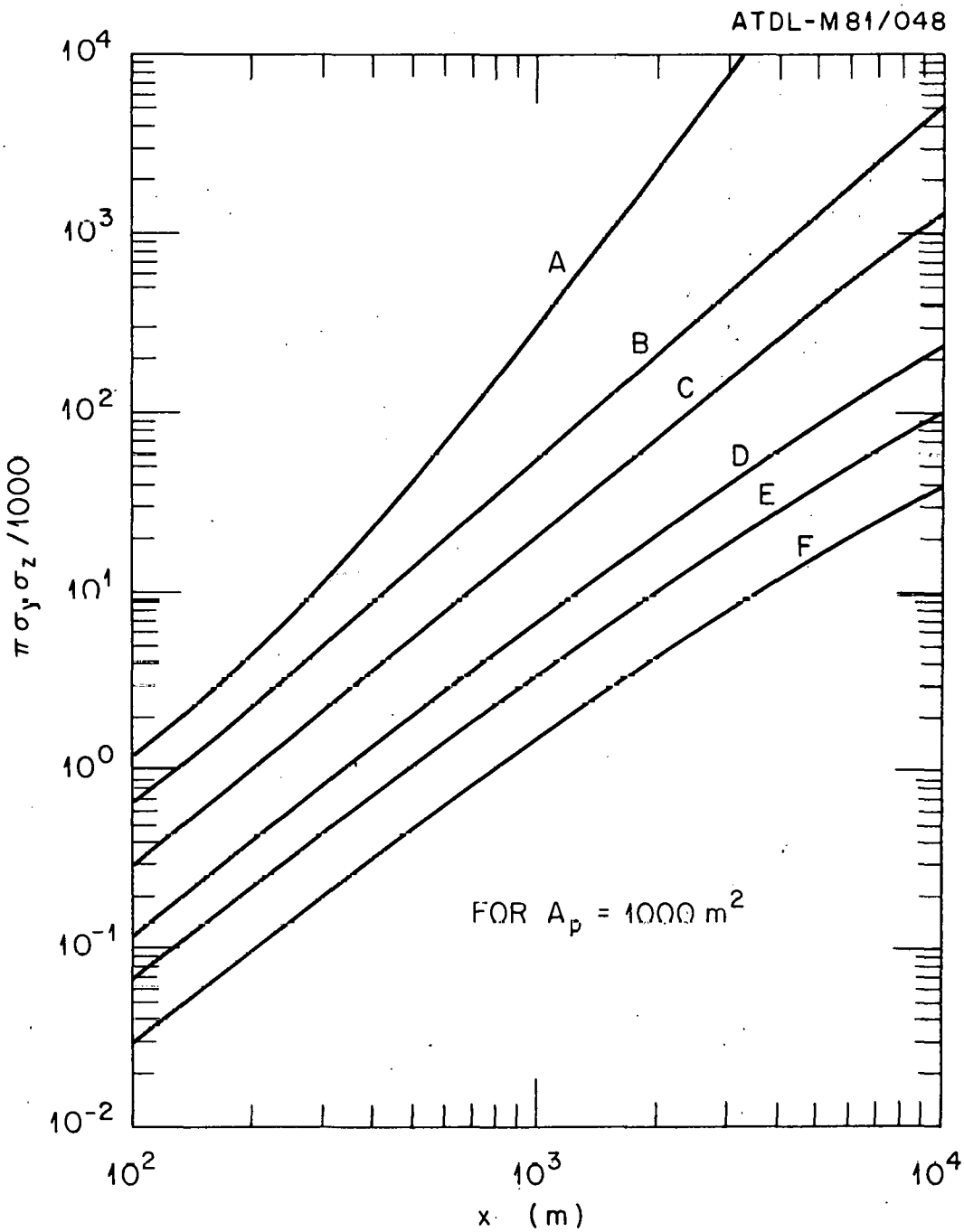

Figure 47. Plot of $\pi\sigma_y\sigma_z/1000$ as function of distance, for various stabilities, for use in Gifford's (1960) initial dilution wake concentration model. Use with arbitrary building frontal area A_p by multiplying by $1000/A_p$.

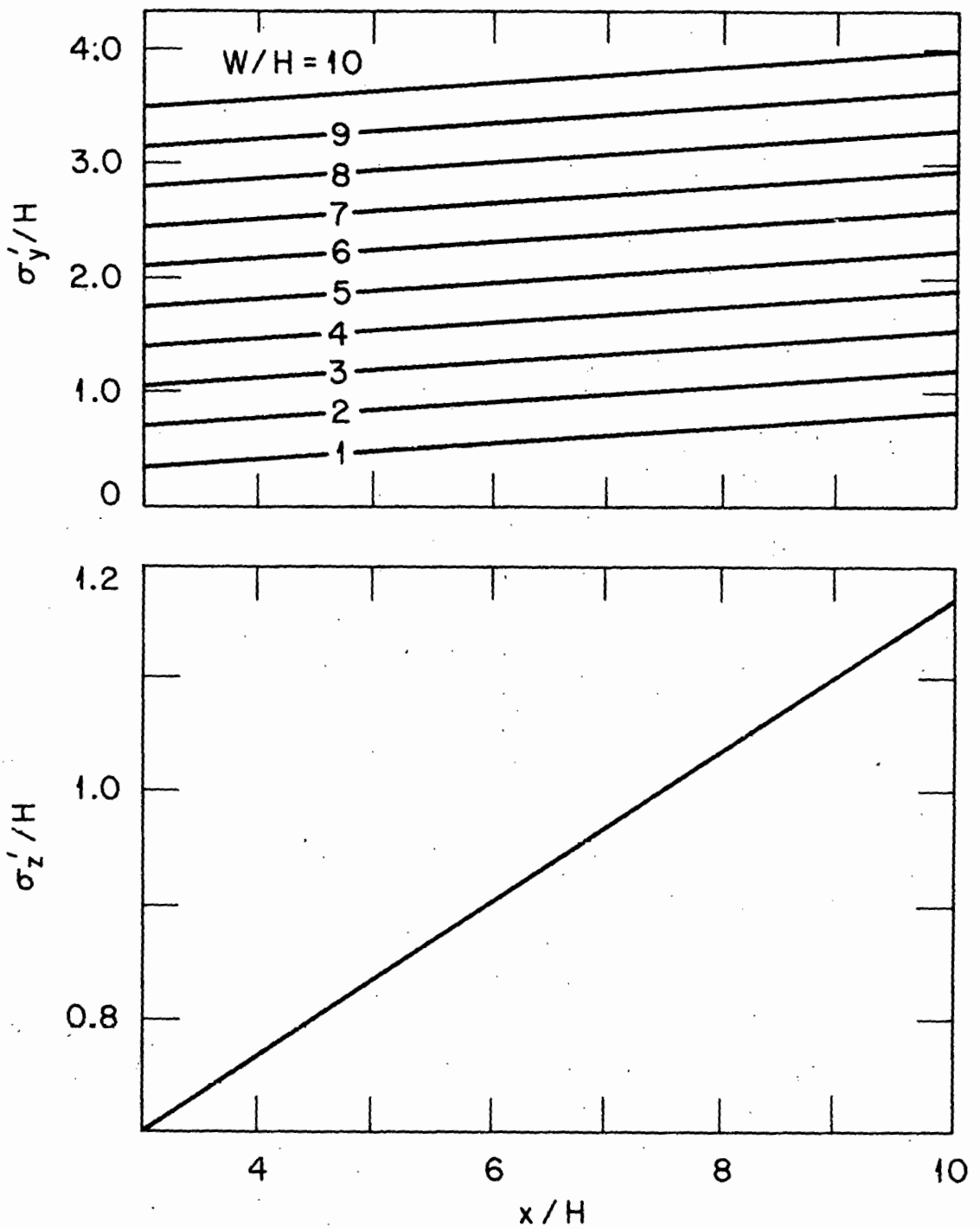

Figure 48. Huber and Snyder's (1976) estimate of dispersion parameters in building wake for 3 H ≦ x ≦ 10 H, for several building aspect ratios W/H.

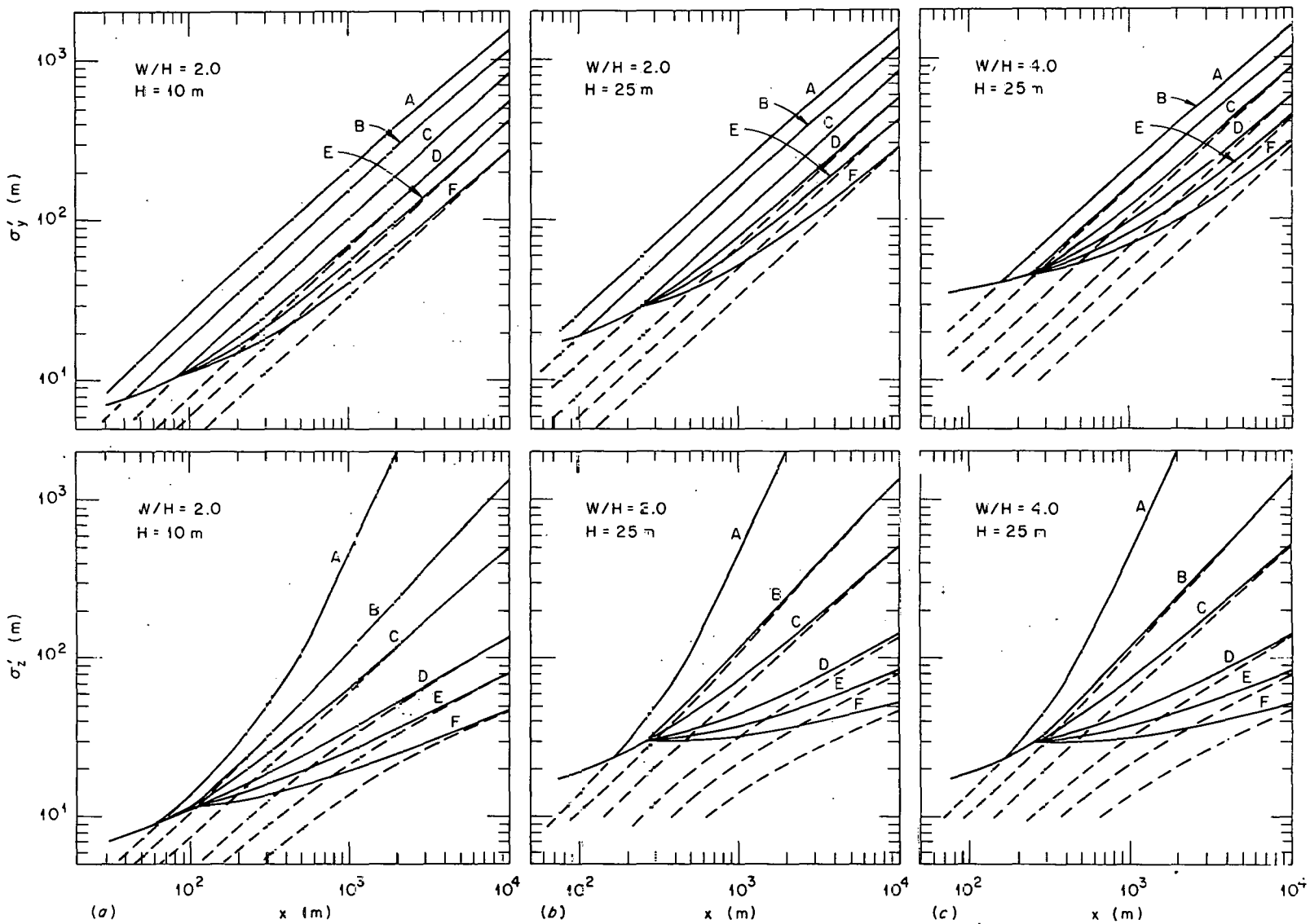

Figure 49. Sample evaluation of Huber's (1977, 1979) recommended lateral and vertical wake-enhanced dispersion parameters to demonstrate effect of changes in building height H (a and b), and width W (b and c). Standard Pasquill-Gifford values for σ_y and σ_z are shown as broken lines.

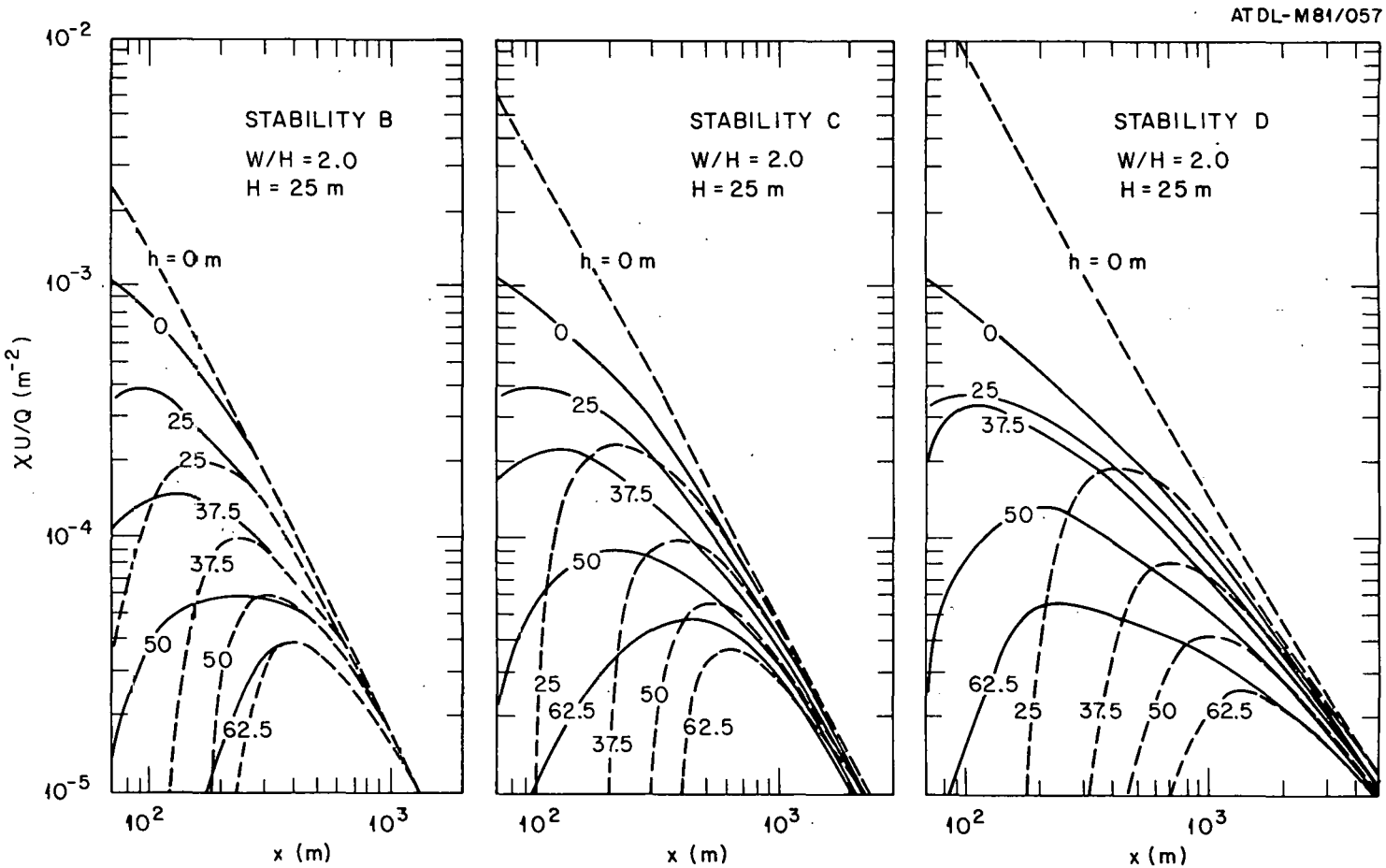

Figure 50. Huber's (1979) estimates of $\chi U/Q$ using wake-enhanced dispersion coefficients (solid lines) compared to usual point-source Gaussian model results with no wake effect (broken lines).

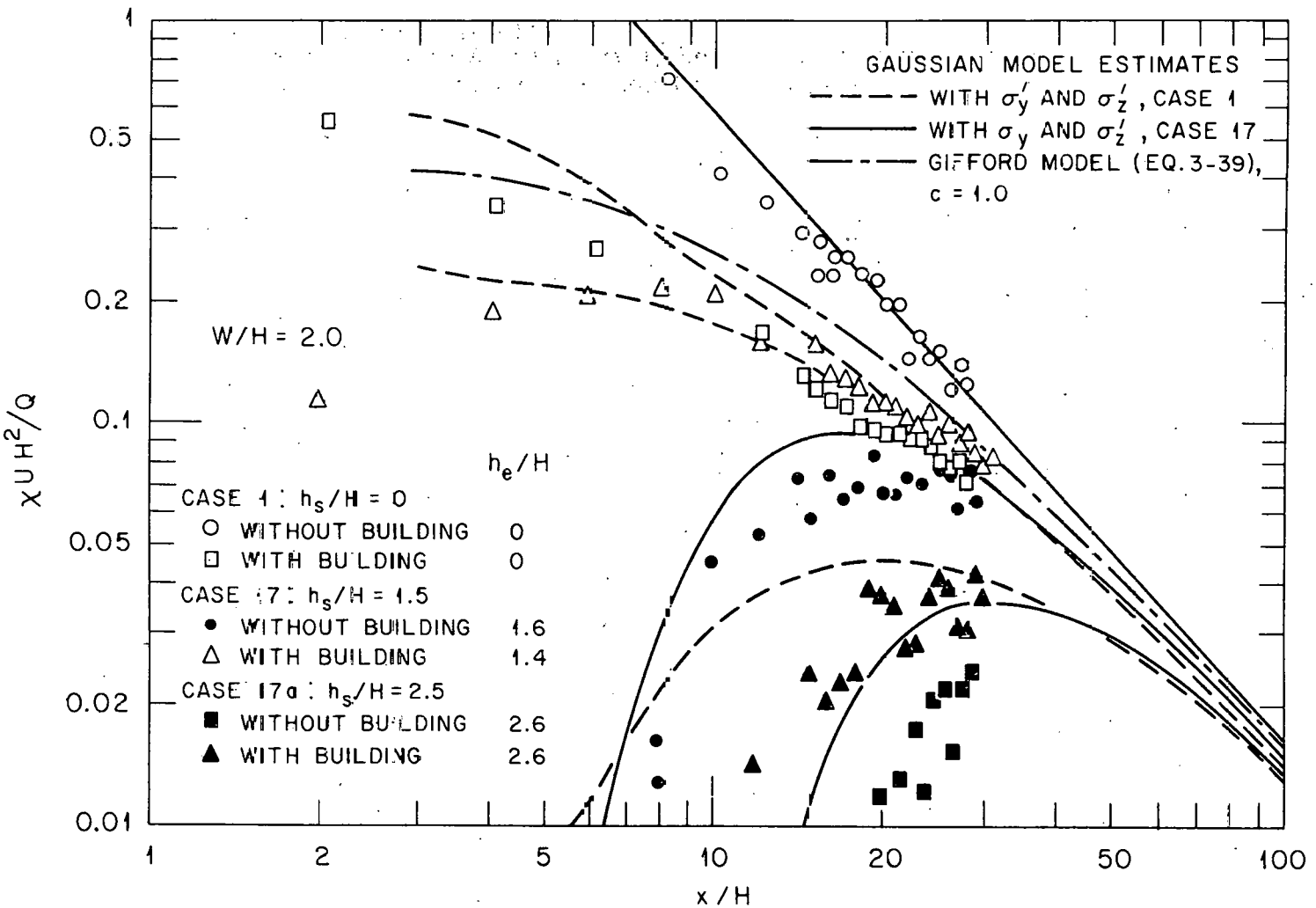

Figure 51. Comparison of wind tunnel data with Huber's (1977,1979) recommended wake concentration model (dashed and solid lines), and with Gifford's (1960) initial dilution wake model (from Huber et al., 1980).

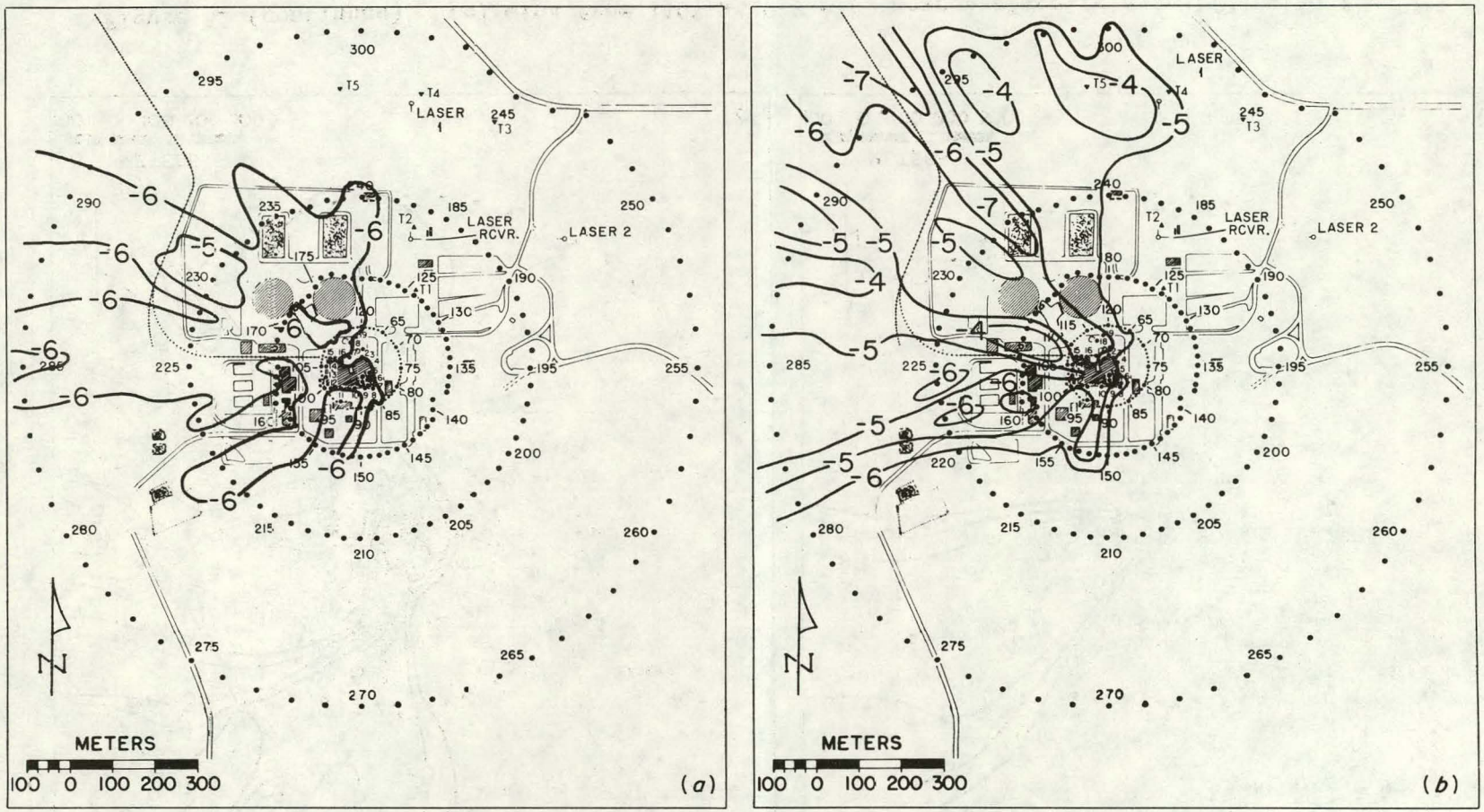

Figure 52. Concentration isopleths of $\chi U/Q$, as negative powers of ten, for different wind directions at a reactor complex (from Start et al., 1977). (a) wind from 161° at 1.8 m/s, $\sigma_\theta \cong 32°$ at 10 m, rooftop release; (b) wind from 100° at 1.7 m/s, $\sigma_\theta \cong 20°$ at 10 m, rooftop release.

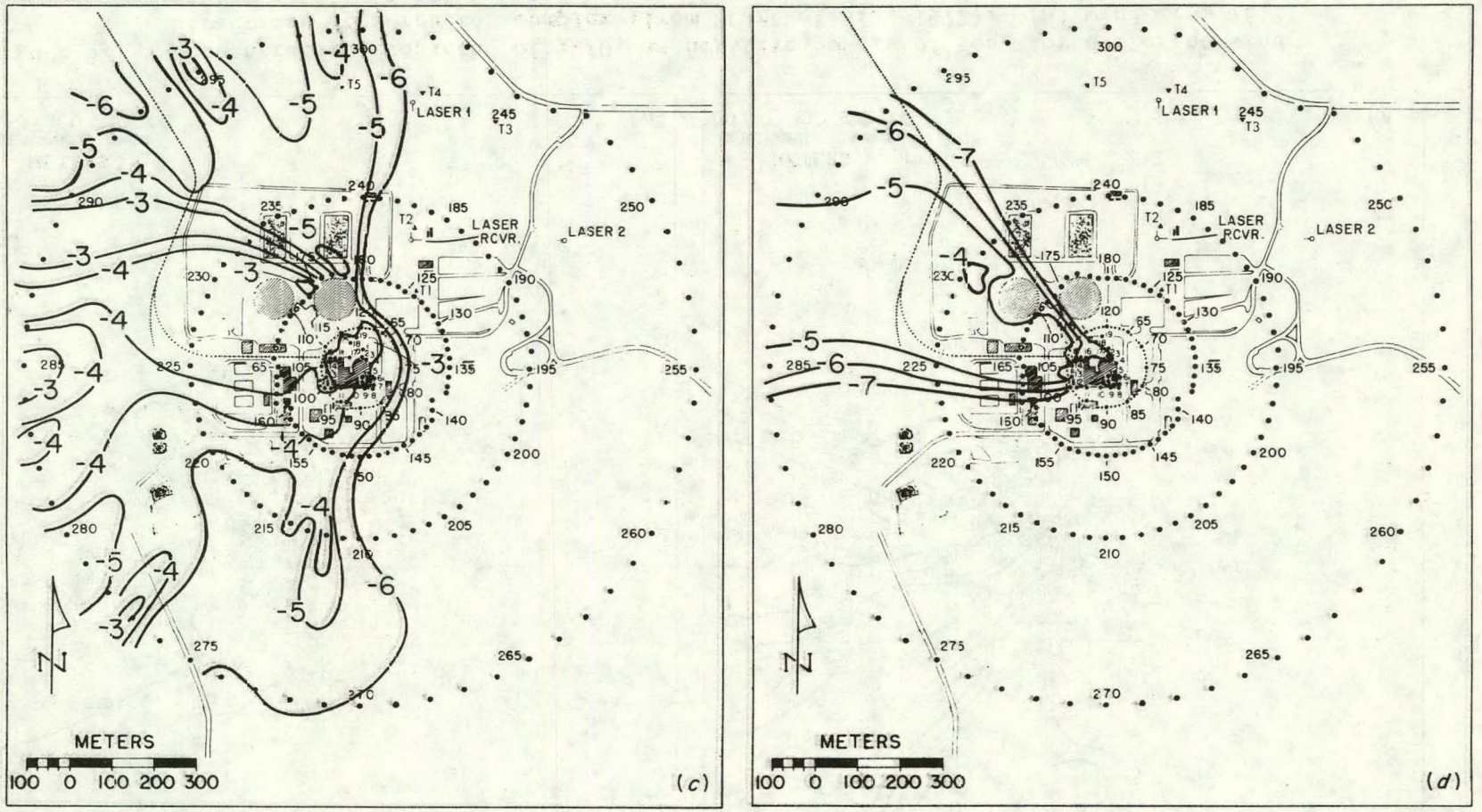

Figure 52 (continued). (c) wind from 110° at 0.9 m/s, near-surface release; (d) wind from 110° at 2.5 m/s, $\sigma_\theta \cong 19°$ at 10 m, rooftop release.

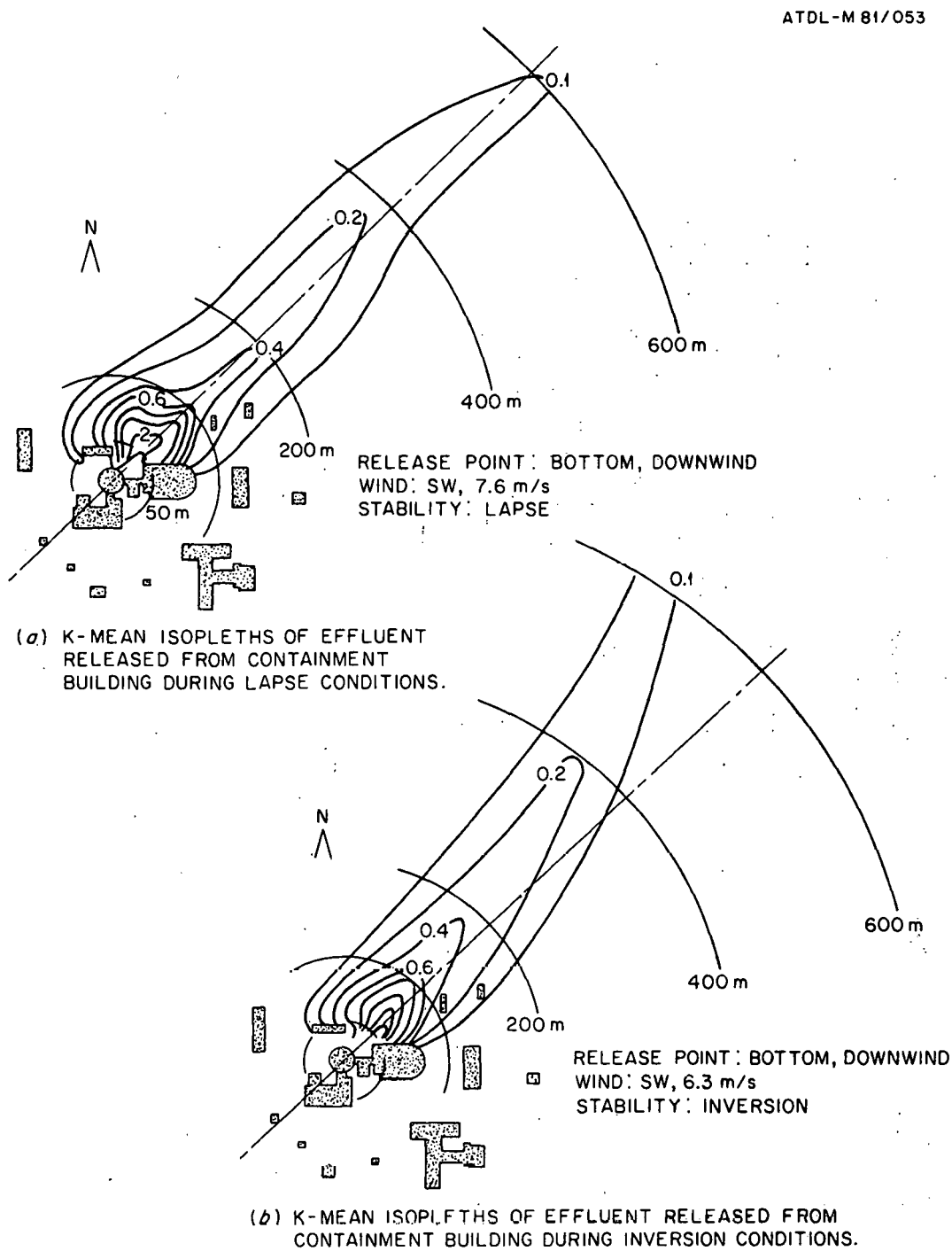

Figure 53. Ensemble-average isopleths of concentration coefficient $K = \chi UA_p/Q$ measured at EBR-II complex, with $A_p = 665\ m^2$ = projected area of containment building only (from Dickson, Start, and Markee, 1969).

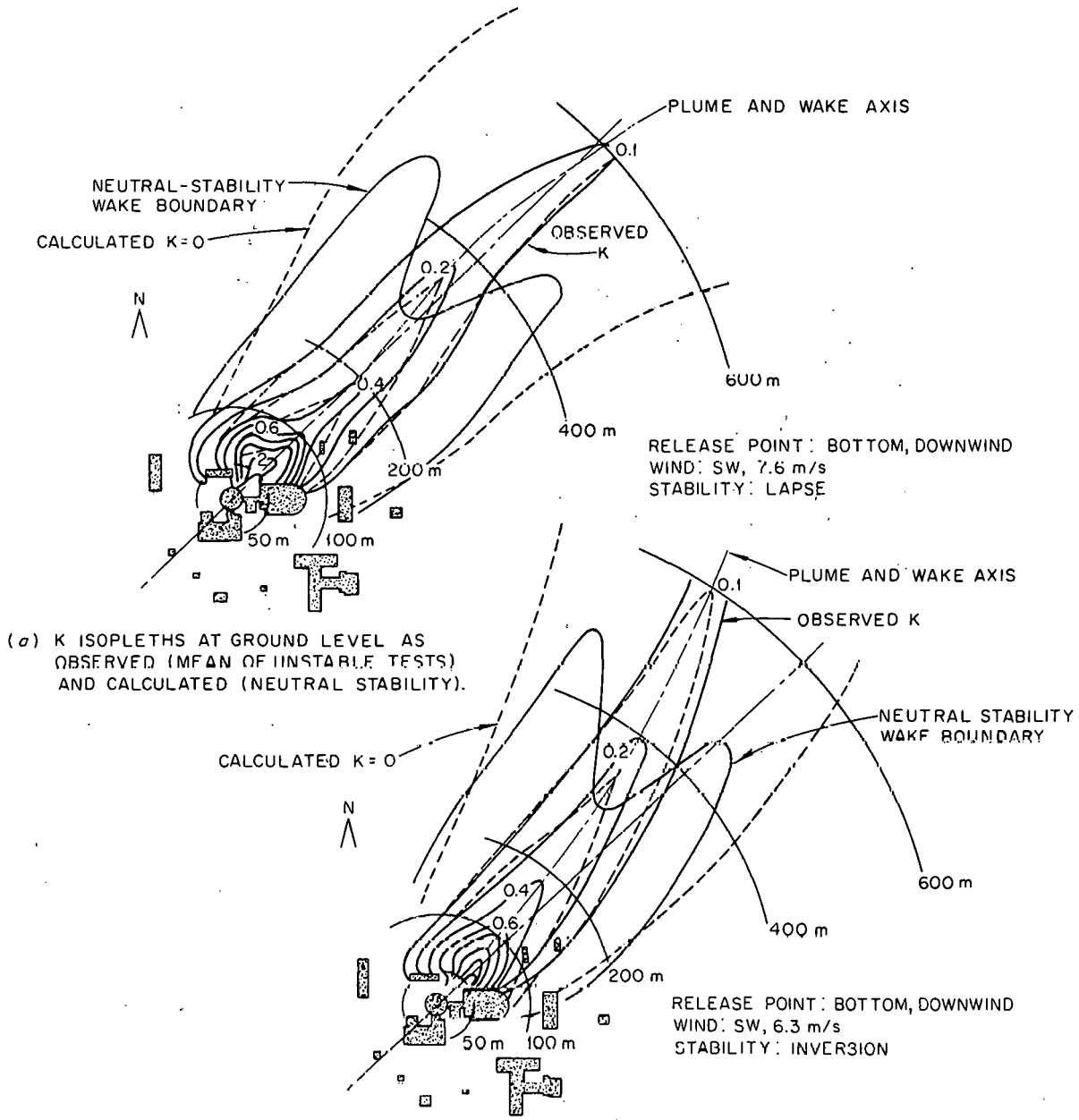

Figure 54. Comparisons of observed (solid lines) and calculated (broken lines) ensemble-average concentration isopleths behind EBR-II complex (from Halitsky, 1977). (a) unstable tests; (b) stable tests.

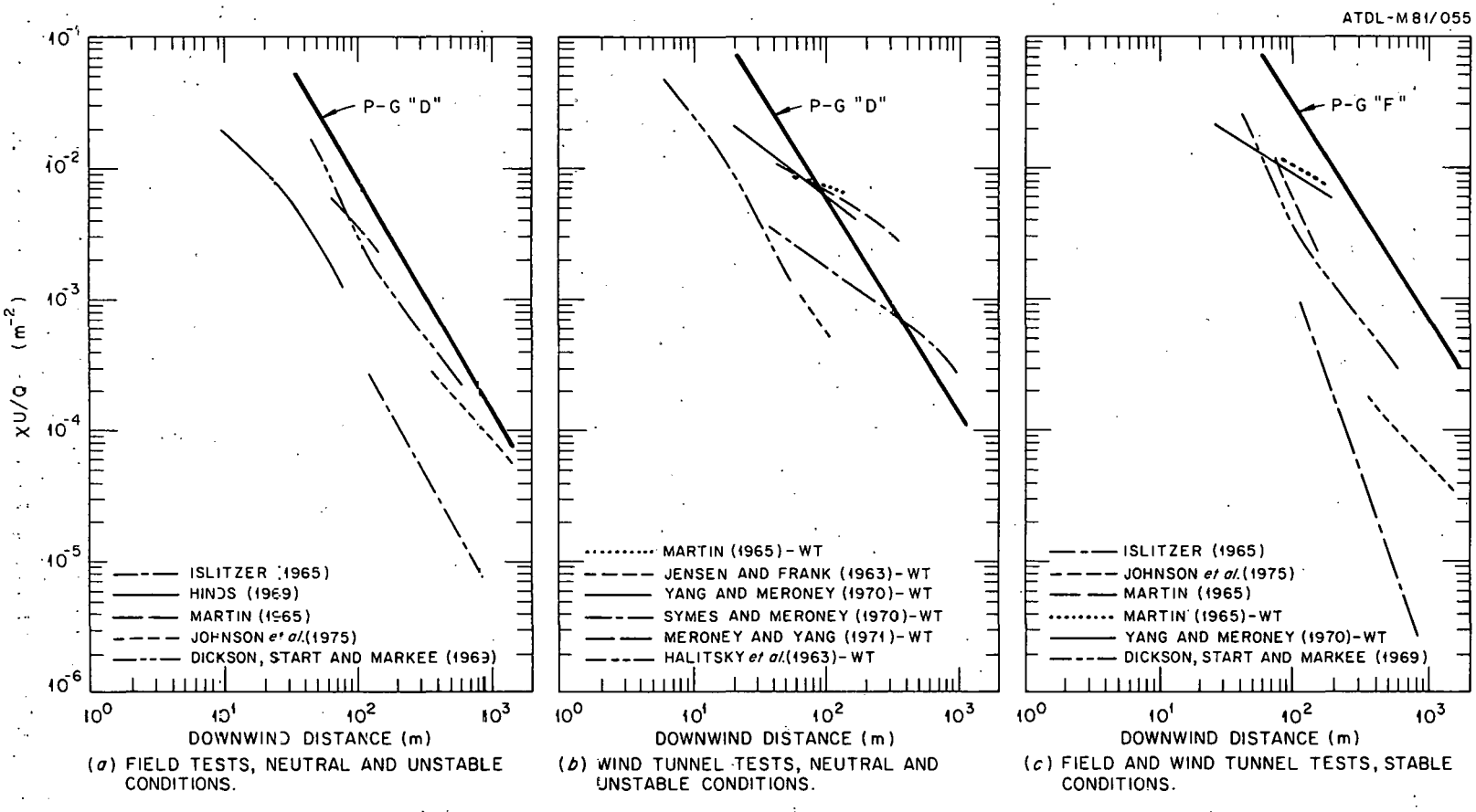

(a) FIELD TESTS, NEUTRAL AND UNSTABLE CONDITIONS.

(b) WIND TUNNEL TESTS, NEUTRAL AND UNSTABLE CONDITIONS.

(c) FIELD AND WIND TUNNEL TESTS, STABLE CONDITIONS.

Figure 55. Summary of far wake concentration decay with distance behind building clusters (from Abbey, 1976).

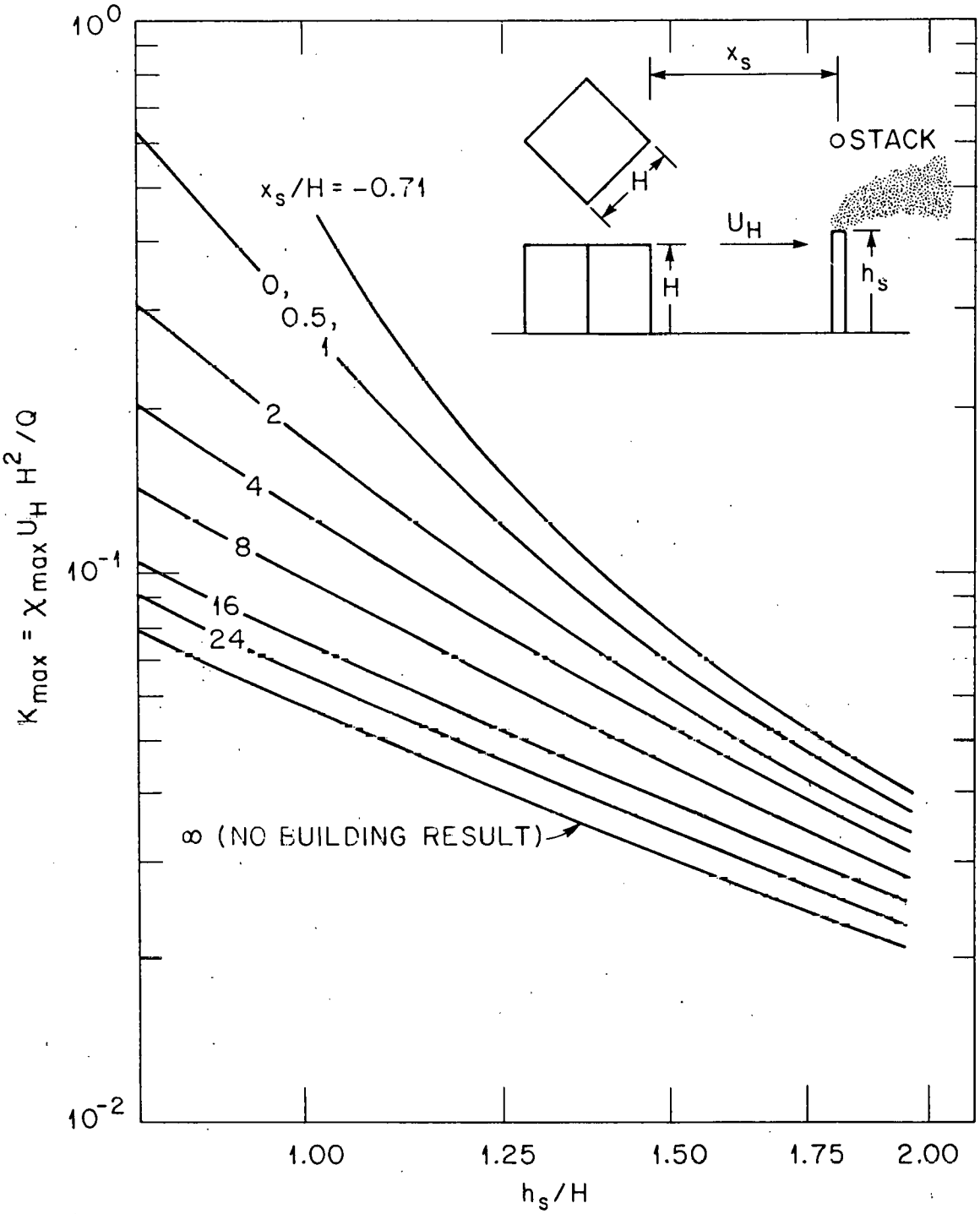

Figure 56. Maximum ground-level concentration as function of stack height, for stack at various distances downwind of building at 45° to incident wind (from Barrett, Hall, and Simmonds, 1978).